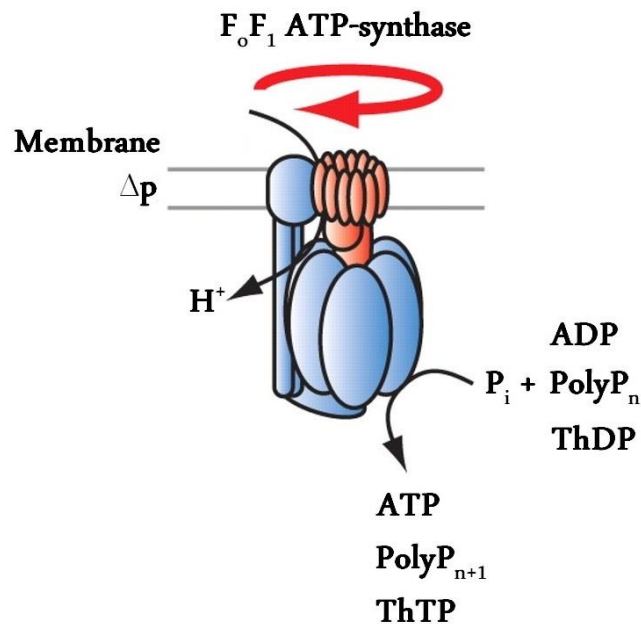


Metabolic significance of inorganic triphosphate, thiamine triphosphate and their hydrolyzing enzymes

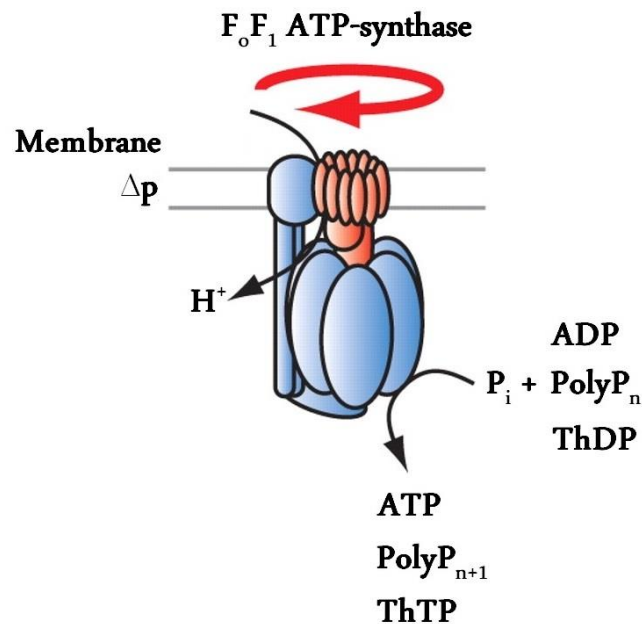


Mémoire présenté par Grégory Kohn,

Titulaire d'un Master en Sciences Biomédicales,

en vue de l'obtention du grade de Docteur en Sciences Biomédicales et
Pharmaceutiques

Metabolic significance of inorganic triphosphate, thiamine triphosphate and their hydrolyzing enzymes



Mémoire présenté par Grégory Kohn,

Titulaire d'un Master en Sciences Biomédicales,

en vue de l'obtention du grade de Docteur en Sciences Biomédicales et
Pharmaceutiques

*“La Science n’est plus à même de fournir
aucune certitude, mais des propositions temporaires
qui se métamorphoseront aussi vite
que nos certitudes d’hier.”*

*Ilya Prigogine
(1917-2003, physicien Belge, Prix Nobel de Chimie en 1977)*

Our laboratory has been interested for many years in thiamine triphosphate (ThTP), an unusual triphosphate derivative of thiamine (vitamin B1) found in nearly all organisms. In mammalian tissues, ThTP is hydrolyzed by a very specific cytosolic thiamine triphosphatase (ThTPase) belonging to an ancient superfamily of proteins called CYTH. Several members of this superfamily have been characterized and they all have in common that they act on triphosphorylated substrates. Some bacterial members (the *N. europaea* specifically) hydrolyze inorganic triphosphate (PPP_i) which raises the question of the physiological significance of this compound.

We first studied the tripolyphosphatase activity in mammals and in bacteria and we showed that it is widely distributed in all organisms. We attempted to identify the enzymes responsible for this activity. We showed that the *E. coli* CYTH enzyme, ygiF, although highly specific for PPP_i plays only a minor role in the cytosolic PPPase activity, while most of the activity is due to inorganic pyrophosphatase. In animal tissues, most PPPase activity is due to the short-chain exopolyphosphatase prune, which hydrolyzes PPP_i with high catalytic efficiency. We hypothesize that PPP_i may be formed as a by-product of metabolism and the major role of PPPase activities may be to keep PPP_i concentrations very low to avoid toxic effects linked to interference with Ca²⁺ metabolism. In order to check this hypothesis, it would be important to have a specific and sensitive method for measuring intracellular PPP_i concentrations. Such a technique is presently not available.

In the second part of our work, we tried to manipulate intracellular ThTP concentrations in order to get insight into the physiological role of this compound. Expression of mammalian ThTPase in *E. coli* prevented ThTP accumulation, but did not affect the growth of the bacteria. We then reduced ThTPase expression in zebrafish embryos using morpholino oligomers. This led to severe malformations of the embryos. Finally, we attempted to produce a ThTPase knockout mouse. However, we found that the spermatogenesis of ThTPase-null sperm cells was impaired and the chimerae were unable to transmit. In conclusion, our results suggest that ThTPase inactivation results in heavy developmental consequences, possibly as a result of ThTP toxicity.

List of abbreviations :

| | |
|--------------|---|
| ADP | Adenosine diphosphate |
| AMP | Adenosine monophosphate |
| AThDP | Adenosine thiamine diphosphate |
| AThTP | Adenosine thiamine triphosphate |
| ATP | Adenosine triphosphate |
| CoA | Coenzyme A |
| CYTH | CyaB-Thiamine triphosphatase |
| E1o | 2-Oxoglutarate dehydrogenase |
| E1p | Pyruvate dehydrogenase |
| E2o | Dihydrolipoamide succinyltransferase |
| E2p | Dihydrolipoamide acetyltransferase |
| E3 | Dihydrolipoamide dehydrogenase |
| EDTA | Ethylenediaminetetraacetic acid |
| ES cell | Embryonic stem cell |
| GC | Glycine cleavage complex |
| Hpf | Hour post-fertilization |
| IPTG | Isopropyl β -D-1-thiogalactopyranoside |
| k_{cat} | Catalytic constant |
| K_m | Michaelis constant |
| KOMP | Knockout Mouse Project |
| LC-ESI/MS/MS | Liquid chromatography Electrospray ionization mass spectrometry |
| NAD | Nicotinamide adenine dinucleotide |
| NADP | Nicotinamide adenine dinucleotide phosphate |
| NCBI | National Center for Biotechnology Information |
| NMP | Nucleotide monophosphate |
| NMR | Nuclear magnetic resonance |
| NTP | Nucleotide triphosphate |
| OGDH | 2-Oxoglutarate dehydrogenase complex |
| PCR | Polymerase chain reaction |
| PDH | Pyruvate dehydrogenase complex |
| P_i | Inorganic phosphate |
| PolyP | Inorganic polyphosphate |
| PPase | Pyrophosphatase |
| PP_i | Inorganic diphosphate |
| PPK | Polyphosphate kinase |
| PPPase | Triphosphatase |
| PPP_i | Inorganic triphosphate |
| PPX | Exopolyphosphatase |

List of abbreviations

| | |
|----------|---|
| qPCR | quantitative PCR |
| SD | Standard deviation |
| SDS-PAGE | Sodium dodecyl sulfate Polyacrylamide gel electrophoresis |
| SL | Standard length |
| SLC | Solute carrier (gene) |
| SOC | Swim-out - central part |
| SOP | Swim-out - peripheral part |
| SUL | Swim-up - lower part |
| SUS | Swim-up - superior part |
| TCA | Trichloroacetic acid |
| ThDP | Thiamine diphosphate |
| ThMP | Thiamine monophosphate |
| ThTP | Thiamine triphosphate |
| ThTPase | Thiamine triphosphatase |
| THTR | Thiamine transporter (protein) |
| TTM | Triphosphate tunnel metalloenzyme |
| WT | Wild-type |

Après 10 ans passés à écumer les couloirs, les amphis et les laboratoires de l'université, il y a beaucoup de personnes que je me dois de remercier pour le soutien qu'ils m'ont apporté de différentes manières. J'oublierai sûrement de citer certains d'entre eux mais ils savent qu'ils sont malgré tout dans mes pensées.

Tout d'abord, bien entendu, je tiens à remercier ma famille et surtout mes parents à qui revient tout le mérite de mon parcours, même si je ne leur ai probablement pas souvent fait ressentir. Et un merci tout spécial à mon grand-père qui n'est malheureusement plus là pour assister à l'aboutissement de cette entreprise.

Il y a quelques personnes à qui mon parcours scientifique doit énormément. Tout d'abord, le Pr Lucien Bettendorff qui m'a conseillé et guidé au cours de toutes mes années de doctorat ; le Dr Pierre Wins, la bibliothèque vivante perpétuellement remise à jour que tout jeune chercheur devrait avoir la chance de rencontrer ; le Dr Bernard Lakaye et ses précieux conseils qui m'ont permis d'éviter nombre de pièges au cours de ces cinq années et Ilca pour sa gentillesse.

Ensuite, bien entendu, le Dr David Delvaux pour m'avoir appris les bases du travail scientifique et pour toujours avoir été de bon conseil quand je débutais ma carrière. Également les Dr Marjorie Gangolf et Tiziana Gigliobinaco avec qui j'ai partagé bien plus qu'un bureau lors de mes premiers pas de chercheur et Arlette Minet et son esprit d'aventure.

Un merci spécial va ensuite à Julie Vignisse avec qui j'ai partagé pas mal des joies et des peines survenues aux cours de mon master d'abord et de ma thèse ensuite. Et bien sûr, un grand merci à Coralie Pasquet pour les pauses-café et Margaux Sambon pour ses "Greeeeeg" présageant toujours une question. Une dédicace spéciale

à mon admiratrice secrète pour avoir refait la décoration du bureau et pour son “ théobromine-tactisme” exacerbé.

Je tiens aussi à remercier les Dr Laurence de Nijs et Nathalie Wolkoff pour avoir contribué à la bonne atmosphère de notre équipe ainsi que Sophie Harray qui a partagé avec moi une première expérience d'élevage de N.A.C. et Laurie Medard pour sa folie et sa bonne humeur.

Je tiens à remercier tous les étudiants qui ont transité pour quelques mois par notre labo et tout spécialement Franciska, pour m'avoir fait découvrir et repousser les limites de la patience, ainsi que Cindy pour m'avoir rendu foi dans le travail fourni par la nouvelle génération d'étudiant.

Je ne peux pas oublier non plus ceux avec qui j'ai collaboré, Marc Muller et tous les membres de l'équipe du Laboratoire de Biologie Moléculaire et Génie Génétique, surtout Marie Winandy pour son écolage ; les membres du Laboratoire de Génétique et de Physiologie Bactérienne de l'ULB, surtout Johan Timmermans pour son aide, et enfin Fabien Ectors pour la production et le croisement de nos chimères.

Enfin, merci à ceux qui étaient là avant, pendant et seront toujours là après tout ça, Pierre et Laulau, Bruno, Jen et Benoit, Loïc, Léon et Cath.

And last but not least, un grand merci aux membres du GIGA-Neurosciences : tout d'abord aux techniciens Bernard, Alexandra, Alice, Laurent, P-B, les Patricia et Guérin qui ont toujours été là pour répondre à mes questions ; ensuite à nos dévouées secrétaires Lari et Jess sur qui on peut toujours compter ;

Et enfin à tous les autres, doctorant, PI ou autres qui ont fait et font du centre ce qu'il est.

I have now to switch to English to thank many people that were or were not already cited in the first part. To all of you who will be included in the next part, thank you for the different experiences and opinions shared and for the free English class. As I have always said: sorry to fail as a local for not teaching you any French and instead using you to improve my English.

First, I want to thank all the “expats” from the GIGA-Neurosciences, and specially the two “douche” Arash and Deb for all the good time and Sita and Asya for all the good music, live or on vinyl.

Also all the others members of the so called “Liege Expats group” with a special thanks to Sophie who made me an expat in my own city. Thank you all for the trips, parties, pic-nics, museum visit and so on and so forth that we've made together.

I also want to thank my climbing partners Todd, Katya, Rohan, Amy, Stephane, Brett and Cyrine; nothing is as good as getting high (15 meters high) with nice people after a good day of work.

“But standing in water up to their knees three very unimportant little people were doing the best they could with an idea and that's about all they had and I don't know maybe that night these three people were making history but anyway what I'm telling to tell you folks is: here we are!” J.Steinbeck. –We all had many discussions that made me think about that sentence, sharing our experience all around the globe.

I also want to thank all the members of the "Institut für Physiologie und Pathophysiologie" in Heidelberg for their warm welcome. First, the Prof. Dr.med. Andreas Draguhn who made it possible, then a special thank for Azra who taught me most of what I know about electrophysiology and Antonio because my stay there would never have been the same without him. Of course I also want to thank all the others: Jana, Xiao-min, Cédric Rachel, Pascal, Christian, Ismini, Joshua, Dimitri, Alistair, Miguel, Suse and Pierre and all the others I forgot.

"No one looks back on their life and remembers the nights they got plenty of sleep"

Introduction

| | |
|--|----|
| Chapter 1: Thiamine and its phosphorylated derivatives | 1 |
| Chemistry: | 1 |
| Physiology: | 1 |
| Different derivatives: | 3 |
| Thiamine diphosphate: | 3 |
| Thiamine monophosphate: | 5 |
| Thiamine triphosphate..... | 5 |
| Adenylated thiamine derivatives | 6 |
| ThTP production in E. coli: | 6 |
| Chapter 2: The mammalian 25-kDa ThTPase: | 8 |
| Discovery and characterization | 8 |
| Phylogeny | 8 |
| Catalytic properties..... | 10 |
| Translational control of the expression | 11 |
| Chapter 3: The inorganic polyphosphates | 13 |
| Nomenclature: | 14 |
| Synthesis and degradation: | 14 |
| Function: | 15 |
| Energy and P _i storage: | 15 |
| Regulatory role in mammals | 15 |
| Chapter 4: The zebrafish..... | 16 |
| Phylogeny: | 16 |
| Description: | 16 |
| Growth and mortality: | 17 |
| Reproduction: | 17 |
| Genetics: | 17 |

| | |
|---|----|
| The zebrafish as a tool for the scientist..... | 17 |
| CYTH in fish..... | 18 |
| Morpholino: | 21 |
| Anti-sense knockdown of gene expression: | 21 |
| Aims of the work | |
| Aims o the work..... | 24 |
| Material and methods | |
| Material | 25 |
| Solvents and Reagent | 25 |
| Morpholino solution..... | 25 |
| Zebrafish solution | 26 |
| Bacteria culture medium: | 26 |
| Strains of E. coli used: | 26 |
| Methods..... | 28 |
| Determination of the tripolyphosphatase activity | 28 |
| Collection of the sample | 28 |
| Measurement of the activity | 28 |
| Pig brain PPPase activity identification | 28 |
| E. coli PPPase activity identification | 29 |
| In-gel enzymatic activity..... | 30 |
| Detection of thiamine and its derivatives in E. coli | 30 |
| Determination of acetyl-CoA levels | 31 |
| Polymerase chain reaction | 31 |
| Insertion of the mammalian ThTPase coding sequence in the E.coli genome | 33 |
| Zebrafish maintenance | 34 |
| Zebrafish breeding and eggs generation | 35 |
| Morphant generation, characterization and maintenance | 35 |
| Zebrafish embryo RNA isolation..... | 35 |
| zThTPase mRNA cloning and expression | 36 |

| | |
|--|----|
| Mouse genotyping | 36 |
| Sperm isolation | 36 |
| Swim up | 37 |
| Swim out | 37 |
| Quantitative PCR:..... | 38 |
| Results | |
| Chapter 1: Tripolyphosphatase activity..... | 39 |
| Tripolyphosphatase activity of mammalian tissues:..... | 39 |
| Characterization | 39 |
| Identification | 39 |
| Tripolyphosphatase activity of E. coli supernatant fraction:..... | 41 |
| ygiF is not the main tripolyphosphatase of E. coli..... | 41 |
| Identification of the enzyme responsible for the tripolyphosphatase activity in E. coli: | 41 |
| Characterization of the tripolyphosphatase activity of the EcPPase | 42 |
| PPase, ygiF or PPX? | 43 |
| PPase and PPPase activities over growth of the bacteria | 44 |
| Conclusions: | 44 |
| Chapter 2: ThTP production in E. coli | 47 |
| ThTP synthesis and PDH mutants:..... | 48 |
| ThTP synthesis and OGDH mutant:..... | 49 |
| ThTP synthesis, OGDH mutant and glyoxylate cycle over-activation: | 51 |
| ThTP synthesis and the two first enzymatic activities of the Krebs cycle: | 53 |
| ThTP production and inhibition of the F ₀ F ₁ ATP-synthase by octyl- α -cetoglutarate:..... | 54 |
| Mammalian ThTPase expression in E. coli:..... | 55 |
| ThTP synthesis and oxidative stress:..... | 57 |
| Conclusions | 58 |
| Chapter 3: Possible role of THTP and 25-kDa zThTPase on zebrafish development | 61 |
| Characterization of the zTHTPA gene: | 61 |
| Morpholino-induced zThTPase expression reduction..... | 63 |
| HPLC measurement of thiamine derivatives in zebrafish embryo:..... | 70 |

Conclusions..... 70

Chapter 4: Knock-out of the mouse ThTPase:..... 72

 Thiamine triphosphatase knock-out methods 72

 Results obtained from the THTPA chimerae:..... 75

 Conclusions..... 77

Discussion and conclusion

Possible biological role(s) of tripolyphosphate..... 80

Role of ThTP and the 25-kDa ThTPase in animal tissues 81

Bibliography

Appendix 1

Delvaux D., Murty MR, Gabelica V., Lakaye B., Lunin VV, Skarina T., Onopriyenko O., Kohn G., Wins P., De Pauw E., Bettendorff L. 2011. A specific inorganic triphosphatase from *Nitrosomonas europaea*: structure and catalytic mechanism. *J. Biol. Chem.* 286 (39) 34023-35. doi: 10.1074/jbc.M111.233585.

Appendix 2

Kohn G., Delvaux D., Lakaye B., Servais AC, Scholer G., Fillet M., Elias B., Derochette JM, Crommen J., Wins P., Bettendorff L. 2012. High inorganic triphosphatase activities in bacteria and mammalian cells: identification of the enzymes involved. *PLoS One.* 7 (9) e43879. doi: 10.1371/journal.pone.0043879.

Appendix 3

Delvaux D., Kerff F., Murty MR, Lakaye B., Czerniecki J., Kohn G., Wins P., Herman R., Gabelica V., Heuze F., Tordoir X., Marée R., Matagne A., Charlier P., De Pauw E., Bettendorff L., 2013. Structural determinants of specificity and catalytic mechanism in mammalian 25-kDa thiamine triphosphatase. *Biochim. Biophys. Acta* 1830 (10) 4513-23. doi: 10.1016/j.bbagen.2013.05.014.

Appendix 4

Bettendorff L., Lakaye B., Kohn G., Wins P. 2014. Thiamine triphosphate: a ubiquitous molecule in search of a physiological role. *Metab. Brain Dis.* 29 (4) 1069-82. doi: 10.1007/s11011-014-9509-4.

Introduction

Chapter 1: Thiamine and its phosphorylated derivatives

Thiamin (vitamin B1) was the first vitamin to be discovered and characterized as an “antianeuric factor” more than a century ago. A vitamin is defined as an organic compound required by humans in only small amounts and that they are unable to synthesize in sufficient amounts. Hence, the main source of vitamins is the diet. There are a total of 13 vitamins universally recognized, that are divided in two categories: the lipophilic vitamins (A, D, E, K) and the water-soluble vitamins (B1, B2, B3, B5, B6, B7, B9, B12, C). All the B vitamins are coenzymes (or coenzyme precursors) in metabolism of all living cells. For some of them, non-coenzyme roles have also been suggested. This is the case for vitamin B1 (thiamine), a vitamin essential for brain function. Our laboratory has been interested for many years in studying non-cofactor roles of thiamine and its phosphorylated derivatives.

Chemistry:

Thiamine (2-{3-[(4-amino-2-methylpyrimidin-5-yl)methyl]-4-methylthiazol-5-yl}ethanol) is composed of a pyrimidine ring linked to a thiazolium ring by a methylene bridge. The C5 of the thiazolium ring bears an ethanol moiety that can be esterified, leading to the formation of phosphate esters. Diphosphorylated thiamine (thiamine diphosphate, ThDP) is an important cofactor in cell metabolism. Other phosphate esters are thiamine monophosphate (ThMP) and thiamine triphosphate (ThTP), whose roles remain unknown. Recently, the existence of adenylated thiamine derivatives, adenosine thiamine triphosphate (AThTP) and adenosine thiamine diphosphate (AThDP) has been reported in our laboratory (Bettendorff *et al.* 2007) (figure 1)

Physiology:

Thiamine can be synthesized by bacteria, fungi and plants (Manzetti *et al.* 2014) but not by animals. Because of the positive charge in the thiazolium heterocycle and the polar character of the molecule, thiamine does not diffuse freely through biological membranes and its transport requires specific transporters. In mammals, thiamine is absorbed in the intestine by two specific transporters: THTR 1 ($K_d < 10 \mu\text{M}$) and THTR 2 ($K_d < 100 \text{ nm}$) encoded respectively by the SLC19A2 and SLC19A3 genes. After crossing the intestinal epithelium, thiamine can reach the blood stream and then be distributed into the whole body. In the blood, total thiamine is roughly found for 75% in erythrocytes, 15% in leucocytes and 10% in plasma (Weber and Kewitz, 1985).

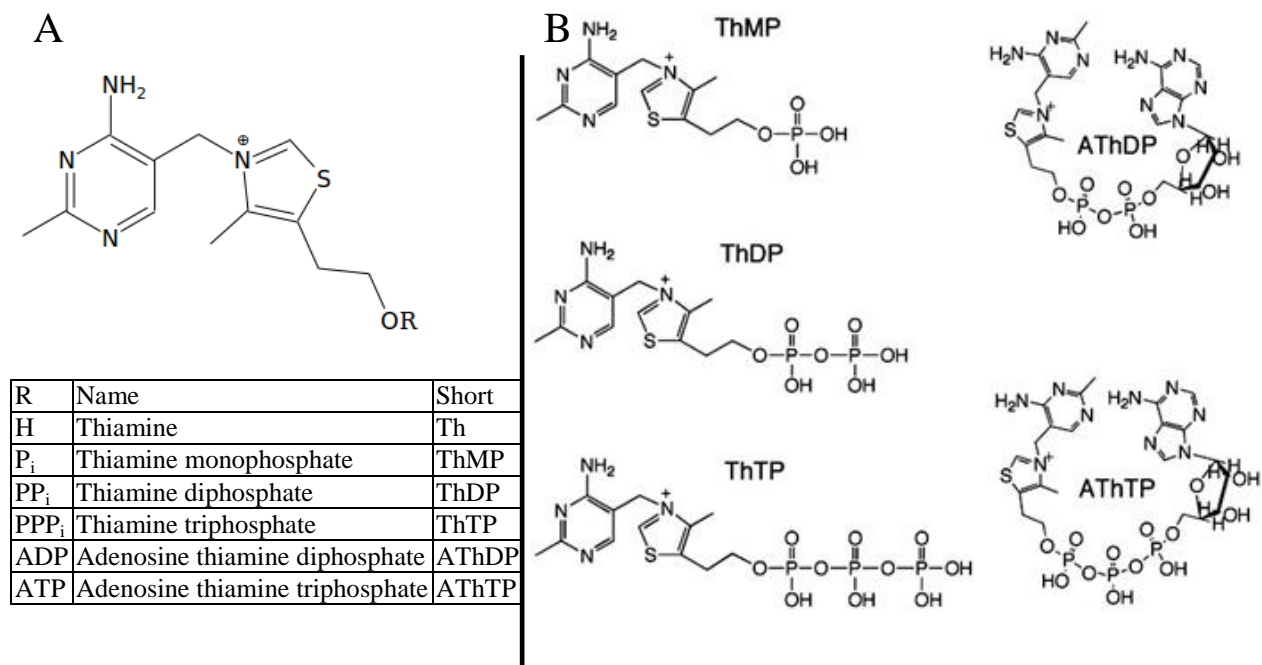


Figure 1: thiamine and its derivative. A: thiamine and the different chemical groups naturally found attached to the alcohol function; B: thiamine monophosphate (ThMP), thiamine diphosphate (ThDP), thiamine triphosphate (ThTP), adenosine thiamine diphosphate (AThDP) and adenosine thiamine triphosphate (AThTP) (right panel from Bettendorff, 2012).

In plasma, thiamine half-life is approximately one hour, then it has either been excreted by the kidney or absorbed by the tissues (Tallaksen *et al.* 1993).

Once thiamine enters a mammalian cell, it is pyrophosphorylated to ThDP by a cytosolic thiamine pyrophosphokinase (EC 2.7.6.2). ThDP is the cofactor for the cytoplasmic transketolase and for the mitochondrial oxoglutarate and pyruvate dehydrogenases. ThDP is the precursor of other thiamine derivative (figure 2), it can be:

- hydrolyzed by a thiamine diphosphatase to thiamine monophosphate (ThMP), which in turn can be hydrolyzed to thiamine by a thiamine monophosphatase. Neither of these enzymes has been characterized to date.
- phosphorylated in the mitochondria by the F₀F₁-ATP synthase (EC 3.6.3.14) to form ThTP (Gangolf *et al.*, 2010). ThTP in turn can be hydrolyzed to ThDP by the 25-kDa ThTPase (EC 3.6.1.28) in the cytoplasm.
- converted to AThDP or AThTP by a ThDP-adenyl transferase (EC 2.7.7.65), depending whether the other substrate is ADP or ATP. They can be turned back into ThDP and AMP by unknown hydrolases.

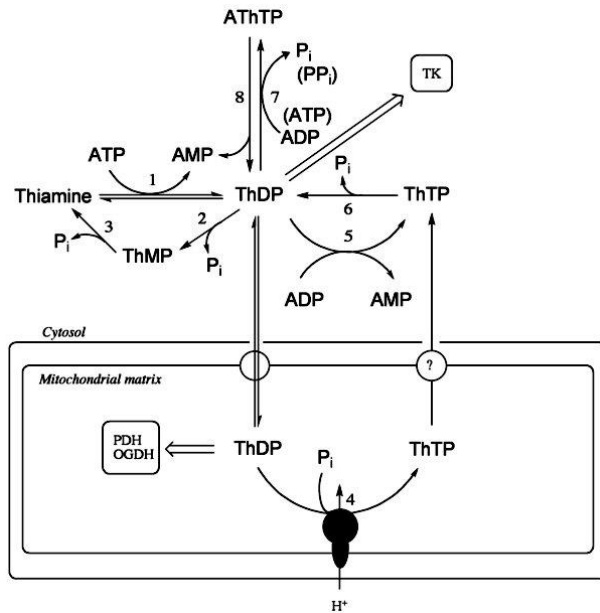


Figure 2: Thiamine and its derivatives in eukaryotic cells. Thiamine diphosphate (ThDP) is formed by pyrophosphorylation of thiamine. ThDP can bind to cytosolic transketolase or be transported (in eukaryotic cells) into mitochondria, where it can bind to pyruvate dehydrogenase complex (PDH) or oxoglutarate dehydrogenase complex (OGDH). Free ThDP is the precursor for the synthesis of thiamine monophosphate (ThMP), thiamine triphosphate (ThTP) and adenosine thiamine triphosphate (AThTP). Hydrolysis of ThDP yields ThMP, which can in turn be hydrolyzed to thiamine. ThTP can be formed in the cytosol by adenylate kinase and in mitochondria by a chemiosmotic mechanism, probably involving F_0F_1 -ATP synthase. AThTP formation is catalyzed by a cytosolic adenyllyl thiamine diphosphate transferase, either from ATP or from ADP. Similar reactions are involved in thiamine metabolism in prokaryotes, except that the mitochondrial part takes place in the cytosol.

1, thiamine pyrophosphokinase; 2, thiamine diphosphatase; 3, thiamine monophosphatase; 4, ThTP synthase (could be identical to ATP-synthase); 5, adenylate kinase; 6, 25-kDa thiamine triphosphatase; 7, ThDP adenyllyl transferase (can use both ATP and ADP as substrate); 8, AThTP hydrolase. (from Bettendorff 2012).

Different derivatives:

Thiamine diphosphate:

Thiamine diphosphate is the main active form of the vitamin and accounts for 75-85% of total thiamine content of most cells. After transport into the cells, thiamine is pyrophosphorylated into ThDP according to the reaction: $\text{thiamine} + \text{ATP} \rightleftharpoons \text{ThDP} + \text{AMP}$, further favoring thiamine entry into the cell. The ThDP formed can then be transported into the mitochondria through the SLC25A19 transporter which is an antiporter, probably exchanging cytoplasmic ThDP against mitochondrial nucleotides (Lindhurst *et al.* 2006). In many cells, including neurons, most of the ThDP is bound to apoenzymes. However, in erythrocytes, hepatocytes and skeletal muscle, a larger part of ThDP is cytosolic and free (not bound to apoenzymes). Those tissues may therefore act as storage compartments of the vitamin (in the form of ThDP) when extracellular thiamine concentrations are high.

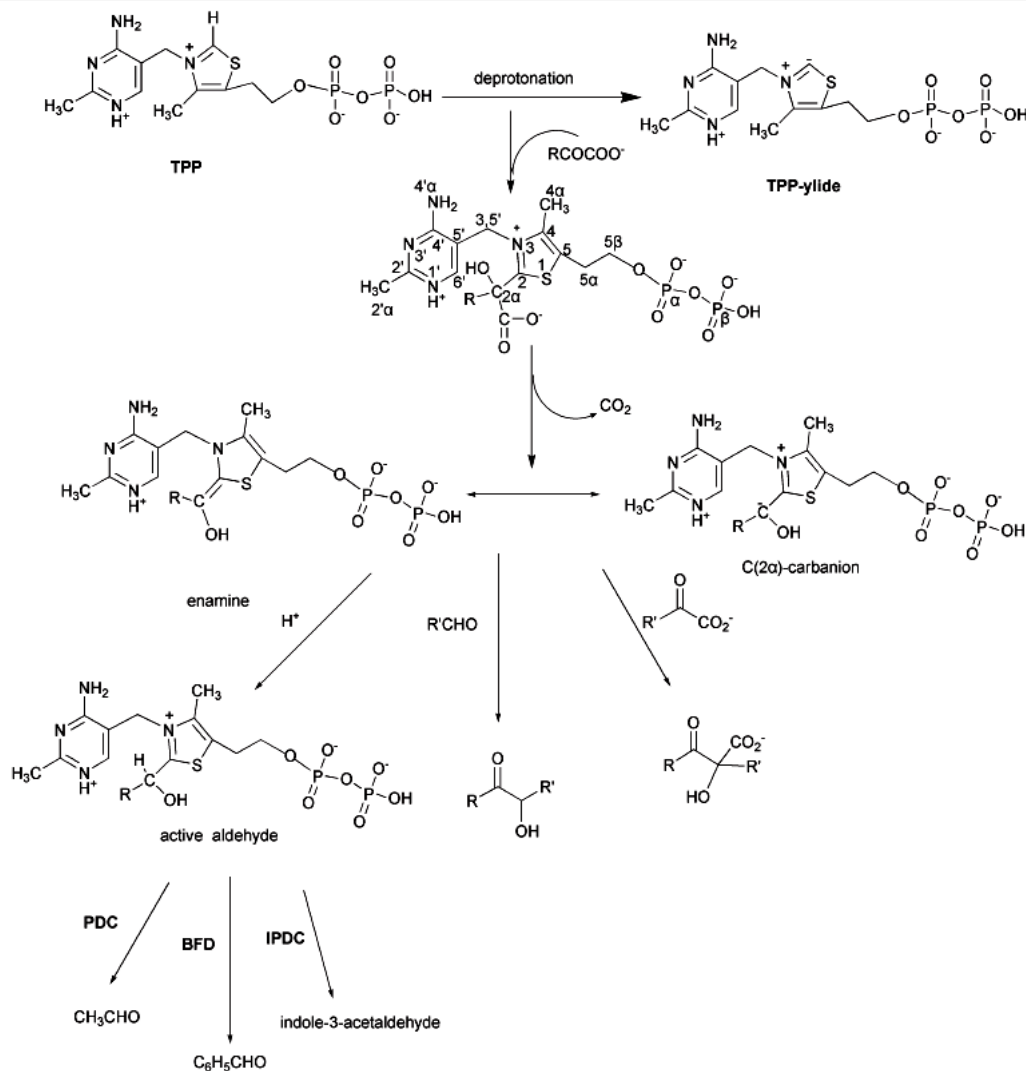


Figure 3: catalytic mechanism of α -ketoacid decarboxylation by the cofactor ThDP. Decarboxylation is initiated by formation of a C(2) carbanion of ThDP, that interacts with the C(2) of the substrate α -ketoacids to form a nucleophilic adduct, followed by CO_2 release and formation of the C(2 α)-carbanion/enamine. Subsequent protonation leads to the 'active aldehyde' intermediate whose metabolism depends on the specific enzyme involved. Finally, decarboxylation with subsequent release of an aldehyde molecule is the main reaction of all α -ketoacid decarboxylases. In the presence of a further aldehyde or α -ketoacid molecule acting as an acceptor, the C(2 α)-carbanion/enamine yields 2-hydroxyketones or hydroxyketoacids.

PDC: pyruvate decarboxylase, part of the ODH complex; BFD benzoylformate decarboxylase; IPDC indolpyruvate decarboxylase (Malandrinos et al. 2006)

ThDP-dependent enzymes are found in almost every major metabolic pathway, they are members of 9 superfamilies of enzymes. An overview of their annotated sequences can be found in the ThDP-dependent Enzyme Engineering Database (TEED, <http://www.teed.biocatnet.de>). Their main role is the decarboxylation of an α -ketoacid to an aldehyde and a CO_2 molecule

(RCOCOOH \rightarrow RCHO + CO₂) (figure 3) whether by oxidative or non-oxidative mechanisms (Malandrinos *et al.* 2006, Hailes *et al.* 2013).

Thiamine monophosphate:

Thiamine monophosphate does not have any known role in eukaryotes but in prokaryotes it is an important intermediate in the synthesis of thiamine and ThDP. In mammalian cells it amounts to 5 to 15% of total thiamine in the cells and it is the only phosphorylated thiamine derivative found in plasma and in the cerebrospinal fluid.

In mammalian cells, ThMP is formed through enzymatic hydrolysis of ThDP but no specific ThDPase has been characterized so far. Some phosphohydrolases have been shown to hydrolyze ThDP but they are not specific for ThDP over nucleoside diphosphates. The same goes for ThMPase, an activity is found in tissues and even used as a marker of small-diameter dorsal root ganglia neurons, but no specific enzyme was characterized so far.

Thiamine triphosphate

Thiamine triphosphate was the first organic triphosphorylated compound other than nucleotides to be discovered (Velluz *et al.* 1948). ThTP is found (generally in low amount) in all mammals tissues but also in all major phyla tested (bacteria, fungi, plants and metazoa) (Makarchikov *et al.* 2003). It generally amounts to less than a few percent of the total cellular thiamine. In neurons, it is mainly found in mitochondria. In some animal tissues (pig and chicken skeletal muscles or *Electrophorus electricus* electric organ) it accumulates in the cytoplasm as a result of the absence of cytosolic thiamine triphosphatase (ThTPase, see below). Under specific conditions (amino-acid starvation) it transiently accumulates in *E. coli* and it can reach up to 50% of the total thiamine content.

In neurons, ThTP synthesis occurs in the mitochondria from ThDP and P_i and is linked to the respiratory chain (Gangolf *et al.* 2010). As in *E. coli* cells, the enzyme responsible for its synthesis seems to be the F₀F₁-ATP synthase (Gigliobianco *et al.* 2013) and the energy is provided by the proton gradient dissipation. In skeletal muscle, where a high adenylate kinase activity is present, ThTP synthesis can also occur in the cytoplasm according to the reaction ThDP + ADP \rightleftharpoons ThTP + AMP. ThTP is hydrolyzed by a specific 25-kDa ThTPase which was characterized at the molecular level (Lakaye *et al.* 2002; Song *et al.* 2008; Delvaux *et al.* 2013). It seems that the ThTP concentration in cells is inversely proportional to the ThTPase activity. For

instance, in mice, it is very low ($< 10^{-7}$) due to the high efficiency of ThTPase while in pig tissues it is relatively high because of the low activity of the enzyme. In humans, where the efficiency of ThTPase is lower than in mice, it is intermediate.

Adenylated thiamine derivatives

Two new thiamine compounds, adenosine thiamine diphosphate (AThDP) and adenosine thiamine triphosphate (AThTP) were recently discovered in our laboratory (Bettendorff *et al.* 2007; Frédéricich *et al.* 2009). AThTP is found in several tissues but it is not as widespread as ThTP. It has been shown *in vitro* to be an inhibitor of PARP-1 (poly(ADP-ribose)transferase-1) thanks to its structural analogy with NAD^+ . PARP-1 is over-activated in stress condition leading to a deleterious decrease of the NAD^+ level in the cells. This suggests a potential interest in the study of AThTP metabolism (Tanaka *et al.* 2011). In *E. coli*, AThTP accumulates during energy stress (Gigliobianco *et al.*, 2010). AThDP was only found in low amount in rodent liver and *E. coli*.

ThTP production in *E. coli*:

In *E. coli*, we could not find any significant amounts of ThTP under normal growth conditions but we know that the metabolic status of the bacteria is a key factor for ThTP accumulation. The biggest production of ThTP was obtained in M9 minimal medium (which does not contain any amino acids) in the presence of some specific carbon sources, mainly the ones that lead to the decarboxylation of pyruvate to acetyl-CoA such as glucose or pyruvate (figure 4). The yield was always better in the presence of oxygen but some carbon sources such as malate, fail to induce any accumulation of ThTP (Lakaye *et al.* 2004c; Gigliobianco *et al.* 2013; Bettendorff *et al.* 2014).

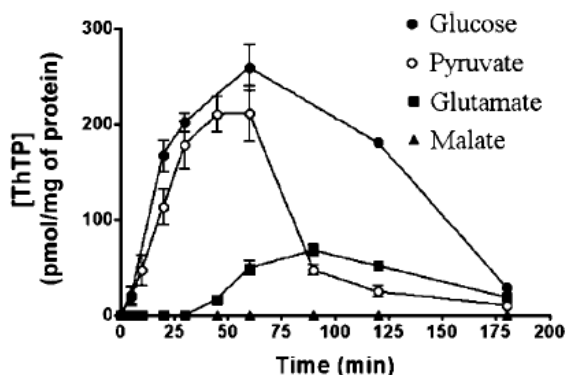


Figure 4: Kinetics of ThTP accumulation by *E. coli* in the presence of various carbon sources (10 mM) in M9 minimum
From Lakaye *et al.* 2004c

ThTP synthesis is specifically catalyzed by the F_0F_1 ATP-synthase thanks to the energy from the proton-motive force of the electrochemical proton gradient generated by the respiratory chain. The synthesis occurs according to the reaction: $\text{ThDP} + \text{P}_i \rightarrow \text{ThTP} + \text{H}_2\text{O}$. It was suggested that during amino-acid starvation and in the presence of an adequate carbon source, an activator, presumably derived from acetyl-CoA, is synthesized and induces a conformational change in the F_0F_1 ATP-synthase which becomes then a ThTP-synthase (Gigliobianco *et al.* 2013; figure 5).

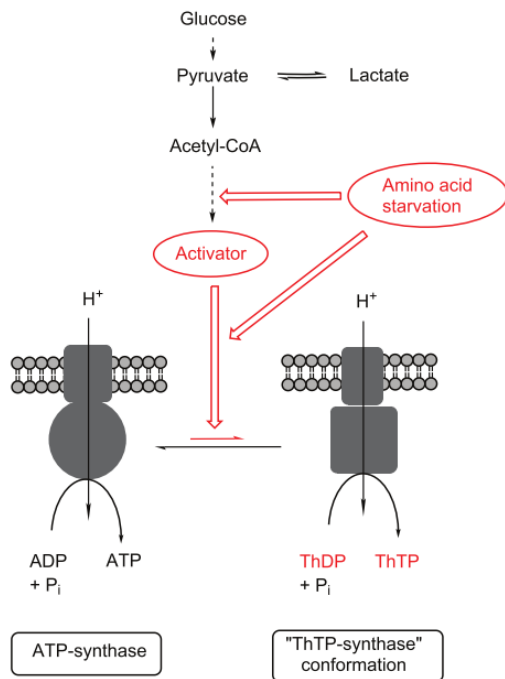


Figure 5: Mechanism and regulation of ThTP synthesis in *E. coli*. Under conditions of amino acid starvation and in the presence of an energy substrate yielding pyruvate, a hypothetical activator would be formed. This would shift F_1 from the normal conformation to a ThTP synthase conformation, binding ThDP rather than ADP. Both ATP and ThTP synthesis are energized by the proton-motive force generated by the respiratory chain. From Gigliobianco *et al.* 2013

Chapter 2: The mammalian 25-kDa ThTPase:

Discovery and characterization

The existence of a soluble thiamine triphosphatase in mammalian tissues was first reported in 1972 (Hashitani and Cooper, 1972). It was mainly localized in the cytoplasm and seems to be ubiquitously present in mammalian tissues. It was first purified to homogeneity from bovine brain in 1992 and shown to migrate as a single 25-kDa band after SDS-PAGE (Makarchikov and Chernikevich, 1992). The remarkable finding was its very high specificity for ThTP as substrate: it had virtually no activity towards ThDP, ThMP and nucleoside tri- and di-phosphates. Its molecular characterization was achieved in 2002 (Lakaye *et al.* 2002). The 219 amino acid sequence revealed that the protein contained a high proportion of charged residues and above all that it had no homology with any other mammalian protein.

Phylogeny

Shortly after the molecular characterization of the mammalian 25-kDa ThTPase (Lakaye *et al.* 2002), bioinformatics studies showed that this enzyme shared a small signature sequence with the adenylyl cyclase 2 from *Aeromonas hydrophila*, CyaB (Iyer and Aravind, 2002) (figure 6). This enzyme has a sequence which is unrelated to the main prokaryote adenylate cyclase family. Iyer and Aravind showed that proteins carrying this signature sequence were present in nearly all organisms in the three kingdoms of life and could be traced to the last common ancestor of all living organisms. They proposed the existence of a new protein superfamily that they named CYTH, according to the names on its two founding members: CyaB – ThTPase (Iyer and Aravind, 2002).

Later, it was shown that most of the CYTH family members are also members of a superfamily carrying the CYTH signature sequence but also sharing a common structural feature at least in the presence of the substrate. Members of this superfamily are indeed characterized by a triphosphate-binding tunnel composed of eight antiparallel β -strand and they all require either Mg^{2+} or Mn^{2+} to be active. Therefore this superfamily, which includes the yeast RNA-triphosphatase Cet1, is the Triphosphate Tunnel Metalloenzyme (TTM) superfamily (Gong *et al.* 2006; Keppetipola *et al.* 2007).

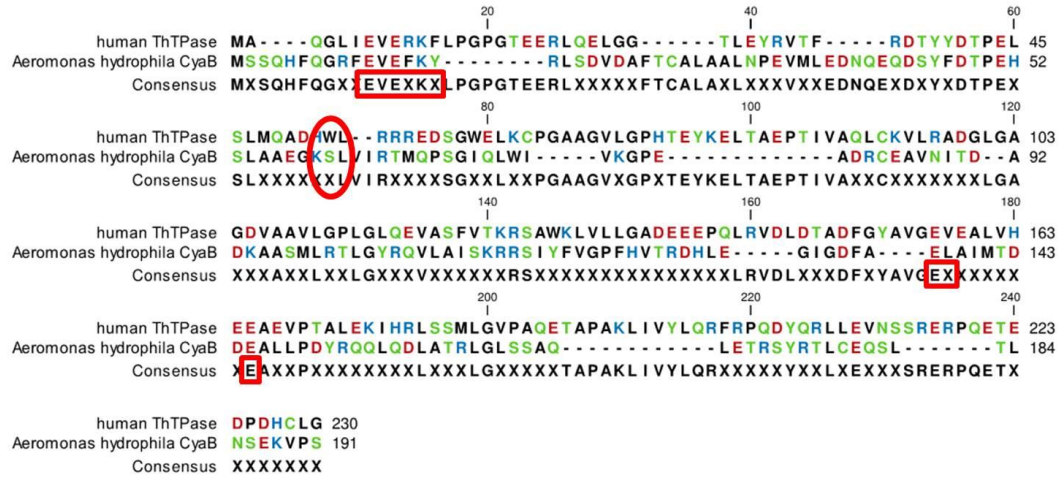


Figure 6: Alignment of the human thiamine triphosphatase amino-acid sequence with the *Aeromonas hydrophila* adenylate cyclase, CyaB. The consensus sequence is also shown. The three red squares show the signature of the CYTH family while the red circle shows the tryptophan 53 on the human ThTPase, the amino that confers the specificity to ThTP and appears later in the evolution. The nonpolar amino acids are in black, the polar and neutral are in green, the acidic are in red and the basic are in blue. The alignment was performed with CLC SEQUENCE VIEWER, Version 7.6 (CLC bio A/S).

While the CYTH gene was initially considered to be ubiquitously present in animals, a notable exception became apparent once several bird genomes became available: indeed, no CYTH gene was found in the genomes of the chicken (*G. gallus*), the diamond mandarin (*T. guttata*) and wild turkey (*Meleagris gallopovo*). Alongside the *thtpa* gene, 30 selected genes of the same region on the human chromosome 14 have disappeared in the bird genome. The lizard Carolina anole (*A. carolinensis*) genome contains 26 of those 30 selected genes on the same chromosome 14 while in zebrafish, the *thtpa* and the two neighboring genes have moved as a cluster to the chromosome 24 and the other selected genes have been scattered on many other chromosomes. The disappearance of the *thtpa* gene seems restricted to a small evolutionary branch leading to dinosaurs and birds (recent data show the presence of CYTH protein in the american alligator : NCBI Reference Sequence: XP_006261269.1) but not to the whole phylum of diapsids (Bettendorff and Wins, 2013; Delvaux *et al.* 2013) (figure 7).

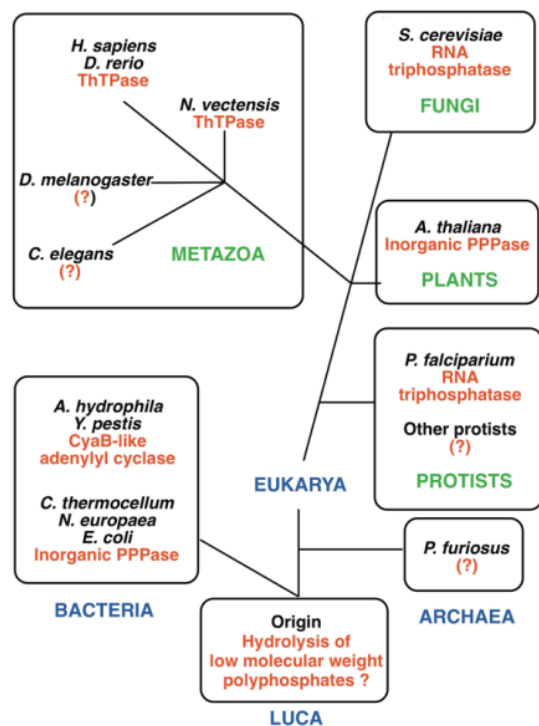


Figure 7: Reconstitution of the phylogenetic tree of the CYTH superfamily. Currently, four different enzyme activities have been identified for members of the CYTH superfamily: tripolyphosphatase (in *C. thermocellum*, *N. europaea*, *E. coli*, and *A. thaliana*), adenylyl cyclase (AC) (in *A. hydrophila* and *Y. pestis*), RNA triphosphatase (in fungi and some protozoans), and ThTPase (in some metazoans, including vertebrates). We hypothesize that the original activity was the hydrolysis of low molecular mass polyphosphates.

From Bettendorff and Wins, 2013

Catalytic properties

There is a high variation in 25-kDa ThTPase activity, depending on the tissues and the species studied (Makarchikov *et al.* 2003). Important differences between different mammalian species were observed concerning the catalytic properties of the purified recombinant enzyme (table 1). However, in all cases, Mg^{2+} was a good activator while Ca^{2+} was inhibitory.

| Animals | K_m (μM) | Catalytic constant (k_{cat} , s^{-1}) | Catalytic efficiency (k_{cat}/K_m , $s^{-1} \cdot M^{-1}$) | Reference |
|--------------|-------------------|---|--|---------------------------------|
| Calf | 39 ± 7 | 240 | $6 \cdot 10^6$ | Lakaye <i>et al.</i> 2002 |
| Human | 154 ± 22 | 140 ± 30 | $9,1 \cdot 10^5$ | Lakaye <i>et al.</i> 2004b |
| Pig (WT) | n.d. | $\sim 2,5$ | n.d. | Szyniarowski <i>et al.</i> 2005 |
| Pig (K85E) | 200 | $\sim 17,5$ | $\sim 87 \cdot 10^3$ | Szyniarowski <i>et al.</i> 2005 |
| Mouse (WT) | 8 ± 2 | 23 ± 3 | $3 \cdot 10^6$ | Delvaux <i>et al.</i> 2013 |
| Mouse (K65A) | 9 ± 2 | $0,019 \pm 0,002$ | $2 \cdot 10^3$ | Delvaux <i>et al.</i> 2013 |
| Mouse (W53A) | 550 ± 90 | $4,4 \pm 0,2$ | $8 \cdot 10^3$ | Delvaux <i>et al.</i> 2013 |

Table 1: catalytic properties of the ThTPase (WT and some mutant) in some mammals

Site-directed mutagenesis, sequence analysis, NMR and crystallography allowed the determination of the amino acids essential for specificity and catalytic activity of the enzyme (Figure 8). Tryptophan 53 is the amino acid responsible for the specificity for ThTP by binding to the thiamine moiety; this explains the high increase in K_m of the W53A mThTPase mutant. It was also shown that the appearance of the W53 in the CYTH sequence is concomitant with the

appearance of ThTPase activity. Lysine 65 and tyrosine 39 are essential for catalytic activity and probably form a catalytic dyad. In particular, the K65A mutation leads to a dramatic decrease in enzyme activity (Table 1), while the tridimensional structure is conserved (Delvaux *et al.* 2013).

In pig, the activity of the enzyme is very low compared to the other mammalian ThTPases tested. There are 16 mutated amino acids compared to the conserved human or mouse sequence, mainly between the 63rd and the 85th amino acid (Szyaniarowski *et al.* 2005). It seems that the most drastic change is that of glutamate 85 to a lysine in the pig enzyme. A higher activity can be restored by replacing the lysine by a glutamate residue in the pig enzyme. The significance of these mutations in pig is not known, but the low ThTPase activity is likely to be the main reason for the high ThTP levels observed in pig tissues (Egi *et al.*, 1986).

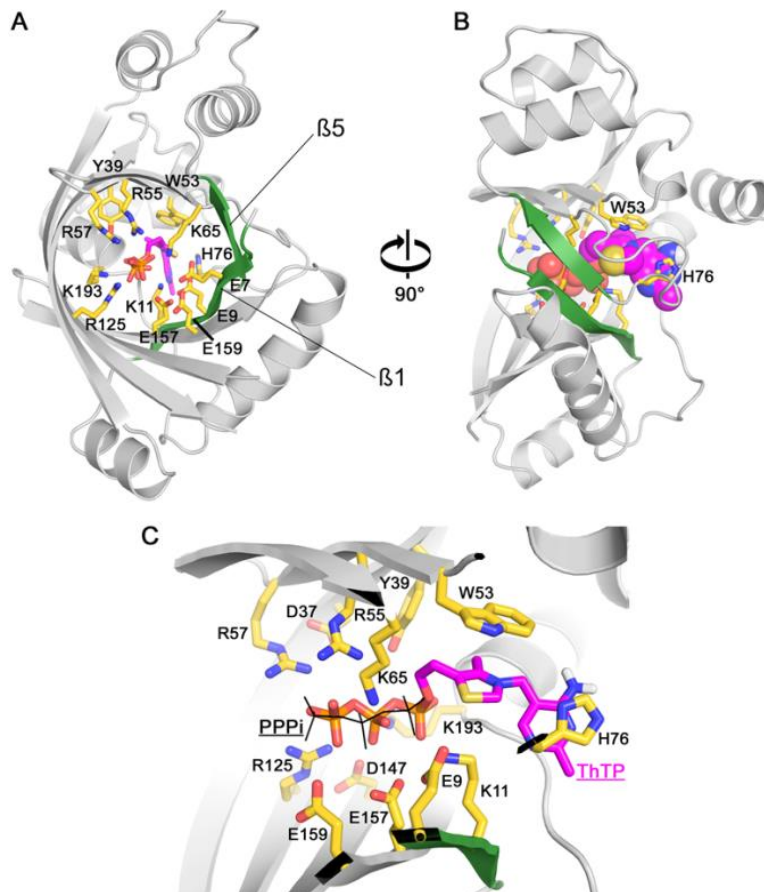


Figure 8: Docking of ThTP in the structure of hThTPase. (A) Representation of the three-dimensional structure of the human ThTPase with ThTP docked in its active site. The two β sheets (residues 5–12 and 78–82) participating in the closing of the tunnel are displayed in green. Important ThTPase residues are shown as yellow sticks and the ThTP molecule as magenta sticks. Antiparallel strands $\beta 1$ and $\beta 5$ are indicated. (B) Same as (A) rotated by 90° with the ThTP molecule shown as spheres. (C) Close up view of the ThTP molecule environment with a PPi molecule from the crystallographic structure superposed and displayed as thin black lines.

From Delvaux *et al.* 2013

Translational control of the expression

In mouse, there is no relation between the specific activity and the mRNA level in the different tissues tested. The activity is highest in liver > kidney > uterus, and rather low in the testis, lung and intestine, while mRNA levels are highest in testis >> lung > skeletal muscle and

lowest in spleen and intestine. In the liver, where the activity is the highest, the mRNA levels are relatively low, a situation opposite to the one found in the testis (figure 9).

To explain those discrepancies, the mRNA was studied in different species (mouse, pig, bovine, macaque, human) and a conserved sequence of more or less 190 nucleotides was found in the 3'UTR (165-180pb after the STOP codon) of the ThTPase (Lakaye *et al.* 2004a). It is possible that this sequence plays a role in the control of translational expression.

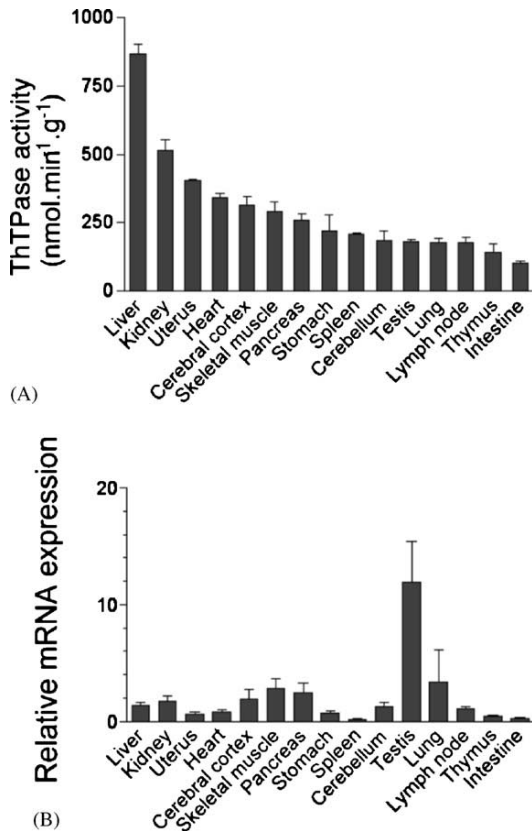


Figure 9: ThTPase activities (A) and mRNA expression (B) in various mouse tissues. ThTPase mRNA expression was determined using quantitative real time PCR and the values were normalized relative to HPRT mRNA. All results are expressed as mean \pm S.D. (n = 3); Kruskal–Wallis test P < 0.0001 From Lakaye *et al.* 2004a

Chapter 3: The inorganic polyphosphates

After oxygen, carbon, hydrogen and nitrogen, phosphorus is the fifth most abundant compound in most life forms. In some animals, calcium is more important in weight but mainly stored in bones. Phosphorus is most often bound to four oxygen atoms under the form of orthophosphate (PO_4^{3-}), either free (P_i) or bound.

Under non aqueous conditions orthophosphoric acid spontaneously polymerize to polyphosphate chains. The shortest polyphosphate is the inorganic diphosphate (pyrophosphate, PP_i), a compound of high physiological significance. In aqueous medium, the phosphoanhydride bond is said to be “energy-rich” because its free enthalpy of hydrolysis is strongly negative; at 37 °C, $\Delta G^0 = -35 \text{ kJ/mol}$. Though thermodynamically unstable in aqueous media, phosphoanhydride bonds are kinetically stable except at extreme pH values. Polyphosphates can be found in living organisms with a length of several hundreds of residues.

Most of the cellular phosphate is attached to organic compounds. The most famous one is probably adenosine triphosphate (ATP) which is the cornerstone compound in the energy metabolism of all organisms. ATP is used as an energy source for many reactions. But phosphate can be found attached to sugar molecules, proteins and lipids and it is part of the backbone of RNA and DNA.

Inorganic pyrophosphate (PP_i) is released in different anabolic processes such as the synthesis of RNA and DNA from ribo- and deoxyribonucleotides ($(\text{NMP})_n + \text{NTP} \rightleftharpoons (\text{NMP})_{n+1} + \text{PP}_i$) or the synthesis of aminoacyl-tRNA (amino acid + tRNA + ATP \rightleftharpoons aminoacyl-tRNA + AMP + PP_i). In each case, PP_i is rapidly hydrolyzed to 2 P_i by an inorganic PPase (EC 3.6.1.1), rendering these reactions globally irreversible. PPases are widely distributed in all organisms and here we show that *E. coli* PPase also has an important PPPase activity.

Polyphosphate chains (polyP) with three or more residue (figure 10) have been found in every cellular type where it was searched (Kornberg *et al.* 1999). They are usually linear chains of inorganic phosphate linked by phosphoanhydride bonds that can reach more than a thousand residues. Since they naturally form, at high temperature, by dehydration from P_i , they were thought to have had a role in the prebiotic world. Until the 90's they were classified as fossil molecules with no known role despite their presence in every organism. Nowadays, there is more and more evidence that they play a role in different metabolic process.

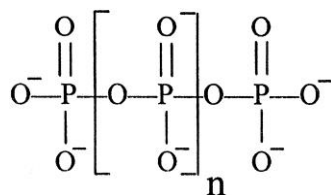


Figure 10: Inorganic polyphosphate. The value for n range from 1 to many hundreds for long chain polyphosphates.
From Kornberg *et al.* 1999.

In eukaryotes, the most studied organism in the polyphosphate field is the *S. cerevisiae* yeast. In this organism the polyP are mainly vacuolar and represent up to 10% of the dry weight of the cell. In rodent polyP is found at concentrations ranging from 25-120 μM (in terms of P_i residues) in many tissues (brain, heart, kidneys, liver, and lungs) and subcellular compartments (nuclei, mitochondria, plasma membranes, and microsomes). Their lengths are usually from 50 to 800 residues but in the brain only the longest are found.

Nomenclature:

| Number of Pi | Full name | | Short name |
|--------------|--------------------------|--------------------|--|
| 3 | Inorganic triphosphate | Tripolyphosphate | PPP _i or PolyP ₃ |
| 4 | Inorganic tetraphosphate | Tetrapolyphosphate | PolyP ₄ |
| 50 | | | PolyP ₅₀ |
| Unknown | Inorganic polyphosphate | Polyphosphate | PolyP |

Table 2: nomenclature of the polyphosphate

Synthesis and degradation:

In *E. coli* there is a specific enzyme responsible for the synthesis of polyphosphate: the polyphosphate kinase (PPK) which was described in the early 90's and catalyzes the reaction: $n\text{ATP} \rightleftharpoons \text{PolyP}_n + n\text{ADP}$ (Akiyama *et al.* 1992; Ahn and Kornberg, 1992). A *ppk* homologous gene was found in different microorganisms but not in all of them, the gene is also absent in yeast and animal genome but polyP are still found in those organisms. PPK can also catalyze the opposite reaction and use polyP to form ATP from ADP.

In eukaryotic cells, the polyP level is highly dynamics and can rapidly change depending on the mitochondrial status. They seem to be constantly synthesized and used and have a rapid turnover. PolyP production is directly linked to mitochondrial respiration and oxidative phosphorylation. The enzyme responsible for their synthesis seems to be the F_0F_1 ATP-synthase and the energy for the reaction is provided by the proton motive force (Pavlov *et al.* 2010).

Two categories of enzyme are directly responsible for their degradation: the exopolyphosphatases which remove the terminal phosphate of the chain and the

endopolyphosphatases which cut inside the chain forming two smaller polyP. The *E. coli* exopolyphosphatase (PPX) is expressed in the same operon then *ppk* but it is not the case in every microorganism with a *ppk* gene. Homologous enzymes with a PPX activity were also found in yeast (Wurst and Kornberg, 1994) and mammals (Tammenkoski *et al.* 2008). The endopolyphosphatases have been mainly characterized in yeast and produce two main kinds of polyP: polyP₆₀ and polyP₃ from longer polyP but an endopolyphosphatase activity was found in calf and rat brain and in most organisms except eubacteria (Kumble and Kornberg, 1996).

Some kinases can use the polyP to phosphorylate their substrate:

- $\text{PolyP}_n + \text{AMP} \rightarrow \text{PolyP}_{n-1} + \text{ADP}$
- $\text{PolyP}_n + \text{ADP} \rightarrow \text{PolyP}_{n-1} + \text{ATP}$
- $\text{PolyP}_n + \text{D-glucose} \rightarrow \text{PolyP}_{n-1} + \text{D-glucose-6-phosphate}$ (Pepin and Wood, 1986)
- $\text{PolyP}_n + \text{NAD} \rightarrow \text{PolyP}_{n-1} + \text{NADP}$ (Kulaev *et al.* 2004)

Function:

Energy and P_i storage:

The energy stored in the bond between the P_i residues can be used to catalyze the transfer of the phosphate to others molecules as shown earlier. PolyP is also a way for the cells to store P_i which is a lot more advantageous on the osmotic point of view compared to free P_i. And that phosphate pool is readily available thanks to exopolyphosphatases (Akiyama *et al.* 1993).

Regulatory role in mammals

In mammals, the dependence to the environment is lower than in prokaryotes. Thus, the phosphate storage role of the polyP is reduced but they still have a regulatory role (Kulaev *et al.* 1999). Among other roles, they are involved in blood coagulation (Smith and Morrissey, 2008), they can form transmembrane voltage gated channels in association with poly-3-hydroxybutyrate and calcium (Pavlov *et al.* 2005) and in mitochondria, they are involved in the maintenance of membrane potential, NADH levels and calcium storage (Abramov *et al.* 2007).

Growth and mortality:

The zebrafish grow quickly during the first three months after hatching and then slowly till their 18th month of life. They generally grow faster in an aquarium (laboratory or private aquarium) than in the wild and females always tend to be larger than males. The domesticated zebrafish have a mean lifespan of 42 months with the oldest individual reaching 66 month while in the wild they rarely reach more than 24 months (Spence *et al.* 2008).

Reproduction:

The reproductive maturity in zebrafish is size-related and starts when they reach a standard length of 24,9 mm for the female and 23,1 mm for the male. A pair of zebrafish left together will spawn frequently but irregularly. A single female can produce batches of eggs of several hundred per spawning (up to 700). The batch size increases with the female size and the inter-spawning interval.

The eggs have a diameter of approximately 0,7 mm, are non-adhesive and sink (figure 13). The hatching takes place 48 to 72h post-fertilization (hpf) (Spence *et al.* 2008).



Figure 13: zebrafish egg, a few minute after spawning

From : http://www.physi.uni-heidelberg.de/~dpietra/leo_css7p1.html

Genetics:

The zebrafish genome is diploid, and organized in 25 chromosomes. It has been almost fully sequenced with a new reference assembly (GRCz10) released on September 2014 (<http://www.ncbi.nlm.nih.gov/projects/genome/assembly/grc/zebrafish/>). The annotation of the genome is still ongoing but on October 2014, 30,741 genes and 63,217 transcripts were already identified. This includes 14,442 genes (14,019 protein-coding) with known RefSeq transcripts, and an additional 16,158 predicted genes (12,459 protein-coding) with model RefSeqs.

The zebrafish as a tool for the scientist

The zebrafish is the most extensively used non-mammalian vertebrate in laboratories throughout the world. It is mainly used in genetics, developmental biology, neurophysiology and biomedicine (Spence *et al.* 2008). There are thousands of laboratories that use zebrafish as a research model worldwide. It has many of the advantages of the fly (*Drosophila melanogaster*)

and of the worm (*Caenorhabditis elegans*) such as a small size, a fast reproduction and the production of a lot of embryos but, as a vertebrate, it is closer to mammals, and especially useful for developmental studies. Its high fecundity has also allowed large-scale screening of drugs, facilitated by the possibility to add the compound to be tested directly to the culture water. The zebrafish development (5 days) is slower than that of the invertebrates mentioned above but still faster than in mice (19 days). Moreover, zebrafish development is external, precluding the study of *in utero* processes, but this has many advantages in terms of manipulation and observation of the embryos. It also allows the study of the same embryo over time. The small transparent embryo of the zebrafish has allowed the scientists to address questions in a whole living organism about the fundamentals of cell metabolism, which before were almost only possible using cultured cells.

Moreover, once the zebrafish model started to be commonly used in the laboratory, forward genetics screens allowed the identification of many genes involved in its development. It has generated a large amount of mutants carrying a specific gene disruption that became available as a tool to study those genes. Surprisingly, the results obtained somewhat disturb the knowledge about certain genes studied in cultured cells and that were thought to be essential and ubiquitous, but whose expression during zebrafish development were spatially and temporally restricted (Vacaru *et al.* 2014).

CYTH in fish

A member of the CYTH-TTM family is present in the genome of every species where it has been searched until now, except for birds. When looking in more detail to the available genomic data about the bony fishes, we could always find a member of that family described as a ThTPase (table 3).

| TaxID | Organism name | GeneID | Description | map_location | Ch |
|--------|---|-----------|-------------|--------------------------------------|------|
| 7955 | Danio rerio (zebrafish) | 100048920 | ThTPase | NC_007135.6 (14451258 14455856 plus) | 24 |
| 8010 | Esox Lucius (northern pike) | 105019498 | ThTPase | NC_025988.1 (8296487 8302233 plus) | LG21 |
| 8208 | Notothenia coriiceps (black rockcod) | 104941948 | ThTPase | | Un |
| 215358 | Larimichthys crocea (large yellow croaker) | 104927511 | ThTPase | | Un |
| 8081 | Poecilia reticulata (guppy) | 103482317 | ThTPase | NC_024350.1 (4865958 4868263 plus) | LG20 |
| 244447 | Cynoglossus semilaevis (tongue sole) | 103376930 | ThTPase | NC_024309.1 (4104666 4107137 minus) | 3 |
| 144197 | Stegastes partitus (bicolor damselfish) | 103365356 | ThTPase | NW_007578563.1 (54169 58029 minus) | Un |
| 48698 | Poecilia Formosa (Amazon molly) | 103135322 | ThTPase | NW_006799963.1 (997484 999811 minus) | Un |
| 8030 | Salmo salar (Atlantic salmon) | 100194700 | ThTPase | | Un |
| 8078 | Fundulus heteroclitus (mummichog) | 105918316 | ThTPase | | Un |
| 7950 | Clupea harengus (Atlantic herring) | 105890182 | ThTPase | | Un |
| 106582 | Maylandia zebra (zebra mbuna) | 101465435 | ThTPase | | Un |
| 8090 | Oryzias latipes (Japanese medaka) | 101157256 | ThTPase | NC_019878.1 (10172950 10176117 plus) | 20 |
| 31033 | Takifugu rubripes (torafugu) | 101073828 | ThTPase | NC_018899.1 (471583 473914 minus) | 10 |

Table 3: state of art in July 2015 about the thiamine triphosphatase gene in bony fish in the “gene” pubmed database. TaxID: Identification number of the taxon; GeneID: identification number of the gene; Ch: Chromosome number (Un: undetermined; LG: linkage group associated with the gene)

When the protein sequences are aligned with the consensus sequence obtained from the alignment of typical representatives of the CYTH protein superfamily (Bettendorff and Wins, 2013), we can see that the bony fish proteins are indeed members of this family. Moreover, we could observe that they have a tryptophan homologous to the tryptophan 53 from the human ThTPase, which is thought to be the key amino-acid for the recognition of the thiamine moiety of the ThTP. They also have residues homologous to Tyrosine 39 and lysine 65, which are the catalytic dyad in the mammalian ThTPase (figure 14).

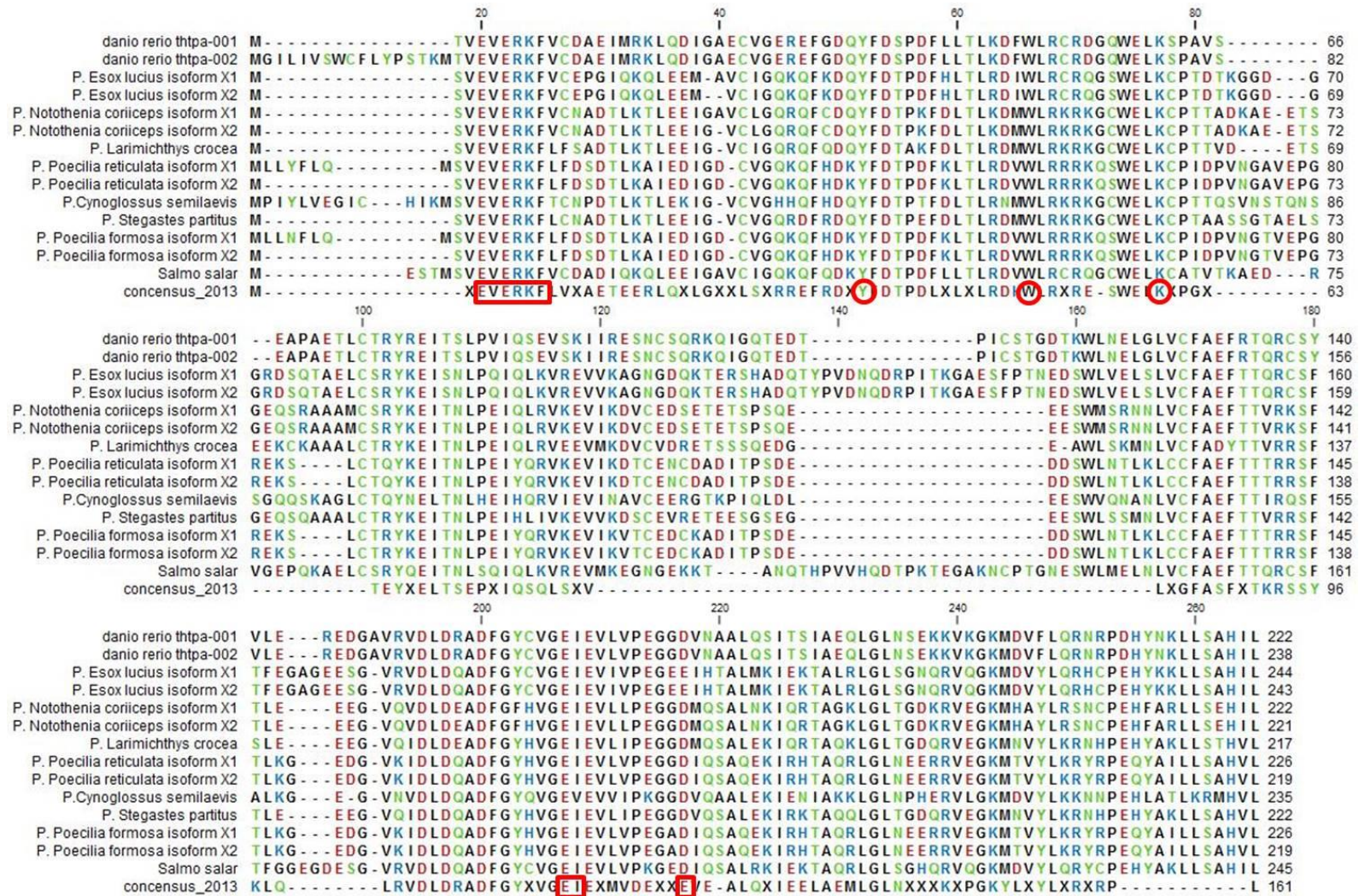


Figure 14: Alignment of the CYTH protein sequences available in bony fishes and of the consensus sequence for CYTH protein (Bettendorff and Wins, 2013). The P. before most of the fish sequences means that those sequences are “Predicted” sequence. The three red squares show the signature of a member of the CYTH family while the red circle shows the amino acid homologous to the human tyrosine 39, tryptophan 53 and lysine 65. The nonpolar amino acids are in black, the polar and neutral are in green, the acidic are in red and the basic are in blue. The alignment was performed with CLC SEQUENCE VIEWER, Version 7.6 (CLC bio A/S).

Morpholino:

The anti-sense morpholino oligomers that are currently used in zebrafish experiments are based on the morpholino phosphorodiamidate derivatives (figure 15). They were first developed as suitable for in vivo use in 1996 (Hudziak *et al.* 1996; Taylor *et al.* 1996; Summerton and Weller, 1997). They are chemically modified oligonucleotides that use a base stacking similar to natural RNA: they have a morpholine moiety instead of the ribose, and the phosphorodiamidate linkage results in a neutral charge instead of the negative phosphate link. This modified oligomer is highly soluble and can hybridize with a high affinity to the single stranded nucleic acid sequences (Ekker, 2000).

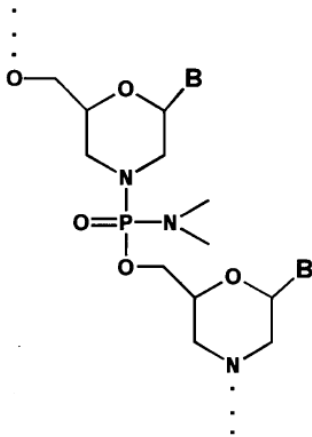


Figure 15: Model of morpholino oligomers. They are composed of a chain of morpholino rings bearing a nucleotide on the C2 with a dimethylaminophosphoryl intersubunit linkage.
From Hudziak *et al.* 1996

B = adenine, cytosine, guanine, uracil

The morpholino oligonucleotides are the anti-sense knockdown strategy most commonly used in zebrafish but this could change in the near future. Indeed, recent studies tend to show that the results obtained by knocking down gene with morpholino are not always reproducible when the target gene is deleted from the genome by knock-out methods (Kok *et al.* 2015), which suggests some nonspecific effect of the morpholino.

Anti-sense knockdown of gene expression:

There are different strategies to interfere with a specific transcript or protein levels in the zebrafish using morpholino. They can act in the cytoplasm but also in the nucleus and can either inhibit the splicing of the pre-mRNA, the initiation of translation or the miRNA signaling.

Splicing inhibition:

The morpholino can interact with the pre-mRNA splicing site and prevent its interaction with the splicing machinery. The misspliced mRNA product will then comprise an insertion of part or the totality of the targeted intron. It can either induce a frameshift or insert a stop codon that will lead to a truncated protein or the insertion will produce an aberrant protein (Schmajuk *et al.* 1999)

The morpholinos inhibiting the splicing site have the characteristics of targeting only the zygotic mRNA but not the maternal one as they were already spliced in the unfertilized egg. The efficiency of the inhibition can be evaluated by amplifying a PCR product with primers directed at the exon sequences flanking the targeted intron (Draper *et al.* 2001). The spliced sequence will be reduced or become undetectable in the morphant compared to the non-injected embryo and a longer misspliced sequence can appear as a PCR product.

Translation initiation site inhibition:

The morpholino is designed to interact with the translation initiation site of the mRNA and prevent its interaction with the translation machinery (Ekker, 2000). Those morpholinos will target maternal and zygotic mRNA, which in turn can affect the very early developmental stages and thus prevent the observation of more specific effects during the organogenesis for example.

miRNA signaling inhibition:

The micro RNAs (miRNAs) are small non-coding RNA molecules found in eukaryotes and in some viruses. To quickly summarize their synthesis, they are first transcribed into pri-microRNA then cleaved into pre-microRNA by the ribonuclease Drosha. They are again cleaved by the endoribonuclease Dicer into microRNA duplexes that can be used by the RISC complex to induce the cleavage, repress the translation or induce the deadenylation of their specific target mRNAs.

The morpholino can block the maturation of miRNAs either at the Drosha or the Dicer cleavage steps or inhibit their interaction with their target RNA (Choi *et al.* 2007; Kloosterman *et al.* 2007). When the morpholinos are used to block microRNAs, they will increase the mRNA stability or translation by preventing the miRNA to down-regulate them (figure 16). One of the advantages of this approach is that many different morpholinos can be used to inhibit the same microRNA and thus increase the specificity of the conclusion drawn from the morphant.

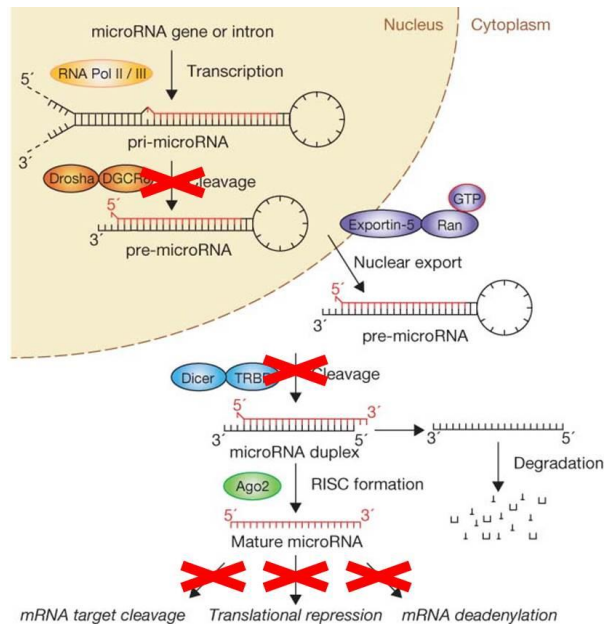


Figure 16: The pathway from the production to the action of the microRNA. The red crosses show the processes that can be blocked by morpholinos. Modified from: Winter *et al.* 2009.

*Aims of
the work*

In this study we will focus our attention on two small compounds with no clearly defined biological roles. These two molecules are the inorganic triphosphate and the thiamine triphosphate. Both are known to be targets of different members of the CYTH superfamily of proteins, some of which are specific inorganic tripolyphosphatase (PPPase) or thiamine triphosphatase (ThTPase).

Inorganic triphosphate (tripolyphosphate, PPP_i) is a short-chain polyphosphate known to accumulate in protozoan acidocalcisomes. It could not be detected in other tissues because of the lack of sensitive methods. However, recently several studies have shown that some enzymes have a highly specific PPPase activity raising the possibility that this compound indeed exists in the cells and may play a metabolic role. We thus decided to study the PPPase activities in mammals and also in *E. coli*.

The second part of this work is focused on thiamine triphosphate (ThTP) with the aim to gain insight into the possible physiological role of this compound. ThTP is synthesized by F_0F_1 -ATP synthase by a chemiosmotic mechanism similar to ATP synthesis. It is therefore impossible to specifically inhibit ThTP synthesis and the only way we have to control intracellular levels is to either increase or decrease its hydrolysis by up and down regulation of the specific ThTPase. We used different organisms (*E. coli*, zebrafish, mice) and strategies (metabolic deregulation, morpholino oligomers and targeted knock-out) in order to study the consequences of increased cellular levels of this compound.

In *E. coli*, ThTP accumulation strongly depends on cultures condition and a transient and important increase of the intracellular ThTP concentration can be induced under amino acid starvation. We studied different mutant strains, commercial or mutated in our lab and the impact of some metabolic inhibitors in order to gain insight into the physiological significance of this compound.

In zebrafish eggs, we used morpholinos directed against ThTPase with the aim of increasing the intracellular concentration of ThTP in order to study its consequences on the development of the fish embryos.

In parallel, we decided to create a mouse knock-out for the gene coding for ThTPase in order to study the effects of this deletion on the phenotype of the animal.

*Material
And
Methods*

Material

Solvents and Reagents

All the solutions were prepared with milli Q water (Millipore S.A. / N.V., Brussels, Belgium).

All the compounds for the bacteria culture medium, the HPLC reagents as well as the D-Glucose were from Merck NV/SA (Oversijse, Belgium).

Antibiotics, isopropyl β -D-1-thiogalactopyranoside (IPTG), Bovine Serum Albumin (BSA), EDTA, sodium triphosphate (PPP_i), proteinase K enzyme, *E. coli* pyrophosphatase, HOCL 30%, thiamine, ThMP and ThDP were from Sigma-Aldrich NV/SA (Bornem, Belgium).

The trichloroacetic acid (TCA) and the Folin-Ciocalteu reagent were from VWR Prolabo (VWR International NV/SA, Louvain, Belgium).

The HPLC solvents and the diethyl-ether were from Biosolve (Valkenswaard, The Netherlands).

The octyl- α -ketoglutarate was from Cayman chemical (Ann Arbor, MI, USA)

The ThTP which is not commercially available was synthesized as described by Bettendorff *et al.* in 2003.

Morpholino solution

Three different morpholinos were ordered from Gene Tools (Gene Tools, LLC 1001 Summerton Way Philomath, OR 97370 USA) and stored as stock solution at -80 °C in the Danieau solution:

- the Gene Tool standard control morpholino: 5' CCTCTTACCTCAGTTACAATTTATA 3'
- the morpholino that inhibit the splicing between the second and third exons of the zThTPase: 5' ATTTAAAACACACCTCCAATATCCT 3'
- the morpholino that inhibits the transcription initiation site of the zThTPase-001 and 003: 5' TCCACTTCTACAGTCATTTTGGAC 3'.

The working solutions that were injected in the eggs were always prepared with a final volume of 10 μ l and stored at -80 °C in between the experiments. They contained the morpholino, 0.5% of rhodamine dextran and eventually the RNA coding the zThTPase or the K61A zThTPase and were bring to 10 μ l with the Danieau solution.

Zebrafish solution

E3 medium

NaCl 5 mM, KCl 0.17 mM, CaCl₂ 0.33 mM, MgSO₄ 0.33 mM, methylene blue 0,05%.

Tricaine (50X)

Final concentration of 4 g per liter of water, bring to pH 9.5 with Tris-HCl 1 M pH 9.5

Danieau

NaCl 58 mM, KCl 0.7 mM, MgSO₄ 0.4 mM, Ca(NO₃)₂ 0.6 mM, HEPES 5 mM, pH 7.6

Bacteria culture medium:

LB medium:

This medium contained 1% (w/v) of peptone from casein, 0.5% (w/v) of yeast extract and 1% (w/v) of NaCl, was autoclaved and stored at 4 °C. For use as an agar plate, we added 1.5% (w/v) of agar prior to the autoclave treatment.

M9 minimal medium:

This medium contained 47.7 mM of Na₂HPO₄, 22.05 mM of KH₂PO₄, 8.55 mM of NaCl and 18.7 mM of NH₄Cl, was autoclaved and stored at 4 °C. Right before use, MgSO₄ and CaCl₂ were add from a 1000x concentrated stock solution (sterilized by filtration); the final concentrations were 1 mM and 0.1 mM respectively.

Strains of *E. coli* used:

Most of the experiments were carried out using the MG1655 strain (WT K12 strain) which was generously offered to us by Dr. M. Cashel (Laboratory of Molecular Genetics, NICHD, National Institute of Health, Bethesda, MD). He also offered us the CF5802 strain lacking the polyP kinase (PPK) and the exopolyphosphatase (Δ ppk-ppx::km) (Kuroda *et al.* 1997)

Different mutant strains from the *E. coli* Genetic Stock Center (Yale University, New Haven CT, USA) were used (table 4).

The NM543 strain was a gift from N. Majdalani NCI, NIH. Two more strains were produced in our lab from that strain: the ThTPase WT I and ThTPase K65A I.

| Name | Mutation | Genotype |
|---------------|----------------------------|--|
| JW3026 | Δ ysiF | F-, Δ (araD-araB)567, Δ lacZ4787(::rrnB-3), l2, Δ ysiF747::kan, rph-1, Δ (rhaD-rhaB)568, hsdR514, CGSC#10312 |
| JW0110 | Δ E1p | F-, Δ (araD-araB)567, Δ aceE732::kan, Δ lacZ4787(::rrnB-3), λ -, rph-1, Δ (rhaD-rhaB)568, hsdR514, CGSC#8392 |
| JW0111 | Δ E2p | F-, Δ (araD-araB)567, Δ aceF733::kan, Δ lacZ4787(::rrnB-3), λ -, rph-1, Δ (rhaD-rhaB)568, hsdR514, CGSC#8393 |
| JW0112 | Δ E3 | F-, Δ (araD-araB)567, Δ lpd-734::kan, Δ lacZ4787(::rrnB-3), λ -, rph-1, Δ (rhaD-rhaB)568, hsdR514, CGSC#8394 |
| JWO715 | Δ E1o | F-, Δ (araD-araB)567, Δ lacZ4787(::rrnB-3), Δ sucA775::kan, λ -, rph-1, Δ (rhaD-rhaB)568, hsdR514, CGSC#8786 |
| JRG465 | Δ E1o iclR const | F-, sucA8, gal-25, λ -, trpA9767, IN(rrnD-rrnE)1, iclR7(Const), trpR47, CGSC#4456 |
| JW0710 | Δ CS | F-, Δ (araD-araB)567, Δ lacZ4787(::rrnB-3), Δ gltA770::kan, λ -, rph-1, Δ (rhaD-rhaB)568, hsdR514, CGSC#8784 |
| JW1268 | Δ acnA | F-, Δ (araD-araB)567, Δ lacZ4787(::rrnB-3), λ -, Δ acnA785::kan, rph-1, Δ (rhaD-rhaB)568, hsdR514, CGSC#9141 |
| JW0114 | Δ acnB | F-, Δ (araD-araB)567, Δ acnB736::kan, Δ lacZ4787(::rrnB-3), λ -, rph-1, Δ (rhaD-rhaB)568, hsdR514, CGSC#8396 |
| NM543 | | MG1655, lacIQ_FLP-scar, mini-lambda::TetR, P-lacO-KanR-sacB. (delta) lacI-lacZ PlacO-kan-sacB |

Table 4: different bacterial strain used, the mutation they carried and their genotypes.

Methods

Determination of the tripolyphosphatase activity

Collection of the sample

All animal experiments were made in accordance with the directives of the Committee for Animal Care and Use of the University of Liège and in accordance with the European Communities Council Directive of November 24, 1986 (86/609/EEC). The protocols were approved by the Committee on the Ethics of Animal Experiments of the University of Liège (# 1253 for mice, # 823 for rats and # 727 for quails). The animals were killed by decapitation and all efforts were made to minimize suffering. Pig brains were obtained from the local slaughterhouse (Abattoirs Publics de Liège & Waremme SC, rue de Droixhe 15, 4020 Liège, Belgium) with the permission to be used for experimental purposes at the University of Liège.

The bacteria were cultured overnight in LB medium at 37 °C under constant stirring (250 rpm) and centrifuged for 10 min at 8000 g at 4 °C. The pellets were solubilized in a Tris-HCl buffer (20 mM) pH 7.4.

Measurement of the activity

The standard incubation medium contained 50 mM buffer, 5 mM MgCl₂, 0.5 mM PPPi and 20 µl of the enzyme at the adequate concentration in a total volume of 100 µl. The mixture was incubated at 37 or 50 °C, the reaction was stopped by addition of 1 ml phosphate reagent (Lanzetta *et al.* 1979) and the absorbance (UV-1800 Shimadzu UV spectrophotometer) was read at 635 nm after 30 min and compared with a standard curve (0–0.5 mM K₂HPO₄) to estimate the release of inorganic phosphate. The buffers used for incubation at different pH values were: Na-MOPS (pH 7.0–7.5), Na-HEPES (pH 7.5–8.0), Na-TAPS (pH 8.0–9.0), Na-CHES (pH 9.0–10.0) and Na-CAPS (pH 10.0–10.5).

Pig brain PPPase activity identification

PPPase was purified from about 500 g of pig brain. All the purification steps were carried out at 4 °C. The tissues were homogenized in Tris-HCl buffer (30 mM Tris-HCl, 50 mM, NaCl, 0.1 mM EDTA, 1.5 mM DTT, pH 7.4). The homogenate was centrifuged at 20,000 g for 20 minutes. The supernatant was brought to 80% saturation in ammonium sulfate and kept under constant stirring for 1 h. After centrifugation at 27,000 g for 30 minutes, the pellet was suspended

in buffer A (20 mM Tris- HCl, 1 mM DTT, pH 7.4) and 5 ml aliquots were placed on a Sephadex G 75 column (3 x 50 cm, GE Healthcare Life Sciences) equilibrated with buffer A. The proteins were eluted with the same buffer at a flow rate of 2 ml/min and all the fractions with high PPPase activity were pooled. The pool was loaded on a DEAE-Sephacel anion exchange column (1.4 x 24 cm, GE Healthcare Life Sciences) equilibrated with buffer A. The proteins were eluted with an exponential concave NaCl gradient from 0 to 0.4 M in buffer A. Fractions with highest PPPase activity were pooled and centrifuged in Amicon ultra-15 centrifugal filter (Ultracel-10 membrane) units (Merck Millipore SA/NV, Overijse, Belgium). The retained proteins were dissolved in buffer B containing 20 mM Tris-HCl and 50 mM NaCl. 25 mg of protein were loaded on a Mono Q column (GE Healthcare Life Sciences) coupled to a Fast Protein Liquid Chromatography apparatus (ÄKTApurifier, Amersham) and elution was made with buffer B using a linear NaCl gradient from 50 to 500 mM. The fractions with the highest PPPase activity were pooled and DTT was added to reach a concentration of 1 mM. The proteins were then separated by non-denaturing polyacrylamide gel electrophoresis. The band with PPPase activity was cut and analyzed by liquid chromatography-mass spectrometry as described below for *E. coli* PPPase activity.

***E. coli* PPPase activity identification**

E. coli wild type strain MG1655 was grown overnight in LB medium at 37 °C under agitation (250 rpm). The bacteria were harvested by centrifugation for 10 minutes, at 8000 g at 4 °C. The pellet was suspended in Hepes-buffer (30 mM Hepes, 50 mM NaCl, pH 7.2–7.4) and the cells were lysed by high pressure using a French press. The lysate was centrifuged for 30 minutes at 40,000 g at 18 °C. The supernatant (called S1) was brought to 50% saturation with ammonium sulfate and kept under constant stirring for one hour at room temperature. After centrifugation for 30 minutes at 20,000 g at 18 °C, the supernatant (called S50) was brought to 80% saturation with ammonium sulfate and kept under constant stirring for one hour at room temperature. After centrifugation 30 minutes at 20,000 g at 18 °C, the pellet was suspended in Hepes-buffer. The preparation obtained (called P80) was loaded on a mono Q column coupled to a Fast Protein Liquid Chromatography (FPLC) apparatus and elution was carried out with a linear NaCl gradient from 50 to 500 mM. The fractions with the highest PPPase activity were pooled (called F1) and placed on a Sephadex G200 column (1 x 25 cm) equilibrated with Hepes buffer. Elution was performed in the same buffer. The fractions with the highest PPPase activity were pooled

(called F2) and used to perform a non-denaturing polyacrylamide gel separation and the PPPase activity was determined as described below. The bands containing PPPase activity were cut and analyzed by liquid chromatography coupled on-line to positive mode electrospray ionization tandem mass spectrometry (UltiMate 3000 Nano LC Systems, Dionex, AmaZone, Bruker) for protein identification.

In-gel enzymatic activity

Non-denaturing polyacrylamide gels (10%) were run in Tris-Glycine buffer (25 mM Tris, 190 mM glycine). After incubation for 30 minutes in a bath containing PPPi (0.5 mM), buffer (20 mM), and MgCl₂ (1 mM), the gel was colored with phosphate precipitation reagent (1% v/v ammonium heptamolybdate, 1% v/v triethylamine, 1 N HNO₃) (Simonović *et al.* 2004). For *E. coli* PPPase, the incubation temperature was 50 °C and the buffer was Na-CHES (pH 9.5) while for pig brain PPPase incubation temperature was 37 °C and the buffer was Na-MOPS (pH 7.1).

Detection of thiamine and its derivatives in *E. coli*

After incubation of the bacteria in M9 minimal medium, 1 ml of the culture was centrifuged for 1 min at max speed on a tabletop centrifuge and the pellet was dissolved in 500 µl of TCA 12% in order to denature and precipitate the proteins. It was then centrifuged for 10 min at 10,000 g at 4 °C. The supernatant was extracted 3 times with 2.5 ml of diethyl-ether to remove the TCA and then analyzed by High Performance Liquid Chromatography (HPLC). The pellet was dissolved in 500 µl of NaOH 0.8 N for the determination of protein concentrations.

The detection of thiamine and its derivative is based on their oxidation into their fluorescent thiochrome derivatives by the potassium ferricyanide (K₃[Fe(Cn)₆]) in alkaline solution prior to their injection on the HPLC column (figure 17). The oxidant solution is composed of 500 µl of a 1% (m/v) solution of potassium ferricyanide and 2.5 ml of NaOH 15% (m/v). 40 µl of the sample are mix with 25 µl of this oxidative solution prior to the injection in the 20 µl injection loop of the HPLC.

Sample thiamine concentrations were calculated from peak areas by comparison with the peak areas of an external standard solution containing known concentration of 250 µM of thiamine, ThMP, ThDP and ThTP. The external standard solution was injected prior to each batch of sample.

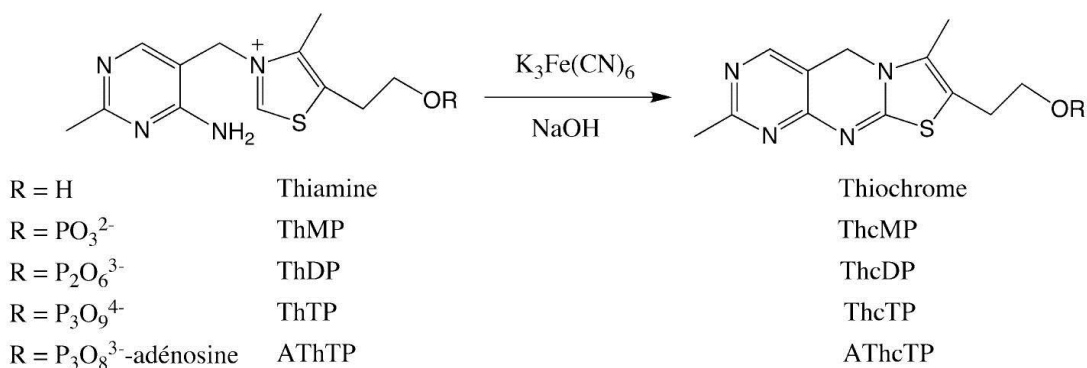


Figure 17 : Oxidation of thiamine and its derivative by potassium ferricyanide ($K_3[Fe(Cn)_6]$) in alkaline solution.

The separation of the derivatives is based on a ion-pair reversed-phase chromatography principle using a alkaline resistant PRP-1 column. This column (150 x 4,1 mm Ø, 5 µm, Hamilton, Reno, USA) is composed of poly(styrene-divinylbenzene) and protected by a pre-column (25 x 2.3 mm Ø) of the same composition. The mobile phase (flow = 0.5 ml/min) is a solution with a pH of 9.5, containing 50 mM of Na₂HPO₄, 25 mM of tetrabutylammonium and 4% of tetrahydrofuran. The column is linked to a fluorescence spectrometer (KONTRON, SFM 25) with excitatory wavelength set at 365 nm and emission wavelength at 433 nm.

Determination of acetyl-CoA levels

The method was adapted from King et al. (King et al. 1988), using a BioSil C18HL reversed phase column (Bio-Rad). The mobile phase was composed of NaH₂PO₄ (0.25 M) containing 5% acetonitrile. The flow-rate was 1 ml/min and 20 µl samples were injected. Acetyl-Coa was detected at 254 nm. The samples were prepared in trichloroacetic acid extracts as for the determination of thiamine derivatives.

Polymerase chain reaction

Every PCR reactions were carried out using the Taq polymerase and dNTP from Promega. All primers were ordered from Integrated DNA Technologies (IDT). The classical protocol was: first, 2 min at 95 °C, then 35 cycles of 30 s at 95 °C, 30 s at the annealing temperature, and an elongation step at 72 °C (time depending on the length of the target sequence) and finally 15 min at 72 °C. The annealing temperature and the elongation time were specific for each set of primers and depend on the length of the target to amplify. All the primers' annealing temperatures and elongations times are listed in table 5.

| Purpose | Forward (5'→3') and reverse primers (5'→3') | Annealing temperature (°C) | Elongation time (s) |
|--|---|-------------------------------|------------------------|
| Amplification of the mouse ThTPase coding sequence (WT or K65A) for insertion in the <i>E. coli</i> genome | For: GTGAGCGGATAACATTGACATTGTGAGCGGATAACAAGATA CTGACGTCAAGGAGGAAAAAATGGCCCAGGGCTTGATTGA Rev: CTAGAAAGTATAGGAACTTCGAAGCAGCTCCAGCCTACACT CAGGATGCTGAGTCCCCTG | 54 | 50 |
| Amplification of the chloramphenicol gene for insertion in the <i>E. coli</i> genome | For: AAGCAGCCAGTTCTGGTGAGGCCACAGGGGACTCAGCATCC TGAGTGTAGGCTGGAGCTGCTTG Rev: CACGGTCACACTGCTTCCGGTAGTCAATATCGGCATTTTCTT TTGCGTTTCATATGAATATCCTCCTTAG | 48 | 50 |
| Verification of the insertion of the ThTPase gene in the bacteria | For: AGGTTTCCCGACTGGAAAGC Rev: CAGCCAGTGGTCAGACAGCA | 52 | 30 |
| Verification of the insertion of the chloramphenicol gene in the bacteria | For: TCAACAGGGACACCAGGAT Rev: AGCCTGAATCAGGCATTTGA | 48 | 30 |
| Amplification of a region of the zebrafish thtpa transcripts that is differentially spliced | For: TGCCCTCATTACACTGATTGA Rev: TCTCTGCATCTCAGCCAGAAAT | 53 | 20 |
| Amplification of a sequence common to the 3 zebrafish thtpa transcripts | For: TGCCCTCATTACACTGATTGA Rev: TCTCTGCATCTCAGCCAGAAAT | 53 | 20 |
| Rescue zebrafish: insertion of the zThTPase in the pCS2+8 | For: AGGATCCGCCACCATGACTGTAGAAG Rev: TCTCGAGTCATAAAATATGAGCACTAA | 55 | 50 |
| Directed mutagenesis of the zThTPase to insert the K61A mutation | For: TGGGAGTTGGCAAGCCCTGCAGTTT Rev: TGCAGGGCTTGCCAACTCCCCT | 62 | 480 |
| Mouse genotyping | For 1-NeoFwd: TCATTCTCAGTATTGTTTTGCC For 2-TDF: GGGTAGGCAGGGAACAGAAC Rev-SD: ACGAGCGGAAATCAATGGAG | 58 | 25 |
| qPCR on the mouse sperm genomic DNA: WT ThTPase allele amplification | For: AACAGAACCGAAGCATGTCCGA Rev: TTCTAGCAGGCGCTGATAGTCCA | 54 | 12 |
| qPCR on the mouse sperm genomic DNA: inactivated ThTPase allele amplification | For: TCATTCTCAGTATTGTTTTGCCAAGTT Rev: AAGTGGCTCCGTTGTAAGGGAA | 54 | 12 |

Table 5: List of the primer, their purposes as well as the annealing temperature and amplification time.

Insertion of the mammalian ThTPase coding sequence in the *E.coli* genome

The strain used to insert the mouse thiamine triphosphatase into the *E.coli* genome was the NM543. In those bacteria, the lactose operon was replaced by a sequence containing the pBR-LacO promoter (Lutz and Bujard, 1997), the kanamycine resistance gene *kan*⁺ and the sucrose susceptibility gene *SacB*. The miniphage λ was also inserted in the genome to allow the recombination, under the dependence of a heat-inducible promoter and followed by a tetracycline resistance gene.

The aim was to replace the *kan*⁺ - *SacB* sequence by our sequence of interest. We inserted two different constructions, both containing a Shine-Dalgarno sequence, followed by either the mouse ThTPase or the K65A mouse ThTPase and by the chloramphenicol resistance gene (*Cm*⁺).

Briefly, the general protocol was as follows: the NM543 bacteria which are resistant to kanamycin thanks to the *kan*⁺ gene, to tetracycline thanks to the *tet*⁺ gene of the miniphage λ but sensitive to sucrose because of the *SacB* gene are grown at 30 °C. A heat choc at 42 °C induced the expression of the miniphage λ and thus of the enzymes required for the homologous recombination. They are then electroporated with the construction containing a sequence homologous to the end of the pBR-LacO promoter and to the sequence between *SacB* and *Lac Z*. After electroporation, the miniphage λ enzymes will act at two different places of the bacterial genome, first by removing the miniphage λ but also by inserting our construction at the targeted site. If they are properly recombined, the bacteria should lose their resistance to kanamycin together with their resistance to tetracycline and their sensitivity to sucrose but should have gained chloramphenicol resistance as well as an inducible ThTPase (WT or K65A) (figure 18).

In practice, a NM543 clone, resistant to kanamycin and tetracycline but which does not grow in the presence of sucrose was grown overnight at 30 °C under constant stirring (250 rpm) in LB medium containing kanamycin and tetracycline. The culture was then diluted 100 times in 160 ml of fresh LB medium, divided in four individual cultures and grown at 30 °C under constant stirring (250 rpm) until the optic density reached 0.4 – 0.6. Next, the four cultures were incubated at 42 °C for 15 min then cooled down on ice for 10 min. Each culture was then centrifuged for 15 min at 3750 g at 4 °C. The supernatants were discarded and each pellet was suspended in 40 ml of sterile water and centrifuged again under the same conditions. The

supernatant was removed again and the bacteria were washed two more times as described above. After the last centrifugation each pellet was suspended in 50 µl of sterile water and then pooled. Of the pool, 40 µl were electroporated (200 Ω, 25 µF, 2500 V), then 1 ml of fresh LB medium was added and the bacteria placed at 37 °C for three to four hour. They are then plated on LB agar containing sucrose (20% w/v) and chloramphenicol (30 µg/ml). Some clones were then tested for their sensitivity to kanamycin and tetracycline and those which had lost their resistance to those antibiotics were assessed by PCR for the insertion of our transgene. The clones that pass this test were then stored at -80 °C in LB-glycerol (1 volume of LB for 1 volume of glycerol) until further use.

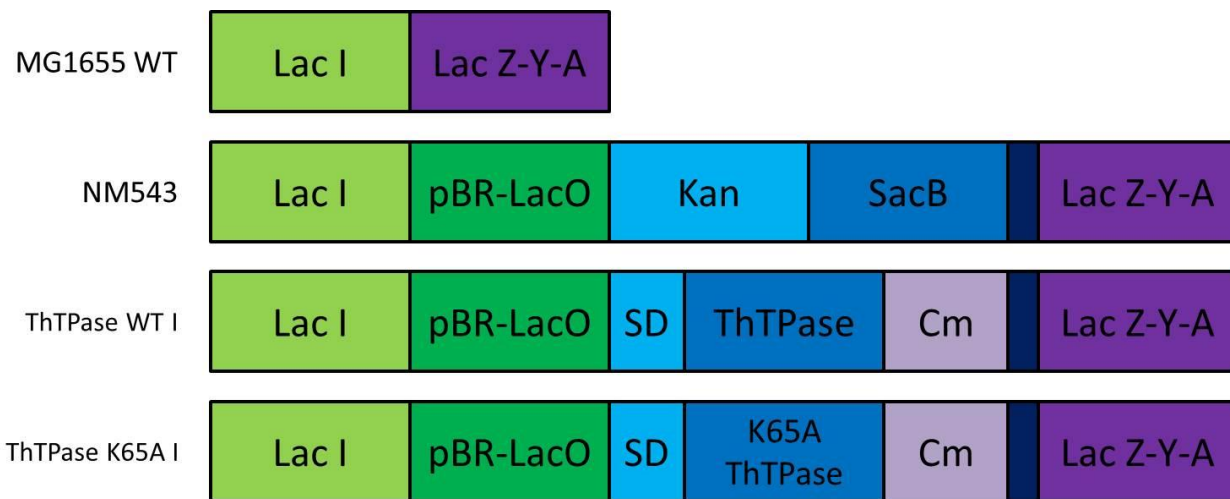


Figure 18: Different lactose operon genes in the different strain: The WT allele in the WT MG1655 strain containing the *Lac I* gene which represses the operon (gene *lac Z*, *lac Y* and *lac A*) in the absence of lactose. In the three next strains, the operon is rendered inactive by the insertion of different genes and in all of them, the pBR-LacO artificial promoter is present right after the *Lac I* gene. In the NM543 gene, the *kan⁺* positive selection gene and the *SacB* negative selection gene were inserted. In the two next strains, those gene were replaced by a Shine-Dalgarno sequence followed by the mouse ThTPase or the K65A mouse ThTPase both followed by the chloramphenicol resistance gene (Cm+).

Zebrafish maintenance

The zebrafish (*Danio rerio*) studied were of the AB strain (ZIRC, Eugene, OR). Those fish were kept in the aquarium at 28 °C as described by Westerfield in 2007. The light/dark cycle was 14/10 h. Animal care and all experimentations were conducted in compliance with Belgian and European laws (Authorization: LA1610002, Ethical commission protocols ULg1076 and ULg624).

Wild-type fish were mated and spawning was stimulated by the onset of light. Then, eggs were collected and placed at 28 °C in Petri dishes containing E3 medium. Embryos and larvae

were staged according to Kimmel et al. (1995). The age of the embryos and larvae is indicated as hours post fertilization (hpf) or days post fertilization (dpf).

Zebrafish breeding and eggs generation

For the production of the eggs, fish were placed in a breeding aquarium as such: 2 male (♂) for 1 female (♀) or 2 ♂ for 2 ♀ or 3 ♂ for 2 ♀ and males separated overnight from the female(s) by a plastic glass. In the morning, the fish were allowed to mate and the eggs were collected in 10 cm Petri dishes containing E3 medium.

Morphant generation, characterization and maintenance

The eggs were manually injected at the one or two cell stage under a binocular microscope (Olympus SZX9) using the Picospritzer II (Parker Hannifin corporation, USA) injector with needles pulled from glass capillary with the PB7 needle/electrode puller (Narishige, Japon). The volume injected per egg was of ~1 nl of the morpholino working solution.

A few hours later, the unfertilized (undeveloped) eggs were removed from the Petri dish and 20 - 24 h after the injection the non-injected or miss-injected embryos were also removed. The correctly injected embryos were counted and categorized 24 h after the injection and the E3 medium was changed for an E3 medium containing 0.2 mM of PTU to prevent the melanization of the embryo. They are counted and categorized again 24 h later.

Zebrafish embryo RNA isolation

Total RNA was isolated with Trizol (Invitrogen, Cergy Pontoise, France) using the RNeasy extraction kit (Qiagen, Venlo, Netherlands) as in Pruvot *et al.* 2014. Briefly, 75 - 100 zebrafish embryos were placed in 600 µl of Trizol and passed 10 times through a G22 needle, followed by 10 passages through a G26 needle with a 1 ml syringe until they were completely dissolved. Then 140 µl of chloroform were added and the samples were vortexed thoroughly for 15 s and incubated under agitation for 2 - 3 min at room temperature (RT). They were centrifuged at 12,000 g for 15 minutes at 4 °C. The upper phase was isolated and 1.5 volumes of ethanol was added and loaded on a column from the Qiagen RNeasy extraction kit. The DNA was removed by application of 80 µl of the RNase-Free DNase Set on the column and incubation for 15 min at RT. The RNA is then isolated following the instruction from the RNeasy extraction kit.

zThTPase mRNA cloning and expression

Zebrafish cDNA was used to amplify the coding sequence of the zThTPase (transcript thtpa-001/3). The forward primer contains a BamHI restriction site, then a Kozak sequence (SJ Grzegorski *et al.* 2014) and the beginning of the coding sequence. The reverse primer adds a XhoI restriction site after the stop codon. This amplicon was inserted into a pGemT vector by TA cloning. Site directed mutagenesis allowed us to change the AAA triplet of lysine 61 into a GCA coding an alanine instead. Both the WT and K61A zThTPase sequences were cloned into BamHI and XhoI sites of the pCS2+8 plasmid. The two plasmids obtained were used to produce *in vitro* the transcripts that will be injected into the zebrafish eggs.

The transcript expression and purification were done using the mMessage mMachine kit from Ambion and the Nucleospin RNA Clean Up kit from Macherey-Nagel after digestion of the two PCS2+8 - zThTPase (WT or K61A) with the NotI restriction enzyme.

Mouse genotyping

Genomic DNA was extracted from tip of the tails, tissues or sperm by overnight incubation at 55 °C in 600 µl of TENS (Tris-HCL 100 mM pH 8,5, EDTA 5 mM, NaCl 200 mM, SDS 0,2% (m/v)) containing 5 µl of proteinase K (20 mg/ml). At the end of the incubation, the samples were centrifuged 10 min at 10,000 g, 500 µl of the supernatant was mixed with 500 µl of isopropanol and centrifuged 15 min at 10,000 g. Supernatants were removed and 600 µl of 70% (v/v) ethanol were added to the pellets before centrifugation (10 min at 10,000 g). The supernatants were removed and the pellets were dried for 5 min at room temperature and then homogenized in 1 ml of TE (Tris-HCl 10 mM pH 8.5, EDTA 1 mM).

The genotype was checked by PCR assay using the primer suggested by the KOMP repository (see table 5) to assess the presence of wild-type and invalidated alleles. Depending on the case, both types of alleles were either detected simultaneously or separately. The amplification was done using an annealing temperature of 58 °C and an elongation time of 25 s for a total of 40 cycles.

Sperm isolation

After the sacrifice of the animals by cervical dislocation, the epididymis and the *ductus deferens* were removed and placed in cold PBS. The sperms were pushed-out of the organs which

are then removed. The PBS containing the sperm was centrifuged for 5 min at 10,000 g in 2 ml microcentrifuge tubes. The supernatant was removed and the pellet used for genotyping.

When the sperm cells were isolated for swim up or swim out experiments, then the epididymis and the *ductus deferens* were placed in pre-warmed (37 °C) DMEM culture medium and the sperms were pushed-out of the organs which were then removed.

Swim up

500 µl of the culture medium containing the sperm are placed in the bottom of a 5 ml sterile culture tube, then 1 ml of fresh pre-warmed (37 °C) culture medium were added without disturbing the medium already in the tube. The tube was then incubated at 37 °C for 30 min in a cell culture incubator (figure 19). At the end of the incubation, 150 µl are removed from the upper part, this fraction was called Swim Up Superior part (SUS) and 150 µl are taken from the lower part, this fraction was called Swim Up Lower part (SUL).

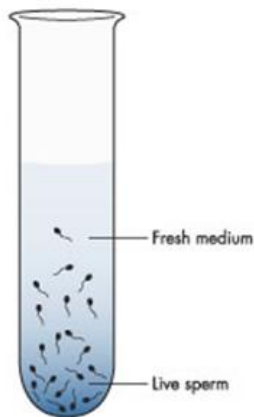


Figure 19: schematic view of the incubation step of the isolation of the mobile sperms through swim-up

Swim out

A 1 ml drop of pre-warmed (37 °C) DMEM culture medium was placed in the center of a 3 cm Ø Petri dish and 5 - 7 droplets of 50 µl of this same medium were placed around it then connected through thin medium bridges to the central drop. Then 500 µl of culture medium containing the sperm were added to the central drop. The Petri dish was then incubated at 37 °C for 30 min in a cell culture incubator (figure 20). At the end of the incubation, the outer droplets were pooled and this fraction was called Swim Out Peripheral part (SOP) and 150 µl were taken from the central drop and this fraction was called Swim Out Central part (SOC).

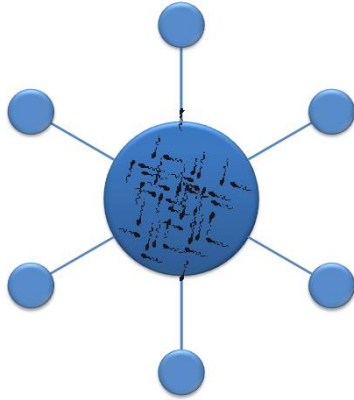


Figure 20: schematic view of the incubation step of the isolation of the mobile sperms through swim-out

Quantitative PCR:

The absolute number of copies per μl of the WT and of the invalidated alleles was measured by performing quantitative PCR (qPCR) on sperm genomic DNA samples. For the establishment of the standard curve, the two allelic sequences amplified during the qPCR were inserted into the pGEM-T plasmid by TA cloning. Plasmids were then purified and their concentration was measured by spectrophotometry. A plot of the absolute number of copies per μl versus the C_t obtained was drawn for each sequences and used to quantify the number of copies of each allele in our samples.

Each sample was analyzed as triplicate. The qPCR mix contained for each of them 10 μl of FastStart Universal SYBR Green Master (Rox) 2x, 0.4 μM of forward primer and 0.4 μM of reverse primer, the DNA sample and water for a total of 20 μl . The qPCR was done in 96 well plates in a LightCycler® 480 Multiwell Plate 96 from Roche.

Results

Chapter 1: Tripolyphosphatase activity

Bacterial CYTH proteins are annotated as predicted adenylate cyclases as one of the founding members of the family is the adenylate cyclase from *Aeromonas hydrophila*, CyaB. In 2011 it was demonstrated in our laboratory that the CYTH enzyme of the bacterium *Nitrosomonas europaea*, NeuTTM, is a specific tripolyphosphatase (Delvaux *et al.* 2011). It was the first time that an enzyme was found to specifically hydrolyze inorganic triphosphate (PPP_i). In 2013, it was shown by Moeder *et al.* that AtTTM3, one of the CYTH enzymes of the plant *Arabidopsis thaliana*, is also a specific inorganic triphosphatase and that this enzyme may be involved in root development.

Tripolyphosphatase activity of mammalian tissues:

The mammalian CYTH ThTPase has been well characterized in our laboratory (Delvaux *et al.* 2013). It hydrolyzes specifically ThTP, with virtually no tripolyphosphatase (PPPase) activity. Nonetheless, supernatant fractions from animal tissues exhibit a high PPPase activity, suggesting that other enzymes (not belonging to the CYTH superfamily) are able to hydrolyze PPP_i.

Characterization

In order to characterize this activity, PPP_i hydrolysis was measured in the supernatant fraction of several quail and rat tissues and also in pig brain (figure 21 A). We found an activity in all tissues tested with the highest activity in the brain. We also tested the dependence of that activity on the pH and on the cation concentration. We found that the activity was not strongly affected by the pH but was optimal around 7 (figure 21 B). On the other hand, the activity was highly dependent on the cation used: Mg²⁺ was a good activator while Mn²⁺ was less effective and no activity was observed in the presence of Ca²⁺ (figure 21 C).

Identification

Since the activity in pig brain was of the same order as in rat or quail brain, we decided for technical and ethical reason to use pig brain from a local slaughterhouse as starting material to identify the enzyme responsible for the PPPase activity in mammalian brain. We used a combination of chromatographic techniques and native polyacrylamide gel electrophoresis, and we carried out the identification by LC ESI/MS/MS. A major protein identified was the pig

homologue of the *Drosophila* protein prune. It was shown that the human ortholog of prune (recombinant protein) is an exopolyphosphatase with higher activity towards short chain polyphosphates such as PPP_i and polyP_4 (Tammenkoski *et al.* 2008). It also hydrolyzes very efficiently adenosine and guanosine tetraphosphates. For PPP_i , the k_{cat} was 13 s^{-1} and the K_m was $2,2 \mu\text{M}$. This suggests that most of the PPPase activity in mammalian tissues is due to prune.

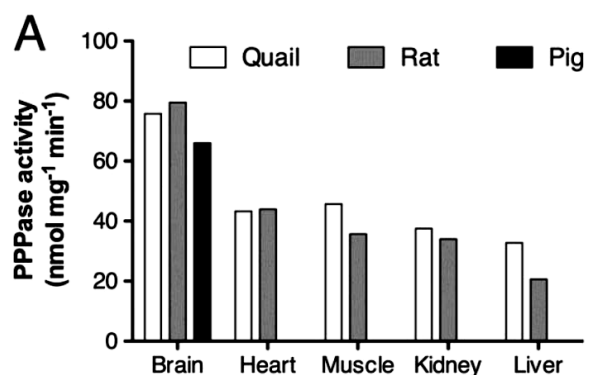


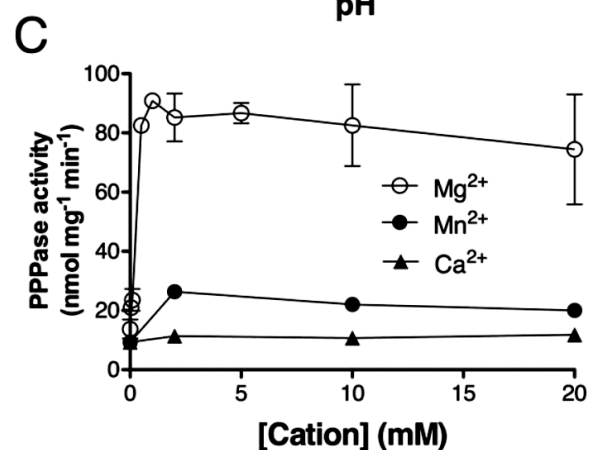
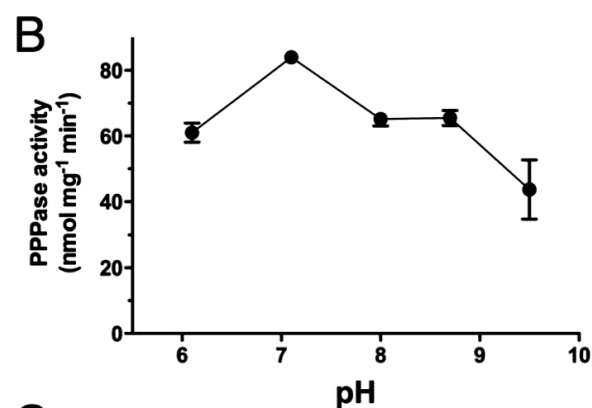
Figure 21: PPPase activities in animal tissue supernatant fractions

(A) PPP_i hydrolysis in various rat and quail tissues, and in pig brain at pH 7.0 in the presence of 5 mM Mg^{2+} ($n = 3-9$).

(B) pH dependence of PPPase hydrolysis in rat brain in the presence of 5 mM Mg^{2+} ($n = 3$).

(C) Activation of PPPase activity by divalent cations. The PPP_i concentration was 0.5 mM and the incubation was carried out at $37 \text{ }^\circ\text{C}$. (Means \pm SD, $n = 3-9$).

From Kohn *et al.* 2012



Mammalian prune proteins (~50 kDa) are orthologs of *Drosophila* prune, which is so-named for the brownish-purple eye color induced by its mutation in the fly. In *Drosophila*, prune has a low phosphodiesterase activity, localizes to the mitochondrial matrix and promotes

mitochondrial DNA replication (Zhang *et al.* 2015). In mammals, the human form (h-prune) also shows low phosphodiesterase activity and its overexpression is associated with cancer progression because it interacts with a known metastasis suppressor (D'Angelo *et al.* 2004). h-Prune belongs to the so-called DHH superfamily (Aravind and Koonin, 1998) and several members of this superfamily are known to exhibit phosphohydrolase activity such as pyrophosphatase in *B. subtilis* (Shintani *et al.* 1998) and exopolyphosphatase in *S. cerevisiae* (Wurst and Kornberg, 1994). This led Tammenkoski *et al.* (2008) to investigate a possible polyphosphatase activity of h-prune. These authors indeed found that h-prune hydrolyzes short-chain PolyP (such as PPP_i , $PolyP_4$ and adenosine tetraphosphate) with high catalytic efficiency. Those polyphosphatase activities were much higher than the previously reported phosphodiesterase activity.

Tripolyphosphatase activity of *E. coli* supernatant fraction:

ygiF is not the main tripolyphosphatase of *E. coli*

Our team noticed that the CYTH enzyme of *E. coli*, *ygiF*, is a specific tripolyphosphatase like its ortholog form *Nitrosomonas europaea*, NeuTTM but with a lower catalytic efficiency. We therefore compared the PPPase activity in the *ygiF* knockout strain JW 3026-2 and in the wild type MG16655 crude extract but no decrease of specific PPPase activity in crude extracts was observed (Figure 22), indicating that the contribution of *ygiF* to PPPase activity is, at best, marginal.

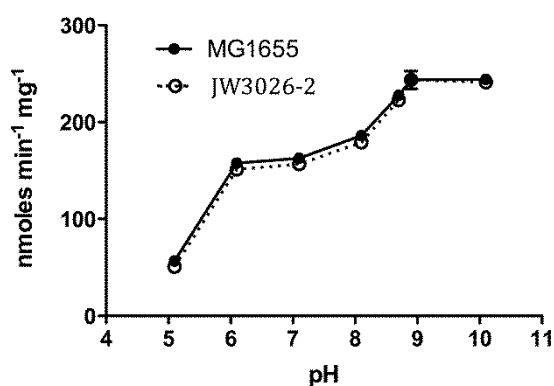


Figure 22: PPPase activity as a function of pH in the supernatants of MG1655 (WT) and JW3026-2 (*YgiF* KO) strains at 37 °C (0.5 mM PPP_i, 5 mM Mg²⁺).

From Kohn *et al.* 2012

Identification of the enzyme responsible for the tripolyphosphatase activity in *E. coli*:

The PPPase activity of a crude extract from wild-type MG1655 *E. coli* (supernatant obtained after sonication and centrifugation at 40,000 g) shows a relatively high Mg²⁺

dependence with an alkaline pH optimum; the specific activity was about $0.2 \mu\text{mol min}^{-1} \text{mg}^{-1}$ at $37 \text{ }^\circ\text{C}$ (with $[\text{PPP}_i] = 1 \text{ mM}$, $[\text{Mg}^{2+}] = 5 \text{ mM}$, pH 9.1). The activity was remarkably heat-stable (up to $80 \text{ }^\circ\text{C}$).

Those properties are reminiscent of *E. coli* inorganic pyrophosphatase (EcPPase) (Josse, 1966; Zyryanov *et al.* 2002). We therefore suspected that PPP_i hydrolysis by *E. coli* extracts might be mainly catalyzed by the PPase, which is abundant in the bacterial cytoplasm (Kukko-Kalske *et al.* 1989).

We partially purified the enzyme responsible for the high PPPase activity in *E. coli* supernatants using various chromatographic techniques (Table 6), followed by native electrophoresis on agarose gels and in-gel activity determination. The band containing the activity was then excised. Analysis by LC-ESI/MS/MS led us to identify inorganic pyrophosphatase (PPase) as a major protein present in the fraction.

| Step | Fraction | Protein (mg) | Activity ($50 \text{ }^\circ\text{C}$) ($\mu\text{mol/min}$) | Specific activity ($\mu\text{mol.mg}^{-1}.\text{min}^{-1}$) | Step purification factor | Total purification factor |
|--------------------------------|----------|--------------|--|---|--------------------------|---------------------------|
| Homogenate supernatant | S1 | 428 | 77 | 0.18 | 1 | 1 |
| Ammonium sulfate precipitation | C80 | 163 | 160 | 0.98 | 5,45 | 5.5 |
| MonoQ | F1 | 4.69 | 24 | 5.1 | 5,17 | 28 |
| Sephadex G200 | F2 | 3.09 | 3 | 7.5 | 1,47 | 41 |

Table 6: Purification of tripolyphosphatase activity from *E. coli* soluble fraction.

Characterization of the tripolyphosphatase activity of the EcPPase

We used a commercially available preparation of purified EcPPase to characterize its PPPase activity (Figure 23). This preparation indeed hydrolyzed PPP_i under the conditions observed above. As expected, it was less efficient for the hydrolysis of PPP_i than for PP_i , considered its natural substrate. With PPP_i , we found a $V_{\text{max}} = 50 \mu\text{mol min}^{-1} \text{mg}^{-1}$ at $25 \text{ }^\circ\text{C}$, about 40% of the V_{max} measured with PP_i under similar conditions ($V_{\text{max}} = 125 \mu\text{mol min}^{-1} \text{mg}^{-1}$). The K_m for PPP_i was $0.91 \pm 0.09 \text{ mM}$, three orders of magnitude higher than for PP_i ($\leq 10^{-6} \text{ M}$) (Avaeva *et al.* 1996).

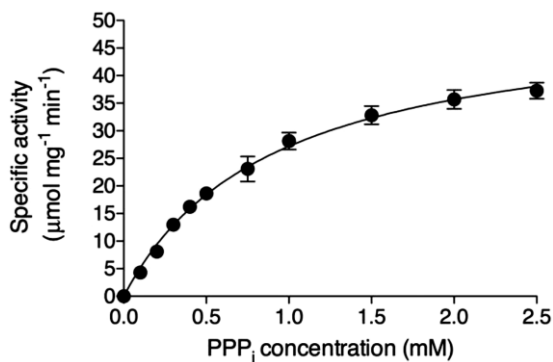


Figure 23: Tripolyphosphatase activity of commercial *E. coli* recombinant pyrophosphatase as a function of PPP_i concentration. The enzyme was incubated in the presence of 10 mM Mg²⁺ in 50 mM CHES buffer at pH 9.1, for 30 min at 25 °C. (Means ± SD, n = 3).

From Kohn *et al.* 2012

Considering a molecular mass of 20 kDa per subunit, we estimated that $k_{\text{cat}} = 16,7 \text{ s}^{-1}$ at 25 °C for PPP_i, compared to 42 s^{-1} for PP_i. Using a different preparation of recombinant *E. coli* pyrophosphatase, Avaeva *et al.* reported, in 1996, a substantially higher value for k_{cat} (389 s^{-1} with PP_i). In any event, due to the very large difference in K_{m} values for PP_i and PPP_i, the catalytic efficiency ($k_{\text{cat}}/K_{\text{m}}$) is much lower for PPP_i ($1,8 \cdot 10^4 \text{ s M}^{-1}$) than for PP_i ($\geq 4,2 \cdot 10^7 \text{ s M}^{-1}$). Considering that the intracellular PP_i concentration is relatively high, except under severe energy stress (Kukko-Kalske *et al.* 1989), it is likely that most of the active sites of pyrophosphatase remain saturated with PP_i and unavailable for PPP_i hydrolysis *in vivo*.

PPase, ygiF or PPX?

It may therefore be argued that, *in vivo*, the pyrophosphatase is ineffective as a PPPase because of its low catalytic efficiency (see above) and ygiF, which is much more specific, might be the main enzyme responsible for PPP_i hydrolysis *in vivo*. However, as already shown, the knockout of ygiF does not affect the tripolyphosphatase activity. The PPase is highly expressed in *E. coli* with nearly 400 copies per cell (Taniguchi *et al.* 2010), whereas only 20 copies of ygiF are expressed per cell. It is therefore not surprising that ygiF does not contribute significantly to PPP_i hydrolysis in a bacterial supernatant fraction. For ygiF to play a significant role in PPP_i hydrolysis, it would require at least a 20-fold upregulation of its expression. Also, in contrast to inorganic pyrophosphatase, ygiF is not an essential protein.

As *E. coli* also contains an exopolyphosphatase which might be responsible for some PPP_i hydrolysis, we used a mutant strain devoid of both polyphosphate kinase and exopolyphosphatase ($\Delta\text{ppk-ppx}::\text{km}$). However, the PPPase activity was the same in this strain and in the wild-type MG1655 strain (Figure 24), suggesting that the exopolyphosphatase does not contribute significantly to PPP_i hydrolysis in an *E. coli* supernatant, in agreement with previous results that showed that PPP_i is not a good substrate for this enzyme (Akiyama *et al.* 1993).

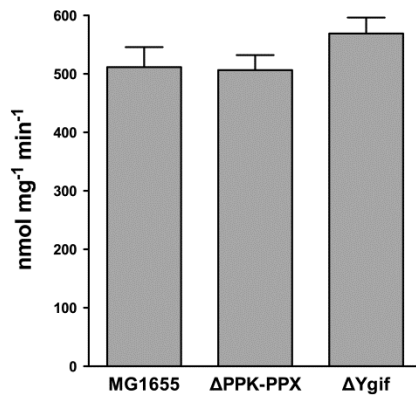


Figure 24: PPPase activity in the supernatants of MG1655 (WT) and Δ PPK-PPX (CF5802) and Δ YgiF (JW3026-2) strains. The supernatants were incubated for 20 min at 50 °C (5 mM PPP_i, 5 mM Mg²⁺ in TAPS buffer at pH 9.5). (Means \pm SD, n=3).

From Kohn *et al.* 2012

PPase and PPPase activities over growth of the bacteria

We also tested whether PPase and PPPase activity changed during growth of *E. coli*, but both PPase and PPPase activities remained relatively constant (Figure 25).

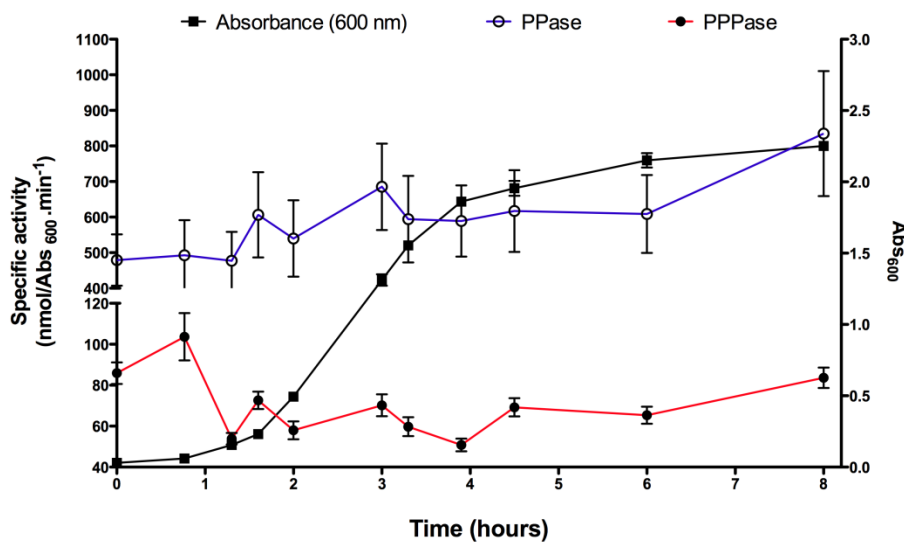


Figure 25: PPase (blue) and PPPase (red) activities as a function of growth in *E. coli*. Growth was measured by following the absorbance at 600 nm (black curve).

From Kohn *et al.* 2012

Conclusions:

In most tissues, phosphate is mainly bound to organic compounds such as nucleotides, metabolic intermediates (such as phosphoenolpyruvate), phospholipids or, in bones, as calcium phosphate salts. In addition to being present in organic molecules, phosphate exists in “free” inorganic form (P_i). Hydrolysis of ATP yields P_i, whose intracellular concentration may exceed 1 mM. P_i is recycled mainly by regeneration of ATP via F₀F₁ ATP-synthase according to the reaction: ADP + P_i \leftrightarrow ATP.

Long chain polyphosphates have been discovered in many organisms (Kumble and Kornberg, 1995; Ault-Riché *et al.* 1998). They are linear chains of up to 1000 P_i residues linked by phosphoanhydride bonds. They may play multiple roles as energy sources, phosphate reservoirs, phosphate donors and chelators of divalent cations. Short-chain polyphosphates are difficult to detect and estimate in tissues, and their possible roles remains unclear. In *E. coli*, polyP is synthesized according to the reaction $(\text{polyP})_n + \text{ATP} \leftrightarrow (\text{polyP})_{n+1} + \text{ADP}$. A recent study suggested that polyP could be synthesized in mammalian cells by a chemiosmotic mechanism requiring F_0F_1 ATP-synthase (Pavlov *et al.* 2010). Polyphosphates may be hydrolyzed by dedicated exopolyphosphatases, but less specific enzymes such as Clostridium thermocellum CYTH protein (Jain and Shuman, 2008) or h-prune (Tammenkoski *et al.* 2008) may also act as exopolyphosphatases.

PPP_i has never been demonstrated to exist in living organisms with the exception of the very specialized protozoan acidocalcisomes (Moreno *et al.* 2000). PPP_i can be generated as the final product of polyPglucose phosphotransferase (EC 2.7.1.63), present in various bacteria (Mycobacterium tuberculosis, Propionobacterium shermanii...). This enzyme uses polyP to form glucose 6-phosphate from glucose ($(\text{polyP})_n + \text{D-glucose} \rightarrow (\text{polyP})_{n-1} + \text{D-glucose 6-phosphate}$; with $n \geq 4$). In animals, an endopolyphosphatase (EC 3.6.1.10) may produce PPP_i (Kornberg *et al.* 1958). PPP_i may also serve as a substrate for the phosphorylation of membrane proteins in rat liver microsomes *in vitro* (Tsutsui, 1986). However this activity is probably not of physiological significance as it is inhibited by micromolar concentrations of ADP and ATP.

The observation that NeuTTM is a highly specific PPPase (Delvaux *et al.* 2011) and that ygiF, which is commonly annotated a predicted adenylate cyclase, is also a relatively specific PPPase raises the question of the existence and possible roles of PPP_i in living cells. This question is even more legitimate as we show for the first time a high PPPase activity in animal tissues, and in particular in brain. This PPPase activity is catalyzed by the homologs of the Drosophila phosphodiesterase prune.

In conclusion, our results demonstrate the occurrence of high PPPase activities in many cells from bacteria to birds and mammals. However, few of these activities come from specific PPPases : the only known specific PPPases are NeuTTM and ygiF. In any event, the physiological importance of PPPase activities remains uncertain.

PPP_i has a very strong chelating power for divalent cations and in particular Ca²⁺, which is the reason why it was extensively used in detergents to control water hardness. The dissociation constant K_d for Ca²⁺ is approximately 10⁻⁷ M (Chang, 1983). This would mean that if it accumulated in cells, it would be expected to interfere with Ca²⁺ signaling. It is therefore possible that the existence of PPPase activities of widely expressed less specific phosphohydrolases is a protective means to prevent accumulation of intracellular PPP_i that may accumulate through the degradation of long chain polyphosphates for instance. From this point of view, specific PPPases such as NeuTTM could thus be considered as metabolite proofreading enzymes, an expression coined by Van Schaftingen and colleagues, by analogy with the proofreading enzymes involved in DNA repair (Linster *et al.* 2011; Marbaix *et al.* 2011), and which protect cells from unwanted toxic metabolic side-products.

On the other hand, it cannot be excluded that PPP_i, which is an energy-rich compound and the simplest triphosphate that can be imagined, may have played a role in energy metabolism in the earliest organisms. Therefore, we recently suggested that PPP_i hydrolysis could be the primitive activity of the CYTH protein family (Delvaux *et al.* 2011). But with the appearance of PPPase side-activity in other abundant phosphohydrolases, CYTH proteins could have evolved towards more complex activities, such as adenylate cyclase in *A. hydrophila* (Sismeiro *et al.* 1998), mRNA-triphosphatase in *S. cerevisiae* and some protozoans (Lima *et al.* 1999; Gong *et al.* 2003; Gong *et al.* 2006) or thiamine triphosphatase in mammals (Lakaye *et al.* 2002; Song *et al.* 2008; figure 7).

Chapter 2: ThTP production in *E. coli*

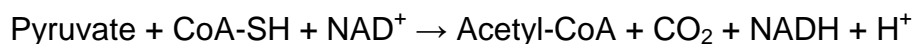
Our interest in the tripolyphosphatase activity was driven, at first, by our interest in the enzymes of the CYTH family of which the mammalian member is the soluble thiamine triphosphatase. Our studies on the latter enzyme were done with the aim of gaining a better insight into the physiological role of the couple ThTP-ThTPase, a topic that started to interest our team in 1987 (Bettendorff and Schoffeniels, 1987).

Thiamine triphosphate is a minor component in most cells (generally 0.1 – 1 % of total thiamine) yet it has been found in most organisms from prokaryotes to mammals (Makarchikov *et al.* 2003). In mammalian cells, the very low ThTP content may be related to the presence of the 25-kDa ThTPase, an enzyme with high catalytic efficiency (Lakaye *et al.* 2002). In other animal species, ThTP can be hydrolyzed by a membrane-bound ThTPase but the specificity of this enzyme is uncertain.

In microorganisms, no ThTPase has been characterized so far and it might therefore be expected that bacterial cells would accumulate relatively high amounts of ThTP. Yet, *E. coli* cells grown aerobically contain no detectable amount of ThTP, but the latter will accumulate transiently (up to 10 - 30% of total thiamine) when the bacteria are transferred to a medium deficient in amino acids (Lakaye *et al.* 2002; Gigliobianco *et al.* 2008). It was therefore suspected that ThTP may act as an intracellular messenger in response to specific condition of nutritional stress (like the alarmone ppGpp). It therefore seemed interesting to study the mechanism of ThTP synthesis and its regulation in *E. coli*. It was found (Gigliobianco *et al.* 2013) that ThTP was produced from ThDP and P_i by a chemiosmotic mechanism: the reaction was catalyzed by F_0F_1 ATP-synthase and energized by respiration. It was hypothesized that, under certain conditions (amino acid starvation and presence of a carbon source yielding pyruvate), the conformation of F_1 was modified so that it catalyzed the $\text{ThDP} + P_i \rightarrow \text{ThTP}$ reaction rather than the usual $\text{ADP} + P_i \rightarrow \text{ATP}$ reaction. However, we cannot exclude the possibility that ThTP may be a “*non-classical metabolite formed by side activities*” of the F_0F_1 ATP-synthase, which accumulates under those specific conditions thanks only to a high ATP-synthase activity and to the absence of an enzyme specifically devoted to the degradation of ThTP (Linster *et al.* 2011).

ThTP synthesis and PDH mutants:

Pyruvate dehydrogenase is an enzymatic complex that catalyzes the oxidative decarboxylation of pyruvate to acetyl-CoA according to the reaction:



This complex is composed of multiple copies of three subunits: the pyruvate dehydrogenase (E1p), dihydrolipoamide acetyltransferase (E2p) and dihydrolipoamide dehydrogenase (E3) (Russell and Guest, 1990).

The reaction catalyzed by the PDH complex seems to be a key point in the control of the ThTP synthesis by *E. coli*. We decided to use three commercially available strains, each with one of the PDH subunits (gene) deleted; JW0110 lacking the E1p gene (Δ E1p), JW0111 lacking the E2p gene (Δ E2p) and JW0112 lacking the E3 gene (Δ E3).

We first checked the acetyl-CoA levels in the different strains cultured in the M9 minimal medium for 1h in presence of 10 mM of glucose. As shown in figure 26, the acetyl-CoA levels of the three strains are in the same range as in the wild type strain MG1655. This suggests that the bacteria produce acetyl-CoA from another source than glucose, either from fatty acid degradation or from direct synthesis from acetate and CoA, a reaction catalyzed by acetyl-CoA synthase.

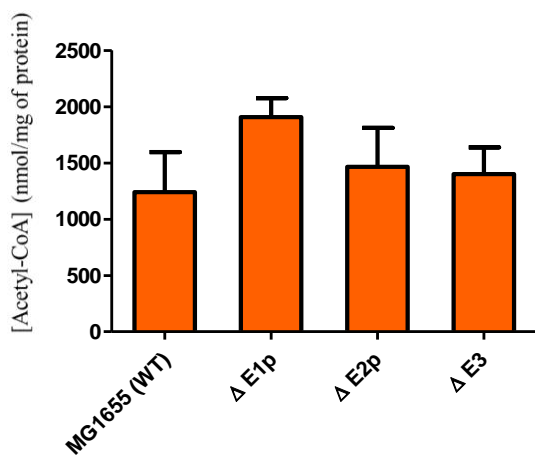


Figure 26: Acetyl-CoA concentration in the WT strain (MG1655) and 3 different strains each mutated for one subunit of the PDH. Estimation were carried out after 1h at 37 °C in M9 medium with 10 mM of glucose.

If we look at the thiamine triphosphate levels as a function of time in those three strains compared to the wild type strain, we observe that in the JW0110 and JW0111 strains (lacking the E1p and E2p gene respectively), ThTP production is slower with a maximum after 2 or 3 hours of incubation. In the JW0112 strain (lacking the E3 gene), no ThTP synthesis was observed during the 4h of the experiment (figure 27).

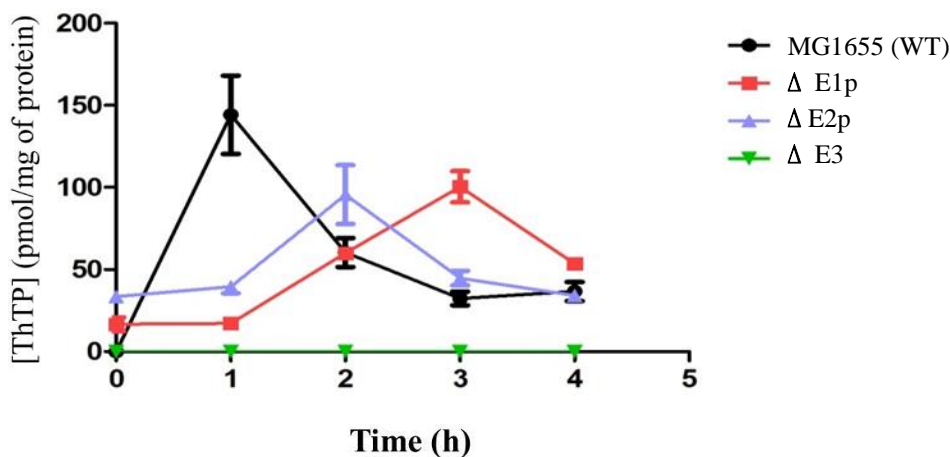
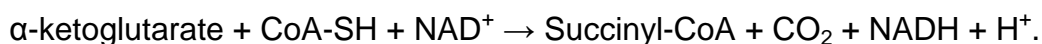


Figure 27: Kinetics of ThTP production in the WT strain (MG1655) and 3 different strains each mutated for one of the subunits of PDH during incubation at 37 °C in M9 medium with 10 mM of glucose. From Pirson, 2011

The absence of ThTP in the JW0112 strain could be due to a general metabolic defect due to the mutation. Indeed, we observed that the growth of that strain was very slow compared to the WT strain. The gene that encodes the E3 subunit of the PDH complex, *lpdA*, also codes for the E3 subunit of the OGDH complex and the L-protein of the glycine cleavage (GC) complex. Moreover, this enzyme is involved in the redox status of the bacteria (Feeney *et al.* 2011). Those multiple defects could provide an explanation for the absence of ThTP. Hence we decided to study strains mutated for the other subunit of the OGDH and GC complexes to assess whether those complexes are involved in ThTP production.

ThTP synthesis and OGDH mutant:

The α -ketoglutarate dehydrogenase is an enzymatic complex that catalyzes the oxidative decarboxylation of α -ketoglutarate to succinyl-CoA according to the reaction:



In *E. coli*, it is composed of multiple copies of three subunits: the α -ketoglutarate dehydrogenase (E1o), the dihydrolipoamide succinyltransferase (E2o) and the dihydrolipoamide dehydrogenase (E3) (Derosier *et al.* 1971).

Since the E3 subunit of the PDH complex is also the E3 subunit of the OGDH complex, we wondered whether the absence of ThTP in the JW0112 mutant was due to the lack of a functional OGDH complex. We decided to study the mutant JW0715 where the E1o subunit gene is deleted (Δ E1o) and studied the time-course of the appearance of ThTP every hour for 4h (figure 28). We could observe that the ThTP synthesis was normal.

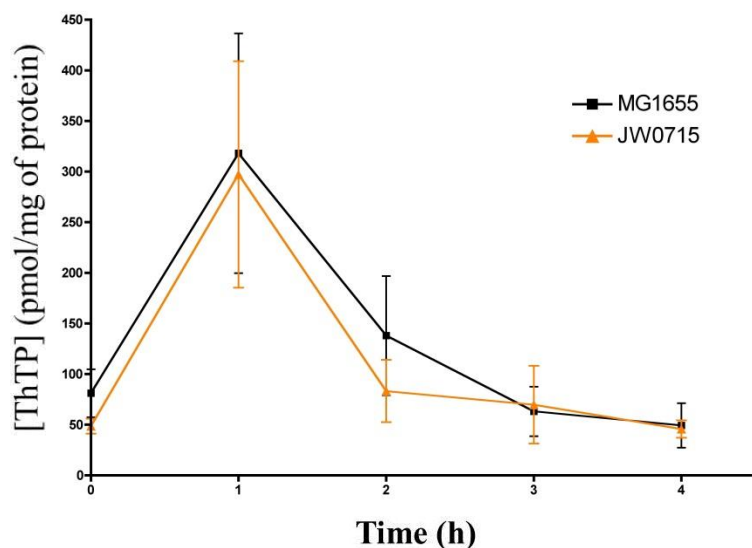


Figure 28: Kinetics of ThTP production in the WT strain (MG1655) and the $\Delta E1o$ strain (JW0715) during incubation at 37 °C in M9 medium with 10 mM of glucose.

From those results, we can conclude that the mutation of E1o gene of the OGDH complex does not affect ThTP production, while the deletion of the E1p and E2p genes of the PDH complex only delays the production of ThTP. The mutation of the subunit specific of the GC complex did not affect the ThTP production either (data not shown). Only the deletion of the *lpdA* gene, which affects all those enzymatic complexes, totally prevents the appearance of ThTP but also strongly impacts on the general metabolism of the bacteria.

There are two points of view to analyze those results, depending whether we consider that ThTP accumulation is due to an activator that changes the conformation of the F_0F_1 ATP-synthase, or that ThTP is a “*non-classical metabolite formed by side activities*” of that same enzyme.

The delay of appearance of ThTP in the mutants E1p and E2p can be due to a delay in the synthesis of the activator or a delay in the activation of the F_0F_1 ATP-synthase due to the lack of PDH activity. When the bacteria are grown in the LB medium, rich in amino acids and in energetic substrates, the metabolism is not much affected by the PDH mutation since the pyruvate can easily be replaced by another source for acetyl-CoA synthesis. When they are placed in minimum medium with glucose as the carbon source, they have to adapt their metabolism. The glutamate necessary for the amino acid production is then derived from the α -ketoglutarate. All those change either delay the production of the activator or delay the production of NADH and $FADH_2$.

ThTP synthesis, OGDH mutant and glyoxylate cycle over-activation:

The Krebs cycle starts with one molecule of oxaloacetate and consumes one molecule of acetyl-CoA. At the end of the cycle, oxaloacetate is restored and two molecules of CO₂ are produced. In bacteria, another metabolic pathway exists, the glyoxylate cycle which also starts with one molecule of oxaloacetate but consumes two molecules of acetyl-CoA. At the end of that cycle, oxaloacetate is restored but instead of releasing two molecules of CO₂ it produces a second oxaloacetate molecule (figure 29). Thanks to that metabolic pathway, the carbon atoms from the acetyl-CoA produced from fatty acid degradation are not lost as CO₂ but instead can be used for neoglucogenesis.

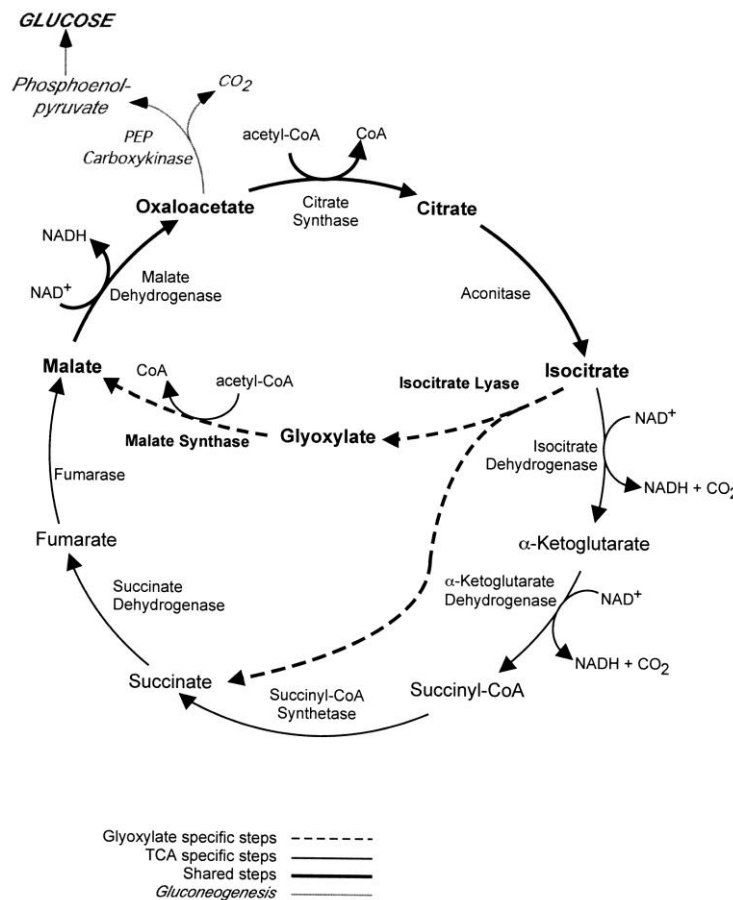


Figure 29: TCA or glyoxylate cycle and gluconeogenesis. The scheme depicts the basic enzymatic steps in the TCA cycle (black lines), which is common to all organisms, those of the glyoxylate cycle (dashed lines), which is specific to microorganisms and plants, and those steps shared by both cycles (bold lines) and the initial reaction of gluconeogenesis (shaded lines). PEP: phosphoenolpyruvate.

From Lorenz and Fink, 2002

We had a mutant strain of *E. coli* with a deletion of the *E1o* gene as in the JW0715 strain but the gene coding for the isocitrate lyase (the enzyme that directs isocitrate from the Krebs cycle to the glyoxylate cycle) was constitutively active ($\Delta E1o$ -*IL*_{const}). That strain, the JRG465, grows at a much slower rate than the WT strain, even in LB (rich) medium, possibly because of the lower levels of NADH produced by the glyoxylate cycle compared to the Krebs cycle.

We compared the kinetics of appearance of ThTP every hour for 4h in the WT strain and in the JRG465 strain. We could observe that only a low amount of ThTP is produced in the mutant, and that there is no ThTP peak (figure 30).

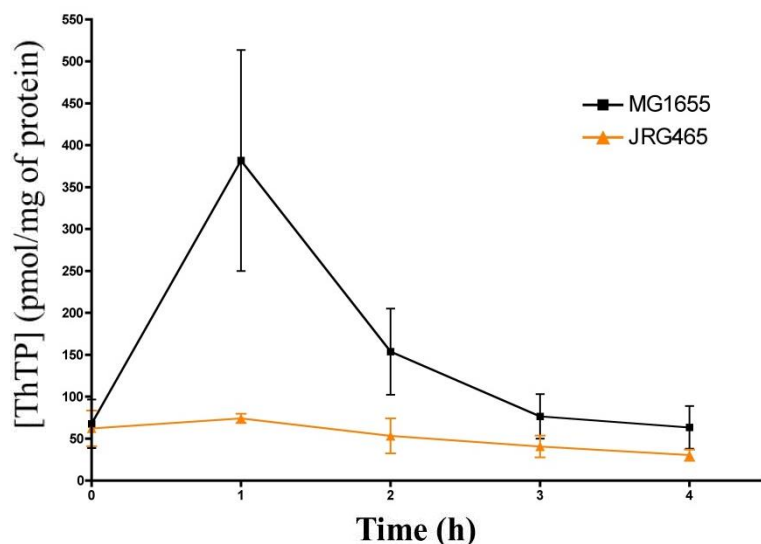


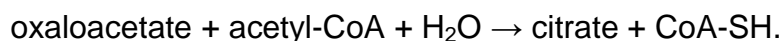
Figure 30: Kinetics of ThTP production in the WT strain (MG1655) and the $\Delta E1o$ -*IL*_{const} strain (JRG465) during incubation at 37 °C in M9 medium with 10 mM of glucose.

Those results suggest that the absence of production of ThTP is due either to the constitutive activation of the glyoxylate cycle which prevents the accumulation of the activator or to the fact that the NADH production is too low to induce a proton-motive force (Δp) required to energize ThTP synthesis.

If the activator is not synthesized in the $\Delta E1o$ -*IL*_{const} mutant strain but reaches normal levels in the *E1o* mutant, it would mean that the activator is either isocitrate or an intermediate of the Krebs cycle upstream of isocitrate or derived from them. Indeed, in the *E1o* mutant, isocitrate can accumulate, while it is consumed by the isocitrate lyase in the JRG465 strain.

ThTP synthesis and the two first enzymatic activities of the Krebs cycle:

In order to investigate the hypothesis of an activator that would involve either citrate or isocitrate, we used 3 different mutant strains: One that was mutated at the level of the citrate synthase gene (Δ CS or JW0710), and two that were mutated for the aconitase A and B gene (Δ AcnA or JW1268 and Δ AcnB or JW0114 respectively). The citrate synthase catalyzes the condensation of the acetyl-CoA with the oxaloacetate into citrate, releasing CoA-SH in the process, according to the reaction:



The aconitase catalyzes the stereo-specific isomerization of citrate into isocitrate according to the reactions:



Three different enzymes are responsible for the total aconitase activity in *E. coli*. Aconitase A is responsible for ~75% of the aconitase activity while aconitase B is responsible of ~20%. In the double knock out (Δ acnAB) *E. coli* strain, there is still 5% of residual aconitase activity but the enzyme responsible is still unidentified (Gruer and Guest, 1994; Blank *et al.* 2002).

Those three mutants had a growth rate similar to the WT strain. If we look at the ThTP levels as a function of time in those strains compared to the wild type when they are grown in a minimal medium with 10 mM of glucose, we observe that the ThTP production is reduced in the citrate synthase and aconitase A mutant (figure 31). The aconitase B mutant strain had a ThTP production that was normal but most of the aconitase activity was conserved, so the metabolism was not much affected (data not show).

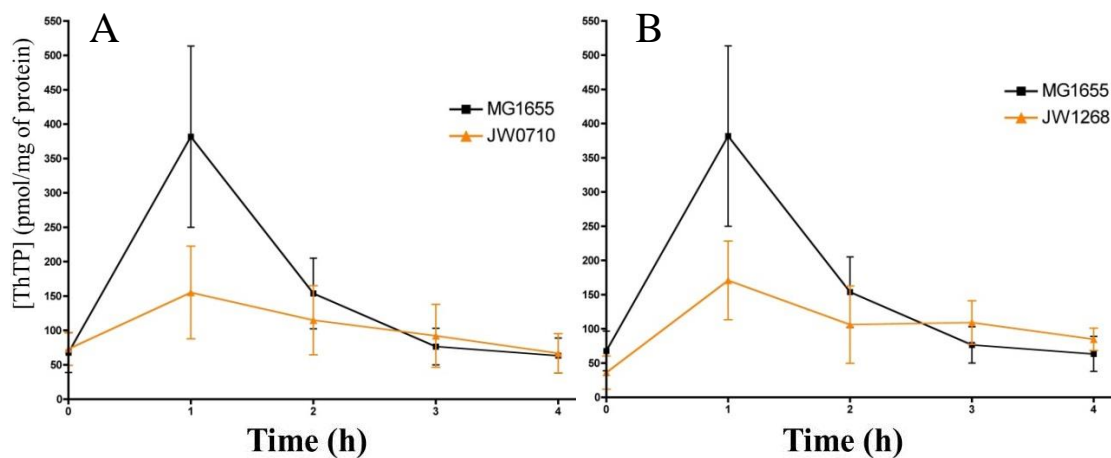


Figure 31: Kinetics of ThTP production in the WT strain (MG1655) and in A: the Δ CS strain (JW0710) or in B: Δ AcnA strain (JW1268) during incubation at 37 °C in M9 medium with 10 mM of glucose.

From those results we can conclude that the production of isocitrate is mandatory for an optimal production of ThTP. Either because the production of the activator needs the accumulation of isocitrate or the impairment of the Krebs cycle in those mutant strains reduces the speed of production of ThTP by the ATP synthase.

ThTP production and inhibition of the F_0F_1 ATP-synthase by octyl- α -ketoglutarate:

Recently, it was shown that intermediates of the Krebs cycle can modulate the F_0F_1 ATP-synthase activity and α -ketoglutarate was shown to inhibit the ATP-synthase but not the respiratory chain (Chin *et al.* 2014). We used the 2-oxo-1-octyl ester pentanedioic acid or octyl- α -ketoglutarate (figure 32), an α -ketoglutarate precursor which can enter the cell by diffusion thanks to its hydrophobic tail. Once in the cells, it is hydrolyzed and α -ketoglutarate is released in the cytoplasm.

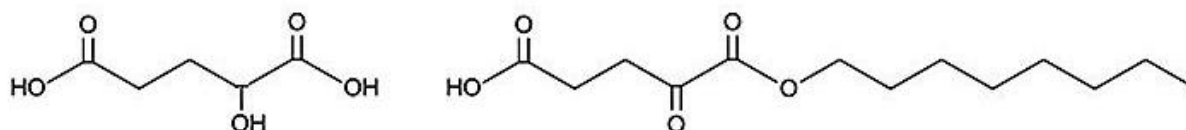


Figure 32: On the left, the α -ketoglutarate and on the right, the octyl- α -ketoglutarate

When we incubated the bacteria in the M9 minimal medium with 10 mM of glucose and increasing concentration of octyl- α -ketoglutarate, we observed a concentration-dependent inhibition of ThTP accumulation after 20 and 60 minutes (figure 33).

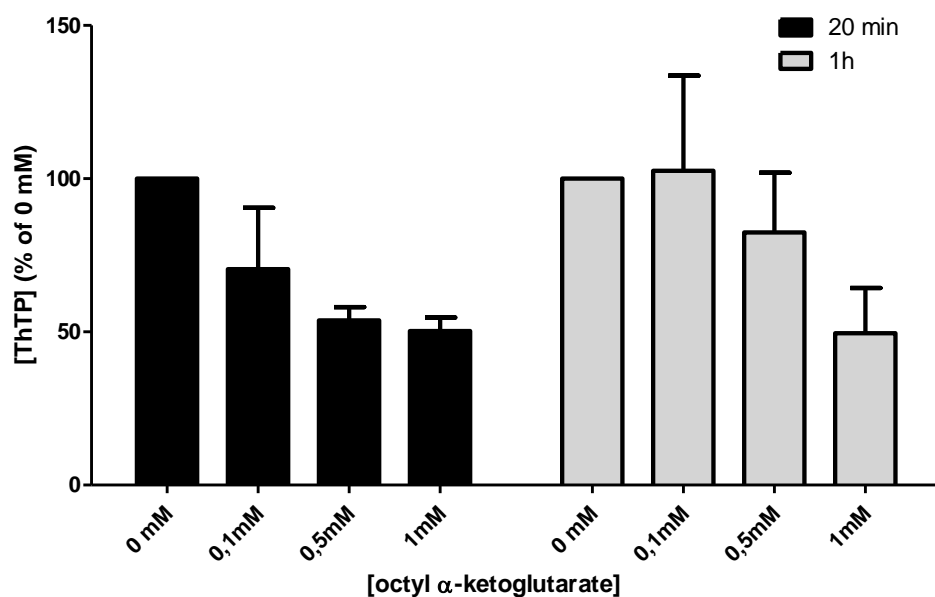


Figure 33: Effect of increasing concentrations of octyl- α -ketoglutarate on the cell ThTP concentration in the WT bacterial strain (MG1655) incubated at 37 °C in M9 medium with 10 mM of glucose.

If we consider those results in the perspective of the activator hypothesis, it is intriguing that the increase of the α -ketoglutarate concentration in the bacteria has a negative impact on the ThTP accumulation while we were expecting an increased activator synthesis. Nevertheless, since the α -ketoglutarate inhibits the ATP-synthase, we can infer that the inhibition of the enzyme is stronger than the increase of the activator. If we consider ThTP as a side product of the ATP-synthase, it is consistent that the inhibition of this enzyme impacts the synthesis of ThTP.

Mammalian ThTPase expression in *E. coli*:

If the bacteria indeed synthesize an activator that acts on the ATP-synthase to increase the production of ThTP, it would mean that the ThTP production helps the bacteria to adapt to a nutritional shift (from the LB (rich) medium to the M9 minimal medium (poor)). It means that if we can degrade the ThTP shortly after its synthesis, it would be unable to fulfill its role and thus affect the bacterial adaptation and delay its growth.

To achieve this goal, we decided to express the specific mammalian 25-kDa ThTPase in the bacteria. In 2004, our lab had already succeeded in overexpressing the human ThTPase in *E. coli* using an expression vector. A slowing down of the growth was observed but only after 5h, i.e. at the end of the transient ThTP peak and during the exponential phase of growth (Lakaye *et al.* 2004c). We decided to include the mouse ThTPase (mThTPase) gene which has a higher catalytic efficiency than the human enzyme, inside the genome of the bacteria. That construction allowed us to express the ThTPase at low levels and thus prevent the strong metabolic disturbance caused by forcing the expression of a high quantity of a heterologous protein. We also expressed, in another clone, the K65A mutant of the mThTPase which is catalytically inactive but where the structure of the protein is conserved (Delvaux *et al.* 2013). It is thus the best control we could get to assess the disturbance due to the expression of a heterologous protein similar to the ThTPase but without any ThTPase activity. Those two proteins were inserted into the NM543 bacteria strain and thus we obtained two new strains where the expression of either the WT or the K65A mThTPase is under the dependence of an inducible promoter.

The WT MG1655 strain, the “mother” strain NM543 and the two newly engineered strains ThTPase WT I and ThTPase K65A I were grown overnight in LB medium, then the expression of the ThTPases was induced for 3h. Afterwards, the bacteria were diluted to an optical density (DO₆₀₀) of 0,03 in the M9 minimal medium with 10 mM of glucose. They were

incubated at 37 °C and the growth was monitored every hour by measuring the DO_{600} . No difference could be observed between the four strains. After 1h, we assessed that the ThTP level was low in the ThTPase WT I strain but normal in the others (figure 34).

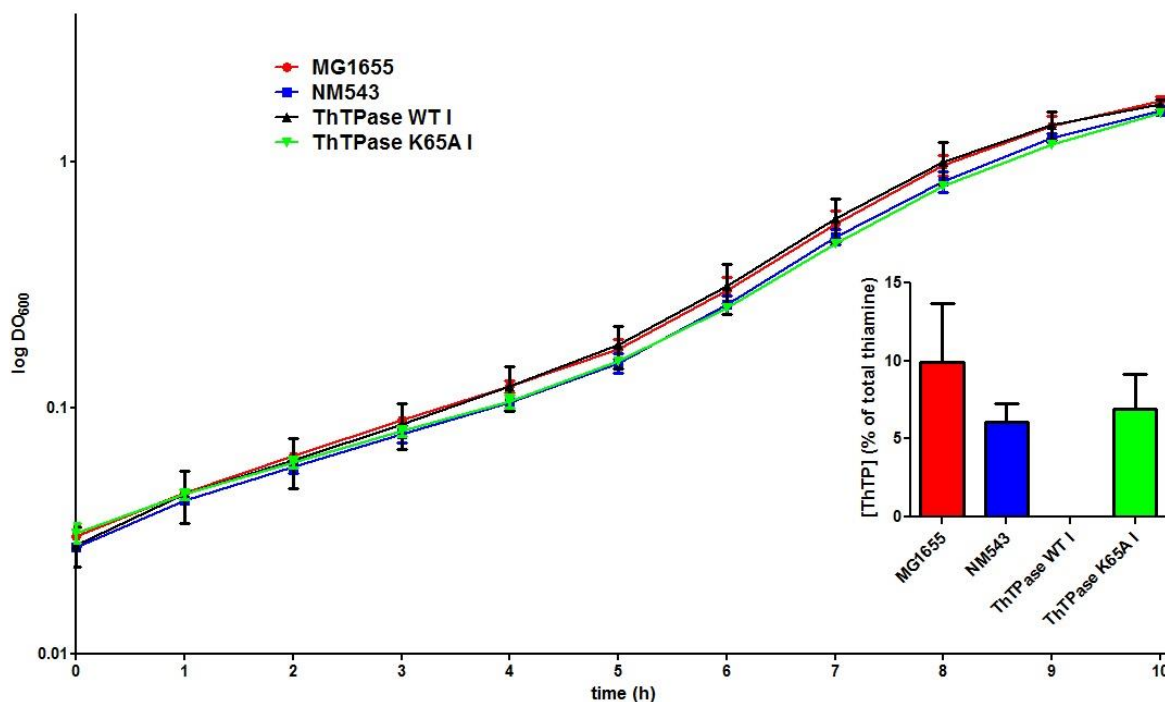


Figure 34: Growth and ThTP production in four bacterial strains incubated at 37 °C in M9 medium with 10 mM of glucose. The ThTP concentration was assessed after 1h of growth.

The absence of effect is not in agreement with what was observed in 2004. However, the expression levels of the protein from a plasmid present in the bacteria in multiple copies was much higher than in our models with only one copy of the gene inserted in the genome. It could be estimated that ThTPase accounted for at least 25% of the total protein in the bacteria. From the present results (obtained without high overexpression of the 25-kDa ThTPase) it appears that ThTP is not required for growth when the bacteria are placed in a condition of amino-acid starvation with glucose as a carbon source. This supports the hypothesis that ThTP is a side product of the ATP-synthase with no apparent physiological role.

Our results also indicated that ThTP is not toxic for the bacteria, as growth is not speeded up by its hydrolysis. While the present results strongly suggest that ThTP plays no important role in bacterial growth or survival, it remains hard to explain why ThTP is produced only under specific conditions, i.e. amino acid deficiency and presence of a substrate yielding pyruvate. If ThTP is a byproduct of ATP synthase activity, it should be correlated with a high proton-motive

force, which itself would occur when the $[NADH] / [NAD^+]$ ratio is high. Further studies are required to assess the exact role of these parameters.

ThTP synthesis and oxidative stress:

The NADH and the $FADH_2$ produced in the Krebs cycle are used to fuel the electron transport chain (ETC), to expel protons from the cell and create an electrochemical gradient. This gradient is used as the energy source that allows the F_0F_1 ATP-synthase to catalyze the formation of ATP or ThTP.

The ETC is also a primary source for reactive oxygen species (ROS) and thus of oxidative stress (Wang *et al.* 2013). In turn, oxidative stress affects the activity of the ATP-synthase by inducing oxidative post-translational modifications (Ox-PTMs) of the enzyme. So, under our conditions where glucose is consumed within minutes, most of NADH and $FADH_2$ is produced through the Krebs cycle. In that process, oxidative stress is more likely to arise.

To test whether the oxidative stress can affect the production of ThTP, we added to the culture medium of the WT bacterial strain increasing concentrations of HOCl ranging from 0 to 100 μM (figure 35).

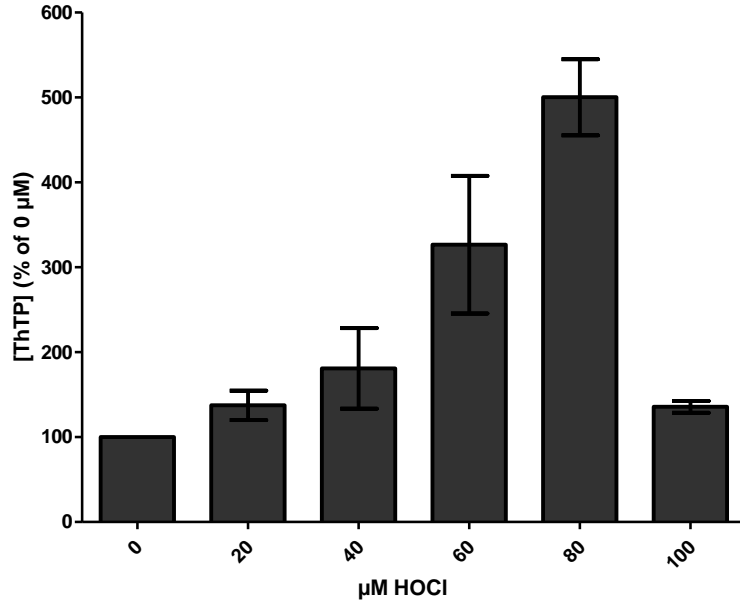


Figure 35: Effect of increasing concentration of HOCl on ThTP concentration in the WT bacterial strain (MG1655) incubated for 1h at 37 °C in M9 medium with 10 mM of glucose.

We could observe that, up to 80 μM , HOCl dose-dependently increased ThTP production but at 100 μM , ThTP production was back to normal and would probably continue to decrease as the excess of HOCl is killing the bacteria. It thus appears that a limited oxidative stress enhances the production of ThTP. It was observed by different authors that oxidative stress affect the F_0F_1 ATP-synthase activity (Hannum *et al.* 1995; Rexroth *et al.* 2012; Wang *et al.* 2013). We can thus hypothesize that it could affect the affinity of the enzyme for different substrates, either by decreasing the affinity for ADP or increasing the affinity for ThDP. Those result are also in favor of the hypothesis that ThTP is a side product of the enzyme.

Conclusions

A summary of the results is shown in table 7, page 60.

Investigations carried out in our laboratory during the last decade have shown that, under specific conditions of cellular stress, *E. coli* cells can accumulate ThTP. This production requires a carbon source yielding pyruvate and occurs in response to a nutritional shift, i.e. amino acid deprivation. It was thus suspected that ThTP could act as an intracellular messenger or “alarmone” required for the adaptation of the bacteria to specific condition of stress. It was intriguing that the energy substrate needed for ThTP synthesis was either pyruvate or yielding pyruvate, e.g. glucose or lactate. No ThTP was produced in the presence of other substrates such as malate (though cellular ATP level was normal). It was therefore postulated (Gigliobianco *et al.* 2013) that a metabolite derived from pyruvate was required to induce ThTP synthesis by F_0F_1 ATP-synthase. Previous results as well as our own suggest that isocitrate (or an unknow compound derived from isocitrate) may act as a modifier of F_1 so that the ATP-synthase catalyzes the synthesis of ThTP rather than ATP.

However, the physiological relevance of the ThTP accumulation after nutritional shift was never assessed. If ThTP is indeed an intracellular messenger produced in response to specific conditions of cellular stress, it should exert some beneficial effects on the metabolism, growth or survival of the bacteria when they are submitted to a nutritional shift. We attempted to answer the question by including a mouse ThTPase in the bacterial genome. As this enzyme hydrolyzes ThTP with high specificity and catalytic efficiency, the mutated bacteria were unable to accumulate any significant amount of ThTP. However, there was no difference in growth rate (after nutritional shift) between wild type bacteria and the mutant. It must be concluded that ThTP plays no important role in the adaptation of *E. coli* cells to amino acid deficiency, at least

as far as survival and growth are concerned. Apparently, the well-known “stringent response” to nutritional shift is sufficient for adaptation of *E. coli* cells. It thus cannot be excluded that ThTP may be a “*non-classical metabolite formed by side activities*” of the F_0F_1 ATP-synthase (Linster *et al.* 2011). We also have results showing that the oxidative stress, which affect the ATP-synthase activity, enhance the ThTP production after the nutritional shift.

Those results, without being a definitive proof, lead us to believe that ThTP production is not dependent of an activator that change the conformation of the F_0F_1 ATP-synthase as we previously claimed (Gigliobianco *et al.* 2013) but is dependent on a high activation of this enzyme. Thus, the high levels of NADH and $FADH_2$, achieved by the entry of high amount of acetyl-CoA in the Krebs cycle are the key for the production of ThTP thanks to the high proton-motive force and the concomitant oxidative stress. In addition, the accumulation of the Krebs cycle intermediate α -ketoglutarate under certain condition may inhibit ThTP synthesis by inhibition of f_0f_1 -ATP synthase.

| Condition | Effect on the bacteria | ThTP production |
|--|---|---|
| Mutant PDH JW0110-JW0111 (E1p – E2p KO) | Loss of the PDH complex activity | The ThTP peak is delayed |
| Mutant JW0112 (E3 KO) | Loss of the PDH, OGDH and GC complex activities, strong perturbation of the metabolism | No ThTP production |
| Mutant JW0715 (E1o KO) | Loss of the OGDH complex activity | ThTP production normal |
| Mutant JRG465 (E1o KO + isocitrate lyase constitutive) | Loss of the OGDH complex activity + constitutive activation of the glyoxylate cycle. General metabolism slightly affected. | No ThTP production |
| Mutant JW0710 (CS KO) | Loss of the citrate synthase activity | Production of ThTP reduced |
| Mutant JW1268 (Aconitase A KO) | Loss of 75% of the aconitase activity | Production of ThTP reduced |
| WT (MG1655) + octyl- α -ketoglutarate | Increased α -ketoglutarate concentration, inhibition of F _o F ₁ ATP-synthase | Dose dependent inhibition of the ThTP production |
| WT (NM543) strain overexpressing the mThTPase | The mouse ThTPase hydrolyzes ThTP as soon as it is produced, no effect on the growth | No ThTP |
| WT (MG1655) + HOCl | Induction of an oxidative stress increasing with the concentration till it induced strong metabolic problems and eventually the death of the bacteria | Dose dependent enhancement of the ThTP production |

Table 7: Summary of the results obtained with the different mutant strain and with the different compound used when the *E. coli* bacteria are incubated at 37 °C in M9 medium with 10 mM of glucose.

Chapter 3: Possible role of ThTP and 25-kDa zThTPase on zebrafish development

ThTP may be a side product in *E. coli* but what about higher organism? It was shown that ThTP can modulate the activity of a high conductance anion channel (Bettendorff *et al.* 1993), that it can phosphorylate some proteins such as the rapsyn (Nghiem *et al.* 2000) and that a highly specific ThTPase is dedicated to its degradation (Lakaye *et al.* 2002). Note that in *E. coli*, no specific ThTP hydrolyzing enzyme has been described.

To study the role of ThTP in eukaryotic cells, there are two possible approaches: to block its synthesis or to induce its accumulation. In mammalian cells, as in *E. coli*, ThTP is synthesized by F₀F₁ ATP-synthase (Gangolf *et al.* 2010). Therefore it would be impossible to block ThTP synthesis without also affecting ATP synthesis. In eukaryotic cells, the only known condition under which ThTP accumulates is when 25-kDa ThTPase activity is very low (e.g. in pig tissues) or when the gene is absent (e.g. in birds). To better understand the role of ThTP, we decided to prevent its degradation. Two different approaches were used to achieve that goal. Both involve interfering with the ThTPase expression. In this chapter we will discuss the use of morpholinos in the zebrafish embryo, while in the next chapter we will discuss the knock-out approach in the mouse.

Characterization of the zTHTPA gene:

In mammals, ThTPase is a ubiquitous enzyme and its only known role is to hydrolyze ThTP. In zebrafish, almost nothing is known about the 25-kDa ThTPase except that the catalytic activity of the recombinant enzyme is 10-100 fold lower than that of the mouse or human enzymes (Delvaux *et al.* 2013). According to the ZFIN database (zfin.org), the ThTPase gene is present on the 24th chromosome and 4 different mRNA seem to exist (figure 36). The transcript thtpa-005 lacks most of the coding sequence and does not seem relevant compared to the others.

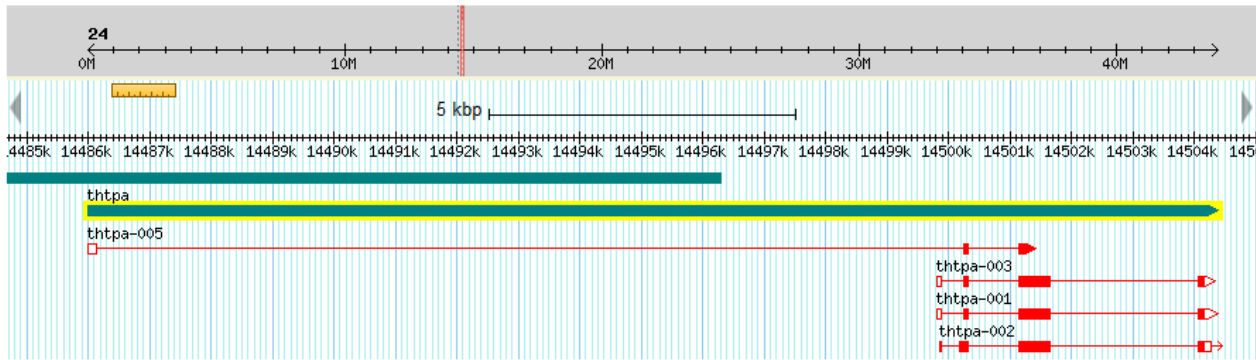


Figure 36: ZFIN database data for the different transcripts of zebrafish thiamine triphosphatase (zThTPase). On the top part, we can see the whole 24th chromosome, and below it, the enlargement of the genomic region containing the thiamine triphosphatase gene. The thick blue lines correspond to the genes, the one highlighted in yellow is the zThTPase gene. In red, we can see the different transcripts of the zThTPase. The thin red lines correspond to the introns while the thick one correspond to the exons. The full part of those thick lines corresponds to the coding sequence of the mRNA.

If we look in more detail at the 3 other transcripts, two major differences with the mammalian gene become apparent. First, the existence of 4 exons is a notable difference with the mammalian gene which in most cases comprises only 2 exons. Second we can see that the exon 3 and the coding sequence in exon 4 are the same for all of them. The exon 2 and the coding sequence of the transcripts thtpa-001 and thtpa-003 are also the same, while the exon 2 of the thtpa-002 is longer and the coding sequence is longer by 58 nucleotides, though the reading frame is conserved (figure 37,39).

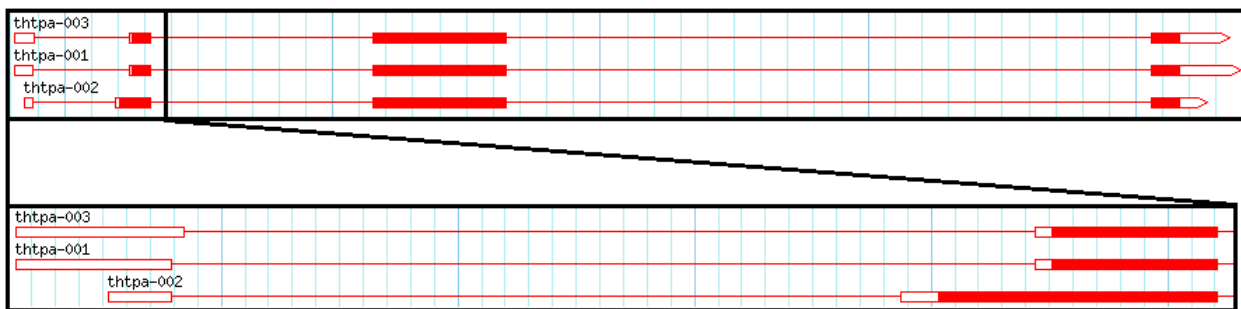


Figure 37: ZFIN database data for the thtpa-001-002-003 transcripts of the zThTPase The thin lines correspond to the introns while the thick ones correspond to the exon. The full boxes of the thick lines correspond to the coding sequences of the mRNA. The second frame is a higher magnification of the two first exons of the three transcripts.

We checked that the thtpa-002 transcript and at least one of the thtpa-001 or thtpa-003 transcripts (there is only a 2 nucleotides difference among them, thus they are impossible to distinguish under our experimental conditions) were expressed in the zebrafish egg at different time points (figure 38). We first isolated the RNA of the fish at 0, 2, 4, 6, 8, 24 and 48 hour post

fertilization (hpf). The RNAs were retrotranscribed into cDNAs and a PCR allowed us to observe the different transcripts. We observed that at least two of the transcripts were expressed at every time point. The sizes of the amplified fragments correspond to the splice forms of the transcripts and thus they are not amplified from the genomic DNA.

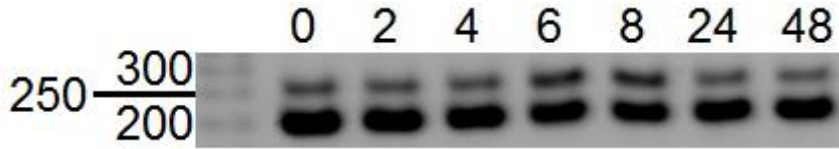


Figure 38: Amplification of the different thtpa transcript: 3% agarose gel; the number on the left are the size in bp of the ladder, the numbers on top are the number of hours after fertilization at which the sample were taken. The expected sizes for the bands were: 195 bp for thtpa-001, 197 bp for thtpa-003 and 252 bp for thtpa-002.

A careful look at the mRNA sequence tells us that in the exon 2, two (or even three for thtpa-002) start codons are in phase. On the thtpa-001-003 transcript, there is a second potential start codon 15 amino acid downstream of the referenced start codon. Those two potential start codons are also included in the thtpa-002 transcript in addition to the start codon which is referenced in the database (figure).

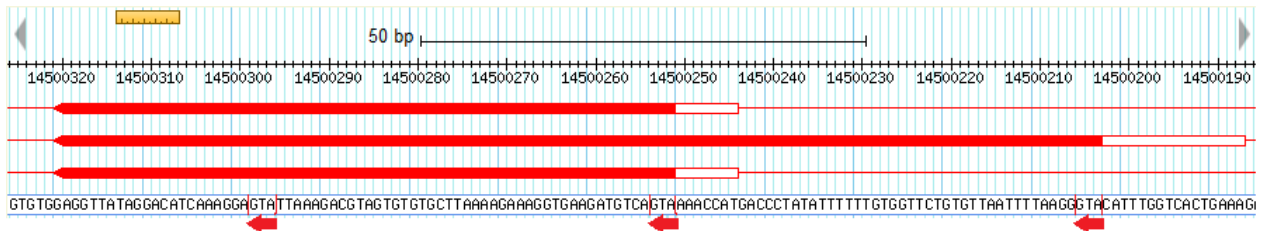


Figure 39: ZFIN database for the exon 2 of the transcript thtpa-001-002-003. The selected frame was inverted to show the complementary sequence which contains the ATG. The three red arrows show the three start codons.

Morpholino-induced zThTPase expression reduction

We decided to use antisense morpholinos directed against the zThTPase to get a better insight in its role in general and especially during embryogenesis. Morpholinos were used because this is a fast and efficient way to reduce the expression of a specific gene in zebrafish embryo.

Two strategies were tested, a morpholino which inhibits the splicing and a morpholino which inhibits the initiation of the translation. The latter was directed against the referenced start codon of the thtpa-001-003 transcript but it blocks neither the potential start codon which is downstream nor the one on the thtpa-002 transcript. It was thus not really efficient (data not shown) and we used only the splicing morpholino in further investigations.

First, a dose-response analysis was made on a total of 1890 injected embryos: the eggs were injected right after spawning with either a control morpholino (4 ng/egg) or with the splicing morpholino directed against the zThTPase (1 – 2 - 4 ng/egg) and observed 24 hours post fertilization (hpf) and 48 hpf.

Although not highly specific, strong phenotypic alterations were observed: there was a general developmental delay or a brain development delay, pericardial edema, cerebral edema, brain necrosis, abnormal somite and abnormal hemostasis (table 8 and 9). The fish were categorized as having a normal, light, moderate or severe phenotype, or dead. We can see that the morpholino act in a dose-dependent manner (Figure 40). Those results are the first showing that the absence of the THTPA transcript alters fish development.


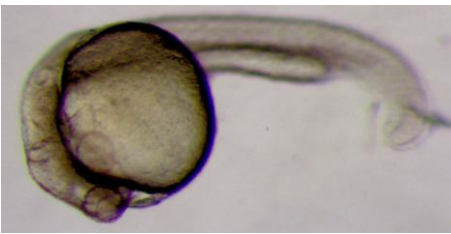


| 24 hpf | |
|---|--|
| <u>Normal</u> |  |
| <u>Light</u> Developmental delay |  |
| <u>Moderate:</u> malformation + brain necrosis (arrow) |  |
| <u>Severe:</u> Strong developmental defect |  |

Table 8 : List of the phenotype observe in zebrafish embryos 24 hpf and the most common alteration observed.

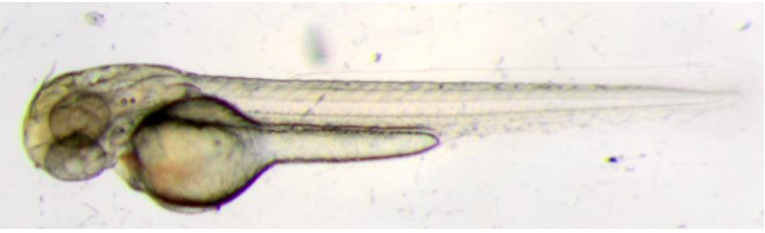
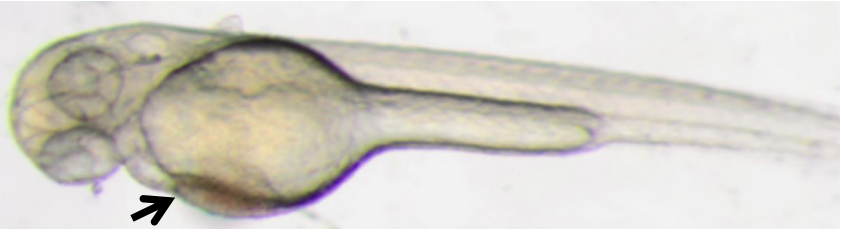

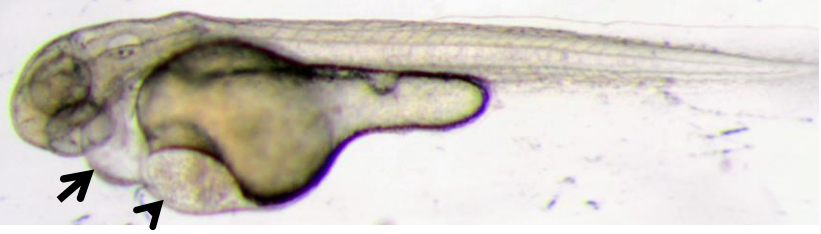
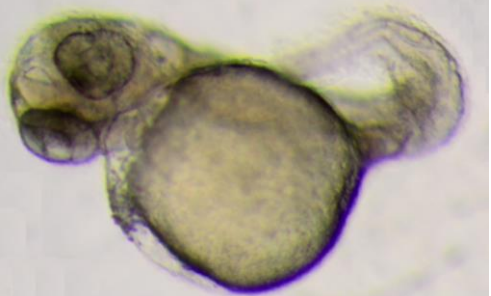
| 48 hpf | |
|--|--|
| <u>Normal</u> |  |
| <u>Light:</u> hemostasis (arrow) |  |
| <u>Moderate:</u> cerebral edema (arrow) |  |
| <u>Moderate:</u> pericardial edema (arrow) and hemostasis (arrow head) |  |
| <u>Severe:</u> No heart at all + strong malformation |  |

Table 9: List of the phenotype observe in zebrafish embryos 48 hpf and the most common alteration observed.

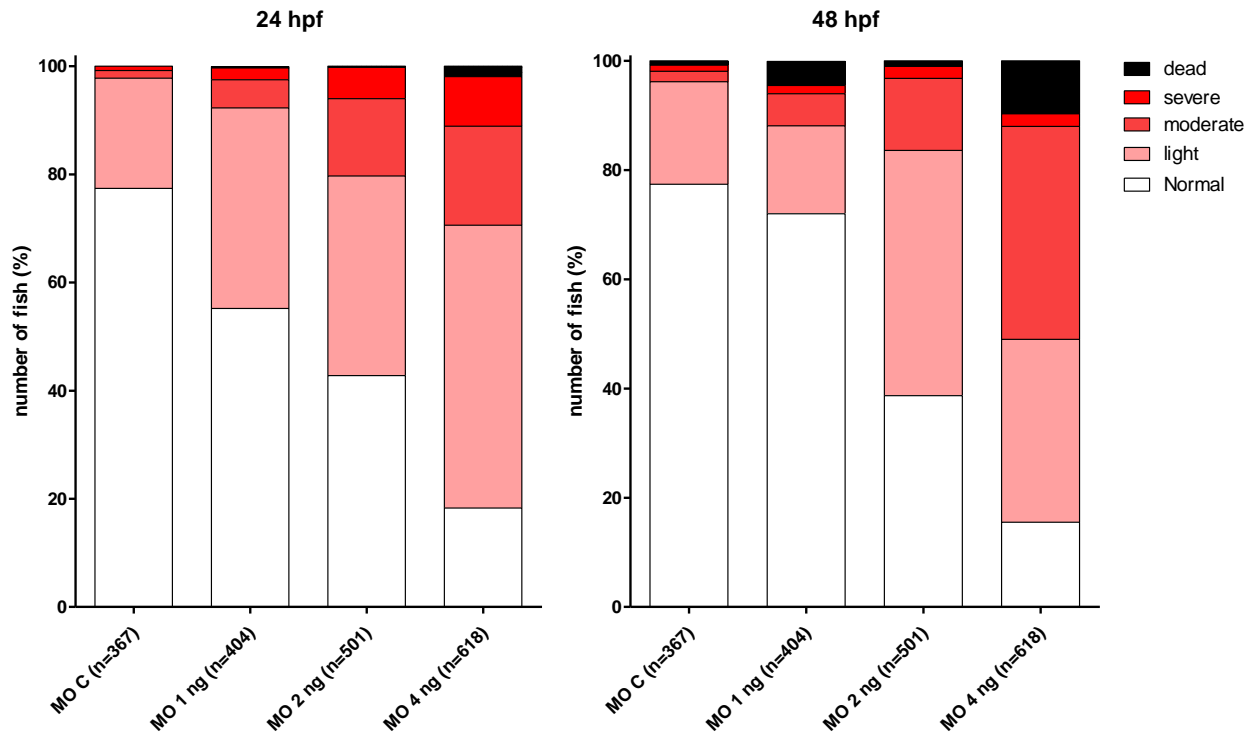


Figure 40: Dose response effect of the splicing morpholino directed against the zThTPase after injection into zebrafish embryos. For each condition, phenotypes are classified as normal, light, moderate, severe or dead and expressed as a percentage of the total number of eggs for that condition. Fish were observed at 24 hpf and 48hpf.

When we take a closer look at the results, we observe that in the fish injected with the control morpholino, almost 80% of the embryos are normal and most of the remaining 20% are only slightly affected, with almost no distinction between the two days of observation.

In the fish injected with the morpholino directed against the zThTPase at 24 hour post fertilization, we can observe a decrease in the percentage of normal fish down to less than 20 % for the 4 ng injected fish. The percentage of only lightly affected fish doubled compared to the control for the 1 or 2 ng and almost tripled for the 4 ng injected fish. The percentages of moderately and severely affected fish also increased from 1 to 4 ng injected fish.

The next day, 48 hpf, we can see that the percentage of normal fish remains almost constant except for the 1 ng injected that seemed to slightly recover. We can also observe that most of the severely affected fish were either dead or had to some extent recovered to moderately affected. The 4 ng injected fish are the most affected with almost 10 % of dead fish, about 70% of the surviving fish were affected, half of them lightly and the other half moderately.

In order to attribute the above-described effects to the morpholino, it is important to demonstrate a reduction of the spliced zThTPase transcript level. We used two different primer

sets, the first being the same as the one used for the detection of the different transcripts and the second targeting a region common to the three transcripts to increase the sensitivity. In both cases, there was a strong reduction of the spliced transcript level in the injected embryo compared to the non-injected one. We can only see a remaining shadow of the spliced amplicons in the zThTPase morphant. We could also observe that the transcript levels were similar between the control morphant and the non-injected fish.



Figure 41: detection of the sliced transcripts of the zThTPase: 3% agarose gel; the numbers on the left of each gel are the size in bp of the ladder; each lane is the result of the PCR on a specific sample: lane 1, cDNA from 24hpf eggs injected with the splicing morpholino against the zThTPase; lane 2, cDNA from 24hpf eggs injected with the control morpholino; lane 3, cDNA from 24hpf non-injected eggs. The expected sizes for the bands on the gel on the left are: 195bp for thtpa-001, 197bp for thtpa-003 and 252bp for thtpa-002, while the expected size for the band on the gel on the right is 140bp.

To confirm the specificity of the observed effects, we tried to rescue the phenotype by injecting the transcript of the mature zThTPase mRNA together with the morpholinos. As the morpholino used is impairing the splicing, our rescue mRNA will not be affected. We chose to work with a fixed concentration of 2 ng of morpholino injected per fish in order to target an intermediate effect, leaving room for improvement or worsening of the effect. The eggs were injected right after spawning with either a control morpholino (2 ng/egg) or with the splicing morpholino directed against the zThTPase (2 ng/egg), in each case, with or without the rescuing mRNA (100 pg/egg). The fish were observed at 24 hpf and 48 hpf. (figure 42).

If we look at the rescue results at 24 hpf, the injection of the morpholino directed against the zThTPase induces a decrease of the normal fish to 50% with again a doubling of the lightly affected fish compared to the control morpholino. We can also observe that the injection of the mRNA coding the zThTPase leads to a distribution of the phenotype that is similar whether it is injected together with the zThTPA or the control morpholino and close to the distribution observed when the control morpholino was injected alone.

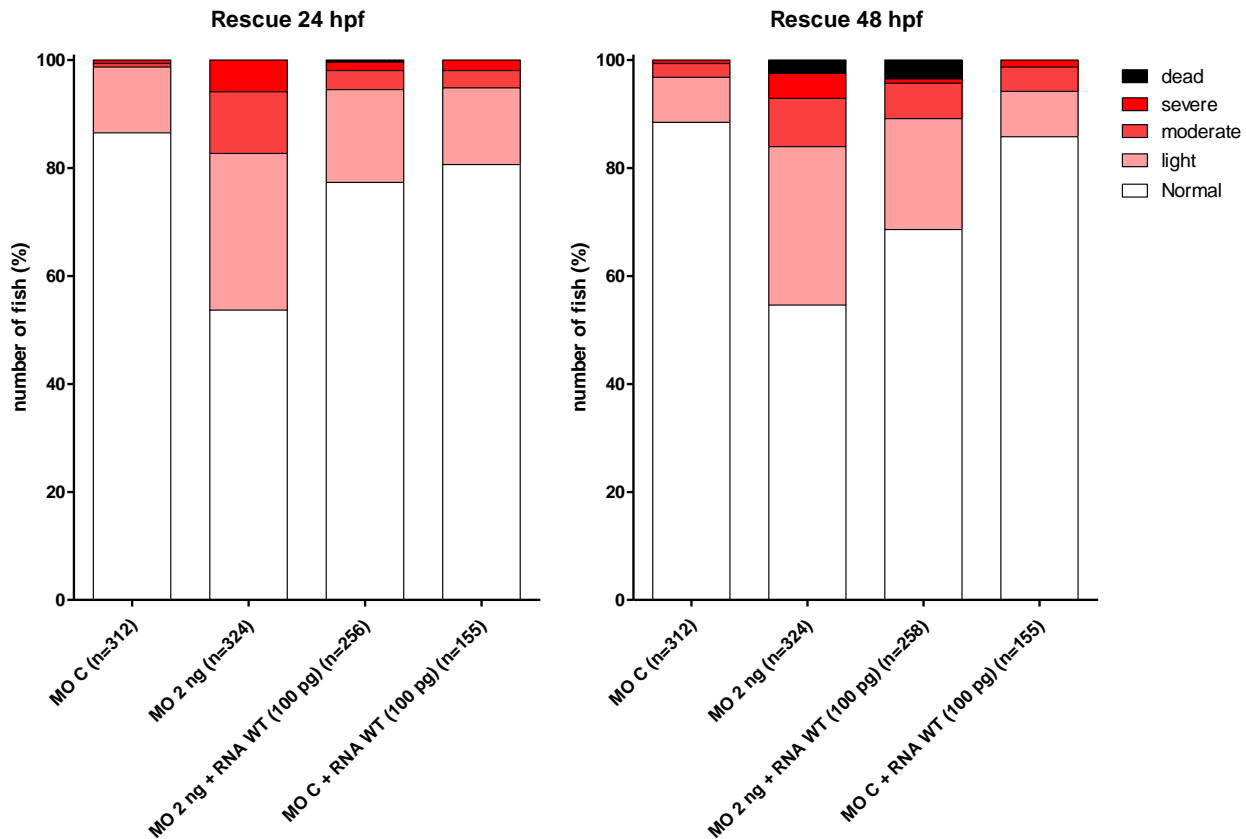


Figure 42: Effect of the rescuing mRNA coding for the zThTPase on the phenotype of zebrafish embryo injected with control or zThTPase splicing inhibitor morpholino. For each condition, phenotypes are classified as normal, light, moderate, severe or dead and expressed as percentage of the total number of eggs for that condition. Fish were observed at 24 hpf and 48 hpf.

At 48 hpf, we can see that the rescued fish have a more intermediate distribution of the phenotype, which can be explained by the degradation and the dilution of the RNA. These results show that the fish phenotype is indeed rescued by co-injection of the zThTPase mRNA with the morpholino suggesting that our zThTPase morpholino is indeed specific. Hence, the lack of the ThTPase induces an unspecific but general impairment of the embryogenesis of the zebrafish.

To further confirm the specificity of the observed effects and to assess whether the activity of the enzyme is required to rescue the phenotype, we decided to try the rescue protocol using the coding sequence of the zThTPase with the K61A mutation. That lysine in zebrafish ThTPase coding sequence is homologous to the lysine 65 (K65) in mouse or human. As already mentioned, the mutation of the K65 to an alanine drastically reduces the catalytic activity but does not affect the tridimensional structure of the enzyme (Delvaux *et al.* 2013).

The transcript of the mature K61A zThTPase mRNA was injected with the morpholinos. Once again, this transcript was not affected by the morpholino. We worked with the same concentration of 2 ng of morpholino and 100 pg of RNA injected per fish. The eggs were injected right after spawning with either the control morpholino (2 ng/egg) or with the splicing morpholino directed against the zThTPase (2 ng/egg), in each case, with or without the K61A zThTPase RNA (100 pg/egg). The fish were observed at 24 hpf and 48 hpf (figure 43).

As previously observed, injection of the morpholino (2 ng) was toxic for the embryos. In contrast to what we observed with the WT mRNA, co-injection of the K61A mRNA appeared to worsen the phenotype (both at 24 hpf and 48 hpf); in any event, no rescue was observed (figure 43). When the K61A RNA was co-injected with the control morpholino the phenotype distribution was similar or slightly worsened compared to the control morpholino injected alone.

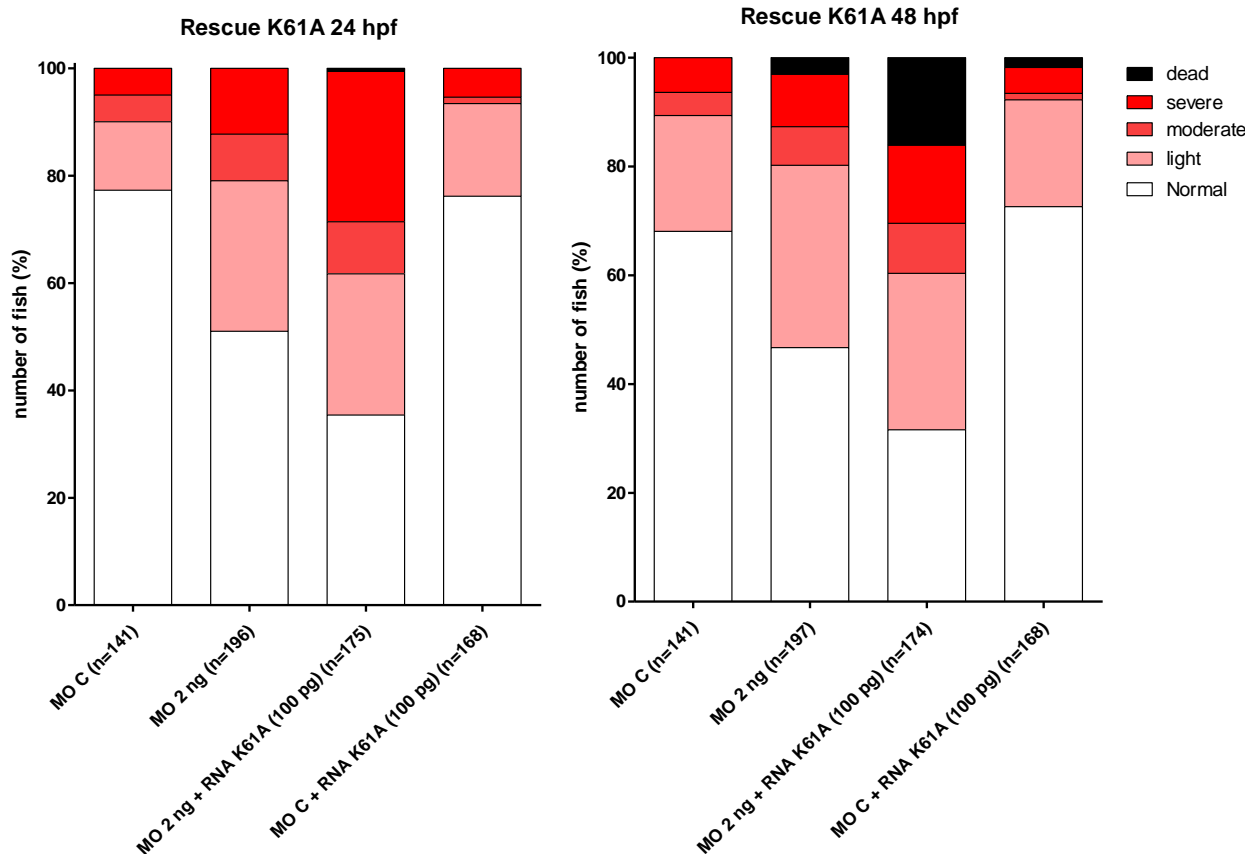


Figure 43: Effect of the rescuing mRNA with the coding for the K61A mutant of the zThTPase on the phenotype of zebrafish embryos injected with control or zThTPase splicing inhibitor morpholino. For each condition, phenotypes are classified as normal, light, moderate, severe or dead and expressed as a percentage of the total number of eggs for that condition. Fish were observed at 24 hpf and 48hpf.

HPLC measurement of thiamine derivatives in zebrafish embryo:

We wanted to measure ThTP and other thiamine derivatives in the embryo of zebrafish and assess the increase of the ThTP levels in the injected fish but unfortunately, in the zebrafish those measurements were impossible with the classical HPLC method (Bettendorff *et al.* 1991) because of the presence of an auto-fluorescent compound that prevents the detection of any thiamine derivative.

Conclusion

The organization of the ThTPase gene in the zebrafish is quite different from the one found in its human or mouse counterparts. While the mammalian THTPA gene usually has two exons and only one transcript, the zebrafish gene contains four exons and can be spliced in different ways. We could observe that the different transcripts were present already in the egg right after spawning, which means that the transcript is present before the fertilization of the eggs. In the zebrafish, till 4 hpf, no new mRNA transcripts are synthesized. During the first hours, the embryos start their development using only the maternal mRNA present in the egg. After those initial 4 hours, the different transcripts were present at least till 48 hpf, which means that the ThTPase could be involved in the development of the embryo.

When the ThTPase expression was reduced by the injection of a morpholino, we could observe that the fish show developmental defects. The phenotype was partly restored when we co-injected the morpholino with the mRNA coding for the ThTPase (rescue) but not when we attempted the rescue with the K61A mutant of the ThTPase. Those results indicate that even if the credibility of morpholinos as a tool for RNA interference has been questioned in the recent literature (Kok *et al.* 2015), the effects that we observe seem specific and are likely caused by the decrease in ThTPase activity.

To make sure that the decrease of ThTPase expression indeed increases the ThTP concentration in embryos, it would have been interesting to measure the ThTP levels, but unfortunately this was impossible for technical reasons.

From those results, we can wonder whether the phenotypes observed are due to the ThTP accumulation which could be toxic for the developing embryo or if the ThTPase has some role other than ThTP hydrolysis (as suggested by Delvaux 2012) which would be necessary for the normal development of the fish.

As previously discussed, both in mammalian brain and in *E. coli*, ThTP can be produced either by cytoplasmic adenylate kinase or by F_0F_1 ATP-synthase. In both cases, ThTP production could not be clearly related to a physiological function and accumulation of high amounts of ThTP (e.g. in pig muscle and electrophorus electric organ) had apparently no toxic effects. However, in the zebrafish, ThTP accumulation seems to interfere with the development of the fish. If ThTP is indeed a side-product of enzyme producing ATP which is toxic in eukaryote cells, the evolution of enzyme of the CYTH family towards hydrolysis of ThTP would prevent the deleterious consequences of its accumulation on normal metabolism.

Chapter 4: Knock-out of the mouse ThTPase:

Much information is available about mammalian ThTPase and the level of ThTP in different organisms and tissues. Yet their metabolic function(s) or the pathways they may be involved in, are still largely unknown.

For that reason, and in parallel to the zebrafish morphant which allows only the study of developing animals and is based on the reduction of the protein levels by interfering with the mRNA, we wanted to obtain a strain of mice knock-out for ThTPase.

Thiamine triphosphatase knock-out methods

In order to generate the THTPA KO transgenic line of mice, we ordered embryonic stem (ES) cells clones from the Knockout Mouse Project (KOMP) repository at UC Davis (www.komp.org). At the end of the validation test, they could provide us with two ES cell clones: BC03 and BA09. In those cells, one allele of the ThTPase gene was deleted and replaced by the “tm1(KOMP)Vlcg” cassette (figure 44). That cassette contained in the 5’ to 3’ order:

- the coding sequence of the beta-galactosidase (*lacZ*),
- the SV40 polyadenylation signal,
- the first lox site,
- the hUBC promoter (the promoter of the human Ubiquitin C),
- the em7 promoter (a synthetic promoter based on the T7 promoter, allowing bacterial expression of the downstream gene),
- the coding sequence of the neomycin resistance gene,
- the mouse phosphoglycerate kinase (mPkg) polyadenylation signal,
- the second lox site.

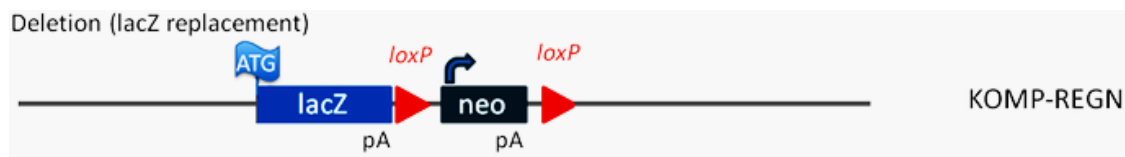


Figure 44: Scheme of the “tm1(KOMP)Vlcg” cassette used to replace the THTPA gene in the BC03 and the BA09 clones.

We sequenced the junction site between the mouse DNA and the cassette to make sure that it was well inserted. As we can see on figure 45, no other known gene was affected by the

deletion and the whole coding sequence of the ThTPase was removed, while the 5' and 3' untranslated regions were conserved.

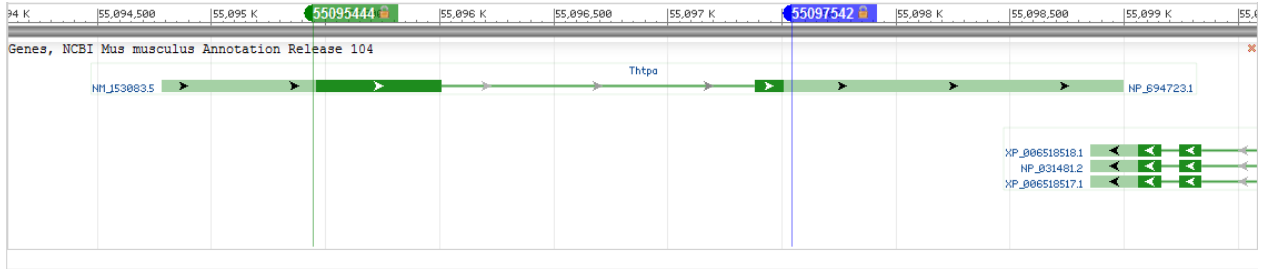


Figure 45: NCBI annotation of the *Mus musculus* genome on the surrounding region of the THTPA gene of the 14th chromosome. The numbers on the top line correspond to the sequence of the chromosome, the green horizontal lines represent the genes along this sequence (light green: untranslated region, dark green: coding sequence, thin green line: intron). The green and the blue vertical lines are there to show the part of the genome that was deleted and replaced by the tm1(KOMP)Vlcg cassette.

The ES cells were injected into blastocysts that were then implanted into the uterus of a foster mother mouse. The surviving blastocysts developed into the mouse uterus until the delivery. Some of the pups were chimerae which, as they grew, became black and white (figure 46) since their cells were derived either from the ES cells or the blastocysts. The genetic background of the ES cells is C57BL/6NTac and thus black, while the blastocysts were generated from mouse from Charles River with a CD-1® IGS (part of the International Genetic Standardization program) white genetic background. By looking at the proportion of black fur we could estimate the percentage of chimerism of our animals. This percentage gave us an idea of the general chimerism but it did not reflect the percentage of chimerism among the stem cells producing the sperm.



Figure 46: picture of a 60% chimeric mouse.

Since the ES cells have a male genotype (XY), they are unable to differentiate into mature oocytes and thus only the male chimerae are of interest. The male chimerae obtained were crossed with wild type (WT) C57Black female mice. While the females could only transmit a black genetic background, the males could transmit either a white or a black genetic background.

Hence, the descendants are either brownish or black. If the pups obtained have a brownish fur, it means that the sperm from the chimerae that has fertilized the oocyte was derived from the blastocyst. On the other hand, if the pups are black, it means that the sperm was derived from the ES cells and thus has a chance to carry the mutation.

As only one of the ThTPase alleles of the ES cells is invalidated, only half of the sperms derived from them carry the mutated allele of the ThTPase. It means that among the black pups, half should be WT while the others half should be heterozygous with respect to the ThTPase gene (figure 47).

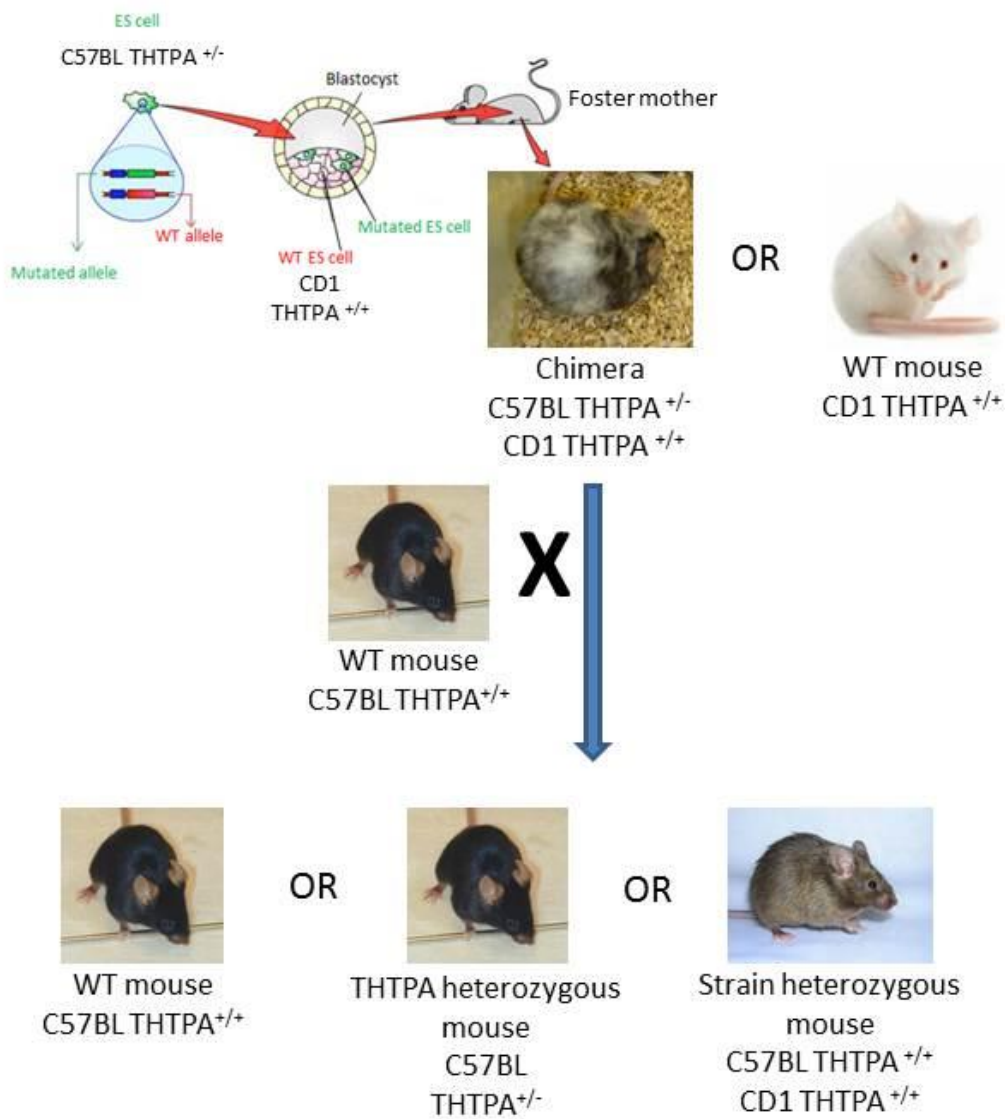


Figure 47: diagram of the process to obtain heterozygous mice from the heterozygous embryonic stem cells.

Results obtained from the THTPA chimerae:

Twelve chimerae were generated and a total of 455 pups were obtained. We genotyped all of them and, surprisingly, they were all wild type (figure 48). Among them, 306 were black, which means that statistically we should have had around 153 heterozygous pups.

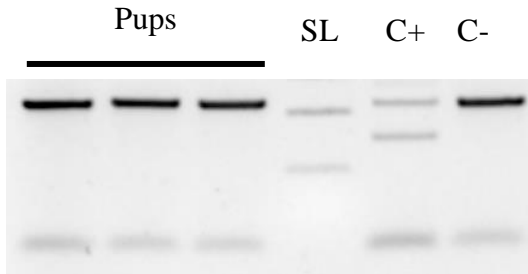


Figure 48: detection of the WT and invalidated allele of the ThTPase: 2% agarose gel: electrophoresis of the PCR product of the genotyping of the chimeric pups. The three first lanes correspond to three different pups, the fourth is the size ladder (from top: 400 bp-200 bp), followed by the positive control (DNA from the mutated ES cells), and then the negative control (DNA from a WT mouse). The two expected sizes for the amplicon were: 307 bp for the mutated gene and 444 bp for the WT allele.

In order to check whether our chimerae were indeed carrying the mutation, we sacrificed two of them and collected tissue samples from different organs (the brain, the lungs, the heart, the skin and the testis). We extracted the genomic DNA from those samples and genotyped them. Those tissues derived from the ES cells and from the blastocyst are partly THTPA^{+/+} and partly THTPA^{+/-}. We indeed observed a signal specific of the mutated gene in every sample tested. That signal was of variable intensity depending of the ratio between the two genetic identities in the cells composing the sample tested (figure 49).

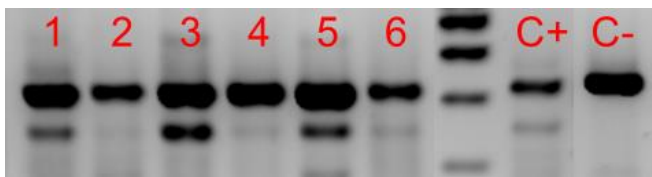


Figure 49: detection of the WT and invalidated allele of the ThTPase: 2% agarose gel of the PCR product of the genotyping of different chimerae tissues: 1:brain; 2:lung; 3:heart; 4:liver; 5:skin; 6:testis; size ladder (from top: 800-600-400-200 bp); C+:ES cells; C-:WT mouse.

Since the chimerae carried the mutation but never transmitted it, we decided to analyze the sperm of those animals. We had two chimerae with a sex reversal. A sex reversal means that the phenotypic sex of the chimera is different from the genotypic sex of the blastocyst. That phenomenon is made possible by the male genotype of the mutated ES cells. When those cells are injected in a female blastocyst, they can drive the phenotypic sex to be male (by producing the

SRY peptide). In that case, all the germ cells derive from the injected ES cells since the XX blastocyst cells cannot differentiate into mature sperms. We could detect the chimerae with a high probability of sex reversal because all their pups were black. In the chimerae with a sex reversal, after meiosis, half of the immature sperm cells would be WT and the other half knock-out for the *ThTPA* gene. The ratio between them should thus be close to one.

We thus decided to analyze, by qPCR, the genomic DNA extracted from the sperm of two mice with a sex reversal to obtain the ratio between the WT and the mutated allele. First, the sperm cells were collected from the epididymis and the *ductus deferens*, and then we purified part of the mobile sperm cells using two isolation methods: the swim-up and the swim-out. We thus obtained four different fractions per chimera: the Swim Up Lower part (SUL), the Swim Up Superior part (SUS), the Swim Out Central part (SOC) and the Swim Out Peripheral part (SOP). After qPCR we obtained a ratio of 1 KO sperm for 100 or 1000 WT sperm. We did not see any difference between the mobile fraction (SUS-SOP) and the mixed fraction (SUL-SOC), except that the amount of material for the SUS fraction of the 10% chimera was too low to detect any signal for the mutated allele (figure 50).

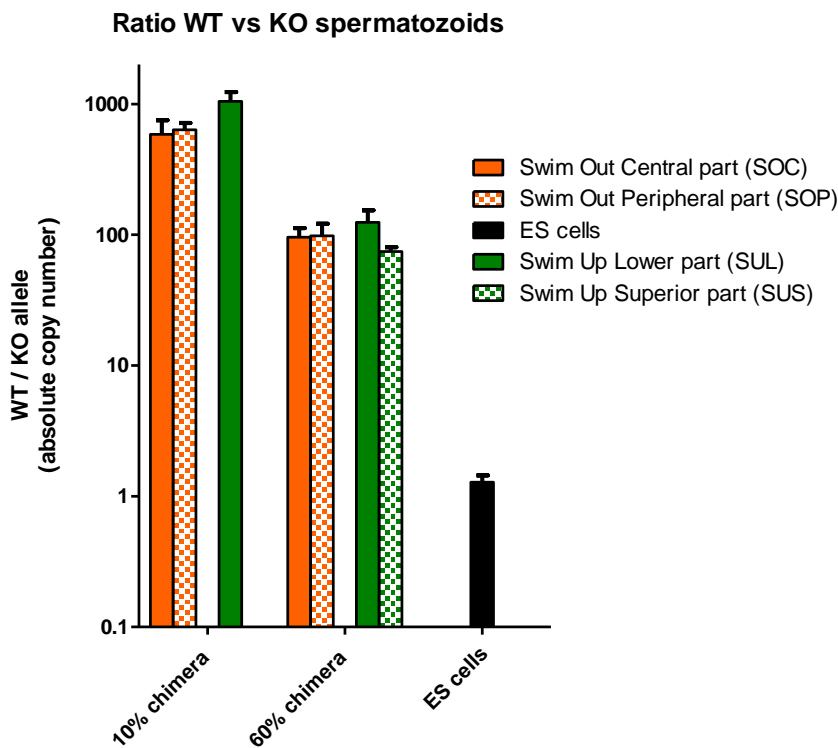


Figure 50: Ratio of the WT and invalidated allele of the *ThTPase* in the genomic sperm DNA.

Conclusions

Even after genotyping more than 300 pups with the expected fur color, we were unable to obtain heterozygous mice for the ThTPase and thus to obtain any KO mouse. Those results are not very surprising if we consider the results obtained with the morphant zebrafish. A decrease in the ThTPase expression appeared to be harmful for the developing embryos; in mice, the total absence of the enzyme after meiosis is apparently harmful for the developing sperm cells as well.

Once again, those results are in agreement with the conclusions drawn from our results in bacteria and in the zebrafish: ThTP appears to be a side product of the F₀F₁ ATP-synthase and its accumulation might be harmful, at least in some cell types. The sperm middle piece is rich in mitochondria and thus could produce a localized accumulation of ThTP in the KO cells. If, as hypothesized in the zebrafish, ThTP is toxic in some way, it could prevent the development of the sperm and thus the transmission of the ThTPA invalidation to the next generation.

From those results, it would appear that, in vertebrates, the 25-kDa ThTPase can play an essential role in some instances, but this seems to be restricted to particular cell types. ThTPase activity may be essential for the development of fish embryos and, in mammals, the protein could play a role in sperm differentiation. In the pig, however, the protein is largely expressed but is nearly inactive. Therefore, pig tissues contain higher amounts of ThTP, apparently with no harmful effects. The same is true for birds, where the ThTPase gene is lost.

It must be concluded that, although genes of the CYTH superfamily are present in most organisms and ThTPase activity is conserved from Cnidarians (*Nematostella*) to vertebrates, this enzyme may be required for the degradation of the unwanted thiamine derivative, ThTP, in some but not all animal cells.

*Discussion
And
Conclusion*

When one thinks about triphosphorylated molecules, nucleoside triphosphates immediately come to mind. Indeed they (and in particular ATP) represent the overwhelming majority of triphosphorylated molecules in the cells. Thiamine triphosphate (ThTP) has been shown to exist in many cells from bacteria to mammals (Makarchikov *et al.* 2003). It might be the only organic molecule containing a triphosphate chain in cells that is not a nucleotide. Our laboratory has been interested in ThTP for many years, in particular because of the existence of an extremely specific ThTPase hydrolyzing this compound (Makarchikov *et al.* 1992; Lakaye *et al.* 2002). This enzyme was first sequenced in our laboratory and it became rapidly evident that it belongs to a family of proteins, the CYTH superfamily (Figure 6), with members found in nearly all known genomes except birds (Iyer and Aravind, 2002; Delvaux *et al.* 2013; Bettendorff and Wins, 2013, see Figure 7). Moreover, while members of this family with known enzyme activities may have various substrates, these are always triphosphates and they are generally cleaved by hydrolysis of their terminal phosphate, with the exception of the *A. hydrophila* and *Y. pestis* members that are adenylate cyclases. While testing the hypothesis that the *N. europaea* CYTH protein might be a ThTPase, we found that it had only negligible ThTPase and ATPase activities. However, the recombinant protein hydrolyzed inorganic triphosphate (PPP_i) with high catalytic efficiency ($k_{\text{cat}} = 288 \text{ s}^{-1}$; $k_{\text{cat}}/K_{\text{M}} = 7.2 \cdot 10^6 \text{ s}^{-1}/\text{M}^{-1}$) (Delvaux *et al.* 2011). Moreover, it was later shown that the *A. thaliana* CYTH enzyme, the only plant member of this family characterized until now, was also a specific PPPase (Moeder *et al.* 2013) and its knock-down seems to negatively impact root development. It is intriguing to find that certain organisms (*N. europaea* and *A. thaliana* for instance) contain a highly specific PPPase. Would this imply that the substrate may be formed *in vivo*? Actually, its existence in free form has never been demonstrated in living organisms. From a chemical point of view, PPP_i is extremely difficult to determine and existing methods lack sensitivity, but it seems that it could exist at low concentrations (< 1 μM) in *E. coli* (Kohn *et al.* 2012).

While ThTP is known to exist in most cells in low amounts (< 1% of total thiamine), some animal cells seem to accumulate it to as much as 70-90% of total thiamine. These are for instance *E. electricus* electric organ (Bettendorff *et al.* 1987), chicken skeletal muscle (Shioda *et al.* 1991) or pig skeletal muscle (Egi *et al.* 1986). *E. electricus* and pig skeletal have an extremely low ThTPase activity while, as mentioned above, the enzyme is absent in birds. Hence, there seems to be a clear inverse relationship between ThTPase activity and ThTP content of the cells,

suggesting that intracellular ThTP concentrations are controlled by ThTPase. Note that in mouse tissues ThTPase activity is very high and ThTP is nearly undetectable, while in human tissues ThTPase activity is lower and ThTP represents from 1 % of total thiamine in the brain to 5 % in muscles (Gangolf *et al.* 2010).

How about ThTP synthesis? The mechanism of ThTP synthesis has been studied for many years and it became clear that there are at least two mechanisms (Bettendorff *et al.* 2014). It was shown by Kawasaki and colleagues that adenylate kinase 1 (myokinase) is able to synthesize ThTP according to the reaction $\text{ThDP} + \text{ADP} \rightleftharpoons \text{ThTP} + \text{AMP}$ (Shikata *et al.* 1989). The reaction is very slow, but might be sufficient to accumulate ThTP in tissues such as electric organs, pig and chicken skeletal muscles where adenylate kinase is abundant and ThTPase activity is very low or absent. Only recently it became clear that in mammalian brain ThTP is synthesized by F_0F_1 ATP-synthase by a mechanism similar to ATP (Gangolf *et al.* 2010). We are facing the paradoxical condition, where an energy-rich compound is synthesized by two mechanisms dedicated to ATP synthesis, but on the other hand there is a very specific enzymes (at least in animals) for its hydrolysis, thereby controlling its intracellular concentration.

In *E. coli*, the situation is not more obvious. In contrast to mammalian cells where ThTP concentrations seem to be in a steady state with little variations, in *E. coli* ThTP may accumulate under specific conditions of amino acid starvation. While it was shown that, as in mammalian brain, ThTP is synthesized by F_0F_1 ATP-synthase (Gigliobianco *et al.* 2013), no specific ThTPase has been characterized in bacteria and ThTPase activities are low in *E. coli* extracts (Nishimune and Hayashi, 1987).

The fact that ThTP is present in most organisms raises the question of its possible physiological role, which is one of the issues we wanted to investigate in the present work. One way to do this would be to manipulate intracellular ThTP concentrations by over- or down-regulating its synthesizing or its hydrolyzing enzymes.

Adenylate kinase 1 knock-out mice have normal ThTP levels (Makarchikov *et al.* 2002) and the knock-down of F_0F_1 ATP-synthase would be lethal because of its impact on ATP synthesis. Therefore we decided to manipulate ThTPase expression. Before our arrival in the laboratory, a transgenic mouse overexpressing bovine ThTPase had been produced with the aim of reducing the cellular ThTP content. However, ThTP levels remained normal (already very low because of the high activity of endogenous ThTPase) and no particular phenotype was observed

(Bettendorff *et al.* 2014). The other alternative, finally adopted was to create a transgenic mouse invalidated in endogenous ThTPase.

Possible biological role(s) of tripolyphosphate

In the first part of our work we focused on the PPP_i issue. As specific PPPases (all from the CYTH family) have been shown to exist, we wanted to check whether animal cells contain specific PPPases (remember that the animal CYTH protein is a specific ThTPase). Moreover, *E. coli* CYTH protein, ygiF, has not been previously characterized and we wanted to check whether it has any PPPase activity.

We were surprised to find high PPPase activities in all mouse tissues tested as well as in *E. coli* supernatants. After purification and sequencing we could identify the enzyme prune (an exopolyphosphatase targeting the short-chain polyphosphate) as the main enzyme responsible for PPPase hydrolysis in mammalian tissues. We also showed that the bacterial ygiF is a specific PPPase, but most of PPPase hydrolysis in *E. coli* supernatants is due to inorganic pyrophosphatase (PPase). As PPPase activity is 500 times lower than its PPase activity (Yoshida *et al.* 1982) it remains to be seen whether PPP_i is efficiently hydrolyzed *in vivo*.

It is well known that long-chain polyphosphates (> 100 units) accumulate in *E. coli* but also in mammalian cells where they may have various physiological roles, among which is energy storage (Akiyama *et al.* 1993). It is also known how these polyphosphates can be shortened or elongated. However it is not known if and how they are formed *de novo*. We can hypothesize that phosphorylation of PP_i could form PPP_i which could act as a precursor for the *de novo* formation of new polyphosphate molecules.

On the other hand, PPP_i has a very high affinity for Ca^{2+} and it is well-known that calcium phosphates are highly insoluble salts. Hence, accumulation of PPP_i inside cells would chelate Ca^{2+} ions and therefore interfere with its very important role as a second messenger in cell-signaling processes. High PPPase activity would thus contribute to protect cells from the toxic effects of PPP_i formed by side metabolic reactions (possibly degradation of polyphosphates). It is difficult to have a final answer concerning the possible physiological role of PPP_i in the absence of a clear idea of its intracellular concentrations. This would require the development of sensitive analytical tools.

Role of ThTP and the 25-kDa ThTPase in animal tissues

The second part of our work was focused on the ThTP/ThTPase couple using three different approaches:

- Expression of mammalian ThTPase in *E. coli* in order to prevent ThTP accumulation during amino acid starvation;
- Inactivation of ThTPase in the zebrafish using morpholinos;
- Production of a ThTPase knock-out mouse.

As *E. coli* cells produce ThTP only under specific conditions of amino acid starvation it was hypothesized that this compound may be important for adaptation to stress conditions (Lakaye *et al.* 2004c). Hence, if we prevent ThTP accumulation under these conditions by expression of the ThTP-hydrolyzing mouse ThTPase, we should observe a slow-down of bacterial growth. This was however not observed and the growth of the bacteria under these conditions was not different from bacteria expressing a mutated ThTPase without enzymatic activity. This could suggest that ThTP accumulation is a side-reaction of F_0F_1 ATP-synthase and that the compound has no physiological role. On the other hand ThTP accumulation occurs only under very specific conditions of amino acid starvation: it requires a carbon source leading to pyruvate oxidation. This is understandable as F_0F_1 ATP-synthase requires a transmembrane proton gradient. This condition is however not sufficient as malate oxidation by malate dehydrogenase does not lead to ThTP production. It came as a surprise that some polycarboxylic Krebs cycle intermediates are potent physiological inhibitors of F_0F_1 ATP-synthase in animals (Chin *et al.* 2014). We tested octyl- α -ketoglutarate, a diffusible analog of α -ketoglutarate, on ThTP synthesis in *E. coli*. This compound indeed inhibited ThTP synthesis. Therefore, ThTP synthesis in *E. coli* requires an oxidizable carbon source to energize F_0F_1 ATP-synthase, but the situation is more complicated and the difference between pyruvate and malate may arise from the fact that pyruvate, a monocarboxylate, is not an inhibitor of F_0F_1 ATP-synthase, while malate, a dicarboxylate, is an inhibitor of this enzyme complex. The observation that ThTP accumulation only occurs under amino acid starvation may be due to the fact that amino acids (most bacterial culture media contain high concentrations of amino acids) are channeled towards glutamate, which yields α -ketoglutarate inhibiting ThTP synthesis by F_0F_1 ATP-synthase.

In a second approach, we wanted to down-regulate the endogenous ThTPase in zebrafish embryos using morpholinos. In the zebrafish embryo, the ThTPase transcript is present in the egg as soon as it is laid and at least till 48 hour post-fertilization (hpf). We induced a decrease of the spliced ThTPase transcript by the injection of morpholino oligonucleotides in the eggs. The different developmental defects observed were rather severe but relatively unspecific. The normal phenotype was restored by the injection of the mRNA coding for the zThTPase. Moreover, when the K61A zThTPase mRNA, yielding a transcript without enzymatic activity, was co-injected with the morpholino, no phenotype restoration was observed. Thus, even if morpholinos are more and more questioned in the literature, we are quite confident in the results obtained showing that reduction of the zThTPase expression alters the normal development of the fish. Unfortunately, for technical reasons, it has not been possible to assess the increase of the ThTP levels.

In order to have a better insight in the role of the ThTPase in the developing embryos and in the adult fish, a knock-out of the zThTPase would be interesting and could be achieved using the CRISPR-Cas technology, which is now more and more routinely used in laboratories. However, in view of the results we obtained with the mouse knock-out, it is possible that this mutant will not be able to reproduce.

In the last part of our work, we attempted to produce a ThTPase knock-out mouse strain. We obtained the embryonic stem (ES) cells from the KOMP repository and produced chimerae with respect to the ThTPase gene. However, after crossing the chimerae, we were unable to obtain a single heterozygous pup, suggesting that ThTPase-null sperm were either not viable or unable to fertilize an oocyte. We showed that, in the sperm cells collected from the epididymis and the *ductus deferens*, only 1 in 100 - 1000 sperm contained the ThTPase-null mutation. It therefore appears that ThTPase-null sperm probably have an incomplete spermatogenesis or else have a high death rate.

Our results show that the strategy of producing a conventional knock-out is probably doomed for failure. This issue can be bypassed by generating a conditional knock-out. In the case of a conditional knock-out, the gene is not deleted but a coding region of the gene is flanked by two LoxP sequences introduced in the non-coding region of the gene. Those small sequences (34 bp) allow the excision of the sequence present between them by the Cre-recombinase (Hamilton and Abremski, 1984).

This approach was not considered initially because (1) we did not expect such a drastic effect of the ThTPase deletion; (2) the ThTPase gene is composed of only two exons. In a classical conditional knock-out protocol, the coding region targeted by the deletion would be chosen so that the LoxP sequences are not added into the 3' or 5' untranslated region (UTR) but in the intron to avoid a modification of the cis regulatory elements present in those regions (promotor, polyadenylation sequence,...). In a gene containing only two exons, this is impossible. Moreover, in the case of the ThTPase, most of the coding sequence is in the first exon, thus one of the LoxP sites, has to be in the promotor region and we cannot exclude that it would affect the ThTPase expression. Nonetheless, a classical KO could not be obtained so the production of a conditional knock-out should be considered.

As it had not been possible to separate ThTPase-null from WT sperm, we were unable to measure intracellular ThTP levels. However, we know that mouse ThTPase is an extremely efficient and specific enzyme, even when ThTP is present at low concentrations ($k_{cat}/K_M = 7.2 \cdot 10^6 \text{ s}^{-1}/\text{M}^{-1}$). Thus, we can assume that in WT sperm it is efficiently hydrolyzed.

Taken together, our results obtained on the zebrafish and mouse models suggest that ThTPase deficiency leads to serious problems in embryo development in the first and spermatogenesis in the second. This is probably due to decreased hydrolysis of ThTP, though we were unable to prove it unambiguously. It is thus possible that ThTP accumulation might lead to toxic effects. It was previously shown that ThTP can activate high conductance anion channels present in plasma membranes (Bettendorff *et al.* 1993) and phosphorylate proteins (Nghiem *et al.* 2000). Hence, ThTP could be viewed as a toxic by-product of metabolism and CYTH enzymes would have evolved towards ThTPase activity in animals as part of a metabolite damage control system (Linster *et al.* 2013). An alternative hypothesis suggested by Linster *et al.* in 2013 would be that ThTP synthesis by cytosolic adenylate kinase 1 and mitochondrial F_0F_1 ATP-synthase would remove the essential cofactor ThDP and trap it in a catalytically inactive form.

This might be true in some cases but on the other hand:

- ThDP is generally largely in excess compared to what is required as cofactor. During thiamine deficiency neurological symptoms appear when ThDP levels are reduced by $\geq 70 \%$.
- Pig ThTPase is largely inactive (Szyniarowski *et al.* 2005) and as a result ThTP accounts for a much higher proportion of total thiamine than in other mammals. It

could be argued that pigs were artificially selected for generations by man to increase profitability and we cannot exclude that, while they were becoming a fatter and faster breeding strain, they acquired a resistance to ThTP and ThTPase mutated towards an inefficient form. To assess this theory, it would be interesting to analyze the tissues of wild boar for instance, and measure the ThTP levels and ThTPase activity.

- Birds have no ThTPase at all, leading to high intracellular ThTP concentrations. The whole region of the human chromosome 14 containing the ThTPase gene as well as 29 other genes has been lost. Indeed, the 30 selected genes in that region are present in the mouse genome, while 26 are still found in the lizard *A. carolinensis*, but none of them in the bird genomes available so far. Sequencing of the genome of the American alligator showed the presence of the ThTPase gene in this species too. Therefore, it seems that this gene was selectively lost in the branch leading to dinosaurs and birds.
- In *E. coli*, ThTP may accumulate under specific metabolic conditions without apparent harm. No specific ThTPase is present in *E. coli*.

Considering all these data we cannot exclude the hypothesis that ThTP may be a toxic by-product of metabolism, at least in vertebrates. The shift in the activities of the enzymes of the CYTH superfamily throughout evolution from specific PPPases (*N. europaea*, *E. coli*, *A. thaliana*) to specific ThTPases (animals) could thus be viewed as an adaptation to cope with increasing sensitivity of the organisms to ThTP toxicity, while some organisms (e.g. birds and domestic pigs) acquired ThTP resistance.

We cannot help wondering which processes would be so sensitive to ThTP. This first hypothesis that comes to mind would implicate F_0F_1 ATP-synthase, the enzyme responsible for mitochondrial ThTP synthesis. However, ThTPase being cytosolic will not prevent accumulation of ThTP inside mitochondria and *E. coli* F_0F_1 ATP-synthase seems to be insensitive to ThTP. The other ThTP-synthesizing enzyme, adenylate kinase 1, has a very low affinity for ThTP compared to ATP and intracellular ThTP concentrations are orders of magnitude lower than ATP concentrations suggesting that even if ThTP accumulates to some extent, it will not inhibit adenylate kinase 1. However, the fact that ThTP and ATP metabolism are so intimately entangled nonetheless suggests that ThTP might interfere with ATP-dependent process.

Bibliography

Bibliography

- Abramov AY, Fraley C., Diao CT, Winkfein R., Colicos MA, Duchon MR, French RJ, Pavlov E. 2007. Targeted polyphosphatase expression alters mitochondrial metabolism and inhibits calcium-dependent cell death. *Proc. Natl. Acad. Sci. U.S.A.* 104 (46) 18091-6.
- Ahn K., Kornberg A. 1992. Polyphosphate kinase from *Escherichia coli*. Purification and demonstration of a phosphoenzyme intermediate. *J. Biol. Chem.* 265 (20) 11734-9.
- Akiyama M., Crooke E., Kornberg A. 1992. The polyphosphate kinase gene of *Escherichia coli*. Isolation and sequence of the *ppk* gene and membrane location of the protein. *J. Biol. Chem.* 267 (31) 22556-61.
- Akiyama M., Crooke E., Kornberg A. 1993. An exopolyphosphatase of *Escherichia coli*. The enzyme and its *ppx* gene in a polyphosphate operon. *J. Biol. Chem.* 268 (1) 633-9.
- Aravind L., Koonin EV. 1998. A novel family of predicted phosphoesterases includes *Drosophila* prune protein and bacterial RecJ exonuclease. *Trends Biochem. Sci.* 23 (1) 17-9.
- Ault-Riché D., Fraley CD, Tzeng CM, Kornberg A. 1998. Novel assay reveals multiple pathways regulating stress-induced accumulations of inorganic polyphosphate in *Escherichia coli*. *J. Bacteriol.* 180 (7) 1841-7.
- Avaeva S., Ignatov P., Kurilova S., Nazarova T., Rodina E., Vorobyeva N., Oganessyan V., Harutyunyan E. 1996. *Escherichia coli* inorganic pyrophosphatase: site-directed mutagenesis of the metal binding sites. *FEBS Lett.* 399 (1-2) 99-102.
- Bettendorff L., Schoffeniels E. 1987. Thiamine triphosphatase activities and bioelectrogenesis. *Bull. Mem. Acad. R. Med. Belg.* 142 (2-3) 228-36.
- Bettendorff L., Peeters M., Jouan C., Wins P., Schoffeniels E. 1991. Determination of thiamin and its phosphate esters in cultured neurons and astrocytes using an ion-pair reversed-phase high-performance liquid chromatographic method. *Anal. Biochem.* 198 (1) 52-9.
- Bettendorff L., Kolb HA, Schoffeniels E. 1993. Thiamine triphosphate activates an anion channel of large unit conductance in neuroblastoma cells. *J. Membr. Biol.* 136 (3) 281-8.
- Bettendorff L., Nghiê m HO, Wins P., Lakaye B. 2003. A general method for the chemical synthesis of gamma-32P-labeled or unlabeled nucleoside 5(')-triphosphates and thiamine triphosphate. *Anal. Biochem.* 322 (2) 190-7.
- Bettendorff L., Wirtzfeld B., Makarchikov AF, Mazzucchelli G., Frédéric h M., Gigliobianco T., Gangolf M., De Pauw E., Angenot L., Wins P. 2007. Discovery of a natural thiamine adenine nucleotide. *Nat. Chem. Biol.* 3 (4) 211-2.
- Bettendorff, L. (2012). Chapter 5: The chemistry, biochemistry and metabolism of thiamin (vitamin B1). In *B Vitamins and Folate: Chemistry, Analysis, Function and Effects (Food and Nutritional Components in Focus No 4*, pp. 71-92). Cambridge: RSC Publishing.

Bibliography

- Bettendorff L., Wins P. 2013. Thiamine triphosphatase and the CYTH superfamily of proteins. *FEBS J.* 280 (24) 6443-55. doi: 10.1111/febs.12498.
- Bettendorff L., Lakaye B., Kohn G., Wins P. 2014. Thiamine triphosphate: a ubiquitous molecule in search of a physiological role. *Metab. Brain Dis.* 29 (4) 1069-82. doi: 10.1007/s11011-014-9509-4. (Appendix 4)
- Blank L., Green J., Guest JR. 2002. AcnC of *Escherichia coli* is a 2-methylcitrate dehydratase (PrpD) that can use citrate and isocitrate as substrates. *Microbiology.* 148 (Pt 1) 133-46.
- Chang DM. 1983. The binding of free calcium ions in aqueous solution using chelating agents, phosphates and poly(acrylic acid). *JAOCS* 60: 618-622.
- Chin RM, Fu X., Pai MY, Vergnes L., Hwang H., Deng G., Diep S., Lomenick B., Meli VS, Monsalve GC, Hu E., Whelan SA, Wang JX, Jung G., Solis GM, Fazlollahi F., Kaweeteerawat C., Quach A., Nili M., Krall AS, Godwin HA, Chang HR, Faull KF, Guo F., Jiang M., Trauger SA, Saghatelian A., Braas D., Christofk HR, Clarke CF, Teitell MA, Petrascheck M., Reue K., Jung ME, Frand AR, Huang J. 2014. The metabolite α -ketoglutarate extends lifespan by inhibiting ATP synthase and TOR. *Nature.* 510 (7505) 397-401. doi: 10.1038/nature13264.
- Choi WY, Giraldez AJ, Schier AF. 2007. Target protectors reveal dampening and balancing of Nodal agonist and antagonist by miR-430. *Science.* 318 (5848) 271-4.
- D'Angelo A., Garzia L., André A., Carotenuto P., Aglio V., Guardiola O., Arrigoni G., Cossu A., Palmieri G., Aravind L., Zollo M. 2004. Prune cAMP phosphodiesterase binds nm23-H1 and promotes cancer metastasis. *Cancer Cell.* 5 (2) 137-49.
- Delvaux D., Murty MR, Gabelica V., Lakaye B., Lunin VV, Skarina T., Onopriyenko O., Kohn G., Wins P., De Pauw E., Bettendorff L. 2011. A specific inorganic triphosphatase from *Nitrosomonas europaea*: structure and catalytic mechanism. *J. Biol. Chem.* 286 (39) 34023-35. doi: 10.1074/jbc.M111.233585. (Appendix 1)
- Delvaux D. 2012. Thèse de doctorat. Mécanisme catalytique et structure des enzymes de la superfamille CYTH. pp. 112
- Delvaux D., Kerff F., Murty MR, Lakaye B., Czerniecki J., Kohn G., Wins P., Herman R., Gabelica V., Heuze F., Tordoir X., Marée R., Matagne A., Charlier P., De Pauw E., Bettendorff L., 2013. Structural determinants of specificity and catalytic mechanism in mammalian 25-kDa thiamine triphosphatase. *Biochim. Biophys. Acta* 1830 (10) 4513-23. doi: 10.1016/j.bbagen.2013.05.014. (Appendix 3)
- Derosier DJ, Oliver RM, Reed LJ. 1971 Crystallization and preliminary structural analysis of dihydrolipoyl transsuccinylase, the core of the 2-oxoglutarate dehydrogenase complex. *Proc. Natl. Acad. Sci. U.S.A.* 68 (6) 1135-7.
- Draper BW, Morcos PA, Kimmel CB. 2001. Inhibition of zebrafish fgf8 pre-mRNA splicing with morpholino oligos: a quantifiable method for gene knockdown. *Genesis.* 30 (3) 154-6.

Bibliography

- Egi Y., Koyama S., Shikata H., Yamada K., Kawasaki T. 1986. Content of thiamin phosphate esters in mammalian tissues--an extremely high concentration of thiamin triphosphate in pig skeletal muscle. *Biochem. Int.* 12 (3) 385-90.
- Ekker SC. 2000. Morphants: a new systematic vertebrate functional genomics approach. *Yeast.* 17 (4) 302-306.
- Feeney MA, Veeravalli K., Boyd D., Gon S., Faulkner MJ, Georgiou G., Beckwith J. 2011. Repurposing lipoic acid changes electron flow in two important metabolic pathways of *Escherichia coli*. *Proc. Natl. Acad. Sci. U.S.A.* 108 (19) 7991-6. doi: 10.1073/pnas.1105429108.
- Frédérich M., Delvaux D., Gigliobianco T., Gangolf M., Dive G., Mazzucchelli G., Elias B., De Pauw E., Angenot L., Wins P., Bettendorff L. 2009. Thiaminylated adenine nucleotides. Chemical synthesis, structural characterization and natural occurrence. *FEBS J.* 276 (12) 3256-68. doi: 10.1111/j.1742-4658.2009.07040.x.
- Gangolf M., Wins P., Thiry M., El Moualij B., Bettendorff L. 2010. Thiamine triphosphate synthesis in rat brain occurs in mitochondria and is coupled to the respiratory chain. *J. Biol. Chem.* 285 (1) 583-94. doi: 10.1074/jbc.
- Gigliobianco T., Lakaye B., Makarchikov AF, Wins P., Bettendorff L. 2008. Adenylate kinase-independent thiamine triphosphate accumulation under severe energy stress in *Escherichia coli*. *BMC Microbiol.* 8:16. doi: 10.1186/1471-2180-8-16.
- Gigliobianco T., Lakaye B., Wins P., El Moualij B., Zorzi W., Bettendorff L. 2010. Adenosine thiamine triphosphate accumulates in *Escherichia coli* cells in response to specific conditions of metabolic stress. *BMC Microbiol.* 10:148. doi: 10.1186/1471-2180-10-148.
- Gigliobianco T., Gangolf M., Lakaye B., Pirson B., von Ballmoos C., Wins P., Bettendorff L. 2013. An alternative role of FoF1-ATP synthase in *Escherichia coli*: synthesis of thiamine triphosphate. *Sci. Rep.* 3 1071. doi: 10.1038/srep01071.
- Gong C., Martins A., Shuman S. 2003. Structure-function analysis of *Trypanosoma brucei* RNA triphosphatase and evidence for a two-metal mechanism. *J. Biol. Chem.* 278 (51) 50843-52.
- Gong C., Smith P., Shuman S. 2006. Structure-function analysis of *Plasmodium* RNA triphosphatase and description of a triphosphate tunnel metalloenzyme superfamily that includes Cet1-like RNA triphosphatases and CYTH proteins. *RNA.* 12 (8) 1468-74.
- Gruer MJ, Guest JR. 1994. Two genetically-distinct and differentially-regulated aconitases (AcnA and AcnB) in *Escherichia coli*. *Microbiology.* 140 (Pt 10) 2531-41.
- Grzegorski SJ, Chiari EF, Robbins A., Kish PE, Kahana A. 2014. Natural variability of Kozak sequences correlates with function in a zebrafish model. *PLoS One.* 9 (9) e108475.

Bibliography

- Hailes HC., Rother D., Müller M., Westphal R., Ward JM, Pleiss J., Vogel C., Pohl M. 2013. Engineering stereoselectivity of ThDP-dependent enzymes. *FEBS J.* 280 (24) 6374-94. doi: 10.1111/febs.12496.
- Hamilton DL, Abremski K. 1984. Site-specific recombination by the bacteriophage P1 lox-Cre system. Cre-mediated synapsis of two lox sites. *J. Mol. Biol.* 178 (2) 481-6.
- Hannum DM, Barrette WC Jr, Hurst JK. 1995. Subunit sites of oxidative inactivation of *Escherichia coli* F1-ATPase by HOCl. *Biochem. Biophys. Res. Commun.* 212 (3) 868-74.
- Hashitani Y., Cooper JR. 1972. The partial purification of thiamine triphosphatase from rat brain. *J. Biol. Chem.* 247 (7) 2117-9.
- Hudziak RM, Barofsky E., Barofsky DF, Weller DL, Huang SB, Weller DD. 1996. Resistance of morpholino phosphorodiamidate oligomers to enzymatic degradation. *Antisense Nucleic Acid Drug Dev.* 6 (4) 267-72.
- Iyer LM, Aravind L. 2002. The catalytic domains of thiamine triphosphatase and CyaB-like adenylyl cyclase define a novel superfamily of domains that bind organic phosphates. *BMC Genomics.* 3 (1) 33.
- Jain R, Shuman S. 2008. Polyphosphatase activity of CthTTM, a bacterial triphosphate tunnel metalloenzyme. *J. Biol. Chem.* 283: 31047-31057.
- Josse J. 1966. Constitutive inorganic pyrophosphatase of *Escherichia coli*. 1. Purification and catalytic properties. *J. Biol. Chem.* 241 (9) 1938-47.
- Keppetipola N., Jain R., Shuman S. 2007. Novel triphosphate phosphohydrolase activity of *Clostridium thermocellum* TTM, a member of the triphosphate tunnel metalloenzyme superfamily. *J. Biol. Chem.* 282 (16) 11941-9.
- Kimmel CB, Ballard WW, Kimmel SR, Ullmann B., Schilling TF. 1995. Stages of embryonic development of the zebrafish. *Dev. Dyn.* 203 (3) 253-310.
- King MT, Reiss PD, Cornell NW. 1988. Determination of short-chain coenzyme A compounds by reversed-phase high-performance liquid chromatography. *Methods Enzymol.* 166 70-9.
- Kloosterman WP, Lagendijk AK, Ketting RF, Moulton JD, Plasterk RH. 2007. Targeted inhibition of miRNA maturation with morpholinos reveals a role for miR-375 in pancreatic islet development. *PLoS Biol.* 5 (8) e203.
- Kohn G., Delvaux D., Lakaye B., Servais AC, Scholer G., Fillet M., Elias B., Derochette JM, Crommen J., Wins P., Bettendorff L. 2012. High inorganic triphosphatase activities in bacteria and mammalian cells: identification of the enzymes involved. *PLoS One.* 7 (9) e43879. doi: 10.1371/journal.pone.0043879. (Appendix 2)
- Kok FO, Shin M., Ni CW, Gupta A., Grosse AS, van Impel A., Kirchmaier BC, Peterson-Maduro J., Kourkoulis G., Male I., DeSantis DF., Sheppard-Tindell S., Ebarasi L., Betsholtz C., Schulte-Merker S., Wolfe SA, Lawson ND. 2015. Reverse genetic screening reveals poor correlation between morpholino-induced and mutant phenotypes in zebrafish. *Dev Cell.* 32 (1) 97-108. doi: 10.1016/j.devcel.2014.11.018.

Bibliography

- Kornberg SR, Lehman IR, Bessman MJ, Simms ES, Kornberg A. 1958. Enzymatic cleavage of deoxyguanosine triphosphate to deoxyguanosine and triphosphosphate. *J. Biol. Chem.* 233 (1) 159-62.
- Kornberg A., Rao NN, Ault-Riché D. 1999. Inorganic polyphosphate: a molecule of many functions. *Annu. Rev. Biochem.* 68 89-125.
- Kukko-Kalske E., Lintunen M., Inen MK, Lahti R., Heinonen J. 1989. Intracellular P_{Pi} concentration is not directly dependent on amount of inorganic pyrophosphatase in *Escherichia coli* K-12 cells. *J. Bacteriol.* 171 (8) 4498-500.
- Kulaev I., Vagabov V., Kulakovskaya T. 1999. New aspects of inorganic polyphosphate metabolism and function. *J. Biosci. Bioeng.* 88 (2) 111-29.
- Kulaev, I., Vagabov, V. & Kulakovskai^a, T. (2004). The biochemistry of inorganic polyphosphates. Chichester, West Sussex Hoboken, NJ: J. Wiley.
- Kumble KD, Kornberg A. 1995. Inorganic polyphosphate in mammalian cells and tissues. *J. Biol. Chem.* 270 (11) 5818-22.
- Kumble KD, Kornberg A. 1996 Endopolyphosphatases for long chain inorganic polyphosphate in yeast and mammals. *J. Biol. Chem.* 271 (43) 27146-51.
- Kuroda A., Murphy H., Cashel M., Kornberg A. 1997. Guanosine tetra- and pentaphosphate promote accumulation of inorganic polyphosphate in *Escherichia coli*. *J Biol Chem.* 272 (34) 21240-3.
- Lakaye B., Makarchikov AF, Antunes AF, Zorzi W., Coumans B., De Pauw E., Wins P., Grisar T., Bettendorff L. 2002. Molecular characterization of a specific thiamine triphosphatase widely expressed in mammalian tissues. *J. Biol. Chem.* 277 (16) 13771-7.
- Lakaye B., Verlaet M., Dubail J., Czerniecki J., Bontems S., Makarchikov AF, Wins P., Piette J., Grisar T., Bettendorff L. 2004a. Expression of 25 kDa thiamine triphosphatase in rodent tissues using quantitative PCR and characterization of its mRNA. *Int. J. Biochem. Cell. Biol.* 36 (10) 2032-41.
- Lakaye B., Makarchikov AF, Wins P., Margineanu I., Roland S., Lins L., Aichour R., Lebeau L., El Moualij B., Zorzi W., Coumans B., Grisar T., Bettendorff L. 2004b. Human recombinant thiamine triphosphatase: purification, secondary structure and catalytic properties. *Int. J. Biochem. Cell. Biol.* 36 (7) 1348-64.
- Lakaye B., Wirtzfeld B., Wins P., Grisar T., Bettendorff L. 2004c. Thiamine triphosphate, a new signal required for optimal growth of *Escherichia coli* during amino acid starvation. *J. Biol. Chem.* 279(17) 17142-7.
- Lanzetta PA, Alvarez LJ, Reinach PS, Candia OA. 1979. An improved assay for nanomole amounts of inorganic phosphate. *Anal. Biochem.* 100 (1) 95-7.
- Lima CD, Wang LK, Shuman S. 1999. Structure and mechanism of yeast RNA triphosphatase: an essential component of the mRNA capping apparatus. *Cell.* 99 (5) 533-43.

Bibliography

- Lindhurst MJ, Fiermonte G., Song S., Struys E., De Leonardis F., Schwartzberg PL, Chen A., Castegna A., Verhoeven N., Mathews CK, Palmieri F., Biesecker LG. 2006. Knockout of Slc25a19 causes mitochondrial thiamine pyrophosphate depletion, embryonic lethality, CNS malformations, and anemia. *Proc. Natl. Acad. Sci. U. S. A.* 103 (43) 15927-32.
- Linster CL, Noël G., Stroobant V., Vertommen D., Vincent MF, Bommer GT, Veigada-Cunha M., Van Schaftingen E. 2011. Ethylmalonyl-CoA decarboxylase, a new enzyme involved in metabolite proofreading. *J. Biol. Chem.* 286 (50) 42992-3003. doi: 10.1074/jbc.M111.281527.
- Lorenz MC, Fink GR. 2002. Life and death in a macrophage: role of the glyoxylate cycle in virulence. *Eukaryot. Cell.* 1 (5) 657-62.
- Lutz R., Bujard H. 1997. Independent and tight regulation of transcriptional units in *Escherichia coli* via the LacR/O, the TetR/O and AraC/I1-I2 regulatory elements. *Nucleic Acids Res.* 25 (6) 1203-10.
- Makarchikov AF, Chernikevich IP. 1992. Purification and characterization of thiamine triphosphatase from bovine brain. *Biochim. Biophys. Acta.* 1117 (3) 326-32.
- Makarchikov AF, Wins P., Janssen E., Wieringa B., Grisar T., Bettendorff L. 2002. Adenylate kinase 1 knockout mice have normal thiamine triphosphate levels. *Biochim. Biophys. Acta.* 1592 (2) 117-21.
- Makarchikov AF, Lakaye B., Gulyai IE, Czerniecki J., Coumans B., Wins P., Grisar T., Bettendorff L. 2003. Thiamine triphosphate and thiamine triphosphatase activities: from bacteria to mammals. *Cell. Mol. Life Sci.* 60 (7) 1477-88.
- Malandrinos G., Louloudi M., Hadjiliadis N. 2006. Thiamine models and perspectives on the mechanism of action of thiamine-dependent enzymes. *Chem. Soc. Rev.* 35 (8) 684-92.
- Manzetti S., Zhang J., van der Spoel D. 2014. Thiamin function, metabolism, uptake, and transport. *Biochemistry* 53 (5) 821-35. doi: 10.1021/bi401618y.
- Marbaix AY, Noël G., Detroux AM, Vertommen D., Van Schaftingen E., Linster CL. 2011. Extremely conserved ATP- or ADP-dependent enzymatic system for nicotinamide nucleotide repair. *J Biol Chem.* 286 (48) 41246-52. doi: 10.1074/jbc.C111.310847.
- Moeder W., Garcia-Petit C., Ung H., Fucile G., Samuel MA., Christendat D., Yoshioka K. 2013. Crystal structure and biochemical analyses reveal that the *Arabidopsis* triphosphate tunnel metalloenzyme AtTTM3 is a tripolyphosphatase involved in root development. *Plant J.* 76 (4) 615-26. doi: 10.1111/tpj.12325.
- Moreno B., Urbina JA, Oldfield E., Bailey BN, Rodrigues CO, Docampo R. 2000. ³¹P NMR spectroscopy of *Trypanosoma brucei*, *Trypanosoma cruzi*, and *Leishmania major*. Evidence for high levels of condensed inorganic phosphates. *J. Biol. Chem.* 275 (37) 28356-28362.

Bibliography

- Nghiêm HO, Bettendorff L., Changeux JP. 2000. Specific phosphorylation of Torpedo 43K rapsyn by endogenous kinase(s) with thiamine triphosphate as the phosphate donor. *FASEB J.* 14 (3) 543-54.
- Nishimune T., Hayashi R. 1987. Hydrolysis and synthesis of thiamin triphosphate in bacteria. *J Nutr. Sci. Vitaminol.* (Tokyo). 33 (2) 113-27.
- Pavlov E., Zakharian E., Bladen C., Diao CT, Grimbly C., Reusch RN, French RJ. 2005. A large, voltage-dependent channel, isolated from mitochondria by water-free chloroform extraction. *Biophys. J.* 88 (4) 2614-25.
- Pavlov E., Aschar-Sobbi R., Campanella M., Turner RJ, Gómez-García MR, Abramov AY. 2010. Inorganic polyphosphate and energy metabolism in mammalian cells. *J. Biol. Chem.* 285 (13) 9420-8. doi: 10.1074/jbc.M109.013011.
- Pepin CA, Wood HG. 1986. Polyphosphate glucokinase from *Propionibacterium shermanii*. Kinetics and demonstration that the mechanism involves both processive and nonprocessive type reactions. *J. Biol. Chem.* 261 (10) 4476-80.
- Pirson B. 2011. Mémoire de master en science biomédicales. Etude du mécanisme biochimique de synthèse du triphosphate de thiamine. pp. 51
- Pruvot B., Curé Y., Djiotsa J., Voncken A., Muller M. 2014. Developmental defects in zebrafish for classification of EGF pathway inhibitors. *Toxicol. Appl. Pharmacol.* 274 (2) 339-49. doi: 10.1016/j.taap.2013.11.006.
- Rexroth S., Poetsch A., Rögner M., Hamann A., Werner A., Osiewacz HD, Schäfer ER, Seelert H., Dencher NA. 2012. Reactive oxygen species target specific tryptophan site in the mitochondrial ATP synthase. *Biochim. Biophys. Acta.* 1817 (2) 381-7. doi: 10.1016/j.bbabi.2011.11.006.
- Russell GC, Guest JR. 1990. Overexpression of restructured pyruvate dehydrogenase complexes and site-directed mutagenesis of a potential active-site histidine residue. *Biochem. J.* 269 (2) 443-50.
- Schmajuk G., Sierakowska H., Kole R. 1999. Antisense oligonucleotides with different backbones. Modification of splicing pathways and efficacy of uptake. *J. Biol. Chem.* 274 (31) 21783-9.
- Shikata H., Koyama S., Egi Y., Yamada K., Kawasaki T. 1989. Cytosolic adenylate kinase catalyzes the synthesis of thiamin triphosphate from thiamin diphosphate. *Biochem. Int.* 18 (5) 933-41.
- Shintani T., Uchiumi T., Yonezawa T., Salminen A., Baykov AA, Lahti R., Hachimori A. 1998. Cloning and expression of a unique inorganic pyrophosphatase from *Bacillus subtilis*: evidence for a new family of enzymes. *FEBS Lett.* 439 (3) 263-6.
- Shioda T., Egi Y., Yamada K., Kawasaki T. 1991. Properties of thiamin triphosphate-synthesizing activity of chicken cytosolic adenylate kinase and the effect of adenine nucleotides. *Biochim. Biophys. Acta.* 1115 (1) 30-5.

Bibliography

- Simonović AD, Gaddameedhi S., Anderson MD. 2004. In-gel precipitation of enzymatically released phosphate. *Anal Biochem.* 334 (2) 312-7.
- Sismeiro O., Trotot P., Biville F., Vivares C., Danchin A. 1998. *Aeromonas hydrophila* adenylyl cyclase 2: a new class of adenylyl cyclases with thermophilic properties and sequence similarities to proteins from hyperthermophilic archaeobacteria. *J. Bacteriol.* 180 (13) 3339-44.
- Smith SA, Morrissey JH. 2008. Polyphosphate enhances fibrin clot structure. *Blood.* 112 (7) 2810-6. doi: 10.1182/blood-2008-03-145755.
- Song J., Bettendorff L., Tonelli M., Markley JL. 2008. Structural basis for the catalytic mechanism of mammalian 25-kDa thiamine triphosphatase. *J. Biol. Chem.* 283 (16) 10939-48. doi: 10.1074/jbc.M709675200.
- Spence R., Gerlach G., Lawrence C., Smith C. 2008. The behaviour and ecology of the zebrafish, *Danio rerio*. *Biol. Rev. Camb. Philos. Soc.* 83 (1) 13-34.
- Summerton J., Weller D. 1997. Morpholino antisense oligomers: design, preparation, and properties. *Antisense Nucleic Acid Drug Dev.* 7 (3) 187-95.
- Szyniarowski P., Lakaye B., Czerniecki J., Makarchikov AF, Wins P., Margineanu I., Coumans B., Grisar T., Bettendorff L. 2005. Pig tissues express a catalytically inefficient 25-kDa thiamine triphosphatase: insight in the catalytic mechanisms of this enzyme. *Biochim. Biophys. Acta.* 1725 (1) 93-102.
- Tallaksen CM, Sande A., Bøhmer T., Bell H., Karlsen J. 1993. Kinetics of thiamin and thiamin phosphate esters in human blood, plasma and urine after 50 mg intravenously or orally. *Eur. J. Clin. Pharmacol.* 44 (1) 73-8.
- Tammenkoski M., Koivula K., Cusanelli E., Zollo M., Steegborn C., Baykov AA, Lahti R. 2008. Human metastasis regulator protein H-prune is a short-chain exopolyphosphatase. *Biochemistry.* 47 (36) 9707-13. doi: 10.1021/bi8010847.
- Tanaka T., Yamamoto D., Sato T., Tanaka S., Usui K., Manabe M., Aoki Y., Iwashima Y., Saito Y., Mino Y., Deguchi H. 2011. Adenosine thiamine triphosphate (A_{Th}TP) inhibits poly(ADP-ribose) polymerase-1 (PARP-1) activity. *J. Nutr. Sci. Vitaminol (Tokyo).* 57 (2) 192-6.
- Taniguchi Y., Choi PJ, Li GW, Chen H., Babu M., Hearn J., Emili A., Xie XS. 2010. Quantifying *E. coli* proteome and transcriptome with single-molecule sensitivity in single cells. *Science.* 329 (5991) 533-8. doi: 10.1126/science.1188308.
- Taylor MF, Paulauskis JD, Weller DD, Kobzik L. 1996. In vitro efficacy of morpholino-modified antisense oligomers directed against tumor necrosis factor- α mRNA. *J. Biol. Chem.* 271 (29) 17445-52.
- Tsutsui K. 1986. Tripolyphosphate is an alternative phosphodonor of the selective protein phosphorylation of liver microsomal membrane. *J. Biol. Chem.* 261 (6) 2645-53.

Bibliography

- Vacaru AM, Unlu G., Spitzner M., Mione M., Knapik EW, Sadler KC. 2014. In vivo cell biology in zebrafish - providing insights into vertebrate development and disease. *J. Cell. Sci.* 127 (Pt 3) 485-95. doi: 10.1242/jcs.140194.
- Velluz L., Amiard G., Bartos J. 1948. Acide thiamine-triphosphorique. *C. R. Acad. Sci. (Paris)*. 226 735-736
- Wang SB, Murray CI, Chung HS, Van Eyk JE. 2013. Redox regulation of mitochondrial ATP synthase. *Trends Cardiovasc. Med.* 23 (1) 14-8. doi: 10.1016/j.tcm.2012.08.005.
- Weber W., Kewitz H. 1985. Determination of thiamine in human plasma and its pharmacokinetics. *Eur. J. Clin. Pharmacol.* 28 (2) 213-9.
- Westerfield, M. (2007). *The zebrafish book. A guide for the laboratory use of zebrafish (Danio rerio)*. 5th ed., Univ. of Oregon Press, Eugene
- Winter J., Jung S., Keller S., Gregory RI, Diederichs S. 2009. Many roads to maturity: microRNA biogenesis pathways and their regulation. *Nat. Cell Biol.* 11 (3) 228-34. doi: 10.1038/ncb0309-228.
- Wurst H., Kornberg A. 1994. A soluble exopolyphosphatase of *Saccharomyces cerevisiae*. Purification and characterization. *J. Biol. Chem.* 269 (15) 10996-1001.
- Yoshida C., Shah H., Weinhouse S. 1982. Purification and properties of inorganic pyrophosphatase of rat liver and hepatoma 3924A. *Cancer Res.* 42 (9) 3526-31.
- Zhang F., Qi Y., Zhou K., Zhang G., Linask K., Xu H. 2015. The cAMP phosphodiesterase Prune localizes to the mitochondrial matrix and promotes mtDNA replication by stabilizing TFAM. *EMBO Rep.* 16 (4) 520-7. doi: 10.15252/embr.201439636.
- Zyryanov AB, Shestakov AS, Lahti R, Baykov AA. 2002. Mechanism by which metal cofactors control substrate specificity in pyrophosphatase. *Biochem. J.* 367(Pt 3) 901-6.

Appendix 1

A Specific Inorganic Triphosphatase from *Nitrosomonas europaea*

STRUCTURE AND CATALYTIC MECHANISM^{*[5]}

Received for publication, March 17, 2011, and in revised form, August 9, 2011. Published, JBC Papers in Press, August 12, 2011, DOI 10.1074/jbc.M111.233585

David Delvaux^{†1}, Mamidanna R. V. S. Murty^{§2}, Valérie Gabelica^{§3}, Bernard Lakaye^{†3}, Vladimir V. Lunin^{¶4}, Tatiana Skarina[¶], Olena Onopriyenko[¶], Gregory Kohn[‡], Pierre Wins[‡], Edwin De Pauw[§], and Lucien Bettendorff^{‡5}

From the [†]GIGA-Neuroscience and the [§]GIGA Systems Biology and Chemical Biology, University of Liège, B-4000 Liège, Belgium and the [¶]Banting and Best Department of Medical Research, University of Toronto, Toronto, Ontario M5G 1L6, Canada

The CYTH superfamily of proteins is named after its two founding members, the CyaB adenylyl cyclase from *Aeromonas hydrophila* and the human 25-kDa thiamine triphosphatase. Because these proteins often form a closed β -barrel, they are also referred to as triphosphate tunnel metalloenzymes (TTM). Functionally, they are characterized by their ability to bind triphosphorylated substrates and divalent metal ions. These proteins exist in most organisms and catalyze different reactions depending on their origin. Here we investigate structural and catalytic properties of the recombinant TTM protein from *Nitrosomonas europaea* (*NeuTTM*), a 19-kDa protein. Crystallographic data show that it crystallizes as a dimer and that, in contrast to other TTM proteins, it has an open β -barrel structure. We demonstrate that *NeuTTM* is a highly specific inorganic triphosphatase, hydrolyzing tripolyphosphate (PPP_i) with high catalytic efficiency in the presence of Mg²⁺. These data are supported by native mass spectrometry analysis showing that the enzyme binds PPP_i (and Mg-PPP_i) with high affinity ($K_d < 1.5 \mu\text{M}$), whereas it has a low affinity for ATP or thiamine triphosphate. In contrast to *Aeromonas* and *Yersinia* CyaB proteins, *NeuTTM* has no adenylyl cyclase activity, but it shares several properties with other enzymes of the CYTH superfamily, e.g. heat stability, alkaline pH optimum, and inhibition by Ca²⁺ and Zn²⁺ ions. We suggest a catalytic mechanism involving a catalytic dyad formed by Lys-52 and Tyr-28. The present data provide the first characterization of a new type of phosphohydrolase (unrelated to pyrophosphatases or exopolyphosphatases), able to hydrolyze inorganic triphosphate with high specificity.

A large number of phosphohydrolases are able to hydrolyze triphosphorylated compounds, generally nucleoside triphosphates such as ATP or GTP. However, in 2002 we achieved the molecular characterization of a mammalian enzyme that specifically hydrolyzed thiamine triphosphate (ThTP),⁶ a compound unrelated to nucleotides (1). This 25-kDa soluble thiamine triphosphatase (ThTPase), which is involved in the regulation of cytosolic ThTP concentrations (2), has near absolute specificity for ThTP (it does not hydrolyze nucleotides) and a high catalytic efficiency. No sequence homology with other known mammalian proteins could be found.

Shortly thereafter, Iyer and Aravind (3) observed that the catalytic domains of human 25-kDa ThTPase (1) and CyaB adenylyl cyclase (AC2) from *Aeromonas hydrophila* (4) define a novel superfamily of domains that, according to these authors, should bind “organic phosphates.” This superfamily was called “CYTH” (CyaB-thiamine triphosphatase), and the presence of orthologs was demonstrated in all three superkingdoms of life. This suggested that CYTH is an ancient family of proteins and that a representative must have been present in the last universal common ancestor (LUCA) of all extant life forms. It was proposed (3) that this enzymatic domain might play a central role at the interface between nucleotide and polyphosphate metabolism, but this role remains largely undefined; in fact, the two structurally and enzymatically characterized members of the superfamily, AC2 and mammalian 25-kDa ThTPase, are likely to be secondary acquired activities, whereas other prokaryotic CYTH proteins would have performed more ancient and fundamental roles in organic phosphate and/or polyphosphate metabolism (3).

Using multiple alignments and secondary structure predictions, Iyer and Aravind (3) showed that the catalytic core of CYTH enzymes contained a novel $\alpha + \beta$ scaffold with six conserved acidic and four basic residues. At least four of the acidic

* This work was supported, in whole or in part, by National Institutes of Health Protein Structure Initiative Grant P50-GM62413-02 (to Alexei Savchenko (Banting and Best Department of Medical Research, University of Toronto, Toronto, Ontario, M5G 1L6, Canada). This work was also supported by Grants 2.4558.04 and 2.4508.10 from the Fonds de la Recherche Fondamentale Collective of the Fonds de la Recherche Scientifique (to L. B., E. D. P., and B. L.).

[5] The on-line version of this article (available at <http://www.jbc.org>) contains Supplemental Tables S1 and S2 and Figs. S1–S6.

¹ A research fellow of the Fonds pour la Formation à la Recherche dans l'Industrie et dans l'Agriculture.

² Present address: National Centre for Mass Spectrometry, Indian Institute of Chemical Technology, Uppal Rd., Tarnaka, Hyderabad-500607, India.

³ Research Associates of the Fonds de la Recherche Scientifique.

⁴ Present address: Biosciences Center, National Renewable Energy Laboratory, 1617 Cole Blvd. MS 3323 Golden, CO 80401.

⁵ Research Director of the Fonds de la Recherche Scientifique. To whom correspondence should be addressed: Unit of Bioenergetics and cerebral excitability, GIGA-Neurosciences, University of Liège, Avenue de l'Hôpital, 1, 4000 Liège, Belgium. Tel.: 32-4-366-59-67; Fax: 32-4-366-59-53; E-mail: L.Bettendorff@ulg.ac.be.

⁶ The abbreviations used are: ThTP, thiamine triphosphate; ThTPase, thiamine triphosphatase; AC, adenylyl cyclase; Gp₄, guanosine 5'-tetrakisphosphate; P₄, inorganic tetraphosphate; PPPase, inorganic triphosphatase; PPP_i, inorganic triphosphate; TTM, triphosphate tunnel metalloenzyme; *NeuTTM*, *N. europaea* TTM; *CthTTM*, *C. thermocellum* TTM; TAPS, 3-[2-hydroxy-1,1-bis(hydroxymethyl)ethyl]amino]-1-propanesulfonic acid; CHES, 2-(cyclohexylamino)ethanesulfonic acid.

A Specific Inorganic Triphosphatase from *N. europaea*

residues (generally glutamate) are likely to chelate divalent cations required for catalysis, as is the case for adenylyl cyclases, DNA polymerases, and some phosphohydrolases (3, 5, 6).

More recently and independently of those bioinformatic studies, Shuman and co-workers (7) pointed out that RNA triphosphatases of fungi and protozoa exhibit striking similarities with bacterial and archaeal proteins of unknown function that belong to the CYTH superfamily. Although the primary structure conservation is low, the active site folds of the Cet1 RNA triphosphatase from *Saccharomyces cerevisiae* (8) and of several prokaryotic CYTH proteins are remarkably similar; in both cases, an eight-strand antiparallel β -barrel forms a topologically closed tunnel, and triphosphorylated substrates as well as divalent cation activators bind in the hydrophilic cavity. Therefore, Shuman and co-workers (7) called these proteins "triphosphate tunnel metalloenzymes" (TTM). They assumed that TTM was a larger superfamily including Cet1-like and CYTH proteins.

However, it is not established that all members of the CYTH superfamily exhibit the closed tunnel conformation. For instance, the 25-kDa mouse ThTPase has an open cleft structure when free in solution, whereas the enzyme-ThTP complex has a more closed, tunnel-like conformation (9). This suggests that the CYTH domain may be a versatile fold, both structurally and functionally.

Despite the presence of orthologs in most organisms, the general significance of CYTH enzymes remains a matter of conjecture. In unicellular eukaryotes, the essential role of RNA triphosphatases in RNA capping is clearly defined. But, like ThTPase activity in mammals, this is probably a secondary adaptation. In bacteria, two CYTH proteins, from *A. hydrophila* (4) and *Yersinia pestis* (10, 11) are considered as a particular class of adenylyl cyclases (class IV, CyaB), but this enzyme activity was found to be significant only under rather extreme conditions (50–60 °C and pH around 10). In addition, a more efficient class I adenylyl cyclase is also present in *A. hydrophila* (4) and *Y. pestis* (11). Archaeal and bacterial CYTH proteins have since been annotated as hypothetical (CyaB-like) adenylyl cyclases.

However, a bacterial CYTH ortholog from *Clostridium thermocellum* was recently shown to be completely devoid of adenylyl cyclase activity (12). The enzyme, which was characterized by Shuman and co-workers (12, 13) in considerable detail had a rather broad substrate specificity. It hydrolyzed guanosine 5'-tetraphosphate (Gp_4), inorganic triphosphate (triphosphosphate (PPP_i)), and to a lesser extent nucleoside triphosphates and long-chain polyphosphates (12, 13).

In 2005 we obtained the three-dimensional crystal structure of the *Nitrosomonas europaea* CYTH ortholog (*NeuTTM*), the hypothetical protein NE1496 (Protein Data Bank code 2FBL); although labeled as a TTM (12), it exhibits a C-shaped cup conformation, or incomplete β -barrel.

Because of the structural similarities between *NeuTTM* and mouse 25-kDa ThTPase (open cleft rather than closed tunnel), we considered the possibility that ThTP might be a good substrate for *NeuTTM*. Indeed, in *Escherichia coli*, ThTP may be involved in responses to environmental stress (15), but no specific bacterial ThTPase has been characterized so far. However,

the present data show that *NeuTTM* is actually devoid of significant ThTPase activity (as well as of adenylyl cyclase activity) but that *NeuTTM* has a strong preference and high affinity for PPP_i . Furthermore, we show that two residues that are highly conserved in CYTH proteins (Lys-52 and Tyr-28) are important for catalysis. This is the first characterization of a specific tripolyphosphatase (PPPase), raising the question of the existence and possible role of PPP_i in living cells.

EXPERIMENTAL PROCEDURES

Materials—Sodium tripolyphosphate (PPP_i), sodium cyclic triphosphate (trimetaphosphate), polyphosphate (sodium phosphate glass, 65 ± 5 residues), ATP, ITP, GTP, and guanosine 5'-tetraphosphate (Gp_4 , Tris salt) were from Sigma. ThTP was synthesized and purified as previously described (16). Tetraphosphate (P_4) (initially from Sigma) was a gift from Dr. Eric Oldfield, Dept. of Chemistry, University of Illinois, Urbana, IL. The pET15b vector for the expression of *NeuTTM* as a His-tag fusion protein was a gift from Dr. A. Savchenko, University of Toronto, Banting and Best Department of Medical Research, C. H. Best Institute, Toronto, Ontario, Canada).

Overexpression and Purification of *NeuTTM*—BL21(DE3) *E. coli* cells were transformed with a pET15b plasmid containing the sequence of *NeuTTM* with a His₆ sequence at the N-terminal side of the gene. Transformed bacteria were grown overnight at 37 °C in 2 ml of LB medium containing 500 μ g/ml ampicillin. Then the bacteria were cultured in 50–200 ml of 2 \times YT medium containing 250 μ g/ml ampicillin until A_{600} reached 0.6–0.8. Expression of the fusion protein was induced with isopropyl β -D-1-thiogalactopyranoside (1 mM). After 3 h of incubation at 37 °C, the bacterial suspension was centrifuged 15 min at $8000 \times g$ (4 °C). Bacteria were suspended in modified binding buffer (20 mM HEPES instead of phosphate buffer, 0.5 M NaCl, 30 mM imidazole, pH 7.5). After two cycles with a French press disruptor, the lysate was centrifuged 30 min at $50,000 \times g$. The tagged protein was purified on a FPLC system (ÄKTATM Purifier, Amersham Biosciences) coupled to a 5-ml HisTrapTM FF column (GE Healthcare) in the above-mentioned buffer. *NeuTTM* was then eluted in eluting buffer (20 mM HEPES, 0.5 M NaCl, 0.5 M imidazole, pH adjusted to 7.5 with 6 N HCl). Removal of the His tag was achieved by incubating 1 mg of the purified protein with 200 units of AcTEVTM protease (Invitrogen). After 2 h at room temperature, the mixture was purified on the HisTrap column to remove the released tag as well as the protease (also His-tagged). The purified untagged *NeuTTM* was recovered in the first fractions.

Crystallization, Data Collection, and Structure Solution—For crystallographic purposes, the *NeuTTM* gene was expressed as a selenomethionine-substituted protein using standard M9 high yield growth procedure according to the manufacturer's instructions (Shanghai Medicilon; catalogue number MD045004-50) with *E. coli* BL21(DE3) codon plus cells.

Crystals for the *NeuTTM* data collection were obtained with hanging drop vapor diffusion using a 24-well Linbro plate. 1 ml of well solution was added to the reservoir, and drops were made with 1 μ l of well solution and 1 μ l of protein solution. The crystals were grown at 20 °C using 3.5 M sodium formate as a precipitation agent and 0.1 M Bis-Tris propane buffer, pH 7.0.

TABLE 1

X-ray data collection and refinement statistics

Statistics for the highest resolution bin are in parentheses. r.m.s.d., root mean square deviation.

| | |
|--|--|
| Data collection | |
| Space group | P 3 ₂ 2 1 |
| Unit cell (Å, °) | $a = 52.28, b = 52.28, c = 252.48$ $\alpha = \beta = 90.0 \gamma = 120.0$ |
| Wavelength (Å) | 0.97959 |
| Temperature (K) | 100 |
| Resolution (Å) | 42.6–1.9 (1.95–1.9) |
| Observed reflections | 32,810 (2,358) |
| R_{int}^a | 0.057 (0.560) |
| Average redundancy | 6.7 (4.9) |
| $\langle I \rangle / \langle \sigma(I) \rangle$ | 20.5 (2.3) |
| Completeness, % | 99.7 (99.0) |
| Refinement | |
| R/R_{free} | 0.213 (0.304)/0.270 (0.358) |
| Protein atoms | 2424 |
| Water molecules | 324 |
| Other atoms | 20 |
| r.m.s.d. from ideal bond length (Å) ^b | 0.02 |
| r.m.s.d. from ideal bond angles ^b | 2.1° |
| Average B-factor for protein atoms (Å ²) | 30.3 |
| Average B-factor for water molecules (Å ²) | 39.8 |
| Ramachandran plot statistics (%) ^c | |
| Allowed | 100 |
| Favored | 98.3 |
| Outliers | 0 |

^a $R_{\text{int}} = \sum |I - \langle I \rangle| / \sum I$, where I is the intensity of an individual reflection, and $\langle I \rangle$ is the mean intensity of a group of equivalents, and the sums are calculated over all reflections with more than one equivalent measured.

^b From Ref. 23.

^c From Ref. 22.

The *NeuTTM* crystal was briefly dipped into a 5- μ l drop of cryoprotectant solution (3.8 M sodium formate, 0.2 M NaCl, 4% sucrose, 4% glycerol, 4% ethylene glycol, and 0.1 M Bis-Tris propane buffer, pH 7.0) before flash-freezing in liquid nitrogen. Data collection was performed at the 19-ID beamline at the Advanced Photon Source, Argonne National Laboratory. One dataset was collected using 0.97959 Å wavelength. Data were indexed and processed with the HKL-2000 package (17).

Intensities were converted into structure factors, and 5% of the reflections were flagged for R_{free} calculations using programs F2MTZ, Truncate, CAD, and Unique from the CCP4 package of programs (CCP4, 1994). The program BnP (18) was used for the determination of the selenium atom positions and phasing. ARP/wARP package (19) was used to build an initial model of the protein. Refinement and manual correction was performed using REFMAC5 (20) Version 5.5.0109 and Coot (21) Version 0.6. The final model included two protein chains (from residue 4 to residue 153 in chain A and from residue –1 to residue 153 in chain B), 3 molecules of ethylene glycol, 8 sodium ions, and 324 water molecules. The MOLPROBITY method (22) was used to analyze the Ramachandran plot and root mean square deviations of bond lengths, and angles were calculated from ideal values of Engh and Huber stereochemical parameters (23). Wilson B-factor was calculated using CTRUNCATE Version 1.0.11 (CCP4, 1994). The figures were created using PyMOL. The data collection and refinement statistics are shown in Table 1.

Native Electrospray Mass Spectrometry—Electrospray mass spectrometry experiments in native conditions (100 mM

ammonium acetate aqueous solution, pH 6.5) were carried out on a Q-TOF Ultima Global mass spectrometer (Waters, Manchester, UK) with the electrospray source in the positive ion mode. The source tuning settings were as follows: capillary = 3 kV, source pirani pressure = 3.3 millibars, cone voltage = 40 V, source temperature = 40 °C, desolvation temperature = 60 °C, collision energy = 10 V. The RF lens 1 voltage was varied from 50 V (soft conditions to preserve the protein dimer) to 150 V (harder conditions to achieve a better desolvation and higher accuracy in the protein mass determination).

Molecular Sieve—A TSK column (G3000SW, 30 × 0.75 cm, 7 mm, Tosoh, Bioscience GmbH, 70567, Stuttgart, Germany) was used in 20 mM Hepes-Na (pH 6.8) and 200 mM NaCl at a flow rate of 0.5 ml/min.

Site-directed Mutagenesis of NeuTTM—Point mutations were introduced by the QuikChange method. The expression plasmid containing the coding sequence of *NeuTTM* was amplified with two mutagenic primers and *Pfu* DNA polymerase (Promega). Template DNA was removed by digestion with DpnI (Promega) for 2 h at 37 °C. The DNA was then introduced into *E. coli* cells, and single clones were isolated. The presence of the mutations was checked by DNA sequencing (Genotranscriptomics Platform, GIGA, University of Liège). The sequences of the oligonucleotides used are given in supplemental Table S1.

Determination of Phosphohydrolase Activities—The standard incubation medium (100 μ l) contained 50 mM buffer, 5 mM MgCl₂, 0.5 mM PPP_i, and 20 μ l of the enzyme at the adequate concentration. The mixture was incubated at 37 or 50 °C, and the reaction was stopped by the addition of 1 ml of phosphate reagent (24). The absorbance was read at 635 nm after 30 min and compared with a standard curve to estimate the released inorganic phosphate. When P₄ was the substrate, the absorbance was read after only 15 min, as acid hydrolysis was rapid in the phosphate reagent. The buffers used for incubation at different pH values were: Na-MES (pH 6.0–7.0), Na-MOPS (pH 7.0–7.5), Na-HEPES (pH 7.5–8.0), Na-TAPS (pH 8.0–9.0), Na-CHES (pH 9.0–10.0), and Na-CAPS (pH 10.0–10.5).

Determination of In-gel Enzyme Activities—In-gel activities were measured as described (25). The gel was colored in phosphate precipitation reagent (1% w/v ammonium heptamolybdate, 1% w/v triethylamine, 1 N HNO₃).

Determination of ATP, ADP, and cAMP—Purified *NeuTTM* was incubated under standard assay conditions with ATP (0.1 mM). The reaction was stopped by the addition of 12% trichloroacetic acid. After extraction of the acid with 3 × 1.5 ml of diethyl ether, nucleotides were determined by HPLC using UV detection (26).

Statistical Analyses—Data analysis was done with Prism 5 for Mac OS X (GraphPad Software, San Diego, CA) using nonlinear fitting to the Michaelis-Menten equation.

RESULTS

Cloning, Overexpression, and Purification of NeuTTM—The ORF for *NeuTTM* was subcloned in the pET15b vector, modified to allow the expression of N-terminal His-tag fusion proteins. The latter was purified as described under “Experimental Procedures.” The protein obtained after elution from the His-

A Specific Inorganic Triphosphatase from *N. europaea*

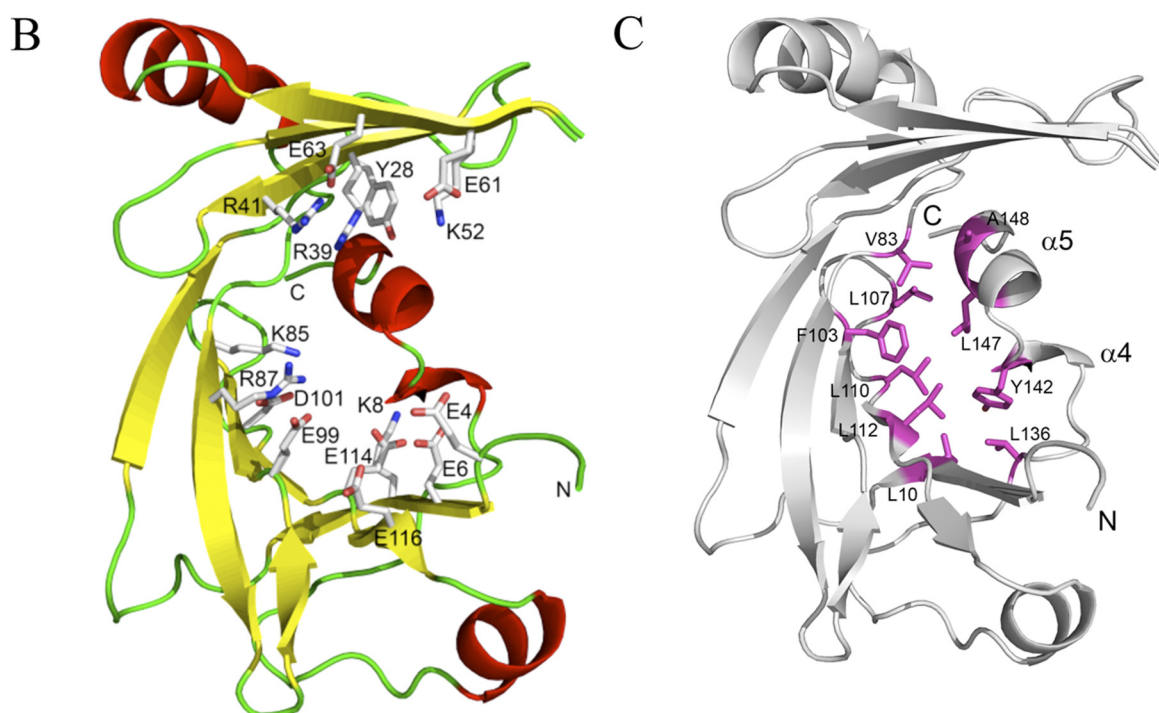
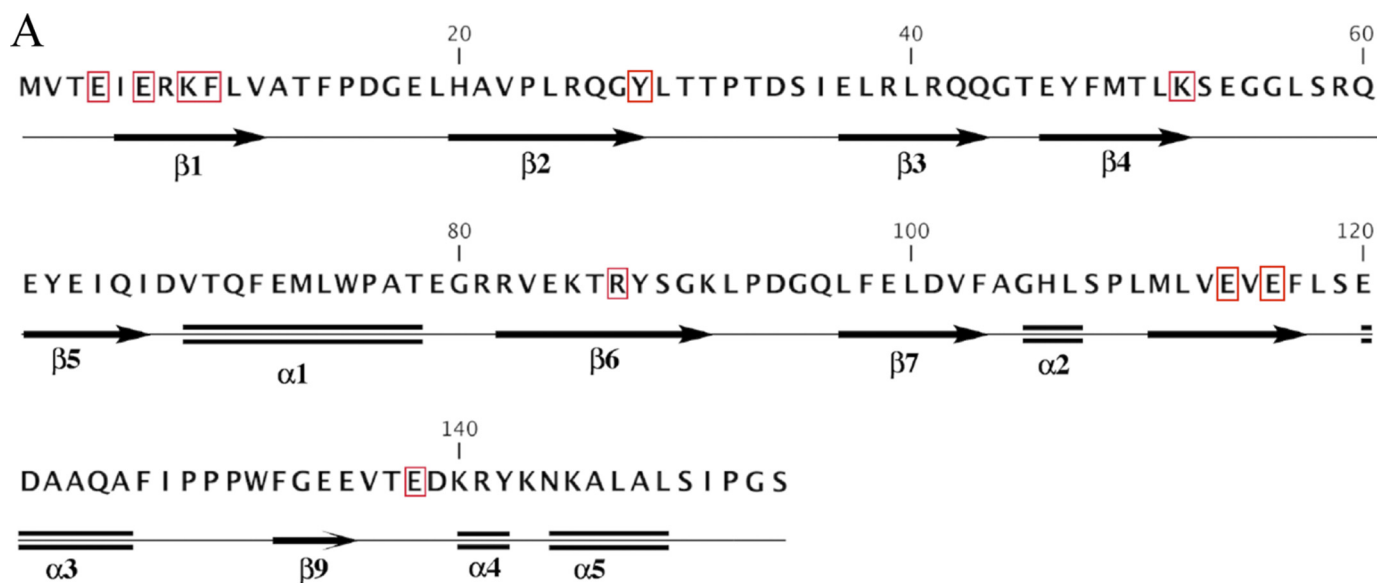


FIGURE 1. Structure of NeuTTM. **A**, amino acid sequence and secondary structure elements are shown. The residues conserved among known CYTH proteins (9) are highlighted by red boxes. **B**, a schematic representation of the NeuTTM monomer is shown. Side chains of residues probably involved in substrate and divalent cation binding and/or catalysis are rendered as sticks and are labeled. **C**, stabilization of the open β -barrel structure by hydrophobic interactions with α -turn 4 and α -helix 5 is shown. The NeuTTM monomer is shown in a schematic representation (gray). The residues forming a hydrophobic patch that stabilizes the protein core are shown in magenta sticks and labeled.

Trap column was essentially pure as judged by SDS-PAGE (supplemental Fig. S1). This poly-His fusion protein could be subsequently cleaved by TEV protease, which considerably increased the triphosphatase activity of the enzyme (see below). For crystallization, NeuTTM was expressed as selenomethionine-substituted protein.

Structural Properties of NeuTTM—The sequence and secondary structure elements are given in Fig. 1A. Crystallographic data show that NeuTTM, like 25-kDa ThTPase (9), has an open cleft structure in the absence of bound substrate (Fig. 1B). Several residues projecting into the cleft have been indicated. They

seem to be important for substrate and metal binding and/or catalytic activity, as in the case of the closely related *Cth*TTM, extensive mutational analysis (12) has revealed that most of these homologous residues are required for full PPPase activity. Four glutamate residues (Glu-4, -6, -114, -116, and possibly Glu-61 and -63) are supposed to be required for Mg^{2+} (or Mn^{2+}) binding, whereas Arg-39 and -41 (and possibly Arg-87) probably interact with substrate phosphoryl groups. According to Keppetipola *et al.* (12), Lys-8 in *Cth*TTM would form a hydrogen bond with a backbone carbonyl at the break of the C-terminal α 4- α 5 helix. However, the analysis of the crystal

structure of *NeuTTM* leaves the existence of such a hydrogen bond in question. Although the distance between Lys-8NZ and Tyr-142-O is 2.9 Å, the angle N...O-C is 117 degrees, which is rather far from the ideal geometry. Also, there is a water molecule (W429) located 3.5 Å away from the Tyr-142 carbonyl oxygen with the angle O...O-C of 172 degrees, which makes this water molecule a more likely partner for a hydrogen bond with the Tyr-142 carbonyl than Lys-8NZ.

It seems that the β sheets are prevented from closing into a complete β -barrel by the insertion of a broken C-terminal helix

($\alpha 4$ and $\alpha 5$) into one end of the fold. Such a conformation is stabilized by hydrophobic interactions conferring a relatively rigid structure to *NeuTTM* (Fig. 1C).

Specificity and Kinetic Properties of Recombinant *NeuTTM*—In contrast to what we expected, only a slight ThTPase activity could be detected, indicating that, unlike its mammalian counterpart, *NeuTTM* is not a genuine ThTPase (Fig. 2).

As ATP and other NTPs were hydrolyzed by a number of enzymes of the TTM family (7, 12), we tested these compounds as potential substrates for *NeuTTM*. Nucleoside triphosphatase activity was negligible in the presence of Mg^{2+} , but a small activity was observed in the presence of Mn^{2+} , in particular with GTP (Fig. 2).

By contrast to NTPs, PPP_i was a very good substrate for *NeuTTM* with Mg^{2+} as activator (Fig. 2, Table 2). The enzyme had a strong preference for linear PPP_i compared with cyclic PPP_i (cyclic trimetaphosphate) and to the linear P_4 . The longer chain polyphosphate (containing 65 ± 5 phosphate residues) was not hydrolyzed either. Likewise, guanosine 5'-tetraphosphate ($Gpppp$ or Gp_4), which is a good substrate for *CthTTM* (13), was not significantly hydrolyzed. The *NeuTTM* adenylyl cyclase activity was also checked by incubating the enzyme with ATP plus $MgCl_2$ or $MnCl_2$ at different pH values, but in not cases did we detect the appearance of a cAMP peak by HPLC. Hence, *NeuTTM* appears to be devoid of adenylyl cyclase activity. Note that the closely related *C. thermocellum* CYTH protein (*CthTTM*) was also devoid of any such activity (12). So far the only bacterial CYTH proteins with significant (albeit low) adenylyl cyclase activity are the CyaB enzyme AC2 from *A. hydrophila* (4) and the homologous class IV adenylyl cyclase from *Y. pestis* (10, 11, 27).

General kinetic properties of *NeuTTM* PPPase are displayed in Fig. 3. The optimal temperature was 50–55 °C (Fig. 3A), and the optimum pH was around 9.7 (Fig. 3B). Thermal stability and alkaline pH optimum are characteristic features of several other enzymes of the CYTH superfamily, notably the founding members CyaB-AC2 (4) and human 25-kDa ThTPase (28).

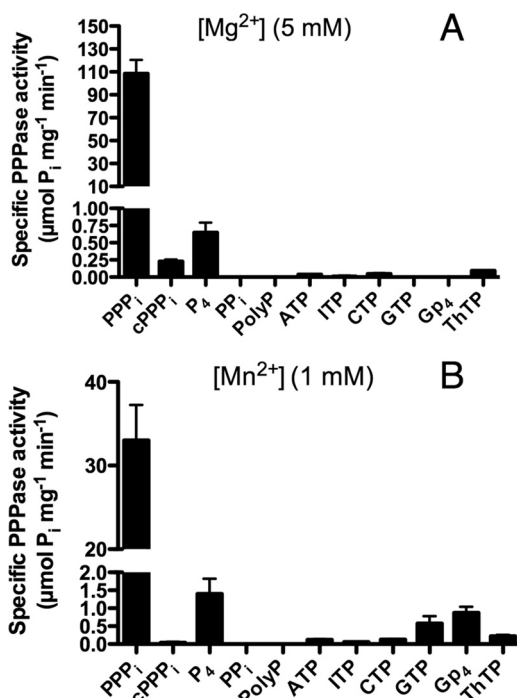


FIGURE 2. Substrate specificity of recombinant His-tagged non-mutated *NeuTTM*. The specificity was tested in the presence of 5 mM $MgCl_2$ (pH 9.7) (A) or 1 mM $MnCl_2$ (pH 10.4) (B). The incubation medium contained either 50 mM Na-CHES (pH 9.7) or 50 mM Na-CAPS (pH 10.4), 0.5 mM substrate, and 5 mM $MgCl_2$ (pH 9.7) or 1 mM $MnCl_2$ (pH 10.4). The temperature was 37 °C. Results are the mean \pm S.D., $n = 2$ –6. $cPPP_i$, cyclic PPP_i .

TABLE 2

Kinetic parameters for non-mutated (WT) and mutated recombinant *NeuTTM*

Data are the mean \pm S.D.; $n = 3$ –4.

| Enzyme preparation | Substrate | Conditions of experiment | K_m app μM | V_{max} $\mu mol\ min^{-1}\ mg^{-1}$ | k_{cat} s^{-1} | K_{cat}/K_m s^{-1}/M^{-1} |
|----------------------------|-----------|--------------------------------------|----------------------|---|-----------------------|----------------------------------|
| WT His-tagged | PPP_i | 50 °C, pH 9.7 $Mg^{2+} = 5\ mM$ | 40 ± 15 | 910 ± 70 | 288 | $7.2 \cdot 10^6$ |
| | | 37 °C, pH 9.7 $Mg^{2+} = 5\ mM$ | 21 ± 3 | 240 ± 30 | 76 | $3.6 \cdot 10^6$ |
| | | 37 °C, pH 7.1 $Mg^{2+} = 5\ mM$ | 58 ± 5 | 60 ± 2 | 19 | $0.33 \cdot 10^6$ |
| WT untagged K8A His-tagged | PPP_i | 50 °C, pH 8.1 $Mn^{2+} = 10\ mM$ | 800 ± 120 | 1.2 ± 0.2 | 0.36 | $0.45 \cdot 10^3$ |
| | | 50 °C, pH 9.7 $Mg^{2+} = 5\ mM$ | 100 ± 20 | $25,000 \pm 2,000$ | 7900 | $79 \cdot 10^6$ |
| K85A His-tagged | PPP_i | 50 °C, pH 9.7 $Mg^{2+} = 5\ mM$ | 390 ± 30 | $2,800 \pm 500$ | 887 | $2.3 \cdot 10^6$ |
| | | 37 °C, pH 9.7 $Mg^{2+} = 5\ mM$ | 280 ± 55 | 235 ± 30 | 74 | $0.19 \cdot 10^6$ |
| | | 50 °C, pH 10.1 $Mn^{2+} = 10\ mM$ | 1200 ± 500 | 12.5 ± 3.2 | 3.96 | $3.3 \cdot 10^3$ |
| K52R His-tagged | PPP_i | 50 °C, pH 9.7 $Mg^{2+} = 5\ mM$ | 720 ± 60 | 65 ± 7 | 21 | $29 \cdot 10^3$ |
| | | 37 °C, pH 9.7 $Mg^{2+} = 5\ mM$ | 2600 ± 400 | 33 ± 3 | 10 | $4 \cdot 10^3$ |
| K52R His-tagged | PPP_i | 37 °C, pH 9.7 $Mg^{2+} = 5\ mM$ | 191 ± 8 | 3.1 ± 0.1 | 0.98 | $5.1 \cdot 10^3$ |
| | | 50 °C, pH 9.7 $Mg^{2+} = 5\ mM$ | | | | |

A Specific Inorganic Triphosphatase from *N. europaea*

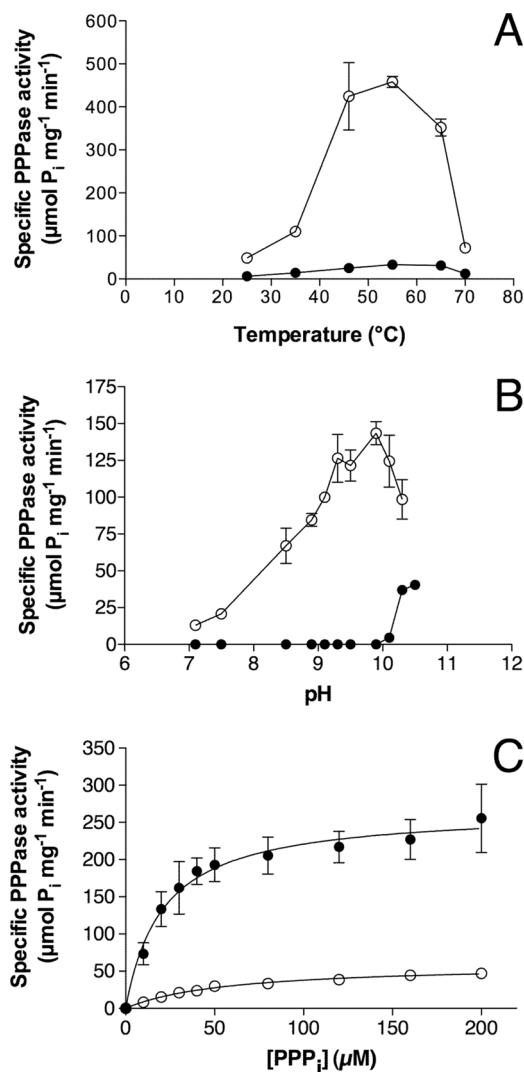


FIGURE 3. Kinetic properties of *NeuTTM* PPPase activity. The PPP_i concentration was 0.5 mM. **A**, dependence on temperature in the presence of 5 mM Mg²⁺ at pH 9.7 (○) or 0.8 mM Mn²⁺ at pH 10.4 (●) is shown. **B**, pH dependence in the presence of 10 mM Mg²⁺ (○) or 1 mM Mn²⁺ (●) at 37 °C is shown. **C**, dependence on substrate concentration at pH 7.1 (○) and 9.7 (●) at 37 °C is shown. The curves were drawn by non-linear regression of the Michaelis-Menten equation ($n = 3$). The buffers used for different pH values are given under "Experimental Procedures." Results are the mean \pm S.D.

As Mn²⁺ is a good substituent for Mg²⁺ in several TTM members (7, 12, 29–31), we tested the possible activating effects of Mn²⁺ ions on *NeuTTM* PPPase activity. We found that it was a very poor substituent for Mg²⁺ at all temperatures tested and in the pH range 7–10 (Fig. 3, **A** and **B**). However, there was a significant Mn²⁺-dependent activity at very alkaline pH (10.0–10.5) (Fig. 3**B**).

Kinetic parameters (K_m , k_{cat} , and catalytic efficiency) were determined with different enzyme preparations and under different experimental conditions (Table 2). Using a freshly prepared His-tagged purified preparation, Michaelis-Menten kinetics were obtained (Fig. 3**C**). At pH 9.7 and 37 °C, K_m was $21 \pm 3 \mu\text{M}$, and V_{max} was $240 \pm 30 \mu\text{mol min}^{-1} \text{mg}^{-1}$ in the presence of 5 mM Mg²⁺. Under such conditions, the substrate is essentially under the form of a Mg²⁺-PPP_i complex, as K_d for the dissociation of the complex is low ($\sim 1.6 \cdot 10^{-6} \text{ M}$). The calculated k_{cat} was 76 s^{-1} under these conditions (assuming a

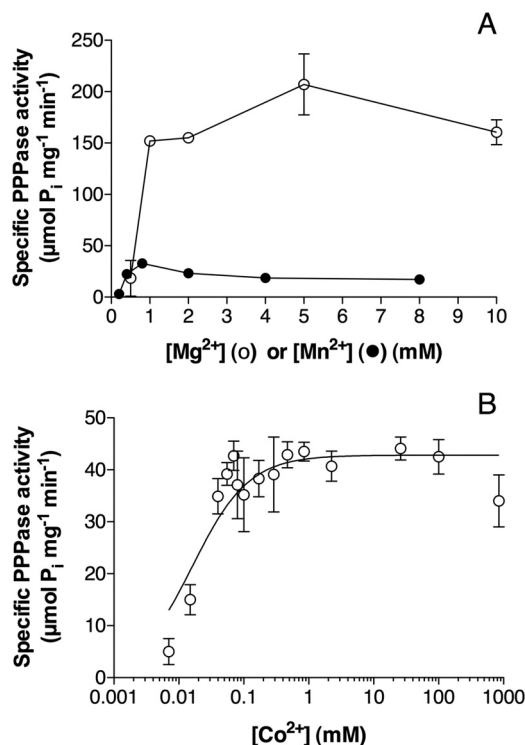


FIGURE 4. Activation of *NeuTTM* PPPase by divalent cations. **A**, shown is dependence of PPPase activity on Mg²⁺ (○) and Mn²⁺ (●) total concentration. The incubation was carried out in the presence of 50 mM Na-CHES (Mg²⁺, pH 9.7) or Na-CAPS (Mn²⁺, pH 10.4) at 37 °C. **B**, shown is the effect of increasing concentrations of Co²⁺ (calculated free Co²⁺ concentration assuming $K_d = 8 \text{ nM}$ for the Co-PPP_i complex) on the PPPase activity. Conditions of experiment: PPP_i, 0.5 mM; Na-CHES, 50 mM, pH 9.5, 45 °C. Results are the mean \pm S.D., $n = 3$.

molecular mass of 19 kDa for the monomeric enzyme with one catalytic site). The catalytic efficiency of *NeuTTM* triphosphatase activity is thus very high, with $k_{cat}/K_m = 3.6 \cdot 10^6 \text{ M}^{-1} \text{s}^{-1}$. At neutral pH, k_{cat}/K_m is about 10 times lower ($3.3 \cdot 10^5 \text{ M}^{-1} \text{s}^{-1}$), but this is still high enough to consider that *NeuTTM* may be a genuine specific inorganic triphosphatase (PPPase). This is all the more plausible as k_{cat} was even higher for the untagged enzyme (up to 7900 s^{-1} at 50 °C and pH 9.7, see Table 2). This is 2 orders of magnitude higher than k_{cat} values obtained for *CthTTM* with its best substrates, PPP_i and Gp₄ (12, 13). This raises the possibility that in *N. europaea* the physiological function of *NeuTTM* might be the degradation of PPP_i. It should be emphasized, however, that any firm conclusion concerning the biological role of this enzyme awaits the demonstration of the presence of inorganic triphosphate in *Nitrosomonas* or any other cell types.

Effects of Different Activators and Inhibitors on Recombinant *NeuTTM*—As their name suggests, enzymes from the TTM family are highly dependent on divalent metal cations. In common with other CYTH enzymes, *NeuTTM* PPPase had an absolute requirement for divalent metal ions, the highest activity being found with Mg²⁺ ions in the concentration range 2–10 mM (Fig. 4**A**). As already mentioned, Mn²⁺ was less effective as an activator (Fig. 4**A**), but half-maximum activation was obtained at 0.4 mM Mn²⁺, which corresponds to a very low concentration of free Mn²⁺.

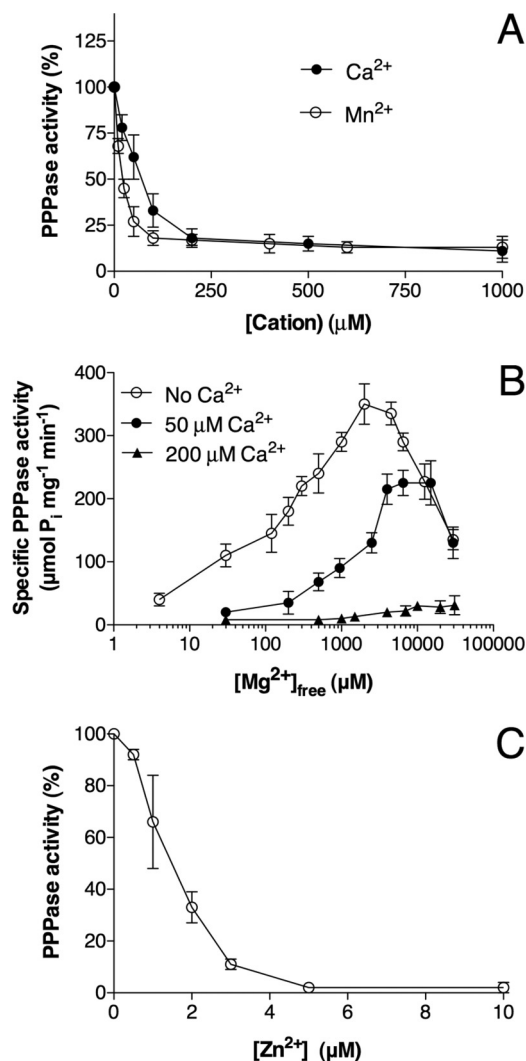


FIGURE 5. Inhibition of *NeuTTM* PPPase by divalent cations. *A*, inhibition by Ca²⁺ and Mn²⁺ in the presence of Mg²⁺ is shown. The incubation medium contained 0.5 mM PPP_i, 5 mM MgCl₂, 50 mM Na-CHES, pH 9.7, at 37 °C. *B*, shown is the effect of increasing concentrations of Mg²⁺ (calculated free Mg²⁺) on *NeuTTM* PPPase activity in the presence or absence of Ca²⁺ ions at 50 °C. The incubation medium contained 0.5 mM PPP_i, 50 mM Na-CHES, pH 9.7. *C*, shown is the effect of increasing concentrations of ZnSO₄ on the PPPase activity of *NeuTTM*. The incubation medium contained 0.5 mM PPP_i, 5 mM MgCl₂, 50 mM Na-CHES, pH 9.7, at 37 °C. Results are the mean ± S.D., *n* = 3.

We also tested the activating effect of Co²⁺, which like Mn²⁺ is a good activator for several TTM enzymes (30). At optimal pH (9.5–9.7), Co²⁺ was a better activator than Mn²⁺, although the maximum activity was less than 10% that measured in the presence of 5 mM Mg²⁺ (Fig. 4*B*). The concentration of free Co²⁺ corresponding to half-maximum activation was extremely low (about 30–50 nM), indicating that the affinity of the binding site for Co²⁺ is even higher than for Mn²⁺.

As already reported for other CYTH enzymes such as Cet1 (30) and 25-kDa ThTPase (28), Ca²⁺ had no activating effect, but it was a potent inhibitor in the presence of Mg²⁺ (Fig. 5*A*); IC₅₀ was 50–100 μM in the presence of 5 mM Mg²⁺. Mn²⁺ was also a potent inhibitor in the presence of Mg²⁺, at least at pH < 10 (IC₅₀ ~ 40 μM). As Mn²⁺ is also a weak activator, the inhibition by Mn²⁺ in the presence of Mg²⁺ was not complete. The curves showing the activating effect of increasing concentra-

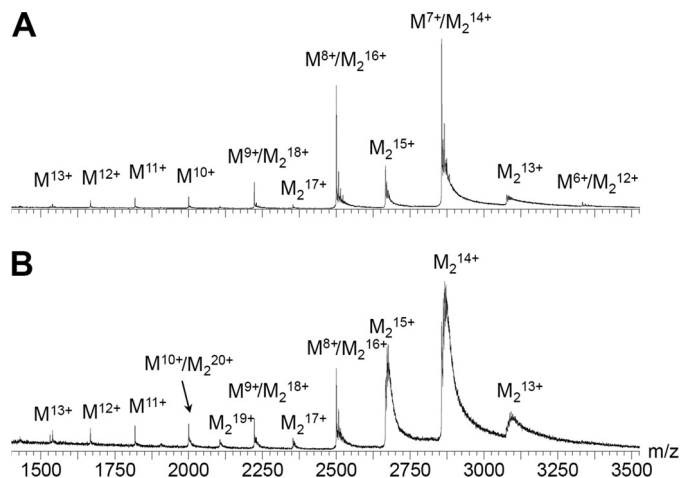


FIGURE 6. Mass spectra of His-tagged *NeuTTM* in the absence of added substrates and divalent cations. *M*, monomer (theoretical mass = 19,987.4 Da); *M*₂, dimer (theoretical mass = 39,974.8 Da). *A*, shown is a spectrum recorded in harsher source conditions (RF lens 1 voltage = 150 V); the dimer was partially destroyed, but the mass accuracy was higher. *B*, shown is a spectrum recorded in soft source conditions (RF lens 1 voltage = 50 V), showing that the dimer is the most abundant species in solution. The protein concentration was 10 μM in 100 mM ammonium acetate, pH 6.5.

tions of Mg²⁺ were shifted to the right in the presence of Ca²⁺ (Fig. 5*B*), suggesting that the latter ion exerts its inhibitory effect at least partially by competition with Mg²⁺. We finally tested the effect of Zn²⁺, which has been shown to be a potent inhibitor of mammalian 25-kDa ThTPase (28). Zn²⁺ inhibited *NeuTTM* PPPase in the lower micromolar range (IC₅₀ ~ 1.5 μM) (Fig. 5*C*). In contrast to Ca²⁺, the inhibitory effect of Zn²⁺ was only marginally affected by the concentration of the activator Mg²⁺ (data not shown), suggesting that the two cations do not compete for the same binding site. This was also the case for 25-kDa ThTPase (28). Those data are in agreement with the assumption that Mg²⁺, Mn²⁺, Ca²⁺, and Co²⁺ may share a common binding site, whereas Zn²⁺ may bind to a peripheral “allosteric” site. In addition to Zn²⁺, Cd²⁺ and Cu²⁺ ions were also inhibitory but with higher IC₅₀ values, 10 and 20 μM, respectively.

Structural and Binding Properties of the *NeuTTM* Protein Analyzed by Native Mass Spectrometry—We first investigated the ability of the 19-kDa recombinant *NeuTTM* to dimerize in solution. The x-ray diffraction data already suggested that the protein crystallized as a dimer (Protein Data Bank code 2FBL). We carried out electrospray mass spectrometry of the concentrated His-tagged protein (total monomer concentration 10 μM) in 100 mM ammonium acetate, pH 6.5 (Fig. 6), and found that the protein was a mixture of monomer (noted *M*) and dimer (noted *M*₂) forms, the dimer being more abundant. The dimer dissociated easily in the gas phase when the RF lens 1 voltage was increased from 50 to 150 V. This suggests that salt bridge interactions do not prevail at the dimerization interface. Indeed, the diffraction data show that the interface is mainly composed of hydrophobic amino acids, among which are Leu-29, -38, -40, -51, and -74 and Ile-36, -64, and -66 (supplemental Fig. S2), and this explains the lability of the dimers in electrospray.

We then studied the complexes of *NeuTTM*, with substrates alone (PPP_i, ATP, and ThTP) in the presence of Mg²⁺. In all

A Specific Inorganic Triphosphatase from *N. europaea*

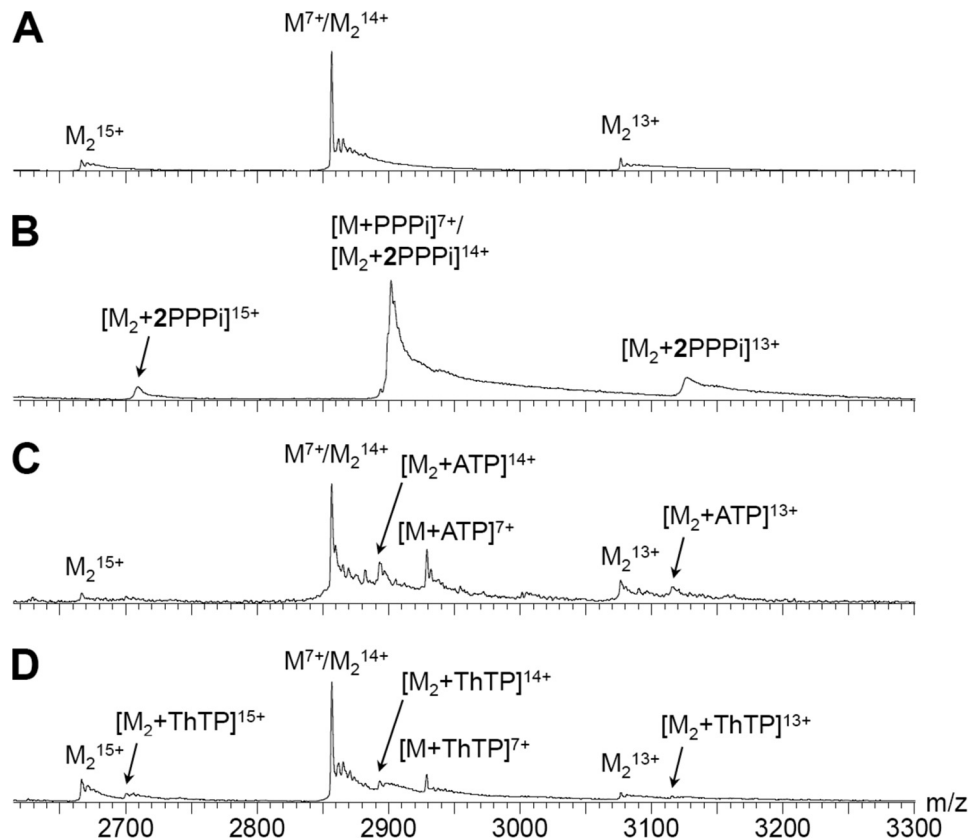


FIGURE 7. Mass spectra showing high specificity of *NeuTTM* for PPP_i compared with ATP and ThTP. *A*, shown is a spectrum of $10 \mu\text{M}$ protein alone in $100 \text{ mM NH}_4\text{OAc}$, pH 6.5. *B*, conditions were as in *A* but with $25 \mu\text{M}$ PPP_i . *C*, conditions were as in *A* but with $20 \mu\text{M}$ protein and $50 \mu\text{M}$ ATP. *D*, conditions were as in *A* with $25 \mu\text{M}$ ThTP instead of PPP_i . *M*, monomer; *M*₂, dimer.

cases the substrates remained tightly bound to *NeuTTM* at all voltages, in line with ionic interactions in these complexes. Fig. 7 shows the mass spectra of *NeuTTM* alone (Fig. 7A) and of the binary mixture with PPP_i (Fig. 7B), ATP (Fig. 7C), and ThTP (Fig. 7D). With PPP_i , at the concentrations used ($10 \mu\text{M}$ *NeuTTM* and $25 \mu\text{M}$ PPP_i), the peak of the free protein is not distinguishable from the noise. It can, therefore, be estimated that the concentration of free protein is less than 8.5% that of the total protein concentration. This means that the dissociation constant for the monomer-substrate complex under the conditions stated above must be lower than $1.5 \mu\text{M}$. Moreover, the protein dimers contain exclusively two PPP_i molecules, as seen from the uneven charge states 15+ and 13+. This strongly contrasts with ATP and ThTP, where the free protein is predominant, and both the monomer and dimer bind one molecule of substrate on average. From the peak intensities, the K_d of the monomer-substrate complex is estimated to be at least $90 \mu\text{M}$ for ATP and ThTP. This is in agreement with the high K_m value ($800 \pm 120 \mu\text{M}$) measured for ATPase activity of *NeuTTM* (Table 2).

Fig. 8 shows the mass spectra of charge state 8+ of the protein monomer in different mixtures with Mg^{2+} and/or PPP_i . The protein alone shows a peak at $m/z = 2499.4$ (Fig. 8A), that remains predominant when the protein is mixed with a 10-fold excess of Mg^{2+} (Fig. 8B). We found that both monomers and dimers bind Mg^{2+} with moderate affinity. We also tested binary mixtures of the protein with Mn^{2+} and Zn^{2+} , and the results suggest a higher affinity for Zn^{2+} (with multiple binding sites)

than for Mg^{2+} and Mn^{2+} (data not shown). This is in agreement with the finding that the PPPase activity of *NeuTTM* is inhibited by micromolar concentrations of Zn^{2+} (Fig. 5C).

A more detailed analysis of the masses of the *NeuTTM*- PPP_i complexes in the absence of divalent cations revealed that they specifically take up two monovalent cations (the peak intensities of the complexes with zero and one monovalent cations being insignificant). Data from Fig. 8C show the presence of a complex with two Na^+ ions. The latter presumably originates from the tripolyphosphate preparation, which is in the form of a pentasodium salt. A *NeuTTM*- PPP_i - Na^+ - K^+ complex was also detected, with K^+ possibly originating from the protein preparation.

Finally, we investigated the properties of the ternary complexes (supposed to be catalytically active) of *NeuTTM*, with the substrate PPP_i and the activator Mg^{2+} . To avoid appreciable hydrolysis of PPP_i , the spectra were recorded immediately after mixing the protein with Mg^{2+} and PPP_i . Despite the high enzyme concentration, PPPase activity is low at room temperature and pH 6.5 (see Fig. 3), and complete hydrolysis of PPP_i under the present conditions would probably take more than a few seconds. With MgCl_2 (0.1 mM) in addition to PPP_i , the enzyme- PPP_i complex took up one Mg^{2+} ion rather than two monovalent cations (Fig. 8D). No free enzyme was observed. We can, therefore, assume that the Mg - PPP_i complex (which is the true substrate) binds to the active site with high affinity, K_d being of the same order of magnitude than for free PPP_i ($<1.5 \mu\text{M}$).

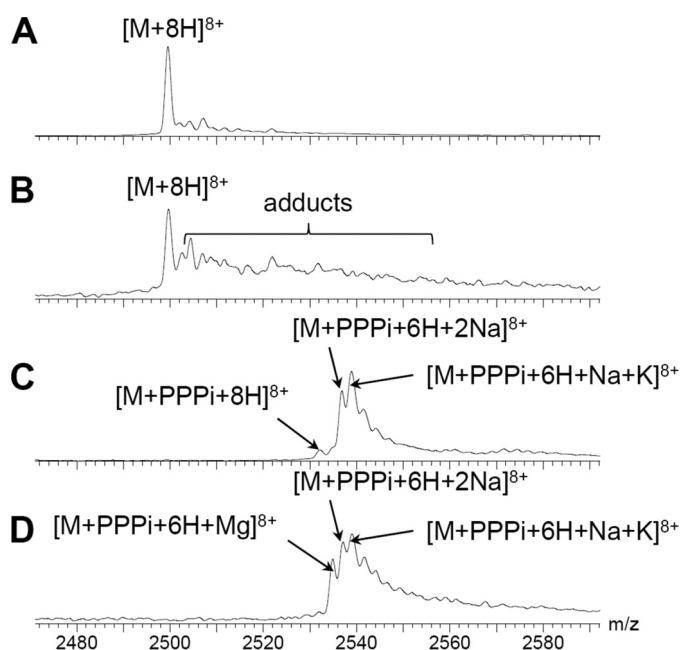


FIGURE 8. Detailed identification of complexes of NeuTTM (10 μM) in binary and ternary mixtures with MgCl_2 (0.1 mM) and/or PPP_i (25 μM). The spectra were all recorded in 100 mM ammonium acetate, pH 6.5, at an RF lens 1 voltage = 150 V for a more accurate mass determination of each complex. *A*, NeuTTM alone at charge state 8+ is shown. The main peak corresponds to the uptake of eight protons, and few sodium or potassium adducts are detected. *B*, NeuTTM binary mixture with Mg^{2+} is shown. The intensity of unresolved adducts peaks increases, but the fully protonated protein remains the most intense peak. *C*, shown is a NeuTTM binary mixture with PPP_i . The fully protonated complex is minor, and the major complexes take up two monovalent cations. *D*, shown is a NeuTTM ternary mixture with PPP_i and Mg^{2+} . The enzyme-substrate complex with the uptake of one Mg^{2+} is clearly detected. *M*, monomer; *M*₂, dimer.

On the other hand, it is clear that the requirement for an activating Mg^{2+} ion is not simply due to the fact that it binds to PPP_i . Although the true substrate is likely to be the Mg^{2+} - PPP_i complex, the divalent metal activator must also bind to a specific site on the protein, as full enzyme activity requires the presence of millimolar free Mg^{2+} in the incubation medium (Figs. 4A and 5B). This was also shown to be the case for RNA triphosphatase from *Trypanosoma* (29), and it is probably a general feature of CYTH proteins (3). In the case of NeuTTM, the metal ion presumably interacts with the carboxyl groups of Glu-4, Glu-6, Glu-114, and Glu-116 (see Fig. 1).

There is no evidence from the present data that the protein might bind more than one Mg^{2+} ion with appreciable affinity. The same conclusion was reached by Song *et al.* (9) for the 25-kDa mouse ThTPase. Although Iyer and Aravind (3) suggested that CYTH proteins may bind two divalent metal activators, this is probably not a general rule for this superfamily of proteins.

In-gel Activity of NeuTTM under Non-denaturing Conditions—In agreement with mass spectrometric data, two peaks of ~20 and 40 kDa were obtained after separation on a size exclusion column (supplemental Fig. S3). The specific activities of the monomer and the dimer were, respectively, 245 and 169 $\mu\text{mol}\cdot\text{min}^{-1}\cdot\text{mg}^{-1}$ with 0.5 mM PPP_i at 50 $^\circ\text{C}$, suggesting that the catalytic activity was not much changed by dimerization. This was also confirmed by in-gel activity determination after polyacrylamide gel electrophoresis under non-denaturing con-

ditions and incubation under optimal conditions (supplemental Fig. S4). Furthermore, when the monomer and the dimer were separated on the size exclusion column and then reinjected, both appeared pure, suggesting that no rapid conversion between the two forms occurs. These results suggest that dimerization may simply be an artifact associated with enzyme purification and without physiological significance.

Site-directed Mutagenesis—Alanine mutation of Lys-8 and Lys-85 were chosen because homologous residues were reported to be important for catalytic activity and substrate specificity of the closely related *Cth*TTM (12). Indeed, the primary structures of *Cth*TTM and *Neu*TTM have 73 positions of side-chain identity (12).

We found that in contrast to the K8A mutant of *Cth*TTM, the K8A mutated *Neu*TTM remained highly active with PPP_i as substrate and Mg^{2+} as activator, with a catalytic efficiency close to that of the recombinant wild-type enzyme, as both K_m and k_{cat} were increased (Table 2). This is an important difference with *Cth*TTM. Indeed, Keppetipola *et al.* (12) found that the corresponding K8A mutation in *Cth*TTM nearly completely abolished the PPPase activity of the enzyme while strongly stimulating its ATPase activity. According to Keppetipola *et al.* (12), Lys-8 would form a hydrogen bond with a backbone carbonyl at the break of the C-terminal helices α_4 - α_5 , stabilizing the open structure of the eight-stranded β -barrel where the substrate binds. Substituting Lys-8 by alanine would prevent this specific interaction between the β_1 strand and α_4 - α_5 helices, making the conformation less rigid. Our own data do not suggest that such a H-bond is required to maintain a rigid structure. Furthermore, with the mutated K8A enzyme, ATP remains a poor substrate (Table 2), even with Mn^{2+} as activator, the catalytic efficiency being 3 orders of magnitude lower than with PPP_i . The present results suggest that either a very rigid conformation is not essential for a high and specific PPPase activity of *Neu*TTM or that Lys-8 is not involved in the stabilization of the enzyme conformation. Note that Keppetipola *et al.* (12) made their assumption on the basis of sequence similarities with *Neu*TTM and that the three-dimensional structure of *Cth*TTM is not known.

Lys-85 is located at the bottom of the cleft that is supposed to contain the catalytic site, close to the arginine residues (Arg-39, -41, and -87) that are thought to bind the substrate phosphoryl groups electrostatically. In the case of the very similar *Cth*TTM protein, the Lys-87 residue, which is homologous to Lys-85 in *Neu*TTM, has been found to be essential for catalysis, but the authors did not determine K_m and V_{max} (12).

The K85A mutant of *Neu*TTM was about 10 times less active than the non-mutated enzyme, but the optimal conditions for activity were essentially the same, *i.e.* pH 9.7, temperature ~50 $^\circ\text{C}$. The mutant was also much less active with ATP than with PPP_i as substrate. The extrapolated V_{max} value yielded a k_{cat} around 21 s^{-1} (at 50 $^\circ\text{C}$) in the presence of 5 mM Mg^{2+} (Table 2), which is 14 times lower than k_{cat} measured under the same optimal conditions for the non-mutated enzyme. On the other hand, the K_m for PPP_i was 1 or 2 orders of magnitude higher than for the non-mutated *Neu*TTM. Note that due to the high K_m , it was not possible to use saturating substrate concentrations, increasing the uncertainty on both K_m and V_{max} .

A Specific Inorganic Triphosphatase from *N. europaea*

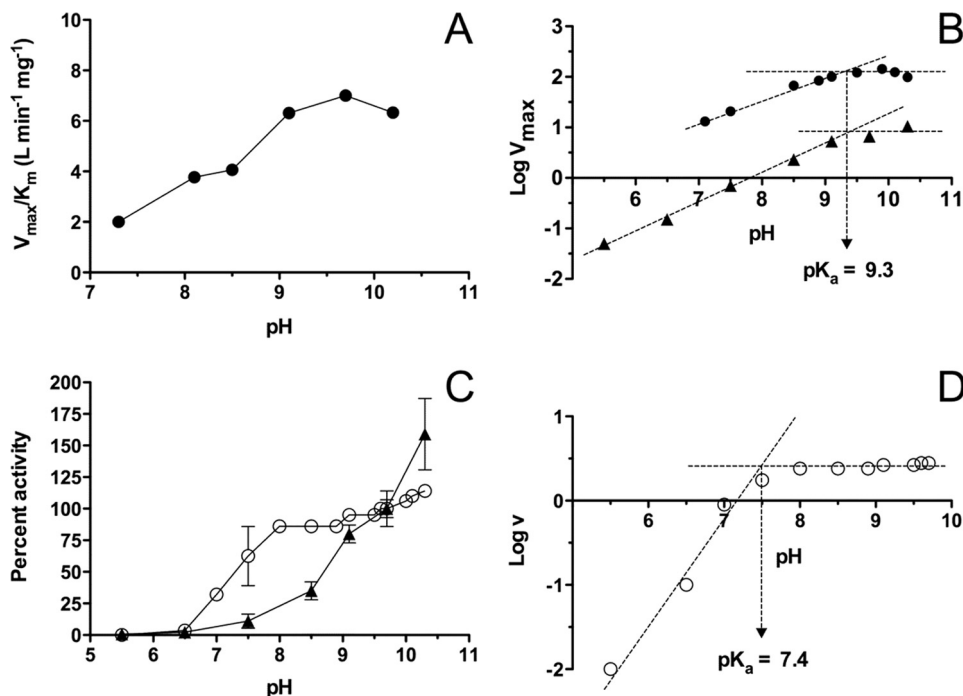


FIGURE 9. pH dependence of non-mutated NeuTTM and of the Y28F and K52R mutants. The reaction was carried out in the presence of 5 mM Mg²⁺ at 37 °C. The control values obtained in the absence of enzyme were subtracted. *A*, shown is V_{\max}/K_m as a function of pH for the non-mutated enzyme. *B*, shown is pH dependence of V_{\max} of non-mutated (●) and K52R-mutated (▲) NeuTTM. *C*, activities of Y28F (○) and K52R (▲) mutants are expressed as the percentage of the respective value obtained at pH 9.7 (100%). The PPP_i concentration was 0.1 mM. *D*, shown is pH dependence of Y29F-mutated NeuTTM, PPP_i = 0.1 mM. Results are the mean ± S.D, *n* = 3–6.

Although the catalytic efficiency of the enzyme appears to be rather strongly decreased by the K85A mutation, it cannot be concluded that Lys-85 is really essential for catalysis, as k_{cat} remains relatively high.

Another important consequence of the K85A mutation is that the effects of divalent cations are profoundly altered; in contrast to the non-mutated enzyme, the K85A mutant is more strongly activated by Mn²⁺ than by Mg²⁺, and the inhibitory effects of Ca²⁺ and Zn²⁺ are less pronounced (supplemental Table S2). Actually, Zn²⁺ can even replace Mn²⁺ as activator, although it is less effective. It thus appears that deleting the positive charge of the side chain at position 85 alters the protein conformation in such a way that cations larger than Mg²⁺ become better activators. This suggests that Lys-85 may act as a “discriminator” residue, ensuring that the smaller and more physiological Mg²⁺ ion is the specific activator. Taken together the data suggest that Lys-85 is not directly involved in catalysis and is more likely to play an important (although not essential) role to properly orient the PPP_i molecule in the enzyme-substrate complex. It is also important for the specificity of Mg²⁺ binding.

As neither Lys-8 nor -85 appear to be essential residues for catalysis, we suspected that Lys-52, which is highly conserved in CYTH proteins (3, 9), might play a more essential role. In *Cih*TTM, mutation of Lys-52 resulted in the loss of 90–99% of the activity, depending on the substrate or activator used (12). In NeuTTM, the conservative K52R mutation resulted in a decreased V_{\max} by about 2 orders of magnitude (Table 2), and as the apparent K_m is strongly increased (supplemental Table S5), the catalytic efficiency is at least 1000 times lower than that of the non-mutated enzyme. Mn²⁺ did not induce a significant

activation of this mutant. Thus, in contrast to K85A, the specificity for activating ions does not appear to be changed. The fact that this conservative mutation strongly decreases the catalytic efficiency of the enzyme suggests that this highly conserved lysine residue plays an important role in the catalytic mechanism.

A puzzling property of NeuTTM as well as other enzymes of the CYTH protein family is their strong activation at alkaline pH (Fig. 3B). To check that this pH profile was not due to impaired binding of the substrate at lower pH, we plotted V_{\max}/K_m as a function of pH (Fig. 9A). Our results show that the K_m does not change much with pH, and the profile obtained is quite similar to the activity versus pH profile (Fig. 3B). We used the Dixon-Webb plot Log V_{\max} versus pH to estimate the pK_a value for the main residue responsible for activity decrease between 9.7 and 7.0. As shown in Fig. 9B, the estimated pK_a was close to 9.3 for the non-mutated enzyme. The same value was found for the K52R mutant. These data are in agreement with the proposal that the catalytic activity depends on a single deprotonation step with $pK_a \sim 9.3$. This may correspond to a general base that removes a proton from water; the resulting OH⁻ would attack a phosphorus atom of the PPP_i substrate.

As the pH-rate profile remains largely unaffected by K52R mutation, the decrease of activity between 9.7 and 7.0 cannot be ascribed to protonation of the Lys-52 amino group. This suggests the involvement of another residue able to interact with Lys-52 and acting as a general base in the hydrolytic mechanism. According to the crystal structure (Fig. 1B), only three residues are in a position to interact easily with Lys-52: Tyr-28, Glu-37, and Glu-61 (see also supplemental Fig. S6). Obviously, the carboxyl groups of glutamate residues could hardly exhibit

such an alkaline pK_a , and we suspected that the residue acting as the general base was Tyr-28 (pK_a for the hydroxyl group of free tyrosine is ~ 10.0). Indeed, the conservative mutation Y28F results in a strong loss of enzyme activity ($\sim 2.6 \mu\text{mol min}^{-1} \text{mg}^{-1}$ at $100 \mu\text{M}$ PPP_i , compared with $\sim 200 \mu\text{mol min}^{-1} \text{mg}^{-1}$ for the non-mutated enzyme, Fig. 3C). Surprisingly, however, the activity continuously increased when PPP_i was raised to 1 mM (the highest testable concentration with our method) with no tendency to saturation (supplemental Fig. S5). This lack of saturation was observed at all pH values tested from 7.0 to 9.0 (data not shown). Thus, the kinetic parameters K_m and V_{max} could not be estimated with this mutant enzyme. The pH optimum of the Y28F mutant is shifted to lower values compared with the non-mutated (Fig. 3B) and the K52R mutant (Fig. 9C). We plotted the log of the specific activity versus pH at 37°C for $\text{PPP}_i = 100 \mu\text{M}$ (Fig. 9D). It is obvious that there is an important shift in pH-rate profile toward lower pH values, and the Dixon-Webb plot yielded a pK_a value ~ 7.4 . This apparent pK_a was not strongly affected by changes in PPP_i concentration (not shown).

This value might possibly reflect the pK_a of the carboxyl group of a neighboring glutamate (Glu-37 or -61) that might also act as a general base, albeit less efficiently than Tyr-28. This would explain that the activity of the Y28F mutant still reaches relatively high values when PPP_i is in large excess (supplemental Fig. S5). Taken together, those data suggest that Tyr-28 plays an important role in *NeuTTM* catalysis (possibly forming a catalytic dyad with Lys-52) and is at least partially responsible for the unusual high pH optimum of the enzyme. The relatively slight decrease in activity at $\text{pH} \geq 10$ could result from a number of possibilities, e.g. charge alterations involving unidentified residues in or near the active site or destabilization of the protein structure.

In the model shown in Fig. 10, we hypothesize that a catalytic dyad is formed by the Tyr-28/Lys-52 pair, the nucleophilic nitrogen of Lys-52 being hydrogen-bonded with the phenolate oxygen of Tyr-28. The latter would act as the general base that removes a proton from water, and the resulting OH^- attacks a phosphorus atom of the substrate PPP_i (Fig. 10). Alternatively, Tyr-28 might act as a nucleophile to directly attack the γ -phosphorus atom of PPP_i (Fig. 10). In the latter case, we would expect a covalent phosphotyrosyl intermediate to be formed that would be unusual for a hydrolase. When the catalytic mechanism involves a phosphoenzyme intermediate, the activity is generally inhibited by sodium orthovanadate acting as a transition state inhibitor. We tested the effect of sodium orthovanadate on the non-mutated *NeuTTM* PPPase activity, but we found no inhibition at concentrations up to 2 mM . However, the activity was very sensitive to fluoride with an IC_{50} as low as $30 \pm 10 \mu\text{M}$ for NaF (results not shown). Fluoride is a well known inhibitor of acid phosphatases, but millimolar concentrations are required. However, inorganic pyrophosphatases are sensitive to fluoride at concentrations lower than 1 mM . In family I pyrophosphatases, where fluoride inhibition involves rapid and slow phases (32), there is much evidence that catalysis proceeds by direct phosphoryl transfer to water rather than via a phosphoryl enzyme intermediate (33, 34). The structure of the F^- -inhibited complex has shown a fluoride ion replacing the nucleophilic water molecule (35). In family II pyrophospha-

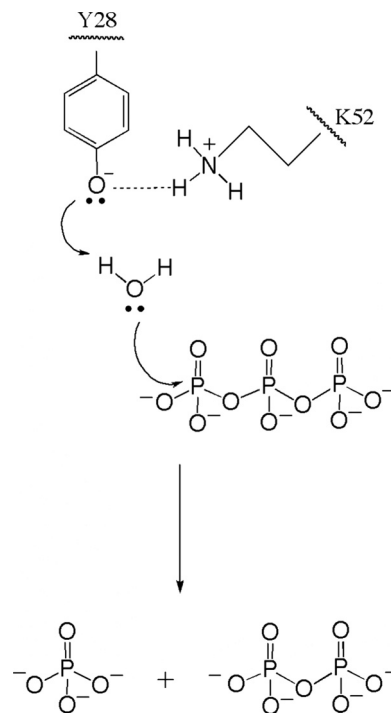


FIGURE 10. Proposed catalytic mechanism for PPP_i hydrolysis by *NeuTTM*. The Lys-52/Tyr-28 pair is considered to form a catalytic dyad. The most simple and plausible mechanism is a general acid-general base catalysis with no covalent acyl-enzyme intermediate.

tases, which belong to the DHH phosphoesterase superfamily (as defined by (5)), the IC_{50} for fluoride inhibition was even lower than for *NeuTTM* ($\sim 12 \mu\text{M}$) (36). In any case fluoride is believed to act as an analog of hydroxide (37). The detailed mechanism of PPP_i hydrolysis by *NeuTTM* requires further investigation, but the lack of effect of vanadate and the strong inhibitory effect of fluoride argue against the existence of a covalent phosphoenzyme intermediate. Therefore, the model proposed in Fig. 10 seems to be the simplest and the most plausible.

DISCUSSION

The present data demonstrate that the hypothetical protein NE1496, present in *N. europaea* (*NeuTTM*), is a functional phosphohydrolase with surprisingly high specificity, affinity, and catalytic efficiency for PPP_i . This is also the first molecular characterization of a specific tripolyphosphatase. Several enzymes hydrolyzing PPP_i have been characterized previously, but they are mainly exopolyphosphatases that, in addition to PPP_i , hydrolyze other substrates such as, for instance, long chain polyphosphates or Gp_4 (38–40). So far, only one enzyme was reported to be strictly specific for PPP_i hydrolysis; it was purified from *Neurospora crassa* and found to be a dimer of 40-kDa subunits (41). Its sequence remains unknown, and unlike *NeuTTM*, it does not appear to have a high affinity for PPP_i .

NeuTTM belongs to the superfamily of CYTH proteins (3) and was first referred to as a hypothetical protein with putative phosphatase or CyaB-like adenylyl cyclase activity by analogy with the *A. hydrophila* CYTH protein (4). However, it has become clear that the functional properties of CYTH proteins

A Specific Inorganic Triphosphatase from *N. europaea*

cannot be predicted from primary or even three-dimensional structure. In fact, the CYTH domain is a functionally versatile protein fold, characterized mainly by its ability to bind triphosphate compounds and catalyze their hydrolysis or other chemical transformations in the presence of divalent metal ion activators. Members of the CYTH superfamily exist in archaea, but none has been functionally characterized so far. In bacteria, two CYTH orthologs were shown to have an adenyl cyclase activity (4, 11, 27), but under physiological conditions this activity is low, and its biological significance is not established. *Cth*TTM, the ortholog from *C. thermocellum* hydrolyzes PPP_i with a relatively good turnover ($k_{\text{cat}} = 3 \text{ s}^{-1}$), but it also hydrolyzes other substrates such as Gp_4 ($k_{\text{cat}} = 96 \text{ s}^{-1}$) and, to a lesser extent, nucleoside triphosphates and long chain polyphosphates (12, 13). Thus, its possible physiological function remains undefined. In contrast, a clear biological role has been demonstrated for the CYTH orthologs of fungi and protozoa, which catalyze the first step of RNA capping in these organisms (7). In pluricellular eukaryotes, only the mammalian 25-kDa ThTPase has been characterized (1, 9, 28). Like *Neu*TTM, the latter enzyme is characterized by a high specificity and a high catalytic efficiency ($k_{\text{cat}}/K_m = 6 \cdot 10^6 \text{ M}^{-1} \text{ s}^{-1}$ for the bovine ThTPase (1)). On the basis that all known CYTH proteins hydrolyze triphosphates and that PPP_i is the simplest triphosphate compound conceivable, PPPase activity might well be the primitive enzymatic activity in the CYTH protein family, which later evolved to hydrolyze more complex organic substrates such as RNA or ThTP in eukaryotes. It should be pointed out that a high affinity for PPP_i was already demonstrated in the case of yeast RNA triphosphatases, where PPP_i is a potent competitive inhibitor, albeit a poor substrate (29, 42, 43).

The present data show that despite low sequence similarity and profound structural differences, *Neu*TTM and 25-kDa ThTPase have several kinetic properties in common, *i.e.* requirement for Mg^{2+} , inhibition by Ca^{2+} by competition with Mg^{2+} , allosteric inhibition by Zn^{2+} , alkaline pH optimum, and an optimal temperature around 50–60 °C. *A. hydrophila* and *Y. pestis* CyaB-like adenyl cyclases are also Mg^{2+} -dependent and have high pH and temperature optima (4, 11, 27). Although more detailed investigations are required, most of these features may possibly be functional signature properties of CYTH enzymes.

Our results shed some light on the particular conformation of the *Neu*TTM protein and the relationship between structural and kinetic properties of the enzyme. The open cleft structure (incomplete β -barrel) is in contrast to the closed tunnel conformation of other TTM proteins (7). It appears to be rather rigid and to be stabilized by hydrophobic interactions between the antiparallel β strands and the broken C-terminal $\alpha 4$ - $\alpha 5$ helix (Fig. 1C). Hence, in contrast to mammalian 25-kDa ThTPase (9), *Neu*TTM is probably unable to form a tunnel-like structure even when a substrate is bound. This is in line with the very different substrate specificities of the two enzymes.

We propose a catalytic mechanism (Fig. 10) in which the hydroxyl group of Tyr-28 hydrogen-bonded to the nucleophilic nitrogen of Lys-52 acts as a nucleophile, attacking a water molecule to form OH^- . Lys-52 was also considered essential in the enzymatic activity of *Cth*TTM (12). To our knowledge, this is

the first lysine-tyrosine dyad proposed for a hydrolase. Such a mechanism strongly contrasts with the classical serine-histidine dyad observed in many phosphatases.

Catalytic dyads based on tyrosyl and lysyl residues seem to be rare (44); nevertheless such a catalytic dyad has been suggested for the enol-keto tautomerization step of the NADP^+ -dependent malic enzyme (45). In that enzyme the Lys \rightarrow Arg and Tyr \rightarrow Phe mutations resulted in a decrease in k_{cat} by 2 orders of magnitude as we observed here.

In the crystal structure described here, the distance between Lys-52 and Tyr-28 is 7.4 Å (supplemental Fig. S6), too much for a hydrogen bond between these two residues. However, as shown for ThTPase, the binding of the substrate induces an important conformational change (9). Such a conformational change in *Neu*TTM might bring the two residues close enough for an interaction.

Four glutamate residues, Glu-4, -6, -114, and -116, protrude from the bottom into the catalytic cleft. They are part of the CYTH consensus sequence and are thought to be involved in Mg^{2+} binding (3, 12). Our data show that the enzyme substrate complex binds only one Mg^{2+} ion (Fig. 8B). We may thus consider the possibility that this Mg^{2+} as well as probably Lys-85 stabilize and orient the substrate PPP_i toward the catalytic dyad projecting from the ceiling of the cleft (Fig. 1B).

Concerning the quaternary structure, it is worth pointing out that *Neu*TTM crystallizes as a dimer (Protein Data Bank code 2FBL) and can also form dimers in solution. However, our results suggest that dimerization is probably not of physiological significance for *Neu*TTM. This is in contrast to yeast RNA triphosphatases Cet1 from *S. cerevisiae* and Pet1 from *Schizosaccharomyces pombe*, where dimerization is important for thermal stability and *in vivo* function (46).

The high affinity and specificity of *Neu*TTM for PPP_i raises the question of the possible biological roles of both PPP_i and the enzymes able to synthesize it. For PPP_i , there are so far very few data concerning its enzymatic synthesis. In *E. coli*, it was shown long ago that PPP_i can be produced by enzymatic cleavage of deoxyguanosine triphosphate (47). On the other hand, it is well known that PPP_i is formed as an intermediate in the enzymatic synthesis of *S*-adenosylmethionine, but in this case it is not released in the cytosol (48). It was also shown that PPP_i is an intermediate in naturally occurring pterins in *Drosophila melanogaster* (49). Like ThTP (50), PPP_i was shown to be an alternative phosphate donor for protein phosphorylation *in vitro* (51), and therefore, like cAMP and possibly ThTP (15), PPP_i might act as an intracellular signal.

However, in contrast to inorganic polyphosphate of higher molecular weight (>10 phosphoryl residues), PPP_i and other very short chain polyphosphates have never been reported to exist in any organism (except in acidocalcisomes, specific organelles rich in calcium and polyphosphates in some protozoans (52)). In all likelihood this is simply due to the present lack of sensitive and specific detection methods. For polyphosphates of longer chain (15–750 residues), the problem was overcome thanks to sensitive assay methods (53). In *E. coli*, polyphosphates play an important role in the response to various forms of environmental stress (14, 54, 55). Polyphosphates may also act as energy stores or divalent cation chelators (14).

The demonstration of similar physiological roles for PPP_i awaits the development of an adequate method to measure its intracellular concentration.

Hence, the present results provide the first detailed characterization of a specific $PPPase$ with high affinity for PPP_i and high catalytic efficiency. Although it is not proven that the physiological function of the protein is to degrade PPP_i *in vivo*, our study is a first step toward the understanding of the possible roles of short chain polyphosphates, which might turn out to be just as important as their long chain counterparts in cell biology.

Acknowledgments—Nucleic acid sequencing was performed by Véronique Dhennin, Genotranscriptomics Platform, GIGA, University of Liège. We thank Dr. Eric Oldfield for the gift of tetrapolyphosphate and Dr. Ilca Margineanu for help with the manuscript and some experiments. We are grateful to Dr. Alexei Savchenko for the gift of the *pET15b* vector for the expression of *NeuTTM* and helpful discussion. The structure of *NeuTTM* was determined by the Midwest Centre for Structural Genomics as part of NIH Protein Structure Initiative Grant GM074942.

REFERENCES

- Lakaye, B., Makarchikov, A. F., Antunes, A. F., Zorzi, W., Coumans, B., De Pauw, E., Wins, P., Grisar, T., and Bettendorff, L. (2002) *J. Biol. Chem.* **277**, 13771–13777
- Gangolf, M., Czerniecki, J., Radermecker, M., Detry, O., Nisolle, M., Jouan, C., Martin, D., Chantraine, F., Lakaye, B., Wins, P., Grisar, T., and Bettendorff, L. (2010) *PLoS One* **5**, e13616
- Iyer, L. M., and Aravind, L. (2002) *BMC Genomics* **3**, 33
- Sismeiro, O., Trotot, P., Biville, F., Vivares, C., and Danchin, A. (1998) *J. Bacteriol.* **180**, 3339–3344
- Aravind, L., and Koonin, E. V. (1998) *Trends Biochem. Sci.* **23**, 17–19
- Tesmer, J. J., Sunahara, R. K., Johnson, R. A., Gosselin, G., Gilman, A. G., and Sprang, S. R. (1999) *Science* **285**, 756–760
- Gong, C., Smith, P., and Shuman, S. (2006) *RNA* **12**, 1468–1474
- Lima, C. D., Wang, L. K., and Shuman, S. (1999) *Cell* **99**, 533–543
- Song, J., Bettendorff, L., Tonelli, M., and Markley, J. L. (2008) *J. Biol. Chem.* **283**, 10939–10948
- Gallagher, D. T., Smith, N. N., Kim, S. K., Heroux, A., Robinson, H., and Reddy, P. T. (2006) *J. Mol. Biol.* **362**, 114–122
- Gallagher, D. T., Kim, S. K., Robinson, H., and Reddy, P. T. (2011) *J. Mol. Biol.* **405**, 787–803
- Keppetipola, N., Jain, R., and Shuman, S. (2007) *J. Biol. Chem.* **282**, 11941–11949
- Jain, R., and Shuman, S. (2008) *J. Biol. Chem.* **283**, 31047–31057
- Rao, N. N., Gómez-García, M. R., and Kornberg, A. (2009) *Annu. Rev. Biochem.* **78**, 605–647
- Lakaye, B., Wirtzfeld, B., Wins, P., Grisar, T., and Bettendorff, L. (2004) *J. Biol. Chem.* **279**, 17142–17147
- Bettendorff, L., Nghiêm, H. O., Wins, P., and Lakaye, B. (2003) *Anal. Biochem.* **322**, 190–197
- Otwinowski, Z., and Minor, W. (1997) in *Methods in Enzymology* (Carter, C. W., Jr., and Sweet, R. M., eds.) pp. 307–326, Academic Press, New York
- Weeks, C. M., Shah, N., Green, M. L., Miller, R., and Furey, W. (2005) *Acta Crystallogr. Sect. A* **61**, C152
- Cohen, S. X., Morris, R. J., Fernandez, F. J., Ben Jelloul, M., Kakaris, M., Parthasarathy, V., Lamzin, V. S., Kleywegt, G. J., and Perrakis, A. (2004) *Acta Crystallogr. D Biol. Crystallogr.* **60**, 2222–2229
- Murshudov, G. N., Vagin, A. A., and Dodson, E. J. (1997) *Acta Crystallogr. D Biol. Crystallogr.* **53**, 240–255
- Emsley, P., and Cowtan, K. (2004) *Acta Crystallogr. D Biol. Crystallogr.* **60**, 2126–2132
- Lovell, S. C., Davis, I. W., Arendall, W. B., 3rd, de Bakker, P. I., Word, J. M., Prisant, M. G., Richardson, J. S., and Richardson, D. C. (2003) *Proteins* **50**, 437–450
- Engh, R. A., and Huber, R. (1991) *Acta Crystallogr. Sect. A* **47**, 392–400
- Lanzetta, P. A., Alvarez, L. J., Reinach, P. S., and Candia, O. A. (1979) *Anal. Biochem.* **100**, 95–97
- Simonović, A. D., Gaddameedhi, S., and Anderson, M. D. (2004) *Anal. Biochem.* **334**, 312–317
- Hill, M., Dupaix, A., Volfin, P., Kurkdjian, A., and Arrio, B. (1987) *Methods Enzymol.* **148**, 132–141
- Smith, N., Kim, S. K., Reddy, P. T., and Gallagher, D. T. (2006) *Acta Crystallogr. Sect. F Struct. Biol. Cryst. Commun.* **62**, 200–204
- Lakaye, B., Makarchikov, A. F., Wins, P., Margineanu, I., Roland, S., Lins, L., Aichour, R., Lebeau, L., El Moualij, B., Zorzi, W., Coumans, B., Grisar, T., and Bettendorff, L. (2004) *Int. J. Biochem. Cell Biol.* **36**, 1348–1364
- Gong, C., Martins, A., and Shuman, S. (2003) *J. Biol. Chem.* **278**, 50843–50852
- Ho, C. K., Pei, Y., and Shuman, S. (1998) *J. Biol. Chem.* **273**, 34151–34156
- Bisaillon, M., and Shuman, S. (2001) *J. Biol. Chem.* **276**, 17261–17266
- Baykov, A. A., Fabrichniy, I. P., Pohjanjoki, P., Zyryanov, A. B., and Lahti, R. (2000) *Biochemistry* **39**, 11939–11947
- Gonzalez, M. A., Webb, M. R., Welsh, K. M., and Cooperman, B. S. (1984) *Biochemistry* **23**, 797–801
- Zyryanov, A. B., Pohjanjoki, P., Kasho, V. N., Shestakov, A. S., Goldman, A., Lahti, R., and Baykov, A. A. (2001) *J. Biol. Chem.* **276**, 17629–17634
- Heikinheimo, P., Tuominen, V., Ahonen, A. K., Teplyakov, A., Cooperman, B. S., Baykov, A. A., Lahti, R., and Goldman, A. (2001) *Proc. Natl. Acad. Sci. U.S.A.* **98**, 3121–3126
- Fabrichniy, I. P., Lehtiö, L., Tammenkoski, M., Zyryanov, A. B., Oksanen, E., Baykov, A. A., Lahti, R., and Goldman, A. (2007) *J. Biol. Chem.* **282**, 1422–1431
- Briley, P. A., Eienthal, R., and Harrison, R. (1975) *Biochem. J.* **145**, 501–507
- Wurst, H., and Kornberg, A. (1994) *J. Biol. Chem.* **269**, 10996–11001
- Fang, J., Ruiz, F. A., Docampo, M., Luo, S., Rodrigues, J. C., Motta, L. S., Rohloff, P., and Docampo, R. (2007) *J. Biol. Chem.* **282**, 32501–32510
- Tammenkoski, M., Koivula, K., Cusanelli, E., Zollo, M., Steegborn, C., Baykov, A. A., and Lahti, R. (2008) *Biochemistry* **47**, 9707–9713
- Egorov, S. N., and Kulaev, I. S. (1976) *Biokhimiia* **41**, 1958–1967
- Gong, C., and Shuman, S. (2002) *J. Biol. Chem.* **277**, 15317–15324
- Issur, M., Despins, S., Bougie, I., and Bisaillon, M. (2009) *Nucleic Acids Res.* **37**, 3714–3722
- Gutteridge, A., and Thornton, J. M. (2005) *Trends Biochem. Sci.* **30**, 622–629
- Kuo, C. C., Lin, K. Y., Hsu, Y. J., Lin, S. Y., Lin, Y. T., Chang, G. G., and Chou, W. Y. (2008) *Biochem. J.* **411**, 467–473
- Hausmann, S., Pei, Y., and Shuman, S. (2003) *J. Biol. Chem.* **278**, 30487–30496
- Kornberg, S. R., Lehman, I. R., Bessman, M. J., Simms, E. S., and Kornberg, A. (1958) *J. Biol. Chem.* **233**, 159–162
- Pérez Mato, I., Sanchez del Pino, M. M., Chamberlin, M. E., Mudd, S. H., Mato, J. M., and Corrales, F. J. (2001) *J. Biol. Chem.* **276**, 13803–13809
- Switchenko, A. C., Primus, J. P., and Brown, G. M. (1984) *Biochem. Biophys. Res. Commun.* **120**, 754–760
- Nghiêm, H. O., Bettendorff, L., and Changeux, J. P. (2000) *FASEB J.* **14**, 543–554
- Tsutsui, K. (1986) *J. Biol. Chem.* **261**, 2645–2653
- Moreno, B., Urbina, J. A., Oldfield, E., Bailey, B. N., Rodrigues, C. O., and Docampo, R. (2000) *J. Biol. Chem.* **275**, 28356–28362
- Ault-Riché, D., Fraley, C. D., Tzeng, C. M., and Kornberg, A. (1998) *J. Bacteriol.* **180**, 1841–1847
- Kuroda, A., Nomura, K., Ohtomo, R., Kato, J., Ikeda, T., Takiguchi, N., Ohtake, H., and Kornberg, A. (2001) *Science* **293**, 705–708
- Brown, M. R., and Kornberg, A. (2008) *Trends Biochem. Sci.* **33**, 284–290

Appendix 2

High Inorganic Triphosphatase Activities in Bacteria and Mammalian Cells: Identification of the Enzymes Involved

Gregory Kohn¹✉, David Delvaux¹✉, Bernard Lakaye¹, Anne-Catherine Servais², Georges Scholer³, Marianne Fillet², Benjamin Elias³, Jean-Michel Derochette⁴, Jacques Crommen², Pierre Wins¹, Lucien Bettendorff¹*

1 GIGA-Neurosciences, University of Liège, Liège, Belgium, **2** Laboratory of Analytical Pharmaceutical Chemistry, Department of Pharmaceutical Sciences, CIRP, University of Liège, Liège, Belgium, **3** Institute of Condensed Matter and Nanosciences, Université catholique de Louvain, Louvain-la-Neuve, Belgium, **4** Prayon S.A., Engis, Belgium

Abstract

Background: We recently characterized a specific inorganic triphosphatase (PPPase) from *Nitrosomonas europaea*. This enzyme belongs to the CYTH superfamily of proteins. Many bacterial members of this family are annotated as predicted adenylate cyclases, because one of the founding members is CyaB adenylate cyclase from *A. hydrophila*. The aim of the present study is to determine whether other members of the CYTH protein family also have a PPPase activity, if there are PPPase activities in animal tissues and what enzymes are responsible for these activities.

Methodology/Principal Findings: Recombinant enzymes were expressed and purified as GST- or His-tagged fusion proteins and the enzyme activities were determined by measuring the release of inorganic phosphate. We show that the hitherto uncharacterized *E. coli* CYTH protein ygiF is a specific PPPase, but it contributes only marginally to the total PPPase activity in this organism, where the main enzyme responsible for hydrolysis of inorganic triphosphate (PPP_i) is inorganic pyrophosphatase. We further show that CyaB hydrolyzes PPP_i but this activity is low compared to its adenylate cyclase activity. Finally we demonstrate a high PPPase activity in mammalian and quail tissue, particularly in the brain. We show that this activity is mainly due to Prune, an exopolyphosphatase overexpressed in metastatic tumors where it promotes cell motility.

Conclusions and General Significance: We show for the first time that PPPase activities are widespread in bacteria and animals. We identified the enzymes responsible for these activities but we were unable to detect significant amounts of PPP_i in *E. coli* or brain extracts using ion chromatography and capillary electrophoresis. The role of these enzymes may be to hydrolyze PPP_i, which could be cytotoxic because of its high affinity for Ca²⁺, thereby interfering with Ca²⁺ signaling.

Citation: Kohn G, Delvaux D, Lakaye B, Servais A-C, Scholer G, et al. (2012) High Inorganic Triphosphatase Activities in Bacteria and Mammalian Cells: Identification of the Enzymes Involved. PLoS ONE 7(9): e43879. doi:10.1371/journal.pone.0043879

Editor: Shuang-yong Xu, New England Biolabs, Inc., United States of America

Received: June 22, 2012; **Accepted:** July 30, 2012; **Published:** September 12, 2012

Copyright: © 2012 Kohn et al. This is an open-access article distributed under the terms of the Creative Commons Attribution License, which permits unrestricted use, distribution, and reproduction in any medium, provided the original author and source are credited.

Funding: LB is a Research Director and BL is a Research Associate at the Funds for Scientific Research – FNRS (Belgium). DD is a Research Fellow of the Fonds pour la Formation à la Recherche dans l'Industrie et dans l'Agriculture (F.R.I.A.). This work was supported by grants of the "Fonds de la Recherche Fondamentale collective" (Grants and 2.4558.04 and 2.4508.10). The funders had no role in study design, data collection and analysis, decision to publish, or preparation of the manuscript.

Competing Interests: One of the authors (Jean-Michel Derochette) is employed by Prayon S.A. This does not alter the authors' adherence to all the PLOS ONE policies on sharing data and materials.

* E-mail: L.Bettendorff@ulg.ac.be

✉ These authors contributed equally to this work.

Introduction

Recently, we have demonstrated for the first time that a bacterial enzyme hydrolyzed inorganic triphosphate (tripolyphosphate, PPP_i) with high specificity and catalytic efficiency [1]. This enzyme from *Nitrosomonas europaea* (referred to as *NeuTTM*) belongs to the CYTH protein superfamily identified in 2002 by Iyer and Aravind [2]. According to these authors the catalytic domains of human 25-kDa thiamine triphosphatase (hThTPase, [3]) and CyaB-like adenylate cyclase from *Aeromonas hydrophila* (AC2, [4]) define a novel superfamily of domains supposed to bind "organic phosphates". This superfamily was therefore called "CYTH" (CyaB-THiamine triphosphatase), and the presence of orthologs was demonstrated in all three superkingdoms of life. Using multiple alignments and secondary structure predictions, Iyer and

Aravind showed that the catalytic core of CYTH enzymes contained a novel $\alpha+\beta$ scaffold with 6 conserved acidic and 4 basic residues. At least 4 of the acidic residues (generally glutamates) are likely to chelate 1 or 2 divalent cations that are required for catalysis, as is the case for nucleotide cyclases, polymerases and some phosphohydrolases [2,5,6]. Independently of those bioinformatic studies, Shuman and coworkers investigated the first step of RNA capping in fungi and protozoa catalyzed by RNA triphosphatases. They showed that the yeast RNA triphosphatase Cet1 belongs to a family of metal-dependent phosphohydrolases, whose active site is located within a topologically closed hydrophilic β -barrel (composed of 8 antiparallel β strands) that they called the "triphosphate tunnel" [7]. Strikingly similar structures were found for several bacterial and archaeal proteins

of unknown function [7]. Since all those proteins carry the CYTH signature, Gong et al., [7] coined the name “Triphosphate Tunnel Metalloenzyme” (TTM) for a superfamily including Cet-1-like RNA triphosphatases and all other CYTH proteins. However, the *NeuTTM* PPPase does not exhibit the closed tunnel structure [1]. On the other hand, bacterial CYTH enzymes have generally been annotated as adenyl cyclases, but only AC2 from *A. hydrophila* [4] and YpAC4 from *Y. pestis* [8] have been found to exhibit adenyl cyclase activity, and its physiological significance in these organisms is unclear.

Only two other bacterial CYTH enzymes have been functionally characterized: *NeuTTM* [1] and *CthTTM* from *Clostridium thermocellum* [9,10]. Both have a high PPPase activity (though *CthTTM* was less specific) but neither had any significant adenyl cyclase activity [1,9]. We thus suspect that PPPase activity might be the ancestral role of CYTH proteins, but the significance of such an activity is by no means clear. Indeed, in contrast to high molecular weight polyphosphates, no data are available concerning the presence or the possible role of PPP_i (and other short chain polyphosphates) in either prokaryotic or eukaryotic cells. However, this lack of data is essentially due to the current absence of sensitive and specific methods to detect short chain polyphosphates. Actually, it is not excluded that these compounds might play very important roles in cell physiology.

The aim of the present investigation was to check whether significant PPPase activities exist in *E. coli* but also in mammalian tissues and what enzymes are responsible for these activities.

Results

Characterization of recombinant *E. coli* ygiF protein

As we have previously shown that the *N. europaea* CYTH protein is a specific tripolyphosphatase [1], we wanted to check whether the *E. coli* ortholog ygiF [2], labeled as a predicted adenylate cyclase, had a similar activity and substrate specificity. YgiF was overexpressed in *E. coli* as a GST-fusion protein and purified (**Figure S1**). The purified fusion protein had indeed a high PPPase activity (**Figure 1**) with a V_{max} of $27 \pm 2 \mu\text{moles} \cdot \text{min}^{-1} \text{mg}^{-1}$ and the K_m was $270 \pm 25 \mu\text{M}$. The optimum pH was 8.5. The enzyme was activated by Mg^{2+} ($\text{EC}_{50} = 1.3 \pm 0.2 \text{ mM}$) and inhibited by Ca^{2+} ($\text{IC}_{50} = 0.6 \pm 0.3 \text{ mM}$). Among other substrates tested, only ThTP was slowly hydrolyzed. No hydrolysis was observed with ATP, ITP, GTP, PP_i or polyphosphate (65 ± 5 residues) as substrates (**Figure 2**).

These results suggest that ygiF, like *NeuTTM*, is a specific tripolyphosphatase, with the characteristic properties of the CYTH protein family, *i. e.* alkaline optimum pH, activation by Mg^{2+} and inhibition by Ca^{2+} .

In *E. coli* supernatants, hydrolysis of PPP_i is mainly catalyzed by inorganic pyrophosphatase

We first estimated the PPPase activity of a crude extract from wild-type MG1655 *E. coli* (supernatant obtained after sonication and centrifugation at $40,000 \times g$). We found a relatively high Mg^{2+} -dependent PPPase activity with alkaline pH optimum: the specific activity was about $0.2 \mu\text{mol} \cdot \text{min}^{-1} \text{mg}^{-1}$ at 37°C (with $[\text{PPP}_i] = 1 \text{ mM}$, $[\text{Mg}^{2+}] = 5 \text{ mM}$, pH 9.1). The activity was remarkably heat-stable (up to 80°C).

Those properties are reminiscent of *E. coli* inorganic pyrophosphatase (EcPPase) [11,12]. We therefore suspected that PPP_i hydrolysis by *E. coli* extracts might be mainly catalyzed by the PPase, which is abundant in the bacterial cytoplasm [13].

We partially purified the enzyme responsible for the high PPPase activity in *E. coli* supernatants using various chromatographic techniques (**Table S1**), followed by native electrophoresis on agarose gels and in-gel activity determination. The band containing the activity was then excised. Analysis by LC-ESI/MS/MS identified inorganic pyrophosphatase (PPase) as a major protein present in the fraction.

We therefore used a commercially available preparation of purified EcPPase to characterize its PPPase activity (**Figure 3**). This preparation indeed hydrolyzed PPP_i under the conditions observed above. As expected, it was less efficient for the hydrolysis of PPP_i than for PP_i , considered its natural substrate. With PPP_i , we found a $V_{max} = 50 \mu\text{mol} \cdot \text{min}^{-1} \text{mg}^{-1}$ at 25°C about 40% of V_{max} measured with PP_i under similar conditions ($V_{max} = 125 \mu\text{mol} \cdot \text{min}^{-1} \text{mg}^{-1}$). The K_m for PPP_i was $0.91 \pm 0.09 \text{ mM}$, three orders of magnitude higher than for PP_i ($\leq 10^{-3} \text{ M}$ compared to $\leq 10^{-6} \text{ M}$) [14].

Considering a molecular mass of 20 kDa per subunit, we estimated that $k_{cat} = 16.7 \text{ s}^{-1}$ at 25°C for PPP_i , compared to 42 s^{-1} for PP_i . Using a different preparation of recombinant *E. coli* pyrophosphatase, Aavaeva *et al.* [14] reported a substantially higher value for k_{cat} (389 s^{-1} with PP_i). In any event, due to the very large difference in K_m values for PP_i and PPP_i , the catalytic efficiency (k_{cat}/K_m) is much lower for PPP_i ($18.10^3 \text{ s} \text{ M}^{-1}$) than for PP_i ($\geq 42.10^6 \text{ s} \text{ M}^{-1}$). Considering that the intracellular PP_i concentration is relatively high, except under severe energy stress [13], it is likely that most of the active sites of pyrophosphatase remain saturated with PP_i and unavailable for PPP_i hydrolysis. In addition, the catalytic efficiency for PPP_i hydrolysis is low. Therefore, it may be argued that, *in vivo*, the pyrophosphatase is ineffective as a PPPase and ygiF, which is much more specific, might be the main enzyme responsible for PPP_i hydrolysis *in vivo*. We thus estimated the PPPase activity in the ygiF knockout strain JW 3026-2. No decrease of specific PPPase activity in crude extracts was observed (**Figure S2**), indicating that the contribution of ygiF to PPPase activity is, at best, marginal. This is not surprising as PPase is highly expressed in *E. coli* with nearly 400 copies per cell [15]. On the other hand, ygiF is expressed at only 20 copies per cell. It is therefore not surprising that ygiF does not contribute significantly to PPP_i hydrolysis in a bacterial supernatant fraction. For ygiF to play a significant role in PPP_i hydrolysis, it would require at least a 20-fold upregulation of its expression. This is however not very plausible as it is constitutively cotranscribed with glutamine synthetase adenyl transferase [16]. Also in contrast to inorganic pyrophosphatase, ygiF is not an essential protein.

As *E. coli* also contains an exopolyphosphatase which might be responsible for some PPP_i hydrolysis, we used a mutant strain devoid of both polyphosphate kinase and exopolyphosphatase ($\Delta\text{ppk-ppx::km}$). However, PPPase activity was the same in this strain as in the wild-type MG1655 strain (**Figure S3**), suggesting that exopolyphosphatase does not contribute significantly to PPP_i hydrolysis in an *E. coli* supernatant, in agreement with previous results that showed that PPP_i is not a good substrate for this enzyme [17].

We also tested whether PPase and PPPase activity changed during growth of *E. coli*, but both PPase and PPPase activities remained relatively constant (**Figure S4**).

CyaB adenylate cyclase has a significant triphosphatase activity but lacks specificity

The *A. hydrophila* CyaB protein, one of the founding members of the CYTH protein superfamily has an adenylate cyclase activity, but is different from class 1 adenyl cyclases present in most

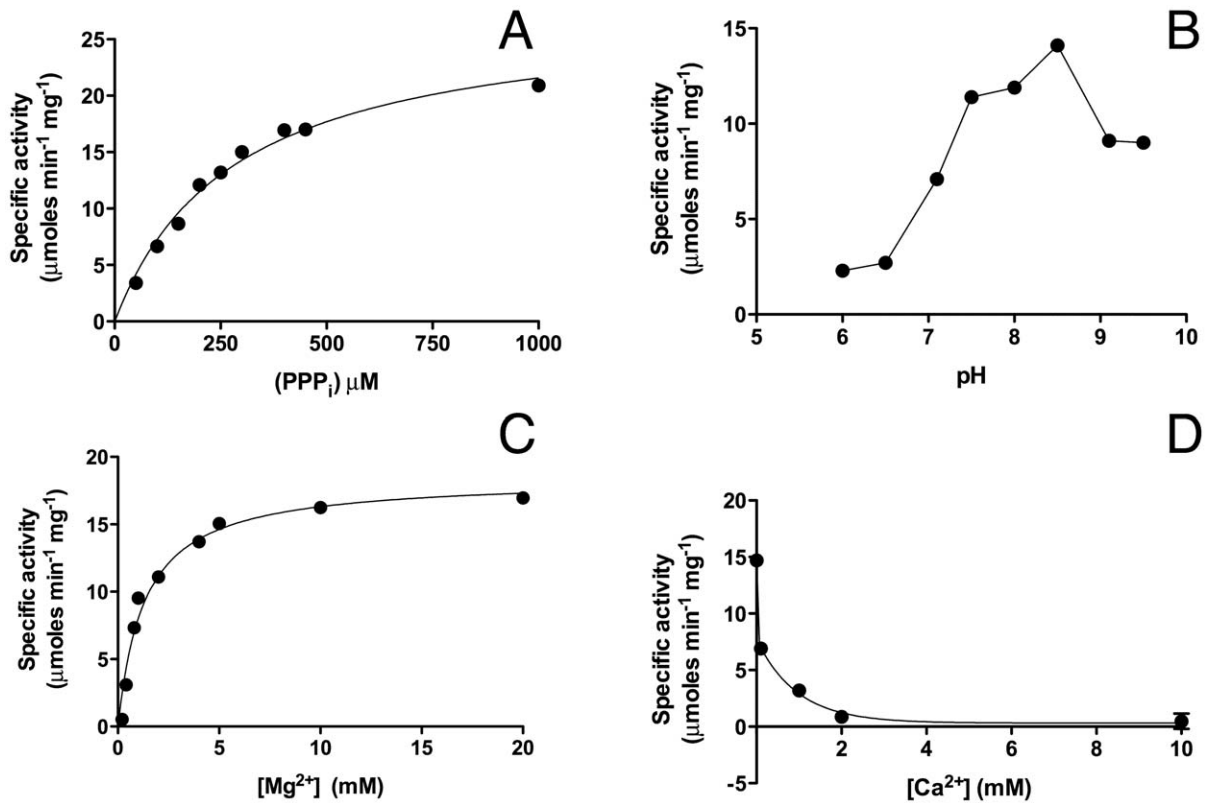


Figure 1. Enzymatic characterization of GST-ygiF PPPase activity. (A) Enzyme activity as a function of PPP_i concentration. The curve was obtained by non-linear fitting to the Michaelis-Menten equation. The Mg²⁺ concentration was 5 mM. (B) PPPase activity as a function of pH at 0.5 mM Mg²⁺. (C) PPPase activity as a function of Mg²⁺ concentration. (D) Inhibition of PPPase activity by Ca²⁺ in the presence of Mg²⁺ (5 mM). If not otherwise stated, the substrate concentration was 0.5 mM and the incubation was carried out at 50°C and at pH 8.5. (Means ± SD, n=3). doi:10.1371/journal.pone.0043879.g001

organisms [4]. Furthermore, CyaB was not expressed under normal laboratory growth conditions. As for ygiF, we wanted to test whether this enzyme is able to hydrolyze triphosphates. Our results show that it indeed hydrolyzes substrates such as ATP, ThTP and PPP_i but at a low rate (Figure 4A). In the presence of Mg²⁺ it has no preference for any of these substrates, while it has a slight preference for ThTP over ATP and PPP_i in the presence of Mn²⁺. The rate of hydrolysis of these substrates is at least an order of magnitude lower than its adenylate cyclase activity previously

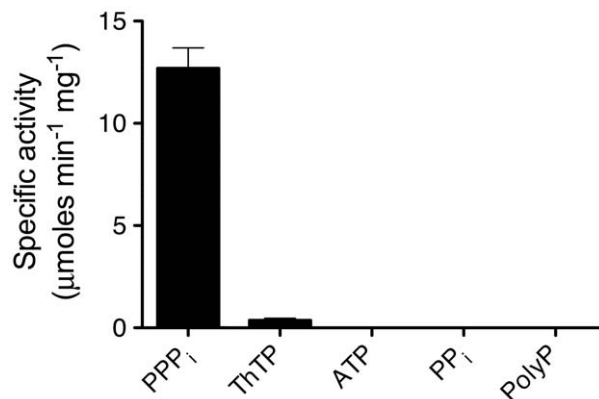


Figure 2. Specificity of GST-ygiF. The various substrates were tested at a concentration of 0.5 mM in the presence of 5 mM Mg²⁺. The incubation temperature was 50°C and the pH 8.5. (Means ± SD, n=3). doi:10.1371/journal.pone.0043879.g002

reported [4] and respectively 2 and 3 orders of magnitude lower than the PPPase activity of ygiF (this study) and NeuTTM [1]. Therefore, this activity is probably not of physiological importance. With ThTP as substrate, the optimum pH is alkaline (Figure 4B) as is usually observed with enzymes of the CYTH superfamily and the activity is highest at a temperature of 50°C (Figure 4C).

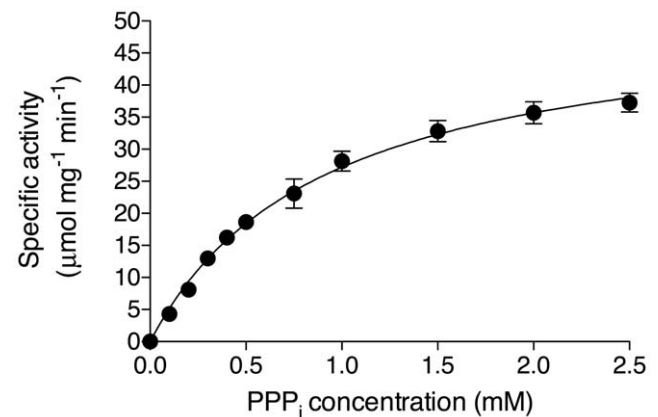


Figure 3. Enzyme activity of commercial *E. coli* recombinant pyrophosphatase as a function of PPP_i concentration. The enzyme was incubated in the presence of 10 mM Mg²⁺ in 50 mM CHES buffer at pH 9.1, for 30 min at 25°C. (Means ± SD, n=3). doi:10.1371/journal.pone.0043879.g003

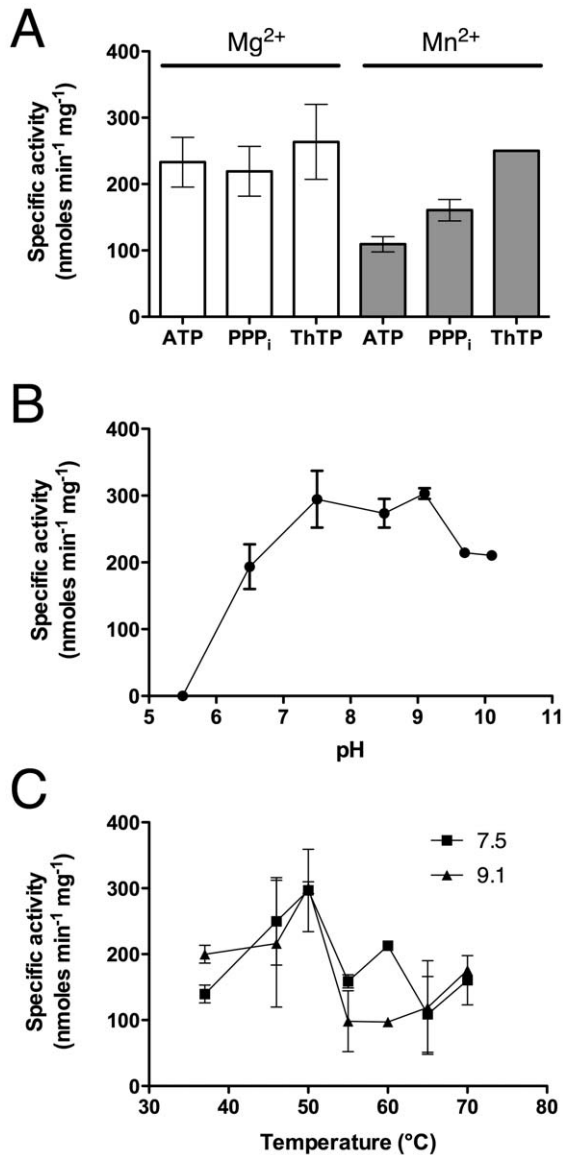


Figure 4. Enzymatic hydrolysis of ATP, PPP_i and ThTP by recombinant CyaB protein. (A) Specificity of CyaB in the presence of 5 mM Mg²⁺ or Mn²⁺ at pH 9.1. (B) pH dependence of ThTPase activity. (C) Temperature dependence of ThTPase activity at pH 7.5 and 9.1. If not otherwise stated, the substrate concentration was 0.5 mM, the Mg²⁺ or Mn²⁺ concentration was 5 mM and a temperature of 50°C was used. (Means ± SD, n=3). doi:10.1371/journal.pone.0043879.g004

PPPase activities in mammalian tissues

As the above results suggest that PPPase activities are rather common in bacteria, we wanted to test whether such activities are also present in mammalian tissues. We measured PPP_i hydrolysis in the supernatant fraction of several rat and quail tissues as well as pig brain (Figure 5A). The specific PPPase activity was highest in brain, only 2–3 times lower than in *E. coli* supernatants under identical conditions. The activity was not strongly pH-dependent but was highest around pH 7 (Figure 5B). PPPase activity was activated by Mg²⁺, to a lesser extent by Mn²⁺, but was insensitive to Ca²⁺ (Figure 5C).

In order to identify the enzyme responsible for PPPase hydrolysis in mammalian brain, we used a combination of

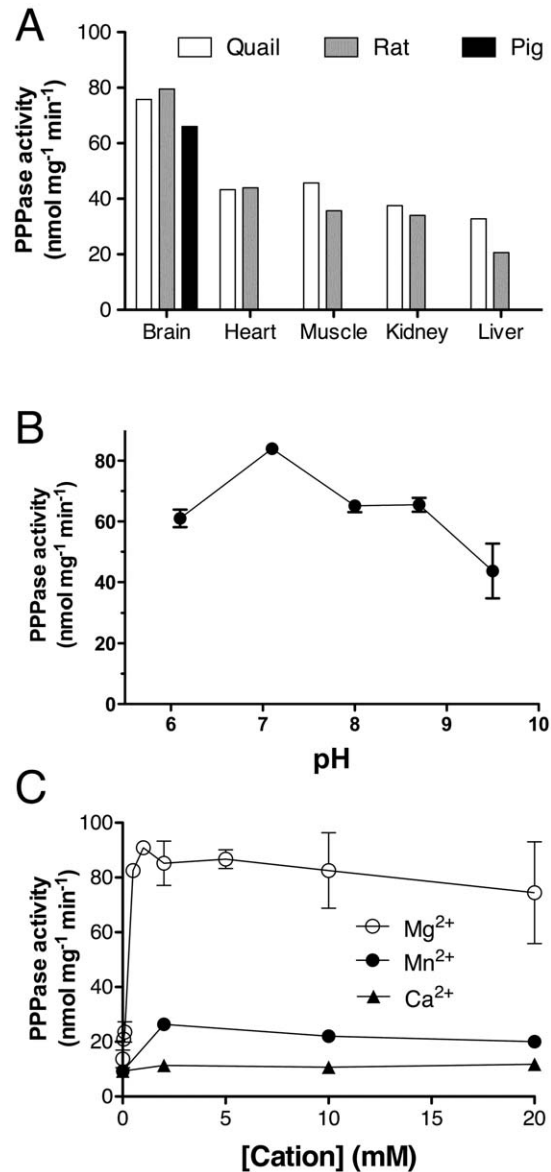


Figure 5. PPPase activities in animal tissue supernatant fractions. (A) PPP_i hydrolysis in various organs of the rat, and the quail, and in pig brain at pH 7.0 in the presence of 5 mM Mg²⁺ (n=3–9). (B) pH dependence of PPPase hydrolysis in rat brain in the presence of 5 mM Mg²⁺ (n=3). (C) Activation of PPPase activity by divalent cations. The PPP_i concentration was 0.5 mM and the incubation was carried out at 37°C. (Means ± SD, n=3–9). doi:10.1371/journal.pone.0043879.g005

chromatographic techniques and native polyacrylamide gel electrophoresis, and we carried out the identification by LC-ESI/MS/MS. A major protein identified was the pig homologue of the *Drosophila* protein prune. It was recently shown that human prune is an exopolyphosphatase with higher activity towards short chain polyphosphates such as PPP_i and P₄ [18]. It also hydrolyzes very efficiently adenosine and guanosine tetraphosphates. For PPP_i, the k_{cat} was 13 s⁻¹ and the K_m was as low as 2.2 μM. This suggests that most of the PPPase activity in mammalian tissues is due to h-Prune. The latter belongs to the DHH protein superfamily named after the characteristic N-terminal Asp-His-His motif. It has no sequence similarities with proteins of the CYTH superfamily (Figure S5).

h-Prune is often overexpressed in metastatic cancer and interacts with the metastasis tumor suppressor nm23-H1, coding for nucleoside diphosphate kinase A (NDPK-A). It was shown that phosphorylation of nm23-H1 by casein kinase 1 leads to complex formation with h-Prune, hence promoting cell motility in breast cancer cells. The role of h-Prune in normal adult brain cells is unknown. H-Prune and nm23-H1 are co-expressed during embryonic development and may play a role in mammalian brain development, while in the adult brain their role may be predominantly linked to their respective enzyme activities [19].

Is PPP_i present in living cells?

Until now PPP_i has not been shown to exist in living cells except for very specialized organelles such as protozoan acidocalcosomes [20]. One of the problems when determining PPP_i is the absence of a specific and sensitive detection method. We first tested a chromatographic separation technique using a Dionex device equipped with a conductivity detector. Such a method was already used to detect exogenously added tripolyphosphate in frozen cod and scallop adductor [21]. We were able to detect in *E. coli* a small peak at the retention time of PPP_i corresponding to a concentration of 1 μM , while no peak was detected in rat brain extracts (Figure 6).

A method using capillary electrophoresis (CE) coupled to a diode array detector was also optimized to detect PPP_i with a limit of detection estimated to 0.5 μM . After fractionation of *E. coli* supernatants on G-25 column, no PPP_i peak could be observed (Figure 7), suggesting that PPP_i , if it exists in living cells, is not a very abundant compound and its concentrations are probably in the low micromolar or even sub-micromolar range.

Discussion

Next to carbon, oxygen, nitrogen and hydrogen, phosphorus is the most abundant element in living organisms. Phosphorus is found mainly under the form of phosphate in many organic

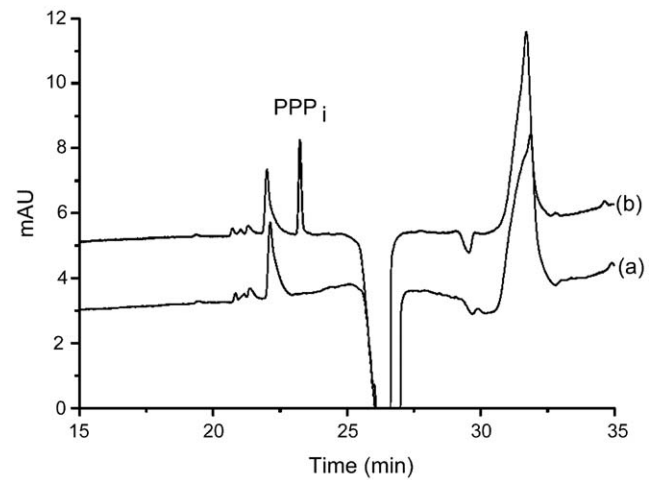


Figure 7. Separation of PPP_i by capillary electrophoresis. Electropherograms of (a) *E. coli* supernatant after fractionation on G-25 column and (b) *E. coli* supernatant after fractionation on G-25 column spiked with 3 μM PPP_i . doi:10.1371/journal.pone.0043879.g007

compounds such as nucleotides, metabolic intermediates (intermediates of glycolysis such as phosphoenolpyruvate for instance), phospholipids or in bones as calcium phosphate salts. In addition to be present in organic molecules, phosphates may exist in free forms. Hydrolysis of ATP yields P_i whose intracellular concentration may exceed 1 mM. P_i is recycled mainly by regeneration of ATP via F_0F_1 -ATP synthase according to the reaction $\text{ADP} + P_i \rightleftharpoons \text{ATP}$.

Inorganic pyrophosphate (PP_i) is released in different anabolic processes such as the synthesis of ribo- and deoxyribonucleotides ($(\text{NMP})_n + \text{NTP} \rightleftharpoons (\text{NMP})_{n+1} + PP_i$) or the synthesis of aminoacyl-tRNA (amino acid + tRNA + ATP \rightleftharpoons aminoacyl-tRNA + AMP + PP_i).

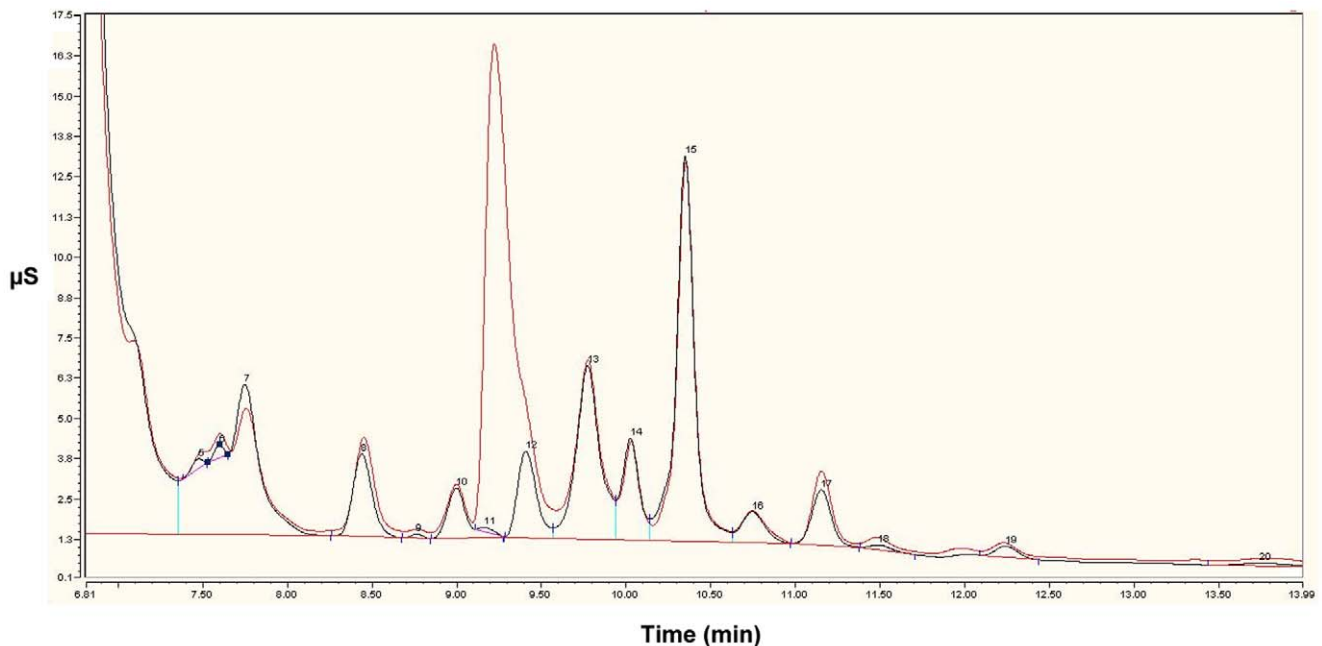


Figure 6. Separation of a *E. coli* extract on a Dionex column. The sample was spiked with exogenous PPP_i (10 mg/L). It can be estimated that peak 11 accounts for less than 0.5 mg/L. doi:10.1371/journal.pone.0043879.g006

In each case, PP_i is rapidly hydrolyzed to 2 P_i by an inorganic PPase (EC 3.6.1.1), rendering these reactions globally irreversible. PPases are widely distributed in all organisms and here, we show that at least *E. coli* PPase also has an important PPPase activity. Hence, PP_i is constantly formed in all organisms, but it is not synthesized *de novo*, at least in animal cells [22], though a pyrophosphate synthase, related to V-type ATPases, has been characterized from *Rhodospirillum rubrum* [23].

Long chain polyphosphates have been discovered in many organisms [24,25]. These polyphosphates are linear chains of up to 1000 P_i residues linked by phosphoanhydride bonds. They may play multiple roles as energy sources, phosphate reservoirs, phosphate donors and chelators of divalent cations. In *E. coli*, they are synthesized according to the reaction $(polyP)_n + ATP \rightleftharpoons (polyP)_{n+1} + ADP$. A recent study suggested that polyP could be synthesized in mammalian cells by a mechanism requiring F_oF_1 -ATP synthase [26]. Polyphosphates may be hydrolyzed by dedicated exopolyphosphatases, but less specific enzymes such as *Clostridium thermocellum* CYTH protein [10] or h-Prune for instance [18] may also act as exopolyphosphatases.

PPP_i has never been demonstrated to exist in living organisms with the exception of the very specialized protozoan acidocalcisomes [20]. PPP_i can be generated as the final product of polyP-glucose phosphotransferase (EC 2.7.1.63), present in various bacteria (*Mycobacterium tuberculosis*, *Propionibacterium shermanii*...). This enzyme uses polyP to form glucose 6-phosphate from glucose (($polyP$)_n+D-glucose \rightleftharpoons ($polyP$)_{n-1}+D-glucose 6-phosphate). In animals, an endopolyphosphatase (EC 3.6.1.10) may produce PPP_i [27]. PPP_i may also serve as a substrate for the phosphorylation of membrane proteins in rat liver microsomes *in vitro* [28]. This activity is probably not of physiological significance as it is inhibited by micromolar concentrations of ADP and ATP.

The observation that *NeuTTM* is a highly specific PPPase raises the question of the existence of this compound in living cells [1]. Moreover, our present results show that *ygiF*, which is commonly annotated a predicted adenylate cyclase, is also a relatively specific PPPase. Its activity is however insignificant compared to PPPase activity resulting from inorganic PPase in *E. coli*.

Figure 8 shows the comparison of the sequences of *NeuTTM* and *ygiF*. It is obvious that *ygiF* is about twice as long as *NeuTTM*. We previously suggested that the catalytic dyad in *NeuTTM* is formed by Tyr-28 and Lys-52. Though the equivalent of Tyr-28 is present in *ygiF*, the equivalent of Lys-52 seems to be absent. Furthermore, the specific activity of *ygiF* is one or two orders of magnitude lower than that of *NeuTTM*. These results suggest that the physiological role of *ygiF* might be different from PPP_i hydrolysis, but it is probably not an adenylate cyclase, as we were unable to detect such activity in purified *ygiF*.

We also studied another protein from the CYTH protein family: the *A. hydrophyla* CyaB protein, which was previously shown to have a significant adenylate cyclase activity. Our data show that CyaB also has PPPase activity, but this activity is lower than its adenylate cyclase activity [4]. Finally, we show for the first time a high PPPase activity in animal tissues, and in particular in brain. This PPPase activity is catalyzed by the homologs of the *Drosophila* exopolyphosphatase prune.

Our results show a high PPPase activity in many cells from bacteria to birds and mammals. However, few of these activities come from specific PPPases: the only known specific PPPases are *NeuTTM* and *ygiF*, though it is questionable that for the latter, this activity is of physiological importance.

In view of the many and important PPPase activities present in cells, the issue is to know whether PPP_i exists as such in living cells. This compound is difficult to detect in small amounts: there are no

specific enzymatic assays and it does not contain any chromophore or fluorophore. We first tested an anion exchange separation method coupled to electrochemical detection. This method is routinely used to test the composition of industrial preparations of small-chain polyphosphates. A small peak with a retention time corresponding to PPP_i was detected in *E. coli* but not in brain extracts. We then developed a method based on a separation of phosphates by capillary electrophoresis. Again, no definite conclusion could be drawn as to the existence of PPP_i in living cells. However, our data allow us to draw the conclusion that if it exists, intracellular concentrations hardly exceed 1 μ M. This would be in agreement with the high PPPase activities observed. Furthermore, many PPP_i hydrolyzing enzymes are proteins that are constitutively expressed with a relatively constant expression (inorganic pyrophosphatase, mammalian prune). It is therefore not likely that intracellular PPP_i concentrations undergo large variations, as it would be the case for a signaling molecule for instance.

PPP_i has a very strong chelating power for divalent cations and in particular Ca^{2+} , which is the reason why it was extensively used in detergents to control water hardness. The dissociation constant K_d for Ca^{2+} is approximately 10^{-7} M [29]. This would mean that if it accumulated in cells, it would be expected to interfere with Ca^{2+} signaling. It is therefore possible that the existence of PPPase activities of widely expressed less specific phosphohydrolases is a protective means to prevent accumulation of intracellular PPP_i that might accumulate from degradation of long chain polyphosphates for instance. From this point of view, specific PPPases such as *NeuTTM* could thus be considered as metabolite proofreading enzymes, an expression recently coined by Van Schaftingen and colleagues, by analogy with the proofreading enzymes involved in DNA repair for instance [30,31], and which should protect cells from unwanted toxic metabolic side-products.

On the other hand, it cannot be excluded that PPP_i, which is an energy-rich compound and the simplest triphosphate that can be imagined, may have played a role in energy metabolism in the earliest organisms. Therefore, we recently suggested that PPP_i hydrolysis could be the primitive activity of the CYTH protein family [1]. But with the appearance of PPPase side-activity in other abundant phosphohydrolases, CYTH proteins could have evolved towards more complex activities, such as adenylate cyclase in *A. hydrophyla* [4], mRNA-triphosphatase in *S. cerevisiae* and some protozoans [7,32,33] or thiamine triphosphatase in mammals [3,34].

Materials and Methods

Materials

Sodium triphosphate (PPP_i), sodium trimetaphosphate (Cyclic PPP_i), polyphosphate (sodium phosphate glass, 65 ± 5 residues), ATP, ITP, GTP, guanosine 5'-tetrphosphate (Gp₄, tris salt) and *E. coli* pyrophosphatase were from Sigma-Aldrich NV/SA (Bornem, Belgium). Thiamine triphosphate (ThTP) was synthesized and purified as previously described [35]. The CyaB expression plasmid pTRC99ACyaB was a gift of Drs Antoine Danchin and Agnieszka Sekowska (AMAbiotics SAS, Genopole Campus 1 - Genavenir 8, 5, rue Henri Desbrùeres, 91030 EVRY Cedex, France). All animal experiments were made in accordance with the directives of the committee for animal care and use of the University of Liège and in accordance with the European Communities Council Directive of November 24, 1986 (86/609/EEC). The protocols were approved by the Committee on the Ethics of Animal Experiments of the University of Liège (# 823 for rats and # 727 for quails). The animals were killed by

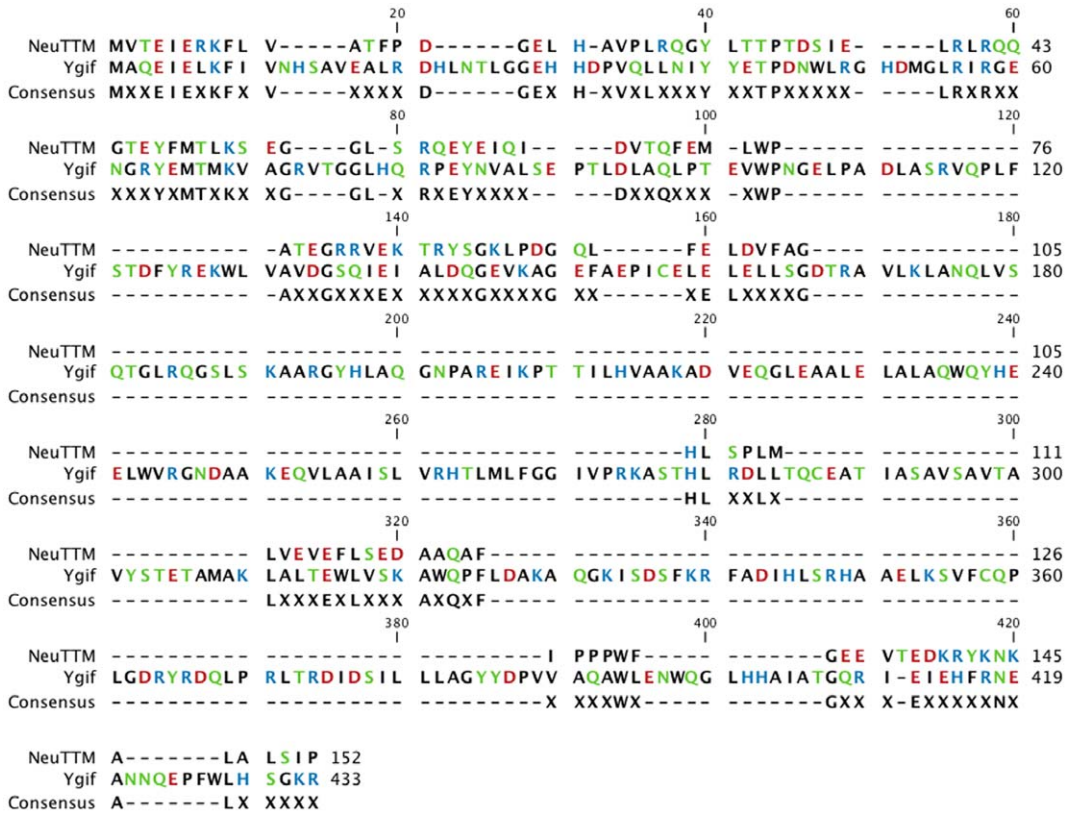


Figure 8. Sequence alignment of NeuTTM and ygif. The sequence alignment was made using CLC Sequence Viewer 6 (CLC bio A/S, 8200 Aarhus, Denmark). doi:10.1371/journal.pone.0043879.g008

decapitation and all efforts were made to minimize suffering. Pig brains were obtained from the local slaughterhouse (Abattoirs Publics de Liège & Waremme SC, rue de Droixhe 15, 4020 Liège, Belgium) with the permission to be used for experimental purposes at the University of Liège.

Bacterial strains

JW3026-2 (F-, Δ(araD-araB)567, ΔlacZ4787(::rrnB-3), λ⁻, ΔygiF747::kan, rph-1, Δ(rhaD-rhaB)568, hsdR514, CGSC#10312) was from the *E. coli* Genetic Stock Center (Yale University, New Haven CT, USA). The CF5802 strain lacking polyP kinase (PPK) and exopolyphosphatase (Δppk-ppx::km) [36] was a gift from Dr. M. Cashel (Laboratory of Molecular Genetics, NICHD, National Institutes of Health, Bethesda, MA).

Determination of phosphohydrolase activities

The standard incubation medium contained 50 mM buffer, 5 mM MgCl₂, 0.5 mM PPP_i and 20 μL of the enzyme at the adequate concentration in a total volume of 100 μL. The mixture was incubated at 37 or 50°C, the reaction was stopped by addition of 1 mL phosphate reagent [37] and the absorbance (UV-1800 Shimadzu UV spectrophotometer) was read at 635 nm after 30 min and compared with a standard curve (0–0.5 mM K₂HPO₄) to estimate the release of inorganic phosphate. The buffers used for incubation at different pH values were: Na-MOPS (pH 7.0–7.5), Na-HEPES (pH 7.5–8.0), Na-TAPS (pH 8.0–9.0), Na-CHES (pH 9.0–10.0) and Na-CAPS (pH 10.0–10.5).

Purification of PPPase activity from *E. coli* supernatants

E. coli wild type strain MG1655 was grown overnight in LB medium at 37°C under agitation (250 rpm). The bacteria were harvested by centrifugation for 10 minutes, at 8000×g at 4°C. The pellet was suspended in Hepes-buffer (30 mM Hepes, 50 mM NaCl, pH 7.2–7.4) and cells were lysed by high pressure using a French press. The lysate was centrifuged for 30 minutes at 40,000×g at 18°C. The supernatant (called S1) was brought to 50% saturation with ammonium sulfate and kept under constant stirring for one hour at room temperature. After centrifugation for 30 minutes at 20,000×g at 18°C, the supernatant (called S50) was brought to 80% saturation with ammonium sulfate and kept under constant stirring for one hour at room temperature. After centrifugation 30 minutes at 20,000×g at 18°C, the pellet was suspended in Hepes-buffer. The preparation obtained (called P80) was loaded on a monoQ column coupled to a Fast Protein Liquid Chromatography (FPLC) apparatus and elution was carried out with a linear NaCl gradient from 50 to 500 mM. The fractions with the highest PPPase activity were pooled (called F1) and placed on a Sephadex G200 column (1×25 cm) equilibrated with Hepes-buffer. Elution was performed in the same buffer. The fractions with the highest PPPase activity were pooled (called F2) and used to perform a non-denaturing polyacrylamide gel separation and the PPPase activity was determined as described below. The bands containing PPPase activity were cut and analyzed by liquid chromatography coupled on-line to positive mode electrospray ionization tandem mass spectrometry (UltiMate 3000 Nano LC Systems, Dionex, AmaZone, Bruker) for protein identification.

In-gel enzyme activities

Non-denaturing polyacrylamide gels (10%) were run in Tris-Glycine buffer (25 mM Tris, 190 mM glycine). After incubation for 30 minutes in a bath containing PPP_i (0.5 mM), buffer (20 mM), and MgCl_2 (1 mM), the gel was colored with phosphate precipitation reagent (1% v/v ammonium heptamolybdate, 1% v/v triethylamine, 1 N HNO_3) [38]. For *E. coli* PPPase, the incubation temperature was 50°C and buffer was Na-CHES (pH 9.5) while for pig brain PPPase incubation temperature was 37°C and buffer was Na-MOPS (pH 7.1).

Overexpression and purification of recombinant ygiF

YgiF was produced in *E. coli* as a GST fusion protein, as previously described [39]. Genomic DNA was isolated from *E. coli* DH5 α bacteria using a standard protocol (Invitrogen). YgiF coding sequence was amplified from 1 μg of genomic DNA using Pfu polymerase and 35 PCR cycles of denaturation (94°C, 20 s), annealing (64°C, 30 s) and elongation (72°C, 90 s) using forward (5'-TTTGGATCCATGGCTCAGGAAATCGAATTAAAG-3') and reverse (5'-TTTGC GGCCGCTTAACGTTTCCGCTGTGCAACC-3') primers. The fragment was then incubated for 15 minutes at 72°C in the presence of Taq polymerase and dATP to add a polyA tail. The 1.3 kb PCR fragment was cloned by TA cloning in the pGEM-T vector (Promega). The plasmid containing the insert was sequenced as described above and then digested by BamHI and NotI. The released fragment was purified on agarose gel and subcloned into pGEX-4T2 (GE Healthcare) to produce the GST-ygiF fusion protein in *E. coli* DH5 α . The GST-fusion protein was purified using a 1 mL GStap HP column (GE Healthcare).

Cloning of the *A. hydrophila* CyaB gene in the PVP16 vector

The plasmid pTRC99ACyaB (gift from A. Danchin and A. Sekowska AMAbiotics SAS, Genopole Campus 1 - Genavenir 8, 91030 EVRY Cedex, France), containing untagged CyaB, was used as starting material. The *A. hydrophila* CyaB gene (Sismeiro *et al.* 1998) was amplified by polymerization chain reaction and inserted in the PVP16 vector (Song *et al.* 2008). To confirm the insertion of the gene, the plasmid was sequenced. The two primers that were used to amplify the gene are: CyaB Forward: 5'-TTGGCGCGCCAGAAACCTGTACTTCCAGTCCATGTCATCACAACACTTTCAGG-3' and CyaB Reverse: 5'-TTACTAGTTCATGAGGGCACTTCTCTGAG-3'. The ATG underlined in the sequence of CyaB Forward corresponds to the codon that encoded the first methionine in the protein sequence.

Overexpression and purification of recombinant *A. hydrophila* CyaB

BL21DE3 were transformed with PVP16CyaB Vector and the expression of the protein was induced by using IPTG. This vector allows the expression of 8-histidine-tagged maltose binding protein (8HIS-MBP) fusion protein. After a first purification on a nickel column (1 mL HisTrapTM HP column (GE Healthcare) [1]), the tag was removed by Tobacco Etch Virus digestion and the purity was checked using Coomassie blue staining after SDS-PAGE.

Purification of PPPase activity from pig brain

PPPase was purified from about 500 g of pig brain. All the purification steps were carried out at 4°C. The tissues were homogenized in Tris-HCl buffer (30 mM Tris-HCl, 50 mM, NaCl, 0.1 mM EDTA, 1.5 mM DTT, pH 7.4). The homogenate

was centrifuged at 20,000 \times g for 20 minutes. The supernatant was brought to 80% saturation in ammonium sulfate and kept under constant stirring for 1 h. After centrifugation at 27,000 \times g for 30 minutes, the pellet was suspended in buffer A (20 mM Tris-HCl, 1 mM DTT, pH 7.4) and 5 ml aliquots were placed on a Sephadex G 75 column (3 \times 50 cm, GE Healthcare Life Sciences) equilibrated with buffer A. The proteins were eluted with the same buffer at a flow rate of 2 mL/min and all the fractions with high PPPase activity were pooled. The pool was loaded on a DEAE-Sephacel anion exchange column (1.4 \times 24 cm, GE Healthcare Life Sciences) equilibrated with buffer A. The proteins were eluted with an exponential concave NaCl gradient from 0 to 0.4 M in buffer A. Fractions with highest PPPase activity were pooled and centrifuged in Amicon ultra-15 centrifugal filter (Ultracel-10 membrane) units (Merck Millipore SA/NV, Overijse, Belgium). The retained proteins were dissolved in buffer B containing 20 mM Tris-HCl and 50 mM NaCl. 25 mg of protein were loaded on a Mono Q column (GE Healthcare Life Sciences) coupled to a Fast Protein Liquid Chromatography apparatus (ÄKTApurifier, Amersham) and elution was made with buffer B using a linear NaCl gradient from 50 to 500 mM. The fraction with the highest PPPase activity was pooled and DTT was added to reach a concentration of 1 mM. The proteins were then separated by non-denaturing polyacrylamide gel electrophoresis. The band with PPPase activity was cut and analyzed by liquid chromatography-mass spectrometry as described above for *E. coli* PPPase activity.

Detection of PPP_i using anion exchange column and electrochemical detection

Ion chromatography coupled with a conductivity detector was used to detect the tripolyphosphate anion. The chromatograph (Dionex ICS-2000) was equipped with an Ion Pac AS 16 2 \times 250 mm column, an Ion Pac AG16 2 \times 50 mm guard column and an ARS 300 suppressor. The KOH gradient necessary for ion separation was generated by an EluGen EGC-KOH cartridge. The gradient profile was the following: start at 20 mM KOH, linear ramp to 45 mM for 4 minutes, step at this level during one minute to fully resolve the tri-meta phosphate from pyrophosphate followed by a second linear ramp up to 70 mM KOH during 3 minutes to elute highly charged polyphosphate ions. The ions were detected by an integrated Dionex DS6 conductivity detector after eluent suppression. The injection volume was 25 μL and the flow rate was 0.36 mL/min.

Development of a method for PPP_i determination by capillary electrophoresis (CE)

CE experiments were carried out on a HP^{3D}CE system (Agilent Technologies, Waldbronn, Germany) equipped with an incorporated diode array detector and a temperature control system (15–60°C \pm 0.1°C). A CE Chemstation (Hewlett-Packard, Palo Alto, CA, USA) was used for instrument control, data acquisition and data handling. Fused-silica capillaries were provided by Thermo-Separation Products (San Jose, CA, USA).

Electrophoretic separations were carried out with uncoated fused-silica capillaries having 50 μm internal diameter and 70 cm length (61.5 cm to the detector). At the beginning of each working day, the capillary was washed with 1 N NaOH, water and the background electrolyte (BGE) for 10 min. Before each injection, the capillary was washed successively with water, for 1 min, 1 N NaOH for 3 min, water for 1 min and then equilibrated with the BGE for 5 min. The applied voltage was 12 kV in the negative polarity mode and UV detection was set at 260 nm. Injections

were made by applying a voltage of -10 kV for a period of 12 s and the capillary was thermostated at 30°C . The composition of the BGE was optimized according to sensitivity and selectivity: the PPP_i peak (N: 233.000) was well separated from PP_i and P_i . The BGE used for electrophoretic experiments was made up of 3 mM sodium molybdate in 200 mM malonate buffer adjusted to pH 3: acetonitrile (ACN) (80:20; v/v). The determination of PPP_i is based on the in-capillary formation of anionic polyoxomolybdate complex in the presence of ACN, as already described for phosphonate, P_i and PP_i [40]. *E. coli* supernatants were injected into the CE system after fractionation on a G-25 column.

Preparation of samples for PPP_i determination

E. coli (MG1655 strain) were grown overnight in 50 ml Luria Bertani medium and centrifuged (10 min at $8000\times g$). The pellet was suspended in 500 μL 20 % TCA and centrifuged for 5 minutes at $13,000\times g$. The TCA suspension was then extracted 10 times with 3 volumes of diethyl ether. The sample was injected onto a 3.9 mL G-25 column and fractions of 500 μl were collected in 10 mM Hepes pH 7. In the control samples, 83 μL of 72% TCA were added to 417 μL 10 mM PPP_i and treated as above.

Supporting Information

Table S1 Purification of tripolyphosphatase activity from *E. coli* soluble fraction.

(DOCX)

Figure S1 Purification of the GST-ygiF fusion protein.

(Lane 1, molecular mass weight markers; Lane 2, bacterial supernatant; lane 3, purified protein after the GST column [2]). (TIFF)

References

- Delvaux D, Murty MR, Gabelica V, Lakaye B, Lunin VV, et al. (2011) A specific inorganic triphosphatase from *Nitrosomonas europaea*: structure and catalytic mechanism. *J Biol Chem* 286: 34023–34035.
- Iyer LM, Aravind L (2002) The catalytic domains of thiamine triphosphatase and CyaB-like adenyl cyclase define a novel superfamily of domains that bind organic phosphates. *BMC Genomics* 3: 33.
- Lakaye B, Makarchikov AF, Antunes AF, Zorzi W, Coumans B, et al. (2002) Molecular characterization of a specific thiamine triphosphatase widely expressed in mammalian tissues. *J Biol Chem* 277: 13771–13777.
- Sismeiro O, Trotot P, Biville F, Vivares C, Danchin A (1998) *Aeromonas hydrophila* adenyl cyclase 2: a new class of adenyl cyclases with thermophilic properties and sequence similarities to proteins from hyperthermophilic archaeobacteria. *J Bacteriol* 180: 3339–3344.
- Aravind L, Koonin EV (1998) A novel family of predicted phosphoesterases includes *Drosophila* prune protein and bacterial RecJ exonuclease. *Trends Biochem Sci* 23: 17–19.
- Tesmer JJ, Sunahara RK, Johnson RA, Gosselin G, Gilman AG, et al. (1999) Two-metal-ion catalysis in adenyl cyclase. *Science* 285: 756–760.
- Gong C, Smith P, Shuman S (2006) Structure-function analysis of Plasmodium RNA triphosphatase and description of a triphosphate tunnel metalloenzyme superfamily that includes Cei1-like RNA triphosphatases and CYTH proteins. *RNA* 12: 1468–1474.
- Gallagher DT, Kim SK, Robinson H, Reddy PT (2011) Active-site structure of class IV adenyl cyclase and transphyletic mechanism. *J Mol Biol* 405: 787–803.
- Keppetipola N, Jain R, Shuman S (2007) Novel triphosphate phosphohydrolase activity of *Clostridium thermocellum* TTM, a member of the triphosphate tunnel metalloenzyme superfamily. *J Biol Chem* 282: 11941–11949.
- Jain R, Shuman S (2008) Polyphosphatase activity of CihTTM, a bacterial triphosphate tunnel metalloenzyme. *J Biol Chem* 283: 31047–31057.
- Josse J (1966) Constitutive inorganic pyrophosphatase of *Escherichia coli*. 1. Purification and catalytic properties. *J Biol Chem* 241: 1938–1947.
- Zyryanov AB, Shestakov AS, Lahti R, Baykov AA (2002) Mechanism by which metal cofactors control substrate specificity in pyrophosphatase. *Biochem J* 367: 901–906.
- Kukko-Kalske E, Lintunen M, Inen MK, Lahti R, Heinonen J (1989) Intracellular P_i concentration is not directly dependent on amount of inorganic pyrophosphatase in *Escherichia coli* K-12 cells. *J Bacteriol* 171: 4498–4500.
- Avaeva S, Ignatov P, Kurilova S, Nazarova T, Rodina E, et al. (1996) *Escherichia coli* inorganic pyrophosphatase: site-directed mutagenesis of the metal binding sites. *FEBS Lett* 399: 99–102.

Figure S2 PPPase activity as a function of pH in the supernatants of MG1655 (WT) and JW3026-2 (YgiF KO) strains at 37°C (0.5 mM PPP_i , 5 mM Mg^{2+}).

(TIFF)

Figure S3 PPPase activity in the supernatants of MG1655 (WT) and DPPK-PPX (CF5802) and DygiF (JW3026-2) strains.

The supernatants were incubated for 20 min at 50°C (5 mM PPP_i , 5 mM Mg^{2+} in TAPS buffer at pH 9.5). (Means \pm SD, n = 3).

(TIFF)

Figure S4 PPase (blue) and PPPase (red) activities as a function of growth in *E. coli*.

Growth was measured by following the absorbance at 600 nm (black curve).

(TIFF)

Figure S5 Sequence alignment of *Drosophila*, pig and human prune.

The sequence alignment was made using CLC Sequence Viewer 6 (CLC bio A/S, 8200 Aarhus, Denmark).

(TIFF)

Acknowledgments

Nucleic acid sequencing was made by the Genotranscriptomics Platform and protein identification by the LC-ESI/MS/MS by the Proteomics Platform, GIGA, University of Liège (<http://www.giga.ulg.ac.be/>).

Author Contributions

Conceived and designed the experiments: LB PW BL ACS MF JC BE. Performed the experiments: GK DD ACS JMD GS. Analyzed the data: GK DD BL ACS MF PW LB. Contributed reagents/materials/analysis tools: ACS GS MF BE JC. Wrote the paper: LB PW.

28. Tsutsui K (1986) Tripolyphosphate is an alternative phosphodonor of the selective protein phosphorylation of liver microsomal membrane. *J Biol Chem* 261: 2645–2653.
29. Chang DM (1983) The binding of free calcium ions in aqueous solution using chelating agents, phosphates and poly(acrylic acid). *JAOCs* 60: 618–622.
30. Linster CL, Noel G, Stroobant V, Vertommen D, Vincent MF, et al. (2011) Ethylmalonyl-CoA decarboxylase, a new enzyme involved in metabolite proofreading. *J Biol Chem* 286: 42992–43003.
31. Marbaix AY, Noel G, Detroux AM, Vertommen D, Van Schaftingen E, et al. (2011) Extremely Conserved ATP- or ADP-dependent Enzymatic System for Nicotinamide Nucleotide Repair. *J Biol Chem* 286: 41246–41252.
32. Lima CD, Wang LK, Shuman S (1999) Structure and mechanism of yeast RNA triphosphatase: an essential component of the mRNA capping apparatus. *Cell* 99: 533–543.
33. Gong C, Martins A, Shuman S (2003) Structure-function analysis of *Trypanosoma brucei* RNA triphosphatase and evidence for a two-metal mechanism. *J Biol Chem* 278: 50843–50852.
34. Song J, Bettendorff L, Tonelli M, Markley JL (2008) Structural basis for the catalytic mechanism of mammalian 25-kDa thiamine triphosphatase. *J Biol Chem* 283: 10939–10948.
35. Bettendorff L, Nghiê m HO, Wins P, Lakaye B (2003) A general method for the chemical synthesis of gamma-32P-labeled or unlabeled nucleoside 5(')-triphosphates and thiamine triphosphate. *Anal Biochem* 322: 190–197.
36. Kuroda A, Murphy H, Cashel M, Kornberg A (1997) Guanosine tetra- and pentaphosphate promote accumulation of inorganic polyphosphate in *Escherichia coli*. *J Biol Chem* 272: 21240–21243.
37. Lanzetta PA, Alvarez LJ, Reinach PS, Candia OA (1979) An improved assay for nanomole amounts of inorganic phosphate. *Anal Biochem* 100: 95–97.
38. Simonovic AD, Gaddameedhi S, Anderson MD (2004) In-gel precipitation of enzymatically released phosphate. *Anal Biochem* 334: 312–317.
39. Makarchikov AF, Lakaye B, Gulyai IE, Czerniecki J, Coumans B, et al. (2003) Thiamine triphosphate and thiamine triphosphatase activities: from bacteria to mammals. *Cell Mol Life Sci* 60: 1477–1488.
40. Himeno S, Inazuma N, Kitano E (2007) Simultaneous determination of phosphonate, phosphate, and diphosphate by capillary electrophoresis using in-capillary complexation with Mo(VI). *J Sep Sci* 30: 1077–1081.

Appendix 3



Structural determinants of specificity and catalytic mechanism in mammalian 25-kDa thiamine triphosphatase



David Delvaux^{a,1}, Frédéric Kerff^b, Mamidanna R.V.S. Murty^{c,2}, Bernard Lakaye^a, Jan Czerniecki^{a,3}, Gregory Kohn^a, Pierre Wins^a, Raphaël Herman^b, Valérie Gabelica^{c,4}, Fabien Heuze^d, Xavier Tordo^d, Raphaël Marée^{d,e}, André Matagne^f, Paulette Charlier^b, Edwin De Pauw^c, Lucien Bettendorff^{a,*}

^a GIGA-Neurosciences, Université de Liège, Avenue de l'Hôpital 1, B-4000 Liège, Belgium

^b Cristallographie des Macromolécules Biologiques, Centre d'Ingénierie des Protéines, Université de Liège, Allée du 6 Août 17, B-4000 Liège, Belgium

^c Physical Chemistry and Mass Spectrometry Laboratory, Department of Chemistry, Université de Liège, Allée de la Chimie 3, B-4000 Liège, Belgium

^d GIGA-Bioinformatics and Modeling, GIGA Systems Biology, Avenue de l'Hôpital 1, B-4000 Liège, Belgium

^e GIGA-Bioinformatics Core Facility, Avenue de l'Hôpital 1, B-4000 Liège, Belgium

^f Enzymologie et Repliement des Protéines, Centre d'Ingénierie des Protéines, Université de Liège, Allée du 6 Août, B-4000 Liège, Belgium

ARTICLE INFO

Article history:

Received 19 February 2013

Received in revised form 24 April 2013

Accepted 9 May 2013

Available online 22 May 2013

Keywords:

CyaB, ThTPase

Triphosphate tunnel metalloenzyme

Thiamine triphosphate

Tripolyphosphate

Divalent cation

ABSTRACT

Background: Thiamine triphosphate (ThTP) is present in most organisms and might be involved in intracellular signaling. In mammalian cells, the cytosolic ThTP level is controlled by a specific thiamine triphosphatase (ThTPase), belonging to the CYTH superfamily of proteins. CYTH proteins are present in all superkingdoms of life and act on various triphosphorylated substrates.

Methods: Using crystallography, mass spectrometry and mutational analysis, we identified the key structural determinants of the high specificity and catalytic efficiency of mammalian ThTPase.

Results: Triphosphate binding requires three conserved arginines while the catalytic mechanism relies on an unusual lysine–tyrosine dyad. By docking of the ThTP molecule in the active site, we found that Trp-53 should interact with the thiazole part of the substrate molecule, thus playing a key role in substrate recognition and specificity. Sea anemone and zebrafish CYTH proteins, which retain the corresponding Trp residue, are also specific ThTPases. Surprisingly, the whole chromosome region containing the ThTPase gene is lost in birds.

Conclusions: The specificity for ThTP is linked to a stacking interaction between the thiazole heterocycle of thiamine and a tryptophan residue. The latter likely plays a key role in the secondary acquisition of ThTPase activity in early metazoan CYTH enzymes, in the lineage leading from cnidarians to mammals.

General significance: We show that ThTPase activity is not restricted to mammals as previously thought but is an acquisition of early metazoans. This, and the identification of critically important residues, allows us to draw an evolutionary perspective of the CYTH family of proteins.

© 2013 Elsevier B.V. All rights reserved.

1. Introduction

Thiamine triphosphate (ThTP), the triphosphorylated form of vitamin B1, has been found in all organisms investigated to date, from

Abbreviations: CD, circular dichroism; PPP_n, inorganic tripolyphosphate; PPPase, tripolyphosphatase; ThDP, thiamine diphosphate; ThMP, thiamine monophosphate; ThTP, thiamine triphosphate; ThTPase, thiamine triphosphatase; TTM, triphosphate tunnel metalloenzyme

* Corresponding author. Tel.: +32 4 366 59 67; fax: +32 4 366 59 53.

E-mail address: L.Bettendorff@ulg.ac.be (L. Bettendorff).

¹ Present address: Angiogenesis and Cancer Research Lab, UCLouvain, 53 Avenue E. Mounier, B-1200 Bruxelles, Belgium.

² Present address: National Centre for Mass Spectrometry, Indian Institute of Chemical Technology, Uppal Road, Tarnaka, Hyderabad 500607, India.

³ Present address: Department of Biology and Pathology of Human Reproduction, Institute of Animal Reproduction and Food Research, Polish Academy of Sciences, Poland.

⁴ Present address: Univ. Bordeaux, IECB, ARNA Laboratory, F-33600 Pessac, France and INSERM, U869, ARNA Laboratory, F-33000 Bordeaux, France.

bacteria to mammals[1]. In *Escherichia coli* cells, ThTP might be a signal transiently produced in response to amino acid starvation [2], while a newly discovered thiamine derivative, adenosine thiamine triphosphate (AThTP) accumulates in response to energy stress [3,4]. In vertebrate tissues, ThTP can phosphorylate certain proteins, especially rapsyn [5], a protein essential for the clustering of acetylcholine receptors at neuromuscular junctions. In addition, ThTP favors the activation of a high-conductance anion channel in excised patches of neuroblastoma cells [6]. Although there is no proof that these effects are of physiological importance, they might suggest that, in animal tissues, ThTP is part of a new cellular signaling pathway. ThTP is synthesized by a chemiosmotic mechanism probably involving a conformationally modified form of F₀F₁-ATP-synthase [7,8].

In mammals, cytosolic ThTP concentration is kept low by a highly specific soluble phosphohydrolase, the 25-kDa thiamine triphosphatase (ThTPase) [9]. This 25-kDa enzyme has a relatively high catalytic efficiency, an alkaline pH optimum, which requires Mg²⁺ as activator

(Ca²⁺ is inhibitory) and its specificity for ThTP is nearly absolute [10]. Its sequence has no homology with any other known mammalian proteins [11]. However, bioinformatic studies showed that human ThTPase (hThTPase) and CyaB adenyl cyclase from *Aeromonas hydrophila* define a new superfamily of proteins with orthologs in the three superkingdoms of life [12]. This was called the CYTH (CyaB, ThTPase) domain and it was proposed to play several roles “at the interface between nucleotide and polyphosphate metabolism” [12]. Multiple alignments and secondary structure predictions indicated that the catalytic core of the CYTH domain contains a novel $\alpha + \beta$ scaffold with six conserved acidic and four basic residues. The latter are likely to bind phosphoryl groups, while four acidic residues (generally glutamate, among which the CYTH signature formed by the initial EXEXK sequence, Fig. 1) bind the divalent metal cations, generally Mg²⁺, required for catalysis [12].

More recently and independently of the above-mentioned bioinformatic studies, Shuman and associates pointed out that RNA triphosphatases of monocellular eukaryotes (yeast and protozoans) and some viruses exhibit striking similarities with bacterial and archaeal proteins belonging to the CYTH superfamily [13]. Despite low amino acid sequence similarity, yeast RNA triphosphatase (Cet1) and prokaryotic CYTH proteins with known crystal structure have a remarkably similar active site fold, consisting of eight antiparallel β strands (β -barrel). This fold forms a topologically closed tunnel with a hydrophilic cavity, where substrates and metal activators bind to conserved charged residues. Therefore, Gong et al. called Cet1 and other CYTH proteins “triphosphate tunnel metalloenzymes” (TTM), assuming that all CYTH proteins exhibit a similar TTM conformation.

However, the closed tunnel conformation may not be a constant feature of CYTH proteins. For instance, the solution structure of mouse 25-kDa ThTPase (mThTPase) was determined by NMR spectroscopy [14] and it was shown that the free protein had an open cleft structure. Yet, the ThTP-enzyme complex had a more closed conformation. In addition, the crystal structure of human 25-kDa ThTPase obtained in the presence of sulfate and citrate has a closed tunnel-like

structure (Protein Data Bank code 3BHD, Structural Genomics Consortium, Toronto, unpublished data). While the latter type of conformation may be restricted to proteins crystallized in the presence of polyanions and possibly enzyme–substrate complexes, free proteins may have open structures.

Here, we characterize in more detail the structural determinants and specific amino acid residues responsible for the catalytic efficiency of mammalian 25-kDa ThTPases and for their high specificity for ThTP. We show that orthologs from other animal phyla are also specific ThTPases. We discuss the implications of these findings for the molecular origin and evolutionary significance of the CYTH-TTM superfamily of protein.

2. Experimental procedures

2.1. Materials

ThTP was synthesized as previously described [15]. The *Nematostella vectensis* cDNA mixture from different embryonic, larval and polyp stages was a gift from Fabian Rentzsch (Sars Centre for Marine Molecular Biology, Bergen, Norway). The zebrafish cDNA was from the GIGA-Zebrafish Facility, University of Liège, Belgium.

2.2. Determination of ThTPase activity

The ThTPase assay was carried out as previously described [16]. The standard reaction medium contained 50 mM Na-TAPS (pH 8.5), 5 mM MgCl₂, variable concentrations of ThTP and 10 μ l of enzyme at the adequate concentration in a total volume of 100 μ l. The mixture was incubated for 10 min at 37 °C. The reaction was stopped by addition of 500 μ l trichloroacetic acid (12%) which was extracted with diethyl ether, and the ThDP formed was determined by HPLC as previously described [17]. When other substrates such as PPP_i were tested, the reaction was stopped by addition of 1 ml phosphate reagent [18]. After 30 min the absorbance was read at 635 nm and

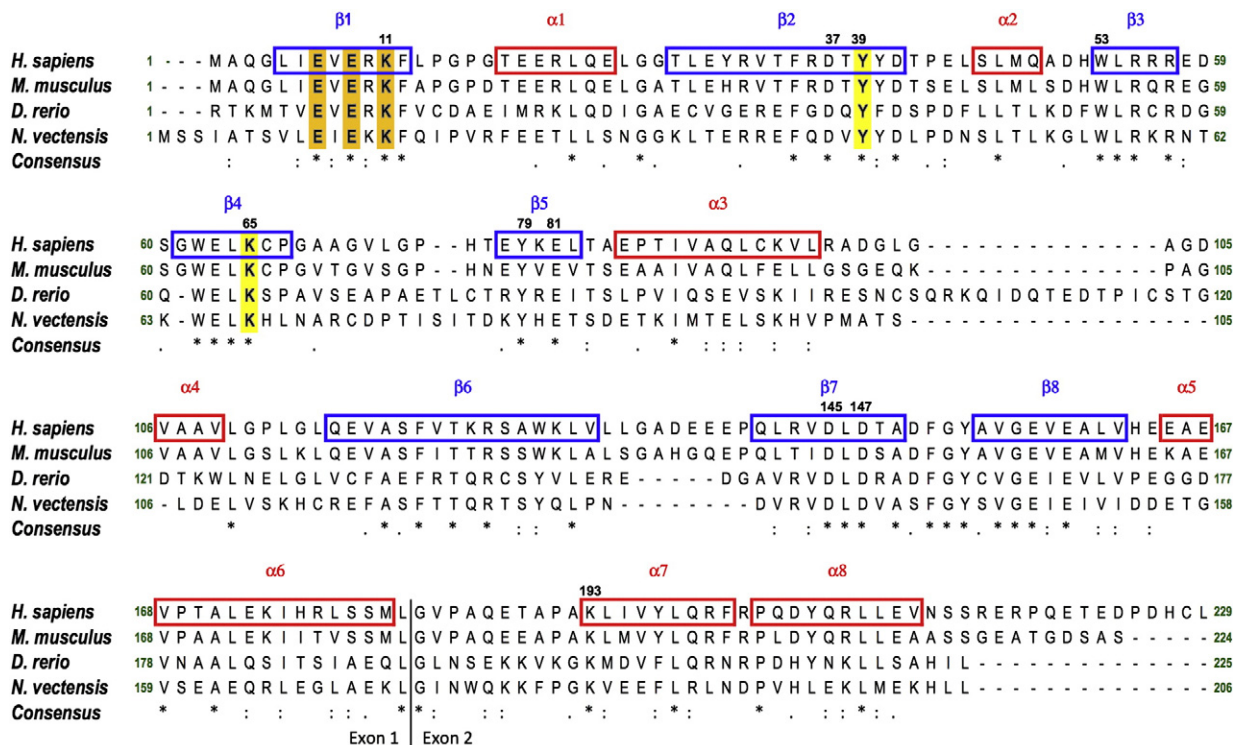


Fig. 1. Alignments of human, mouse, zebrafish and sea anemone ThTPase sequences. β -Sheets (blue boxes) and α -helices (red boxes) are indicated. The CYTH signature EXEXK is evidenced and Tyr-39 and Lys-65 are indicated in yellow. The separation between exon 1 and exon 2 is drawn by a black line.

compared to a standard curve to determine inorganic phosphate concentration. For the determination of enzyme activity as a function of pH, the following buffers were used: succinic acid (pH 5.3–5.7), MES (pH 5.8–6.4), PIPES (pH 6.5–6.9), MOPS (pH 7.0–7.3), HEPES (pH 7.4–7.9), TAPS (pH 8.0–8.8), CHES (pH 8.9–9.9), and CAPS (pH 10.0–10.5). The pH was adjusted with concentrated NaOH.

2.3. Site-directed mutagenesis

Mutants were generated by the QuickChange method using *Pfu* DNA polymerase. The plasmid was transferred to competent *E. coli* DH5 α for selection of ampicillin-resistant clones. Plasmid DNA sequences were checked by sequencing (GIGA, University of Liège).

2.4. Circular dichroism (CD)

CD spectra were collected at 25 °C, with a Jasco J-810 spectropolarimeter (Jasco, Japan), either in the far UV (185–260 nm) or in the near UV (250–300 nm) regions, using protein concentrations of 0.06–0.12 or 0.6–1.2 mg/ml, and 0.1 cm or 1 cm cell path lengths respectively. Proteins were in NaH₂PO₄ 10 mM at pH 7.5 and spectra were acquired at a scan speed of 20 nm/min, with a 0.2 nm data pitch, a 1 nm bandwidth and a 4 s response time. The spectra were averaged after four accumulations and corrected by subtraction of the buffer spectrum obtained under the same conditions. Ellipticity measurements in mdeg were converted in molar mean residue ellipticity, by using a mean residue weight value of 108.7 Da, on the basis of the enzyme composition. Calculation of the secondary structures from analysis of CD data was performed following the procedure of Raussens et al. [19].

2.5. Electrospray ionization mass spectrometry

Experiments were performed on a Q-TOF Ultima Global (Waters, Manchester, UK) electrospray mass spectrometer, in positive ion mode. The capillary voltage was 3.0 kV, the source and desolvation temperatures were 40 °C and 60 °C, respectively, the cone voltage was 40 V, the RF lens 1 voltage was 150 V, and the source pressure was 3.29 mbar. The cone and desolvation gas (nitrogen) were kept at 40 l/h and 400 l/h. Data acquisition and processing were carried out using MassLynx 4.1. All spectra shown are the sum of 150 scans and were smoothed (mean function, 2 \times 15 channels).

2.6. Cloning, expression and purification of zebrafish (*Danio rerio*) and starlet sea anemone (*N. vectensis*) ThTPases

The putative *thtpa* coding sequence of sea anemone and zebrafish were amplified from cDNA by PCR using *Pfu* DNA polymerase and appropriate primer pairs (5'-TTCATATGAGTTCATTGCAACCTCAGTTC-3' and 5'-TTGGATCCTTATAACAAATGCTTTTCCATGAGTTTCTC for sea anemone and 5'-TTCATATGTGCTGACTAGAAAACTGCAGAG-3' and 5'-TTGGATCCTATAAAATATGAGCTAAGAAGTTTGTG-3' for zebrafish). The PCR fragments were cloned into pGEM-T (Promega) and sequenced to check for mutation (GIGA—Genotranscriptomics Platform). Then both coding sequences were cloned into pET-15b (Novagen) to allow the production of His6 tagged proteins in BL21 λ DE3 *E. coli* strain (Novagen). Protein production and purification were performed as described previously [20].

2.7. Crystallization and structure determination of the ThTPase–PPP_i complex

The hThTPase was concentrated to 9.8 mg/ml in 40 mM Tris at pH 6.5 containing 0.2 M EDTA to inhibit the enzyme activity. Crystallization trials were performed at 20 °C using the hanging-drop vapor diffusion method and precipitant solutions similar to the one used for the ThTPase structure with PDB code 3BHD. The drop producing the crystal used for the data collection was composed of 2.5 μ l of protein

solution, 2 μ l of reservoir solution (0.2 M ammonium sulfate, 0.1 M sodium citrate buffer at pH 4.2), 0.5 μ l ethylene glycol 50% and 1 μ l of 0.3 M sodium triphosphate. The crystal was transferred into a cryoprotectant solution containing 50% glycerol before freezing in liquid nitrogen.

The diffraction data were collected at the European Synchrotron Radiation Facility FIP-BM30a beamline. The crystal belongs to the monoclinic P2₁ space group with unit cell parameters $a = 46.38$ Å, $b = 63.53$ Å, $c = 70.95$ Å and $\beta = 108.75^\circ$. The data were indexed, integrated and scaled with XDS [21]. The refinement and model building cycles were respectively performed with the CCP4 program Refmac5 [22] and Coot [23]. A summary of the relevant data collection and refinement statistics is given in Table 2. The structure was deposited in the protein data bank and received the code 3TVL.

2.8. Docking of ThsTP in the ThTPase structures

Each monomer of the crystallographic structures of the hThTPase available in the protein database (PDB code 3BHD) and of the hThTPase–PPP_i complex solved in this study was used to perform the docking experiments with Autodock Vina [24]. The structures of the four different monomers were prepared for the docking study as follows: water molecules were removed from the PDB files and polar hydrogens were added; Gasteiger charges were merged to the receptor. For the ThTP molecule, Gasteiger charges were assigned and non-polar hydrogen atoms were merged. The search space for the docking was defined as 27 Å cube centered on the middle of the tunnel-shaped active site. The default parameters of the Autodock Vina program were used except the exhaustiveness, which was increased from 8 to 100 to enhance the possibility of finding a deeply embedded solution.

2.9. Search for the *thtpa* gene in birds using bioinformatic analysis

Cross-species analysis of the 1 Mb region surrounding the *thtpa* gene was first performed using Synteny (<http://ensembl.org> release 69) that relies on pairwise whole genome alignments to compare the *Homo sapiens* region with *Mus musculus*, and with the chicken (*Gallus gallus*). Additionally, the 15 genes upstream and the 15 genes downstream *thtpa* were selected in *H. sapiens* genome and associated gene name searches were performed in *G. gallus*, zebra finch (*Taeniopygia guttata*), wild turkey (*Meleagris gallopavo*), zebrafish (*D. rerio*), and the green anole (*Anolis carolinensis*), using Ensemble Genome Browser (<http://ensembl.org> release 69) and EntrezGene (<http://www.ncbi.nlm.nih.gov/>).

3. Results

3.1. Zebrafish and sea anemone CYTH proteins are specific ThTPases

While CYTH proteins are present in practically all organisms, a ThTPase activity has been demonstrated only for some mammalian enzymes. In mammalian ThTPases, the sequence identities are nearly 80% [11], a percentage too high to pinpoint those amino acids essential for catalysis and substrate binding. Therefore we wanted to test ThTPase activity of the CYTH proteins of other vertebrates and invertebrates. One of the most obvious possibilities would have been birds, but although several bird genomes are known, they do not seem to contain a sequence corresponding to a CYTH protein (see below), in agreement with our previous studies unable to detect a significant soluble ThTPase activity in chicken tissues [1]. A CYTH sequence was however found in the zebrafish (*D. rerio*) and the starlet sea anemone (*N. vectensis*) (Fig. 1). Therefore, we expressed zebrafish and sea anemone CYTH proteins as His-tagged proteins and purified them to test their activities. Both proteins hydrolyzed ThTP, with a

fairly good specificity for ThTP over other triphosphorylated substrates (Fig. S1).

When comparing the sequences of human, mouse, zebrafish and sea anemone (*Cnidaria*) ThTPases, it can be seen that 47 amino acids are conserved (Fig. 1), including the universally conserved charged residues of the CYTH proteins [12]. Four conserved Glu residues (Glu-7, Glu-9, Glu-157, Glu-159) are thought to be involved in metal cofactor binding. Arg-55, Arg-57 and Arg-125 are probably involved in phosphate binding.

We recently showed that the residues homologous to Tyr-39 and Lys-65 most probably form the catalytic dyad in *Nitrosomonas europaea* TTM protein (*NeuTTM*), which is a specific inorganic tripolyphosphatase [20]. Those residues are also strictly conserved in animal CYTH proteins and therefore could play a role in catalysis in these enzymes too. Other conserved residues are Lys-11, Asp-37, Glu-81 and Asp-147. Furthermore, many uncharged residues are conserved and could play a role in binding the thiamine part of ThTP to the enzyme.

3.2. Absence of the *thtpa* gene in birds

Bioinformatic analysis did not allow us to find a sequence homologous to the mammalian *thtpa* gene in the chicken (*G. gallus*), the diamond mandarin (*T. guttata*) or the wild turkey (*Meleagris gallopavo*) genomes. Moreover, it seems that the whole region (30 selected genes) of the human chromosome 14 containing the *thtpa* gene has disappeared in birds (Table S1). This is in contrast to the mouse where this region is conserved, also on chromosome 14.

This also contrasts with the situation in the Carolina anole (*A. carolinensis*), a lizard containing 26 of the 30 selected genes conserved on the same chromosome 14. In the zebrafish, *thtpa* and its two direct neighbors (*ngdn* and *zfhx2*, Table S1) are localized to chromosome 24, while most other genes of the region have been scattered over many other chromosomes. Therefore, it seems that the disappearance of the *thtpa* gene is restricted to a small evolutionary branch that might include other archosauria (but we have presently no data about crocodylians) but not the whole phylum of diapsids, as a CYTH sequence is present in the lizard *A. carolinensis*.

3.3. Three-dimensional structure of human ThTPase as a complex with inorganic tripolyphosphate (PPP_i)

A crystal structure of human ThTPase (hThTPase), obtained in the presence of sulfate and citrate, was first deposited in the Protein Data Bank (PDB code 3BHD) by the Structural Genomic Consortium (Toronto, Canada). The asymmetric unit of the crystal contained two molecules and each of them presented a closed tunnel-like structure, characteristic of TTM proteins. One year later, the solution structure of the mouse ThTPase was determined by NMR [14]. The latter revealed a more dynamic structure, presenting an open fold in the absence of substrate and a more closed structure in the presence of ThTP. The protein is a monomer, as previously suggested for the soluble ThTPase purified from bovine brain [10].

As already reported [10,11], mammalian 25-kDa ThTPases are very specific for ThTP. In the case of recombinant hThTPase, the rate of hydrolysis of ATP under usual conditions ([S] = 0.5 mM, [Mg²⁺] = 5 mM, pH 8.5) is only 0.5% of that of ThTP. However, the rate of hydrolysis of PPP_i by mThTPase reached nearly 10% of ThTPase activity at V_{max} (with K_m = 0.5 mM) but this was observed at very alkaline pH (9.7) (Fig. S3).

We used these three substrates (ThTP, ATP and PPP_i) in our attempt to obtain crystals of the ThTPase–substrate complex with the human and mouse enzymes. However, the only crystals obtained were with PPP_i and the human ThTPase in the presence of EDTA to inactivate the enzyme. Crystals were difficult to reproduce and the low availability of ThTP prevented us from using similar conditions

(0.3 M stock solution and several cocrystallization trials). The crystallization conditions were similar to those in the previously deposited crystal structure (PDB code 3BHD). We obtained the structure of hThTPase as a co-crystal with PPP_i (Table 1, Fig. 2A). This structure, characterized by a 2.3 Å resolution, contains two molecules in the asymmetric unit. A few residues are not sufficiently defined at the N and C terminal ends as well as in the loop connecting β6 and β7. In monomer A, residues 4 to 132 and 140 to 214 could be built in the electronic density while residues 5 to 132 and 141 to 211 of monomer B are present in the model. No density corresponding to the citrate molecules present in the 3BHD structure could be identified in the active site of the two monomers. Instead, in each active site, a PPP_i molecule has been modeled in the observed density (Fig. 2C, D). The mean B factor calculated for all the atoms of the PPP_i molecules is, however, twice as high as the mean B factor of the protein atoms, meaning that the PPP_i molecules may be characterized by an occupancy significantly lower than 100% and/or some significant flexibility. The positions of these two PPP_i molecules are not exactly identical and the equivalent phosphorus atoms are between 1.2 Å and 1.5 Å apart (Fig. 2E).

In the structure of the hThTPase–PPP_i complex, the general fold of the monomer A and monomer B forming the asymmetric unit is very similar to the equivalent monomers of the previously reported structure with citrate in the active site (PDB code 3BDH). The rms deviation between monomers A of each structure is 0.361 Å over 172 Cα while it is 0.589 Å over 142 Cα for monomers B. The rms deviation between monomer A and monomer B of the hThTPase–PPP_i complex is 0.628 Å over 192 Cα. In monomer A, the largest differences are in the loops connecting α3 to α4 and β6 to β7 (Fig. 2A). The first one is only defined in the hThTPase–PPP_i complex while the second is only observed in the 3BHD structure. In monomer B, as in monomer A, the β6–β7 loop is only present in the 3BHD structure but with a different conformation than in monomer A (Fig. 2B). A larger difference, compared to hThTPase–PPP_i monomer B and the two monomers A, is observed in the region starting from the end of the β8 strand to the beginning of the α7 helix that includes α5 and α6. These helices are slightly displaced and the α6–α7 loop adopts a

Table 1
Diffraction data and refinement statistics.

| Diffraction data statistics | |
|---|------------------------|
| Wavelength (Å) | 0.9797 |
| Space group | P2 ₁ |
| a, b, c (Å) | 46.378, 63.529, 70.950 |
| B (°) | 108.75 |
| Resolution range (Å) | 46.2–2.3 (2.42–2.3) |
| Unique reflections | 16,547 (1969) |
| Completeness (%) | 94.8 (78.2) |
| Redundancy | 3.2 (3.1) |
| R _{merge} (%) | 9.9 (45.1) |
| R _{pim} (%) ^a | 6.3 (29.3) |
| Average I/σ | 9 (2.6) |
| Refinement statistics | |
| Resolution range (Å) | 46.2–2.3 (2.36–2.3) |
| R _{cryst} (%) | 18 (18.9) |
| R _{free} (%) | 26.1 (35.4) |
| No. of non-hydrogen protein atoms | 3160 |
| No. of water molecules | 95 |
| Rms deviations from ideal stereochemistry | |
| Bond length (Å) | 0.014 |
| Bond angles (°) | 1.574 |
| Mean B factor (Å ²) | |
| All atoms | 28.3 |
| Ligand atom | 61.3 |

Values in parentheses correspond to the highest resolution shell.

^aR_{pim}: Precision-indicating merging R factor.

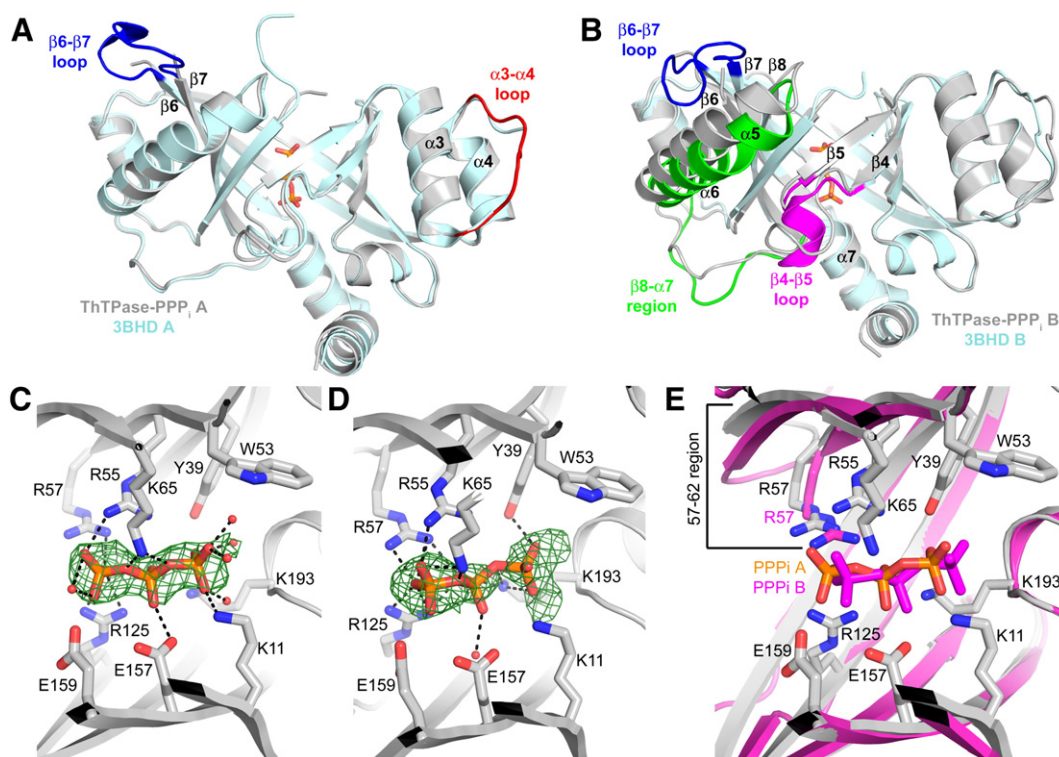


Fig. 2. Crystal structure of the hThTPase-PPP_i complex. (A, B) Cartoon representation of the hThTPase-PPP_i complex structure (gray) superposed to the 3BHD structure (pale cyan) with the major differences highlighted in various colors. (A) Monomer A. (B) Monomer B. (C, D) Representation of the PPP_i molecule inside the active site of each monomer. The difference map calculated in absence of PPP_i is shown in green at a cutoff of 2 σ . (C) Monomer A. (D) Monomer B. (E) Superposition of monomer A (gray) and B (magenta). The 57–62 region which is characterized by the largest difference is highlighted by black line.

completely different orientation in monomer B of 3BHD. This modification is also concomitant with the appearance of a short helix in the β 4– β 5 loop. All these differences are mostly connected to interactions with neighboring molecules in the crystal and do not seem to directly result from the presence of the PPP_i molecules in the active sites.

In monomer A, the PPP_i molecule is within hydrogen-bonding distance (<3.2 Å) of five water molecules and the side chains of five residues (Fig. 2C). The alpha phosphate interacts with the amino group of Lys-11 and four water molecules, the beta phosphate with Lys-65 and the carboxyl group of Glu-157, the gamma phosphate with one water molecule and the guanidinium group of Arg-55, Arg-57 and Arg-125. In addition, Tyr-39 is located at about 3.3 Å from the alpha phosphate and Lys-193 at about 3.5 Å from the beta phosphate. All but one of those residues display an orientation similar to the one observed in monomer A of the 3BHD structure which contains citrate in the active site. The Arg-55 side chain is indeed switched from pointing in the solvent to a position inside the active site tunnel because of the presence of the PPP_i molecule.

In monomer B, the alpha phosphate is closer to the Lys-193 and Tyr-39 side chains than to Lys-11, the β phosphate interacts with Arg-57, Arg-125 and a water molecule, and the γ -phosphate binds to the same three arginine residues as in monomer A (Arg-55, Arg-57 and Arg-125) but also to Lys-65 (Fig. 2D). This different positioning can be correlated with the slight displacement of residues 57 to 62 in monomer B compared to monomer A (Fig. 2E) due to a different environment in the crystal.

In both monomers, the side chains of glutamate residues Glu-7, Glu-9, Glu-157 and Glu-159 are directed towards the active site. These residues, conserved among all the proteins of the CYTH family are involved in Mg²⁺ binding [12]. No cation is observed in the structure because of the presence of EDTA in the crystallization condition to inhibit the enzyme activity. The space between these glutamates and

the PPP_i molecule is large enough to accommodate the Mg²⁺ ions required for the activity but the prediction of their exact positions could not be made with enough confidence.

3.4. Docking solution of the ThTP substrate in the structure of hThTPase

In order to investigate the origin of the specificity of ThTPase for ThTP and because no crystal structure could be obtained with this substrate, we performed docking simulations with the AutodockVina software. For these calculations, we used each monomer of the two crystallographic structures available (3BHD and the complex described above) as fixed entities and searched for the best position (lowest energy) with a flexible ThTP molecule. The solution with the lowest energy (−8.9 kcal/mol) was obtained for monomer A of the ThTPase-PPP_i complex. The result is shown in Fig. 3A–C. In this solution, the ThTP molecule lies inside the active site in an extended conformation, spanning the entire depth of the tunnel (Fig. 3B). The thiazole ring of the thiamine forms a stacking interaction with Trp-53, and the aminopyrimidine ring lies in a pocket defined by His-76, Pro-191 and Ile-195. The triphosphate moiety occupies a similar position as in the ThTPase-PPP_i complex, with interactions involving the side chains of Lys-11, Arg-55, Arg-57, Lys-65, Arg-125 and Lys-193 (Fig. 3C). The 3 phosphorus atoms of ThTP are respectively less than 1.3 Å and 0.8 Å away from the equivalent atoms of the PPP_i molecule in monomer A and monomer B of the ThTPase-PPP_i complex, showing a good agreement between the docking solution and the structure.

This docked solution can also be compared to the CYTH protein from *Yersinia pestis* (YpAC4 class IV adenylyl cyclase) for which the structures of two complexes with non hydrolyzable ATP analogs have been reported [25]. The sequence identity between this adenylyl cyclase and hThTPase is very low (below 15%). The comparison of

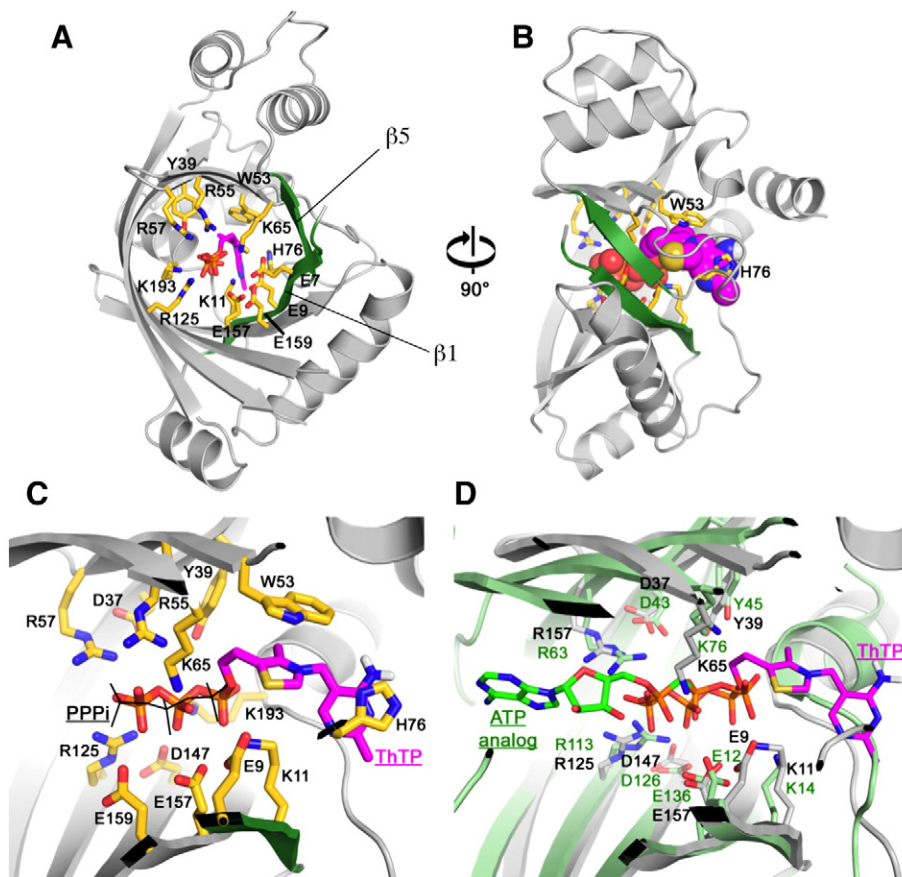


Fig. 3. Docking of ThTP in the structure of hThTPase. (A) Representation of the three-dimensional structure of the human ThTPase with ThTP docked in its active site. The two protein stretches (residues 5–12 and 78–82) participating in the closing of the tunnel are displayed in green. Important ThTPase residues are shown as yellow sticks and the ThTP molecule as magenta sticks. Antiparallel strands $\beta 1$ and $\beta 5$ are indicated. (B) Same as (A) rotated by 90° with the ThTP molecule shown as spheres. (C) Close up view of the ThTP molecule environment with a PPPi molecule from the crystallographic structure superposed and displayed as thin black lines. (D) hThTPase–ThTP complex superposed to the *Y. pestis* adenyl cyclase [25] (light green) with diphosphomethylphosphonic acid adenosyl ester (green) bound in the active site.

these structures to the hThTPase structure was therefore performed by only superimposing the residues conserved in the active site (Fig. 3D). The result reveals a good correlation between the positions of the triphosphate moieties of ATP and ThTP (less than 1.5 \AA between equivalent phosphates) but their adenosine and thiamine parts are located in opposite sides of the tunnel. This apparently surprising observation is in line with the different activities of the two enzymes, as the adenyl cyclase activity involves cleavage between the α and β phosphates while ThTPases cleave between the β and γ phosphates. This further validates the positions obtained for PPPi by crystallography and for ThTP by docking.

3.5. Alanine scanning of conserved residues in the active site: implication for catalytic mechanism and substrate specificity

We have previously used phosphate detection for measuring ThTPase activities. It appeared however that with this method, particularly at high substrate concentration, we often observed activation or inhibition by excess substrate [14]. Therefore, here, we used a highly sensitive HPLC method for the determination of ThDP released. This method is much more sensitive than the phosphate method, leading to a K_m of mThTPase for ThTP of at least an order of magnitude lower, i.e., $8 \pm 2 \text{ \mu M}$, than previously reported [14].

Based on the knowledge of conserved residues in metazoan 25-kDa ThTPases (Fig. 1), as well as on our structural data (Figs. 2 and 3) and on RMN data [14]. The following residues in mThTPase were mutated to alanine: Lys-11, Asp-37, Tyr-39, Trp-53, Lys-65,

Tyr-79, Glu-81, Asp-145, Asp-147 and Lys-193. With the exception of D145A, all the mutations affected at least one kinetic parameter (K_m or k_{cat}) to different extents (Table 2, Fig. S2).

The most dramatic effect on k_{cat} was observed with the K65A mutation: k_{cat} was 10^3 to 10^4 -fold lower for the mutant than for the WT mThTPase, indicating that Lys-65 is essential for catalysis. This is in agreement with our recent observation that Lys-52 (homologous to Lys-65 in mThTPase) in the CYTH protein from *N. europaea* (NeuTMM [20]) is also essential for catalysis in this bacterial triphosphatase.

We mutated two other conserved lysine residues, 11 and 193. Lys-11 is highly conserved in CYTH proteins, being part of the EXEXK CYTH signature [12]. Surprisingly however, the K11A mutation did not

Table 2
Kinetic parameters of wild-type mThTPase and some of its mutants.

| Enzyme | K_m (μM) | V_{max} ($\mu\text{mol min}^{-1} \text{mg}^{-1}$) | k_{cat} (s^{-1}) | k_{cat}/K_m ($\text{s}^{-1} \text{M}^{-1}$) |
|--------|-------------------------|---|-------------------------------|---|
| WT | 8 ± 2 | 59 ± 4 | 23 ± 3 | 3×10^6 |
| E81A | 13 ± 3 | 35 ± 3 | 14.1 ± 1.2 | 1×10^6 |
| K11A | 12 ± 3 | 15 ± 2 | 6 ± 1 | 0.5×10^6 |
| Y79A | 42 ± 17 | 16 ± 4 | 6 ± 2 | 0.14×10^6 |
| D37A | 200 ± 12 | 6.9 ± 0.2 | 2.8 ± 0.1 | 14×10^3 |
| W53A | 550 ± 90 | 11 ± 1 | 4.4 ± 0.2 | 8×10^3 |
| K65A | 9 ± 2 | 0.048 ± 0.005 | 0.019 ± 0.002 | 2×10^3 |
| K193A | 740 ± 130 | 3.7 ± 0.5 | 1.5 ± 0.2 | 2×10^3 |
| Y39A | 620 ± 60 | 1.6 ± 0.1 | 0.64 ± 0.02 | 1×10^3 |
| D147A | 2800 ± 500 | 6.5 ± 0.6 | 2.6 ± 0.2 | 1×10^3 |

significantly increase K_m while k_{cat} was reduced by a factor of only about 4. This was unexpected as our structural data (Figs. 2C–E and 3C) suggest an interaction between Lys-11 and the α -phosphate of ThTP. Thus, we would expect the K11A mutation to increase K_m . Such an effect was observed for the *NeuTTM* PPPase: the corresponding K8A mutation markedly increased K_m without increasing k_{cat} [20]. Therefore, our data suggest that Lys-11 is not important for ThTP binding in the case of mThTPase. Another possibility would be that Lys-11 interacts with the neighboring Glu-9 involved in divalent cation binding and might be important for the specificity of the Mg^{2+} -binding site. However, the activating effects of Mg^{2+} were the same as for the WT mThTPase (EC_{50} about 0.5 mM). It must be concluded that in mammalian 25 kDa ThTPases, this highly conserved Lys-11 residue plays no important role in catalysis.

In contrast to Lys-11, mutating Lys-193 (which is located in exon 2) strongly decreased k_{cat} , though the K193A mutant was still ≈ 80 times more active than K65A. Structural data (Figs. 2 and 3) indicate an ionic interaction with the α -phosphoryl group of the substrate. This suggests that Lys-193 should not be directly involved in catalysis (as the splitting occurs between β and γ groups). Kinetic data (Table 2) show that the mutation increases the apparent K_m about 100-fold. Taken together, those data suggest that Lys-193 is important for binding and correct positioning of the triphosphoryl part of the substrate.

From the mutational analysis concerning the three conserved lysine residues, it appears therefore that only Lys-65 is likely to be directly involved in the catalytic mechanism. The same conclusion had been reached concerning the homologous Lys-52 in *NeuTTM* [20]. In the latter case, it was suggested that Lys-52 forms a catalytic dyad with Tyr-28. We therefore mutated the homologous Tyr-39 to alanine in mThTPase and found a 40-fold decrease in k_{cat} , while K_m increased about 80-fold (Table 2). Note that for the K65A mutant, the k_{cat} is still two orders of magnitude lower than for Y39A. However, as K_m is not significantly affected by the K65A mutation (Table 2), the catalytic efficiency is similar (and very low) for both mutants. It thus seems plausible that Lys-65 and Tyr-39, like the corresponding residues in *NeuTTM*, may form a catalytic dyad, through a mechanism as shown in Fig. 4. The hypothesis is also supported by the crystallographic data: indeed, in the hThTPase–PPP_i complex, Lys-65 and Tyr-39 are close enough so that the nucleophilic nitrogen of Lys-65 can be hydrogen-bonded with the phenolate oxygen of Tyr-39 (Fig. 3C). As in *NeuTTM*, the phenolate oxygen would act as the general base removing a proton from water, and the resulting OH[−] can attack a phosphorus atom of the substrate. Note that such a mechanism could hardly be operative at acid pH, as the tyrosine

phenol group would remain protonated. This is in line with the observation that both *NeuTTM* and mammalian ThTPases have an optimum pH > 8. It is interesting to note that, in the CYTH protein from *Y. pestis* (YpAC4 class IV adenylyl cyclase) recently investigated [25], homologous lysine and tyrosine residues are also present, but the higher distance between Lys-76 and Tyr-45, as well as their unfavorable respective orientations should hardly allow them to function as a catalytic dyad. This is not surprising as YpAC4 has adenylyl and guanylyl cyclase activities but, in contrast to other TTM proteins, had no phosphohydrolase activity.

Note that while mutation of Lys-65 does not affect the K_m , mutation of Tyr-39 leads to a nearly 100-fold increase in the K_m (Table 2). This increase could result from a poor positioning of the Arg-55 and/or Arg-57. Tyr-39 is indeed in the direct vicinity of Arg-55 and forms a hydrogen bond stabilizing Asp-37, which appears to be responsible for the correct orientation of Arg-57.

Surprisingly, while Glu-81 is also a highly conserved residue, from cnidarians to mammals, the E81A mutation resulted in only a small, probably insignificant change, in k_{cat} and K_m (Table 2). The other kinetic properties were not significantly modified. Structural data suggest that the carboxylate of Glu-81 is oriented towards the active site cavity, but no specific interactions with lysine or arginine residues were apparent.

We then investigated the possible role of three aspartate residues, Asp-37, 145 and 147. Asp-37 is strictly conserved not only in animal species but also in the marine choanoflagellate *Monosiga brevicollis* and even in CYTH proteins from *Saccharomyces cerevisiae*, *Y. pestis* and *Pyrococcus furiosus*. The D37A mutation caused a ~ 10 -fold decrease in k_{cat} and a ~ 10 -fold increase in K_m , suggesting that the carboxylate is not directly involved in catalysis but is important for the binding and correct orientation of the substrate. This view is confirmed by structural data (Fig. 3C): the carboxylate indeed strongly stabilizes the Arg-55 side chain responsible for phosphoryl binding by forming a salt bridge with the guanidinium group. The same structural data indicate that Asp-147 plays a similar role through interaction with Arg-125. Indeed, the D147A mutation induced an even stronger decrease in catalytic efficiency than the D37A mutation, mainly through a 300–400-fold increase in K_m (Table 2). The importance of Asp-147 for substrate binding may also be related to its interaction with Lys-193, which binds the α -phosphate of ThTP. As mentioned above, the K193A mutation also causes a strong increase in K_m . It therefore appears that the correctly oriented D147–K193 pair is very important for substrate binding in animal ThTPases.

In contrast to D147A, the D145A mutation had little effect on kinetic parameters (not shown). Like Asp-147, Asp145 is in the active site but probably too far away on the $\beta 7$ sheet to interact with either Arg-125 or Lys-193.

We mutated Tyr-79, a residue well conserved from *M. brevicollis* to human. Moreover, it seems well positioned to interact with Lys-65 and be important for the correct orientation of this catalytic residue. Tyr-79 is also positioned to the side of the pocket harboring the thiazole cycle, suggesting that it might be directly involved in substrate binding through hydrophobic interaction with the thiazole part. However, the Y79A mutation caused only a slight increase in K_m (42 vs 8 μM), thus disproving the above hypothesis. However, k_{cat} was diminished by a factor of at least five (Table 2), suggesting that Tyr-79 may play a role in maintaining a catalytically active conformation of the protein. If Tyr-79 plays no role in binding of the thiamine part of ThTP, we must look for an alternative conserved residue responsible for the specific binding of ThTP. After inspection of the three-dimensional structure of hThTPase with ThTP docked in its active site (Fig. 3), it seems that the strictly conserved Trp-53 residue is ideally positioned to interact with the thiazole cycle through hydrophobic interaction. We indeed found that the W53A mutation caused a 5-fold decrease in k_{cat} while K_m increased ~ 70 -fold. Interestingly, the PPPase activity of 25-kDa ThTPase was increased in the W53A

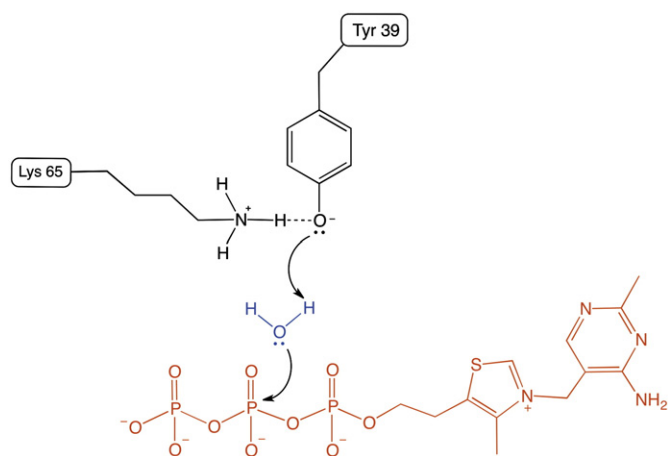


Fig. 4. Proposed catalytic mechanism of 25-kDa ThTPase.

mutant compared to the WT enzyme but remained much lower than its ThTPase activity (Fig. S3): K_m was lower ($97 \pm 9 \mu\text{M}$ compared to $290 \pm 20 \mu\text{M}$ for WT) and k_{cat} was $2.2 \pm 0.1 \text{ s}^{-1}$ compared to $1.6 \pm 0.1 \text{ s}^{-1}$ for WT. Note that Trp-53 is conserved in animal CYTH proteins but not in yeast or prokaryotic CYTH enzymes, which do not hydrolyze ThTP. Bacterial *CthTm* and *NeuTm*, however, do hydrolyze inorganic triphosphate [20,26]. Our results highlight the importance of Trp-53 for ThTP specificity in animal (and possibly choanoflagellate) ThTPases.

3.6. Circular dichroism (CD)

CD measurements were performed in both the near and far UV regions for K65A, D37A and D147A, the mutations that resulted in the most dramatic effect on enzyme activity. Comparison of spectra revealed no significant conformational changes between WT and mutant enzymes; only small variations in intensities were observed, most likely resulting from inaccuracies in the determination of protein concentrations. As an example, the spectra of WT and K65A enzymes are shown in Fig. S4. In spite of the fact that the catalytic activity is nearly abolished by the mutation, there is no evidence for a conformational change. Data collected in the peptide CD band allowed estimation of the secondary structural content, i.e. $37 \pm 4\%$ helices, $15.4 \pm 2\%$ β -sheets, $12.5 \pm 0.5\%$ turns and $31 \pm 3\%$ unordered regions. This is in good agreement with predictions from the sequence (Fig. 1) and structural data (Figs. 2 and 3). Note that the different intensities observed for the wild-type and K65A mutant in the aromatic region (Fig. S4) could result from a different environment of W53 which is located in the vicinity of K65. It is however not very likely that the position of the W53 side chain is altered by the K65A mutation, as the K_m of this mutated protein for ThTP is not affected.

3.7. Electrospray mass spectrometry

Structural and binding properties of human and mouse 25-kDa ThTPases were analyzed by native electrospray mass spectrometry. This was carried out using concentrated purified untagged protein ($5 \mu\text{M}$) in 100 mM ammonium acetate (pH 6.5) in the presence or absence of either ThTP or PPP_i ($25 \mu\text{M}$). For mThTPase, we also compared the WT with the catalytically inactive K65A mutant.

Initial experiments with the human enzyme (Fig. 5A,B) showed that, under these conditions, complexes with both ThTP and PPP_i were formed in the absence of added metal cations. In the presence of $25 \mu\text{M}$ ThTP, about 50% of the protein was in the form of a 1:1

complex, suggesting a K_d around 20–30 μM , not very different from the K_m value estimated from kinetic data (Table 2). Note that the latter data were obtained under conditions very different from those used for mass spectrometry, in particular, the ThTPase activity requires millimolar concentrations of the activator Mg^{2+} and the substrate is essentially a Mg–ThTP complex. We found that the apparent affinities of the substrates were not significantly modified by the presence of Mg^{2+} (0.1 or 0.5 mM, see Fig. S5 for the spectra acquired in 0.1 mM MgCl_2).

In the presence of $25 \mu\text{M}$ PPP_i , a complex was also detected by mass spectrometry. The estimated K_d was somewhat higher but remained ≤ 0.1 mM. For comparison, the K_m estimated at pH 9.5 with Mg– PPP_i as substrate was 0.3–0.5 mM.

The 1:1 complex between hThTPase and ThTP remained stable even under harsh source conditions, indicating that ionic, rather than hydrophobic interactions play a major role in the formation of the enzyme–substrate complex.

Results obtained with the mouse enzyme (WT and mutant K65A–mThTPase) are shown in Fig. 5 (C–F). For the mThTPase, in the presence of $25 \mu\text{M}$ ThTP, most of the protein was in the form of mThTPase–ThTP–complex. As very little protein remained in the free form, K_d is probably in the low micromolar range, one order of magnitude lower than for hThTPase. In contrast, the apparent affinity for PPP_i did not differ significantly between the human and mouse enzymes (around $50 \mu\text{M}$). However, interesting differences were found using the K65A–mThTPase mutant: while the affinity for ThTP remained relatively high (K_d around $5 \mu\text{M}$), there was a large difference in the apparent affinity for PPP_i between the non mutated mThTPase and the K65A mutant, K_d being one order of magnitude higher for the mutant. This suggests that Lys-65 is important for the binding of the triphosphate when it is in the free form but, when the substrate is ThTP, the complementarity of structure and the interaction of Trp-53 with the thiazole ring are sufficient to maintain the high affinity. These data corroborate that Lys-65 is essential for catalysis but not for the formation of the ThTP–enzyme complex.

Taken together, the mass spectrometry data indicate that, although Mg^{2+} is required for ThTPase as well as PPPase activities, it is not required for substrate binding to ThTPases. This is in agreement with data from NMR studies [14] showing that, even in the absence of Mg^{2+} , ThTP binds to mThTPase with high affinity.

We finally tested the possibility that ATP could bind to the ThTPases, but the amount of complex formed was very low, either in the presence or absence of Mg^{2+} (data not shown). This is in line with the previous finding that (at least when Mg^{2+} is the activator), ATP is a very poor substrate for 25-kDa ThTPases [16].

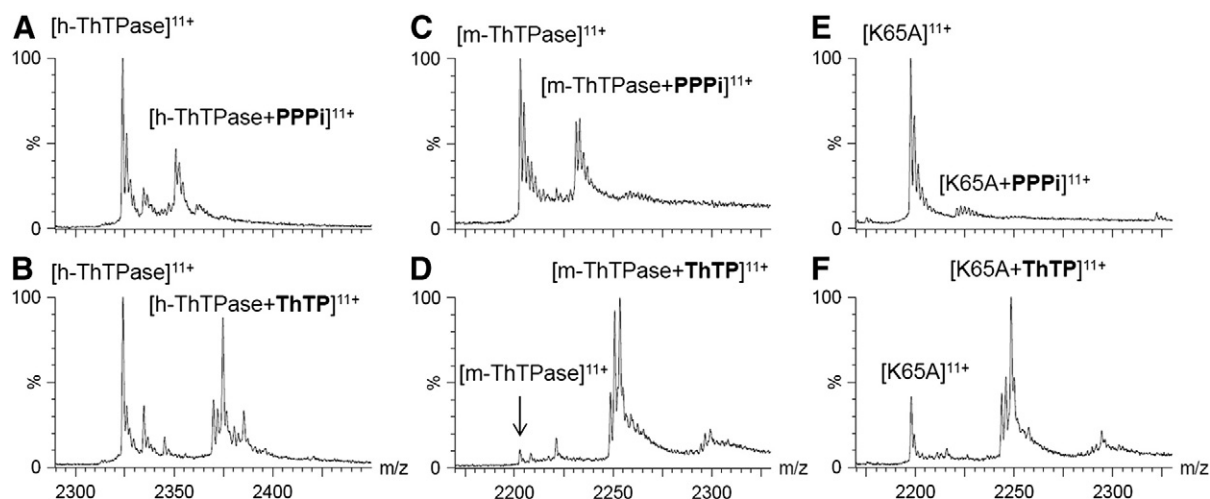


Fig. 5. Electrospray mass spectra of hThTPase, mThTPase and K65A mThTPase. The mixtures contained $5 \mu\text{M}$ enzyme and $25 \mu\text{M}$ substrate in 100 mM aqueous ammonium acetate (pH 6.5). (A) hThTPase + PPP_i , (B) hThTPase + ThTP, (C) mThTPase + PPP_i , (D) mThTPase + ThTP, (E) K65A mThTPase + PPP_i , (F) K65A mThTPase + ThTP.

4. Discussion

The structure of hThTPase described in this report has common features with that of other proteins of the CYTH superfamily crystallized so far. Since the first characterization of Cet1 RNA triphosphatase from *S. cerevisiae* [27], the crystal structures of several prokaryotic CYTH proteins have been reported [13,20,28]. In most cases, the active site is located within a topologically closed tunnel composed of antiparallel β strands with charged residues (involved in substrate binding or catalysis) pointing into the hydrophilic cavity. Although a number of crystallized CYTH proteins have a closed tunnel structure and are therefore referred to as “triphosphate tunnel metalloenzymes” (TTM [13]), it was recently shown that the bacterial tripolyphosphatase from *N. europaea* (*NeuTTM*) has an open, relatively rigid structure, forming only an incomplete β -barrel [20]. On the other hand, the determination of the solution structure of mouse 25-kDa ThTPase [14] has shown that the free enzyme has an open cleft fold, while the ternary enzyme–ThTP–Mg²⁺ complex adopts a tunnel fold. This suggests that crystal structures reported so far for CYTH enzymes are similar to those of the enzyme–substrate complex, rather than of the free enzyme conformation.

In the present study, crystals of human 25-kDa ThTPase were obtained in the presence of the substrate PPP_i instead of the most commonly used citrate and sulfate anions. The structural analysis of the active site using the hThTPase–PPP_i complex enabled us, with a reasonable degree of confidence, to identify the charged residues involved in specific binding of the triphosphate part of the substrate ThTP. Concerning the thiamine part, docking simulations with the whole substrate suggested that the thiazole ring of thiamine forms a stacking interaction with Trp-53. The importance of this residue for ThTP binding and hydrolysis was confirmed by site-directed mutagenesis (Table 2). In animal species, hydrolysis of ThTP remains the only well-characterized function of CYTH enzymes. Until recently, the ThTPase activity of the 25-kDa protein was considered a feature of mammalian cells only [1]. In the present work, we show that non-mammalian orthologs of the 25-kDa ThTPase are also specific ThTPases. Remarkably, such specific ThTPase activity was found not only in orthologs from vertebrates such as the zebrafish but even in the cnidarian *N. vectensis*. Our results suggest that the specificity for ThTP is linked to the presence of a conserved tryptophan residue (Trp-53 in mammalian ThTPase) interacting with the thiazole ring of ThTP. This residue, however, is not conserved in *Caenorhabditis elegans* or *Drosophila melanogaster* [12]. These observations are in agreement with the emerging picture [29] of extensive conservation in gene content, structure and organization between *Nematostella* and vertebrates. According to these authors, even chromosome-scale linkage has been preserved between *Nematostella* and vertebrates. In contrast, nematode and insect model systems have experienced extensive gene and intron loss, as well as rearrangement [30,31].

In the enzyme–ThTP complex, the ThTPase adopts a tunnel-fold, formed by joining of the N-terminal ends of β 1 and β 5 and antiparallel pairing of the latter two strands (Fig. 3A). The same conclusion was reached previously for the ternary mThTPase–Mg–ThTP complex. In the enzyme–substrate complexes, either PPP_i–hThTPase (this study) or ThTP–Mg–mThTPase [14], the compact tunnel-like globular structure is very different from the conformation of free mThTPase in solution. Presumably, strong electrostatic interactions, occurring when the triphosphorylated substrate is bound, are the driving force for closing the cleft, inducing a considerable conformational change of the protein. As suggested in Fig. 3C, ThTP is bound in the extended form, aligning along the groove. Concerning the specificity for a triphosphorylated substrate (which seems to be shared by all CYTH enzymes), it is notable that three arginine residues (Arg-55, -57 and -125) are involved in phosphate binding and that their proper orientation requires the formation of ion pairs with specific acidic residues: Arg-55 and Arg-57 engage in a bidentate salt bridge with Asp-37 while Arg-125 forms a

salt bridge with Asp-147. Not surprisingly, the disruption of any of these ion pairs strongly decreases the catalytic activity.

Such an important conformational change upon substrate binding is in agreement with the highly negative energy (–8.9 kcal/mol) of the docking solution. This also suggests a high affinity for the substrate, in agreement with NMR titration data, suggesting a $K_d \leq 1 \mu\text{M}$ [14], and our electrospray mass spectrometry data showing a tight binding of ThTP to mThTPase (Fig. 5).

Our results provide strong evidence that the highly conserved Lys-65 residue is essential for catalysis in mammalian 25-kDa ThTPase. Assuming that the hydrolytic process occurs through acid–base chemistry (which is the simplest catalytic mechanism), we may expect that the protonated $-\text{NH}_3^+$ group of Lys-65 should act as a catalytic unit comprising at least a second residue acting as general base. In the tunnel conformation as a complex with PPP_i, Tyr-39 (attached to β 3) is very close to Lys-65 (attached to β 4) (Fig. 2C–E). The interaction with the charged $-\text{NH}_3^+$ group might substantially lower the pK_a of the phenol group of tyrosine (from 11 to 7.5), so that Tyr-39 could be in the phenolate form at optimum pH (8.5) and act as general base (Fig. 4). We indeed found that the Y39A mutation strongly decreased the catalytic efficiency of mThTPase. It is therefore plausible that Lys-65 and Tyr-39 form the catalytic dyad. It is noteworthy that the corresponding lysine and tyrosine groups of *NeuTTM* were also recently suggested to form the catalytic dyad which is also a specific tripolyphosphatase [20]. It should also be noted that the putative catalytic dyad Y39–K65, as well as Trp-53, are not conserved in *C. elegans* or *D. melanogaster*, suggesting in the latter two species, the CYTH proteins have a different activity.

Like several other phosphohydrolases (notably CYTH enzymes), 25-kDa ThTPase has a strict requirement for Mg²⁺ as activator (while Ca²⁺ is inhibitory). As shown by mass spectrometry, the ternary ThTP–Mg–ThTPase complex contained only one Mg²⁺ ion, most probably coordinated to Glu-7, -9, -157 and -159. This may seem surprising as, under the usual conditions of enzyme assay, both ThTP and PPP_i are mostly in the form of the complex with Mg²⁺ and it might thus be expected that the substrate would bind to the active site as a complex with Mg²⁺. However, the active site contains several positively charged residues, which are likely to interact directly with the phosphates, so that the presence of a bound Mg²⁺ might have unfavorable effects for substrate binding. We therefore hypothesize that the Mg²⁺ bound to the substrate must dissociate before the triphosphate group can be bound. Thus, Mg²⁺ binding may simply be required for inducing a favorable conformation of the active site of the protein.

CYTH is an ancient family of proteins and a representative must have been present in the Last Universal Common Ancestor (LUCA) of all extant life forms [12]. In the most primitive life forms, CYTH enzymes may have played important metabolic roles in association with PPP_i and possibly other small chain polyphosphate compounds. Enzyme activities such as adenylyl cyclase, RNA triphosphatase and ThTPase are likely secondarily acquired activities of the CYTH domain (Fig. 6).

Another interesting observation concerns the gene organization of the CYTH domain in ThTPases from *Nematostella*, *Danio* and other vertebrate species: in all instances, an intron is present at equivalent positions in the coding region, i.e. between Leu-182 and Gly-183 of the mouse sequence (Fig. 1). The significance of this feature is not clear, however. Furthermore, both in mammals and in fish, the ThTPase gene has the same genes (*zfhx2* and *ngdn*) as neighbors, while all three have disappeared in birds.

In conclusion, here we identified key residues for catalysis (K65) and substrate recognition (W53) of mammalian 25-kDa ThTPase. We propose an unusual catalytic dyad composed of a tyrosine (Y39) and lysine (K65) dyad. We identified three arginine residues involved in phosphate binding. Our results suggest that ThTPase activity is a secondary acquisition of CYTH proteins in early metazoans and was conserved in the lineage leading from cnidarians to mammals. The loss of Y39, K65 and W53 in insects and nematodes suggests that

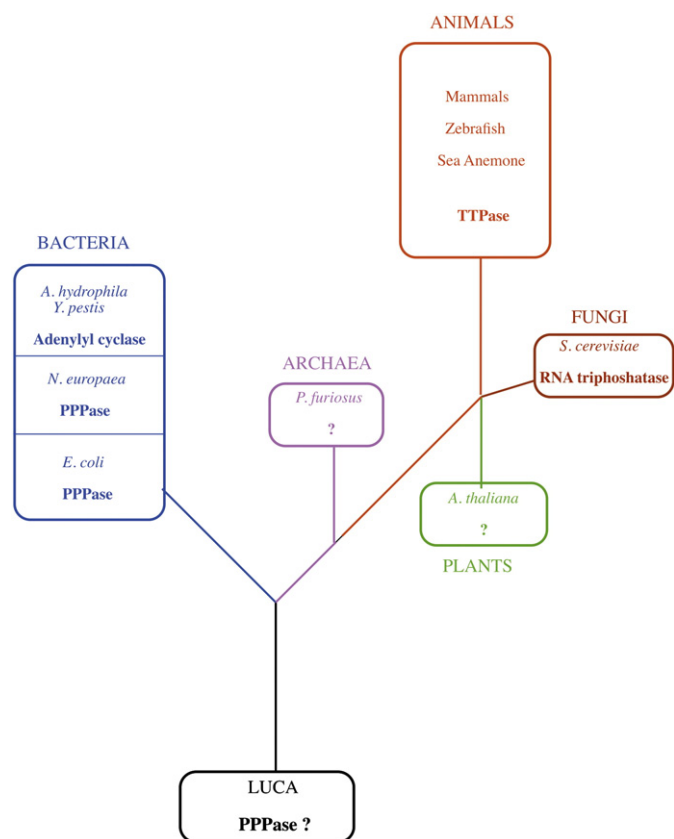


Fig. 6. Possible phylogenetic tree of the CYTH protein family and the activities of its members. Four different enzyme activities have been identified for CYTH proteins. The *Nitrosomonas europaea* and *E. coli* CYTH proteins are specific inorganic triphosphatases. Other enzyme activities such as adenylyl cyclase (in *A. hydrophila* and *Y. pestis*), mRNA triphosphatase (in fungi and protozoans) and ThTPase (in metazoans) activities are secondary acquisitions.

the protein may have a different role in these animals, while the ThTPase gene, as well as its neighbors, was altogether lost in birds.

Accession number

Coordinates and structure factor data have been deposited in the Protein Data Bank under the accession code 3TVL.

Supplementary data to this article can be found online at <http://dx.doi.org/10.1016/j.bbagen.2013.05.014>.

Acknowledgements

The authors wish to thank the “Fonds de la Recherche Fondamentale Collective” (FRFC) for grant numbers 2.4508.10 (LB.) and 2.4530.09 (A.M.). This work was supported by the Fonds de la Recherche Scientifique (IISN 4.4505.09, IISN 4.4509.11) and by the University of Liège (Fonds spéciaux, Crédit classique, C-06/19 and C-09/75). Research at the Centre d'Ingénierie des Protéines is also supported by the Belgian program of Interuniversity Attraction Poles initiated by the Federal Office for Scientific Technical and Cultural Affairs (PAI no P6/19 and no P7/44). LB is a Research Director at the “Fonds de la Recherche Scientifique” (F.R.S.-FNRS). VG, FK and BL are Research Associates at the F.R.S.-FNRS. DD was a Research Fellow of the “Fonds pour la Formation à la Recherche dans l'Industrie et dans l'Agriculture” (F.R.I.A.). RM is supported by the GIGA Center with the help of the Wallonia and European Regional Development Fund (ERDF). Nucleic acid sequencing was made by V. Dhennin, Genotranscriptomics Platform, GIGA, University of Liège, <http://www.giga.ulg.ac.be/>.

References

- [1] A.F. Makarchikov, B. Lakaye, I.E. Gulyai, J. Czerniecki, B. Coumans, P. Wins, T. Grisar, L. Bettendorff, Thiamine triphosphate and thiamine triphosphatase activities: from bacteria to mammals, *Cell. Mol. Life Sci.* 60 (2003) 1477–1488.
- [2] B. Lakaye, B. Wirtzfeld, P. Wins, T. Grisar, L. Bettendorff, Thiamine triphosphate, a new signal required for optimal growth of *Escherichia coli* during amino acid starvation, *J. Biol. Chem.* 279 (2004) 17142–17147.
- [3] L. Bettendorff, B. Wirtzfeld, A.F. Makarchikov, G. Mazzucchelli, M. Frédérick, T. Gigliobianco, M. Gangolf, E. De Pauw, L. Angenot, P. Wins, Discovery of a natural thiamine adenine nucleotide, *Nat. Chem. Biol.* 3 (2007) 211–212.
- [4] T. Gigliobianco, B. Lakaye, P. Wins, B. El Moulaj, W. Zorzi, L. Bettendorff, Adenosine thiamine triphosphate accumulates in *Escherichia coli* cells in response to specific conditions of metabolic stress, *BMC Microbiol.* 10 (2010) 148.
- [5] H.O. Nghiêm, L. Bettendorff, J.P. Changeux, Specific phosphorylation of *Torpedo* 43 K rapsyn by endogenous kinase(s) with thiamine triphosphate as the phosphate donor, *FASEB J.* 14 (2000) 543–554.
- [6] L. Bettendorff, H.A. Kolb, E. Schoffeniels, Thiamine triphosphate activates an anion channel of large unit conductance in neuroblastoma cells, *J. Membr. Biol.* 136 (1993) 281–288.
- [7] M. Gangolf, P. Wins, M. Thiry, B. El Moulaj, L. Bettendorff, Thiamine triphosphate synthesis in rat brain occurs in mitochondria and is coupled to the respiratory chain, *J. Biol. Chem.* 285 (2010) 583–594.
- [8] T. Gigliobianco, M. Gangolf, B. Lakaye, B. Pirson, C. von Ballmoos, P. Wins, L. Bettendorff, An alternative role FoF1-ATP synthase in *Escherichia coli*: synthesis of thiamine triphosphate, *Sci. Rep.* 3 (2013) 1071.
- [9] M. Gangolf, J. Czerniecki, M. Radermecker, O. Detry, M. Nisolle, C. Jouan, D. Martin, F. Chantraine, B. Lakaye, P. Wins, T. Grisar, L. Bettendorff, Thiamine status in humans and content of phosphorylated thiamine derivatives in biopsies and cultured cells, *PLoS One* 5 (2010) e13616.
- [10] A.F. Makarchikov, I.P. Chernikevich, Purification and characterization of thiamine triphosphatase from bovine brain, *Biochim. Biophys. Acta* 1117 (1992) 326–332.
- [11] B. Lakaye, A.F. Makarchikov, A.F. Antunes, W. Zorzi, B. Coumans, E. De Pauw, P. Wins, T. Grisar, L. Bettendorff, Molecular characterization of a specific thiamine triphosphatase widely expressed in mammalian tissues, *J. Biol. Chem.* 277 (2002) 13771–13777.
- [12] L.M. Iyer, L. Aravind, The catalytic domains of thiamine triphosphatase and CybB-like adenylyl cyclase define a novel superfamily of domains that bind organic phosphates, *BMC Genomics* 3 (2002) 33.
- [13] C. Gong, P. Smith, S. Shuman, Structure-function analysis of Plasmodium RNA triphosphatase and description of a triphosphate tunnel metalloenzyme superfamily that includes Cet1-like RNA triphosphatases and CYTH proteins, *RNA* 12 (2006) 1468–1474.
- [14] J. Song, L. Bettendorff, M. Tonelli, J.L. Markley, Structural basis for the catalytic mechanism of mammalian 25-kDa thiamine triphosphatase, *J. Biol. Chem.* 283 (2008) 10939–10948.
- [15] L. Bettendorff, H.O. Nghiêm, P. Wins, B. Lakaye, A general method for the chemical synthesis of gamma-32P-labeled or unlabeled nucleoside 5'-triphosphates and thiamine triphosphate, *Anal. Biochem.* 322 (2003) 190–197.
- [16] B. Lakaye, A.F. Makarchikov, P. Wins, I. Margineanu, S. Roland, L. Lins, R. Aichour, L. Lebeau, B. El Moulaj, W. Zorzi, B. Coumans, T. Grisar, L. Bettendorff, Human recombinant thiamine triphosphatase: purification, secondary structure and catalytic properties, *Int. J. Biochem. Cell Biol.* 36 (2004) 1348–1364.
- [17] L. Bettendorff, M. Peeters, C. Jouan, P. Wins, E. Schoffeniels, Determination of thiamin and its phosphate esters in cultured neurons and astrocytes using an ion-pair reversed-phase high-performance liquid chromatographic method, *Anal. Biochem.* 198 (1991) 52–59.
- [18] P.A. Lanzetta, L.J. Alvarez, P.S. Reinach, O.A. Candia, An improved assay for nanomole amounts of inorganic phosphate, *Anal. Biochem.* 100 (1979) 95–97.
- [19] V. Raussens, J.M. Ruyschaert, E. Goormaghtigh, Protein concentration is not an absolute prerequisite for the determination of secondary structure from circular dichroism spectra: a new scaling method, *Anal. Biochem.* 319 (2003) 114–121 (Erratum in, *Anal. Biochem.* 2359 (2006) 2150).
- [20] D. Delvaux, M.R. Murty, V. Gabelica, B. Lakaye, V.V. Lunin, T. Skarina, O. Onopriyenko, G. Kohn, P. Wins, E. De Pauw, L. Bettendorff, A specific inorganic triphosphatase from *Nitrosomonas europaea*: structure and catalytic mechanism, *J. Biol. Chem.* 286 (2011) 34023–34035.
- [21] W. Kabsch, Automatic processing of rotation diffraction data from crystals of initially unknown symmetry and cell constants, *J. Appl. Cryst.* 26 (1993) 795–800.
- [22] G.N. Murshudov, A.A. Vagin, E.J. Dodson, Refinement of macromolecular structures by the maximum-likelihood method, *Acta Crystallogr. D: Biol. Crystallogr.* 53 (1997) 240–255.
- [23] P. Emsley, K. Cowtan, Coot: model-building tools for molecular graphics, *Acta Crystallogr. D: Biol. Crystallogr.* 60 (2004) 2126–2132.
- [24] O. Trott, A.J. Olson, AutoDock Vina: improving the speed and accuracy of docking with a new scoring function, efficient optimization, and multithreading, *J. Comput. Chem.* 31 (2010) 455–461.
- [25] D.T. Gallagher, S.K. Kim, H. Robinson, P.T. Reddy, Active-site structure of class IV adenylyl cyclase and transphylic mechanism, *J. Mol. Biol.* 405 (2011) 787–803.
- [26] N. Keppetipola, R. Jain, S. Shuman, Novel triphosphate phosphohydrolase activity of *Clostridium thermocellum* TTM, a member of the triphosphate tunnel metalloenzyme superfamily, *J. Biol. Chem.* 282 (2007) 11941–11949.
- [27] C.D. Lima, L.K. Wang, S. Shuman, Structure and mechanism of yeast RNA triphosphatase: an essential component of the mRNA capping apparatus, *Cell* 99 (1999) 533–543.

- [28] D.T. Gallagher, N.N. Smith, S.K. Kim, A. Heroux, H. Robinson, P.T. Reddy, Structure of the class IV adenylyl cyclase reveals a novel fold, *J. Mol. Biol.* 362 (2006) 114–122.
- [29] N.H. Putnam, M. Srivastava, U. Hellsten, B. Dirks, J. Chapman, A. Salamov, A. Terry, H. Shapiro, E. Lindquist, V.V. Kapitonov, J. Jurka, G. Genikhovich, I.V. Grigoriev, S.M. Lucas, R.E. Steele, J.R. Finnerty, U. Technau, M.Q. Martindale, D.S. Rokhsar, Sea anemone genome reveals ancestral eumetazoan gene repertoire and genomic organization, *Science* 317 (2007) 86–94.
- [30] U. Technau, S. Rudd, P. Maxwell, P.M. Gordon, M. Saina, L.C. Grasso, D.C. Hayward, C.W. Sensen, R. Saint, T.W. Holstein, E.E. Ball, D.J. Miller, Maintenance of ancestral complexity and non-metazoan genes in two basal cnidarians, *Trends Genet.* 21 (2005) 633–639.
- [31] F. Raible, K. Tessmar-Raible, K. Osoegawa, P. Wincker, C. Jubin, G. Balavoine, D. Ferrier, V. Benes, P. de Jong, J. Weissenbach, P. Bork, D. Arendt, Vertebrate-type intron-rich genes in the marine annelid *Platynereis dumerilii*, *Science* 310 (2005) 1325–1326.

Appendix 4

Thiamine triphosphate: a ubiquitous molecule in search of a physiological role

Lucien Bettendorff · Bernard Lakaye · Gregory Kohn · Pierre Wins

Received: 16 December 2013 / Accepted: 12 February 2014 / Published online: 4 March 2014
© Springer Science+Business Media New York 2014

Abstract Thiamine triphosphate (ThTP) was discovered over 60 years ago and it was long thought to be a specifically neuroactive compound. Its presence in most cell types, from bacteria to mammals, would suggest a more general role but this remains undefined. In contrast to thiamine diphosphate (ThDP), ThTP is not a coenzyme. In *E. coli* cells, ThTP is transiently produced in response to amino acid starvation, while in mammalian cells, it is constitutively produced at a low rate. Though it was long thought that ThTP was synthesized by a ThDP:ATP phosphotransferase, more recent studies indicate that it can be synthesized by two different enzymes: (1) adenylate kinase 1 in the cytosol and (2) F_0F_1 -ATP synthase in brain mitochondria. Both mechanisms are conserved from bacteria to mammals. Thus ThTP synthesis does not seem to require a specific enzyme. In contrast, its hydrolysis is catalyzed, at least in mammalian tissues, by a very specific cytosolic thiamine triphosphatase (ThTPase), controlling the steady-state cellular concentration of ThTP. In some tissues where adenylate kinase activity is high and ThTPase is absent, ThTP accumulates, reaching ≥ 70 % of total thiamine, with no obvious physiological consequences. In some animal tissues, ThTP was able to phosphorylate proteins, and activate a high-conductance anion channel in vitro. These observations raise the possibility that ThTP is part of a still uncharacterized cellular signaling pathway. On the other hand, its synthesis by a chemiosmotic mechanism in mitochondria and respiring bacteria might suggest a role in cellular energetics.

Keywords Leigh's syndrome · Adenosine thiamine triphosphate · Mitochondria · Adenylate kinase · Brain · Skeletal muscle

L. Bettendorff (✉) · B. Lakaye · G. Kohn · P. Wins
GIGA-Neurosciences, University of Liège, Avenue de l'Hôpital, 1,
4000 Liège, Belgium
e-mail: L.Bettendorff@ulg.ac.be

Introduction

Thiamine (vitamin B1) is essential for energy metabolism and the nervous system is particularly sensitive to its deficiency, which causes specific brain lesions (Hazell and Butterworth 2009). It is thought that this vulnerability results from decreased levels of thiamine diphosphate (ThDP), an indispensable cofactor for several key enzymes such as pyruvate and oxoglutarate dehydrogenases and transketolase.

Indeed, in brain, as in most other mammalian tissues, ThDP is the most abundant thiamine derivative, amounting to 80–90 % of total thiamine. However, five other forms may be present in various proportions: free thiamine and thiamine monophosphate generally account for 5–15 % of total thiamine and have no known physiological function. The three remaining derivatives are thiamine triphosphate (ThTP) and the recently discovered adenosine thiamine triphosphate (AThTP) (Bettendorff et al. 2007) and adenosine thiamine diphosphate (AThDP) (Frédérich et al. 2009). They are minor components, generally amounting to less than 1 % of total thiamine under normal physiological conditions, but they seem more likely to play specific roles as intracellular messengers or metabolic regulators. In particular, we have recently shown (Gigliobianco et al. 2008, 2010; Lakaye et al. 2004c) that, in *E. coli*, either ThTP or AThTP may accumulate (reaching 10–50 % of total thiamine) under different conditions of cellular stress or nutritional downshifts.

ThTP was chemically synthesized in 1948 at a time when the only organic triphosphate compounds known were nucleoside triphosphates (Velluz et al. 1948). The first claims for the existence of ThTP in living organisms were made in rat liver (Rossi-Fanelli et al. 1952) and in baker's yeast (Kiesling 1953), though, ironically, what was measured was probably not ThTP (see below). The presence of ThTP was later suggested in several rat tissues (Greiling and Kiesow 1958) and in plant germs (Yusa 1961). In these studies and until 1979,

ThTP was separated from other thiamine derivatives using a paper chromatographic method, followed by oxidation to fluorescent thiochromes with ferricyanide in alkaline solution (Itokawa and Cooper 1970). This method, however, proved to be not very reliable. In the studies mentioned above, ThTP was reported to be a major thiamine compound in mammalian tissues (about 10 % of total thiamine), much more than suggested by modern HPLC methods.

The development of HPLC techniques in the late 1970's and 1980's by Kawasaki and colleagues in Hiroshima (Ishii et al. 1979a, b; Sanemori et al. 1980) and our own group (Bontemps et al. 1984; Bettendorff et al. 1986, 1991) led to an important simplification, acceleration and increased sensitivity in the determination of ThTP in biological samples (for review see: (Kawasaki 1992b; Lynch and Young 2000)). HPLC methods generally give ThTP levels much lower than previous methods (paper chromatography, paper electrophoresis, low pressure liquid chromatography), casting doubt on at least the quantitative dimension of the earlier findings. Indeed, as we previously showed, under some conditions, especially when poorly selective filter fluorometers are used instead of spectrofluorometers and thiochrome triphosphate is eluted early, chemically unrelated fluorescent compounds present in cells may be detected and mistakenly considered to be ThTP (Bontemps et al. 1984).

The reliability of ThTP determination was an important issue in a particularly controversial case 40 years ago. In 1969, Cooper and associates reported that ThTP levels were strongly decreased in post-mortem brains from patients having died from Leigh's disease, a fatal necrotizing myeloencephalopathy (Cooper et al. 1969, 1970; Pincus et al. 1976). This seemed to substantiate the idea that ThTP plays an important role in brain function. This was however unfounded, as ThTP is always undetectable in post-mortem brains (see below).

The role of thiamine diphosphate (ThDP or cocarboxylase) in the decarboxylation of pyruvate by yeast had been elucidated 15 years before the discovery of ThTP (Lohmann and Schuster 1937) and so it was quite straightforward to test whether ThTP had any cocarboxylase activity in yeast extracts. Although several studies claimed that ThTP could, at least partially, replace ThDP in pyruvate decarboxylation in yeast extracts (Velluz et al. 1949; De La Fuente and Diaz-Cadavieci 1954; Rossi-Fanelli et al. 1955), the use of crystalline ThTP and apo-coarboxylase free of phosphatase activity disproved this possibility (Rossi-Fanelli et al. 1955). An initial communication suggested that ThTP, just like ATP, could phosphorylate hexoses (Greiling and Kiesow 1956), but this was later attributed to impurities in the enzyme and/or substrate preparations (Yusa 1962). The hypothesis that ThTP could act as a reservoir for ThDP is also unlikely because in most tissues ThTP represents only a small fraction of the amount of ThDP. The fact that ThTP is present only in small amounts in most cells (<1 nmol/g of fresh weight) also

excludes that ThTP could be an energy storage compound for the regeneration of ATP, like phosphocreatine for instance.

Here we shall critically review existing data, especially in relation to Leigh's disease, and examine possible cellular roles for ThTP in light of recent data obtained on ThTP synthesizing and hydrolyzing enzymes.

A neurophysiological role for ThTP?

A specific non-cofactor role for thiamine and its phosphorylated derivatives has been suggested for a long time (Cooper and Pincus 1979). The first observation in favor of a specific "neuroactive" role of thiamine was that the electrical stimulation of vagus nerves in vitro induced a release of thiamine into the incubation medium (Minz 1938; Von Muralt 1942, 1947; Von Muralt and Zemp 1943). It was later suggested (Kunz 1956; Cooper et al. 1963; Gurtner 1961) that thiamine release was linked to the dephosphorylation of phosphorylated derivatives such as ThMP; ThDP or ThTP. This led Cooper and associates to suggest that ThTP was the neuroactive form of thiamine (Cooper and Pincus 1979), but no subsequent study could substantiate the idea that ThTP plays any significant role in the regulation of nerve excitability.

ThTP is consistently found in the nervous system of all animal species tested so far, ranging from 0.1 % (mouse brain) to 10 % (Slug cerebral ganglion) of total thiamine (Makarchikov et al. 2003; Frédérick et al. 2009). There are only a few data on the regional distribution of ThTP in brain. In rat brain, it was found to be somewhat more abundant in the stem than in the cerebral hemispheres or the cerebellum (Gangolf et al. 2010a). On the other hand, neurons in primary culture were found to contain more ThTP than astrocytes (Bettendorff et al. 1991).

We studied the effect of intermittent light stimulation on the content of thiamine derivatives in the brain of the photosensitive baboon *Papio papio* (Bettendorff et al. 1989b). Some of these animals are naturally photosensitive and, after intermittent light stimulation, develop paroxysmal discharges in the motor and premotor regions of the brain, responsible for generalized seizures. After intermittent light stimulation, there was a decrease in ThTP levels in the occipital area (containing the visual cortex) of both photosensitive and non-photosensitive animals; however no decrease in ThTP was observed in the motor and premotor areas. This might suggest that the observed decrease is linked to increased stimulation of the visual cortex, but that it is not related to photosensitivity and epileptic discharges. From these experiments, it cannot be inferred whether decreased ThTP levels are a direct consequence of nerve excitability or increased metabolic activity of the neurons during light stimulation. In view of the recent observation that the molecular mechanisms for ThTP and ATP

synthesis (see below) are the same, the latter possibility is the most plausible.

When synaptoneurosome membranes prepared from rat brain membranes were incubated in the presence of ThDP, internal ThTP concentrations increased. Under these conditions, membrane chloride permeability was also increased, suggesting a relationship between ThTP and chloride permeability (Bettendorff et al. 1990b, 1993a, c, 1994a). Indeed, using the patch-clamp technique, we showed that addition of ThTP (1 or 10 μM) to inside-out patches of mouse neuroblastoma cells activated an anion channel of large unitary conductance (Bettendorff et al. 1993b). No effect on cation channels was observed. Maxi anion channels seem to be involved in swelling-induced ATP release, but their molecular identity still remains unknown (Dubyak 2012).

More recently, it was found that in *Torpedo marmorata* electric organ, ThTP specifically phosphorylates rapsyn (Nghiêm et al. 2000), a protein required for the clustering of acetylcholine receptors at the neuromuscular junction (Gautam et al. 1995). Interestingly, ThTP phosphorylated rapsyn on histidyl residues while phosphorylation by ATP occurred on seryl or threonyl residues. ThTP was also shown to phosphorylate some as yet unidentified proteins in rodent brain (Nghiêm et al. 2000). It was therefore suggested that protein phosphorylation by ThTP is part of a new cellular signaling pathway. Until now, the only compound known to phosphorylate proteins in eukaryotic cells was ATP.

Intracellular localization of ThTP

A recent study has shown that ThTP exists not only in mammals, but in all major phyla tested: bacteria, fungi, plants, invertebrates and vertebrates (Makarchikov et al. 2003). It seems that the intracellular localization of ThTP may change from one tissue to another. Thus in *Electrophorus electricus* electric organ, 96 % of ThTP was found in the cytosolic fraction and was not protein-bound (Bettendorff et al. 1987). A similar observation was made concerning ThTP in pig skeletal muscle (Egi et al. 1986). In *T. marmorata* electric organ, ThTP was mainly found in the synaptosomal fraction, either cytoplasmic or associated with membrane structures (Eder and Dunant 1980), but it was not detected inside synaptic vesicles. In this study, the authors report an extremely high total thiamine content of 120 ± 24 nmol / g of fresh weight, only an order of magnitude less than ATP (Eder and Dunant 1980). However, according to our data, the total thiamine content is three orders of magnitude lower in the electric organ of *T. marmorata* (Table 1).

In primary cell cultures, ThTP levels were five times higher in cerebellar granule cells compared to astrocytes (Bettendorff et al. 1991), but there is presently no experimental evidence

that ThTP is also preferentially localized in neurons in the intact adult brain.

In rat brain, the highest content of ThTP was found in synaptosomes. A significant amount was present in the mitochondrial fraction (Bettendorff et al. 1994b; Gangolf et al. 2010b) but only a small percentage was cytosolic. At least part of this ThTP seems to be protein-bound (Bettendorff et al. 1993c). Matsuda et al. homogenized rat tissues in 20 mM Tris-HCl (pH 7.4) – 1 mM EDTA, centrifuged the homogenate at $279,000 \times g$ and assayed ThTP in the particulate and supernatant fractions (Matsuda et al. 1989c): in brain, heart and kidney, ThTP was mainly associated with the particulate fraction, while in white and red skeletal muscle it was present in the supernatant fraction. In liver, it was evenly distributed between both fractions. Matsuda and Cooper (1981a, b) reported the association of thiamine phosphate esters and in particular ThTP with brain synaptosomal membranes. On the other hand, Laforenza et al. (1990) could not find a significant enrichment of synaptosomes compared with total rat brain homogenate. Our recent data is suggested that, in the mammalian brain, ThTP is mainly localized in mitochondria (Gangolf et al. 2010b).

Cytosolic ThTP levels are controlled by a 25-kDa ThTPase

In mammalian cells, concentrations of triphosphorylated thiamine derivatives are generally low, less than 1 % of total thiamine. ThTP levels are kept relatively constant (≤ 1 μM) because the compound is continuously hydrolyzed by a specific 25-kDa cytosolic thiamine triphosphatase (ThTPase, EC 3.6.1.28). This enzyme, first described in 1972 by Hashitani and Cooper (1972), was purified in 1992 and shown to have an absolute specificity for ThTP (Makarchikov and Chernikevich 1992). The molecular characterization revealed that the sequence had no homology with any known mammalian protein (Lakaye et al. 2004a). It is widely distributed in human (Gangolf et al. 2010a) and rodent tissues (Lakaye et al. 2002, 2004b), though it is not a very abundant protein. The catalytic efficiency was high (k_{cat}/K_m is typically in the 10^6 – 10^7 $\text{s}^{-1} \text{M}^{-1}$ range) (Makarchikov and Chernikevich 1992; Lakaye et al. 2002, 2004a; Song et al. 2008; Delvaux et al. 2013). In rodent brain, 25-kDa ThTPase seems to be essentially neuronal, with a high expression in cerebellar Purkinje cells and pyramidal hippocampal neurons (Czerniecki et al. 2004). Using an antibody, staining was observed in cell bodies and in dendrites. In cultured cells, a high labeling was also observed in the nucleus.

Human 25-kDa ThTPase and the so-called cyaB (class IV, (Sismeiro et al. 1998)) adenylyl cyclase from *Aeromonas hydrophila* are the founding members of a novel superfamily of domains that bind triphosphorylated compounds and divalent metal cations (Bettendorff and Wins 2013; Iyer and

Table 1 Thiamine derivatives in various tissues

| nmol/g fresh weight | Thiamine | ThMP | ThDP | ThTP | Total |
|---|-----------|-----------|-----------|-------------|-------|
| Electric organs | | | | | |
| <i>T. marmorata</i> ^a | 38±3 | 26±3 | 9.6±2.3 | 45±4 | 118.6 |
| <i>T. marmorata</i> ^b | 0.03±0.01 | 0.04±0.02 | 0.37±0.06 | 0.024±0.003 | 0.46 |
| <i>E. electricus</i> ^c | 0.06±0.01 | 0.09±0.01 | 0.46±0.08 | 3.9±0.5 | 4.5 |
| Skeletal muscle | | | | | |
| Pig ^d (n=1) | 0.014 | 0.047 | 11 | 20 | 31.1 |
| Pig ^e | 0.38±0.22 | 0.56±0.17 | 7.17±1.90 | 18.24±5.83 | 26.35 |
| Rat ^b (n=5) | 0.10±0.06 | 0.54±0.16 | 6.2±1.0 | 0.39±0.09 | 7.2 |
| Mouse ^f | 0.16±0.02 | 0.49±0.05 | 6.7±0.7 | 0.026±0.006 | 7.38 |
| Rabbit ^b (n=1) | 0.14 | 0.26 | 2.0 | 0.08 | 2.48 |
| Chicken ^d (n=1) | – | 0.33 | 1.2 | 3.7 | 5.23 |
| Quail ^d (n=3) | – | 1.3±0.1 | 16.7±0.1 | 0.34±0.02 | 18.3 |
| Human ^{g, h} (n=11) | 0.08±0.09 | 0.09±0.05 | 2.2±1.6 | 0.13±0.13 | 2.5 |
| Liver | | | | | |
| Rat ^b (n=3) | 0.61±0.04 | 1.8±0.3 | 13.9±1.3 | <0.1 | 16.3 |
| Human ^{g, h} (n=3) | 0.03±0.01 | 0.39±0.26 | 5.9±3.8 | 0.022±0.023 | 6.34 |
| Brain | | | | | |
| Human cerebral cortex ^{g, h} (n=5) | 0.03±0.04 | 0.05±0.03 | 2.7±0.07 | 0.05±0.04 | 2.83 |

^a(Eder and Dunant 1980)^bBettendorff L., unpublished results^c(Bettendorff et al. 1987)^d(Makarchikov et al. 2003)^e(Egi et al. 1986)^f(Makarchikov et al. 2002)^g(Gangolf et al. 2010a)^h Considering that proteins account for about 13 % of wet weight

Aravind 2002). This domain was called CYTH (CyaB and ThTPase) and members of this family, can be traced back to the Last Universal Common Ancestor of all living organisms. ThTPase may represent a relatively divergent acquisition of a new catalytic activity which, so far, appears to be restricted to metazoans (Delvaux et al. 2013; Bettendorff and Wins 2013). The NMR solution structure (Song et al. 2008) and the crystal structure (Delvaux et al. 2013) were obtained for respectively the mouse and the human enzymes. The latter study suggests that the specificity for ThTP is linked to a Trp residue interacting with the thiazolium heterocycle of thiamine.

No sequence homologous to 25-kDa ThTPase and no specific soluble ThTPase activity have been found in birds so far (Makarchikov et al. 2003; Bettendorff and Wins 2013). It seems that the *thtpa* gene has been lost in the reptile branch leading to birds. The fish enzyme seems to have a much lower catalytic activity than its mammalian counterpart (Delvaux et al. 2013). This could be the reason why no soluble ThTPase activity was observed in fish tissues (Makarchikov

et al. 2003). Surprisingly, and due a single amino acid substitution, the pig has a low catalytic activity, though it seems to be expressed according to a similar pattern than in rodent tissues (Szyniarowski et al. 2005). This means that in pig, bird and fish tissues, 25-kDa ThTPase is either absent or its catalytic activity is very low, allowing ThTP to accumulate (Table 1). This suggests that the enzyme indeed plays a major role in the control of cytosolic ThTP concentration. Also, human tissues generally have a much higher proportion of ThTP compared to total thiamine than rodent tissue. This may probably be correlated to the higher abundance and catalytic efficiency of rodent ThTPase compared to the human enzyme (Gangolf et al. 2010a).

In mammalian cells, ThTP seems to be more constitutively synthesized, but in much lower amounts, than in *E. coli*. Nevertheless, we produced a transgenic mouse expressing bovine ThTPase in addition to the endogenous mouse ThTPase. Total ThTPase activity was increased by approximately a factor of two, but ThTP levels were not significantly decreased (Fig. 1). Mouse ThTPase is a very efficient enzyme, and ThTP levels are much lower in this species than in most

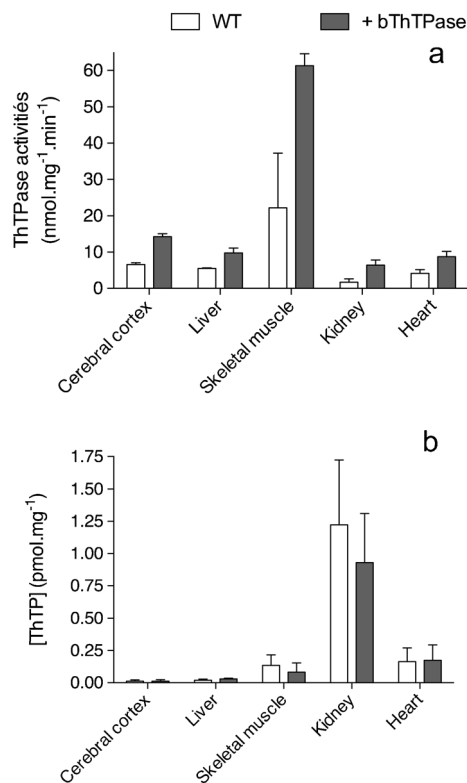


Fig. 1 Thiamine triphosphatase activities and thiamine triphosphate in several tissues of a transgenic mouse overexpressing bovine 25-kDa ThTPase (bThTPase). The bThTPase coding sequence was placed by targeted insertion in the ROSA26 locus using the method described by Srinivas et al. (2001). The mice generated were then mated with EIIaCre female mice (kindly provided by Dr E. Weinsphal) to remove the PGK-Neo cassette and place the bThTPase coding sequence under the control of the ubiquitous ROSA26 promoter. ThTPase activities (a) and ThTP content (b) were measured as previously described (Gangolf et al. 2010a). The results are expressed as means \pm SD for 5 mice. ThTPase activities were significantly increased in all tissues (Two-way ANOVA: $p \leq 0.0001$), but no significant decrease was observed for ThTP ($p = 0.2$)

other species tested. Therefore ThTP levels are hardly affected after increasing cytosolic ThTPase activity by overexpression of the bovine enzyme.

Though ThDP is the major thiamine compound in most living organisms (Makarchikov et al. 2003), a few exceptions have been noted: in pig (Egi et al. 1986) and chicken (Miyoshi et al. 1990) skeletal muscle and the muscle-derived *E. electricus* electric organ (Bettendorff et al. 1987), ThTP is the major thiamine compound accounting for 70–80 % of total thiamine (Table 1). However, such a high ThTP content is by no means a general characteristic of skeletal muscle or skeletal muscle-derived tissues (Table 1). Rat and rabbit skeletal muscle have a much lower ThTP content. In trout, quail and guinea pig skeletal muscle (Makarchikov et al. 2003; Egi et al. 1986), ThTP accounts for less than 10 % of total thiamine. White muscle fibers have a lower ThDP content than red muscle fibers in chicken (Miyoshi et al. 1990), rat, guinea pig and rabbit (Matsuda et al. 1989b) but a higher ThTP content. However, ThTP levels are very low in mouse

white and red skeletal muscle (0.1 % of total thiamine) (Matsuda et al. 1989b; Makarchikov et al. 2002) (Table 2). Thus, there is apparently no obvious relationship between ThTP levels and functional characteristics of the tissue investigated.

In addition to the soluble 25-kDa ThTPase, a membrane-associated ThTPase has also been reported in most animal species (Barchi and Braun 1972; Bettendorff et al. 1987). This enzyme is strongly activated by anions in *E. electricus* electric organ (Bettendorff et al. 1988, 1989a) and mammalian skeletal muscle (Matsuda et al. 1991) but this was not the case for the brain enzyme. The latter is inhibited by ATP but seems to be distinct from membrane-bound ATPases. The membrane-associated ThTPase has not been characterized at the molecular levels and its contribution in the control of intracellular ThTP levels is unknown, but it was recently speculated that it could be identical to a synaptosomal thiamine-binding protein (Sidorova et al. 2009). Indeed, a thiamine-binding protein has been isolated from rat brain synaptosomes (Postoenko et al. 1988). This protein of 107 kDa also binds thiamine phosphate esters with the sequence ThMP > ThTP > ThDP, but its molecular identity is unknown.

ThTP is synthesized in vivo

Despite ThTP being known for nearly 60 years, the mechanism of its biosynthesis remains controversial.

After subcutaneous (Gaitonde and Evans 1983), intracerebro-ventricular (Iwata et al. 1985) or intraperitoneal (Bettendorff et al. 1994b) administration of radiolabeled

Table 2 Soluble 25-kDa ThTPase activities

| | ThTPase activities (nmol. mg ⁻¹ . min ⁻¹) |
|---|---|
| Mammals | |
| Rat brain | 3.4 \pm 0.5 ^a |
| Rat skeletal muscle | 0.40 \pm 0.1 ^a |
| Mouse skeletal muscle | 2.0 \pm 0.2 |
| Pig skeletal muscle | 0.095 ^a |
| Birds | |
| Chicken skeletal muscle (<i>G. gallus</i>) | < 0.01 ^a |
| Quail skeletal muscle (<i>C. coturnix japonica</i>) | < 0.01 ^a |
| Fish | |
| Electrophorus electric organ (<i>E. electricus</i>) | < 0.01 ^b |
| Torpedo electric organ (<i>T. marmorata</i>) | < 0.01 ^b |
| Trout skeletal muscle (<i>S. trutta</i>) | < 0.01 ^a |

ThTPase activities were determined in the supernatants from various tissue homogenates centrifuged at 100,000 \times g

^a Adapted from (Makarchikov et al. 2003)

^b Bettendorff L., unpublished results

thiamine to rats, radioactivity was rapidly incorporated into ThTP, demonstrating that this compound is indeed synthesized in vivo in the brain. A net synthesis of ThTP was obtained after administration of thiamine disulfide derivatives in rat liver (Sanemori and Kawasaki 1982) and brain (Bettendorff et al. 1990a), though at least in the later case, administration of equivalent doses of thiamine was ineffective in raising brain ThTP content.

It came as a surprise that administration of radiolabeled thiamine in rats (Iwata et al. 1985; Bettendorff et al. 1994b; Gaitonde and Evans 1983) or incubation of mouse neuroblastoma cells with radiolabeled thiamine (Bettendorff 1994a) led to a more rapid increase in specific radioactivity in intracellular ThTP and ThMP than in ThDP. Similarly, incubation of brain slices with [³²P]P_i led to a much more rapid incorporation of radioactivity in ThTP than in ThDP (Berman and Fishman 1975). In animal cells, ThDP is directly formed from thiamine by thiamine pyrophosphokinase (thiamine + ATP ⇌ ThDP + AMP) and ThMP can only be formed from ThDP by enzymatic hydrolysis. The fact that, the precursor ThDP has a considerably lower specific radioactivity than its products, suggests that there are two ThDP pools: one small pool of high turnover (which is the precursor of ThTP and ThMP) and a larger pool of lower turnover, probably corresponding to ThDP bound to apoenzymes (Berman and Fishman 1975; Bettendorff 1994a). The high turnover pool probably corresponds to free cytosolic ThDP (≤ 10 % of total thiamine) whereas the low turnover pool consists of ThDP bound to transketolase in the cytoplasm and PDH and OGDH in mitochondria (Bettendorff 1994a). The turnover of ThTP was ~1–2 h, while the turnover of the slow ThDP pool was ~17 h.

A key observation was that in some species cellular ThTP concentrations are not constant. They are generally very low but, under conditions of cellular stress, the intracellular ThTP can increase considerably. This phenomenon was observed in plants during withering (Makarchikov et al. 2003) and in bacteria during amino acid starvation (Lakaye et al. 2004c). The intracellular ThTP concentration is highly regulated in *E. coli*, strongly depending on physiological conditions: in bacteria growing in aerated rich medium, ThTP is barely detectable, but it quickly accumulates (reaching cellular concentrations ≥ 10 μM) when the bacteria are transferred to minimum medium devoid of amino acids but containing a carbon source such as glucose (Lakaye et al. 2004c). Interestingly, this accumulation is transient, reaching a maximum after 1–2 h, then decreasing eventually to zero. How those regulatory mechanisms respond to the nutritional status remains an open question.

When the specific human 25-kDa ThTPase was overexpressed as a GST-fusion protein in *E. coli*, ThTP did not accumulate and the bacterial growth curves displayed an intermediate plateau, suggesting that ThTP is involved in the rapid adaptation of the bacteria to amino acid starvation. As

the expression level of the fusion protein was very high (> 10 % of total protein), toxic effects can however not be excluded, though overexpression of a protein unrelated to thiamine metabolism did not produce this intermediate plateau. This led us to propose that ThTP (as well as AThTP) could act as “alarmones” or signals responding to specific conditions of nutritional downshift or metabolic stress (Lakaye et al. 2004c; Gigliobianco et al. 2008, 2010, 2013). The biochemical mechanisms underlying the production of these signals remain to be clarified.

Mechanisms of ThTP synthesis

ThTP synthesis by a ThDP:ATP phosphotransferase and Leigh’s disease

The most obvious mechanism for the synthesis of a triphosphate compound would be the transfer of a phosphate group from ATP to the diphosphorylated precursor. Such a mechanism, involving a cytosolic ThDP:ATP phosphotransferase (ATP + ThDP ⇌ ADP + ThTP), was already proposed in 1964 (Eckert and Möbus 1964) in acetone powder extracts of supernatants of pig spinal cord, but the enzyme was not characterized.

Years later, an enzyme thought to catalyze such a reaction was partially purified from rat liver hyaloplasm (Voskoboev and Luchko 1980; Voskoboev and Chernikevich 1985). The authors measured the formation of labeled ThTP from [¹⁴C]ThDP in the presence of ATP and Mg²⁺. After a 100-fold purification, the specific activity was still low and two pH optima were found (5.3 and 7.8). In 1984, the same group reported the complete purification of a soluble ThDP kinase from brewer’s yeast (Chernikevich et al. 1984; Voskoboyev et al. 1987). Though the authors give the amino acid composition of their preparation, which seemed to be a multi-subunit complex, we have been unable to identify a possible candidate from current databases. However, the product ThTP was not unambiguously identified. Indeed, it could have been the recently discovered adenosine thiamine triphosphate (AThTP, (Bettendorff et al. 2007)), which is synthesized in the cytosol according to the reaction ThDP + ATP (ADP) ⇌ AThTP + PP_i (P_i) (Makarchikov et al. 2007). Using supernatants from *E. electricus* electric organs or pig brain, which contain no significant soluble ThTPase activity, we were unable to demonstrate any ThTP synthesis by such a mechanism. Likewise, no such activity could be detected in cell-free extracts from *E. coli*.

J. R. Cooper and colleagues at Yale University reported the synthesis of ThTP in a mitochondrial fraction from rat brain by a ThDP:ATP phosphotransferase (Cooper et al. 1969; Itokawa and Cooper 1968). The reaction did not seem to occur in the mitochondrial matrix and no functional mitochondria

were required. A most puzzling observation was that the urine, spinal fluid and deproteinized blood from patients with Leigh's syndrome contained an inhibitor of this reaction. Moreover, no ThTP was detected in the post-mortem brain samples from patients with Leigh's syndrome (Cooper et al. 1969; Pincus et al. 1976; Murphy 1976), while in brain samples from control patients ThTP accounted for ~10 % of total thiamine. This result could not be confirmed, however. Indeed, we were unable to detect any ThTP in post-mortem human brains (Bettendorff et al. 1996). This is probably due to hydrolysis by 25-kDa ThTPase during the post-mortem delay, which is at least 2–3 h, and 25-kDa ThTPase remains highly active in post-mortem human brain (Bettendorff et al. 1996). In cultured mouse neuroblastoma cells (which have a low ThTPase activity, Bettendorff, unpublished results), the half-life of ThTP was ~1 h (Bettendorff 1994a). However, we found significant amounts of ThTP in human brain biopsies (Bettendorff et al. 1996; Gangolf et al. 2010a), but it accounted for only ~1 % of total thiamine, far less than the 10 % reported by Cooper et al. in post-mortem human brains.

Leigh's syndrome (subacute necrotizing myeloencephalopathy), first described by Denis Leigh in 1951 (Leigh 1951), is a rare heterogeneous neurodegenerative disorder of early childhood, characterized by focal, symmetric necrotic brain lesions, leading to death before the age of five (Finsterer 2008). It is now recognized that Leigh's syndrome results from deficits in mitochondrial respiratory chain complexes (I, II, III, IV), F₀F₁-ATP synthase or pyruvate dehydrogenase. In a small percentage of patients (<10 %), particularly when pyruvate dehydrogenase is affected, high-dose thiamine treatment may have beneficial effects (Di Rocco et al. 2000; Naito et al. 1997), but there is probably no involvement of a ThTP deficiency in this disease.

In 1977, Ruenwongsa and Cooper (1977) reported that, in the supernatant fraction from rat liver, labeled ThTP was formed from [γ -³²P]ATP. No addition of ThDP to the preparation was required and the authors concluded that the substrate was ThDP bound to a protein. Schrijver and colleagues reinvestigated this assertion (Schrijver et al. 1978), but they were unable to reproduce any ThTP synthesis by the mechanism described. They suggested a chromatographic artifact resulting from formation of complexes between thiamine and phosphates behaving chromatographically like ThTP (Schrijver et al. 1978). Moreover, Ruenwongsa and Cooper report a synthesis of 1.28 nmol of ThTP per mg of protein in a rat liver homogenate from endogenous ThDP, while total ThDP in rat liver was only about 0.1 nmol/mg of protein (Table 1, see also (Schrijver et al. 1978)). As radioactive [³²P]ATP was used as substrate, it was suggested that the [³²P]ThTP formed (if any) was contaminated by radioactive adenine nucleotides and inorganic phosphate (Cooper et al. 1982).

Finally, in 1983, Cooper and coworkers reported the purification of a 103 000 kDa protein from an acetone powder prepared from what appears to be a bovine brain mitochondrial fraction. They used a purified ThDP-binding protein from liver as substrate (Nishino et al. 1983). Hence, the reaction studied was: ThDP-protein + ATP \rightleftharpoons ThTP-protein + ADP. The enzyme was unstable and inactivated by sulfhydryl reagents. The activity of the purified enzyme was 67 nmol. mg⁻¹. h⁻¹, which would correspond to a *k*_{cat} of 0.11 min⁻¹. The authors attributed this low turnover to the fact that the substrate was protein-bound and its concentration could therefore not be raised to attain the maximum velocity. There was a controversy about the nature of the ThDP-protein complex used as substrate. According to Nishino et al. (1983), this soluble protein (purified from a liver supernatant fraction) was distinct from transketolase, which is a well-known cytosolic protein binding ThDP with high affinity. Voskoboev and Chernikevich (1985) reinvestigated the purification procedure and concluded that the only ThDP-binding protein in the rat liver supernatant fraction was transketolase and, at least in rat liver, the ThDP-transketolase complex was not a substrate for ThTP synthesis. Shortly thereafter, Yoshioka et al. reported the complete purification of liver ThDP-binding proteins (Yoshioka et al. 1987). They found a single band of 68 kDa corresponding to a transketolase monomer. Using immunocytochemistry, these authors also found that the ThDP-binding protein is localized in the cytoplasm in neurons and in nuclei in glial cells. Such differential localizations between neurons and glial cells were later established for transketolase (Calingasan et al. 1995). Therefore, it is very likely that the ThDP-binding protein used by Cooper and colleagues. was transketolase.

How about the enzyme catalyzing the synthesis of ThTP? We checked whether the amino acid composition, as well as the molecular mass of 103 000 of the enzyme purified by Nishino et al. (1983) could match any known protein (Table 3). The only protein with a molecular mass close to 103 000 that gave a significant correlation was hexokinase type I (*R*²=0.80, *p*<0.0001, molecular mass of 103,064; 918 amino acids) (Fig. 2).

Hexokinase type I is highly abundant in brain, and most of it is associated with mitochondria (Sui and Wilson 2002; Wilson 2003), while type II and III isoforms are expressed only at low levels in the brain. Though Nishino et al. claimed that their preparation had no hexokinase activity, this was probably destroyed by the acetone treatment. Furthermore, it is well known that hexokinase activity is quickly lost in the absence of glucose and EDTA (Redkar and Kenkare 1972) and both compounds were absent during the purification procedure described by Nishino et al. In this respect, it may be significant that Nishino et al. report that ThTP-synthesizing activity required a cofactor that they suggest to be glucose (Nishino et al. 1983). This cofactor was supposed to be

Table 3 Comparison of the amino acid content of the protein purified by Nishino et al. from bovine brain and bovine hexokinase HK1

| | Nishino et al. ^a (mol/103,000 g protein) | (%) ^b | Bovine HK1 ^c (%) |
|-----------|--|------------------|--------------------------------|
| Lys | 72.8 | 7.1 | 5.7 |
| His | 19.4 | 1.9 | 2.2 |
| Arg | 53.4 | 5.2 | 5.7 |
| Asp + Asn | 101 | 9.8 | 9.7 |
| Thr | 58.4 | 5.7 | 5.8 |
| Ser | 51 | 5 | 6.9 |
| Glu + Gln | 107.2 | 10.4 | 10.2 |
| Gly | 88.5 | 8.6 | 7.2 |
| Ala | 54.2 | 5.3 | 8.3 |
| Val | 64 | 6.2 | 6.6 |
| Met | 36.4 | 3.5 | 2.4 |
| Ile | 56.7 | 5.5 | 5.2 |
| Leu | 92.5 | 9 | 9 |
| Tyr | 18.5 | 1.8 | 3.2 |
| Phe | 40.3 | 3.9 | 3.9 |

^a From (Nishino et al. 1983)^b Calculated from column 1^c Obtained from the protein sequence [UniProt identifier P27595 (HXK1_BOVIN)], using the ExPasy AACompIdent tool (<http://www.expasy.ch/tools/aacomp/>)

characterized separately and, though they refer to a manuscript in preparation, this was never published. Therefore, it remains a mystery as to what the authors really measured.

Therefore, the mechanisms described by Nishino et al. in bovine brain and by Chernikevich and colleagues in yeast have not been confirmed in other laboratories and there is no compelling evidence that a ThDP:ATP phosphotransferase bearing the enzyme nomenclature number EC 2.7.4.15 really exists.

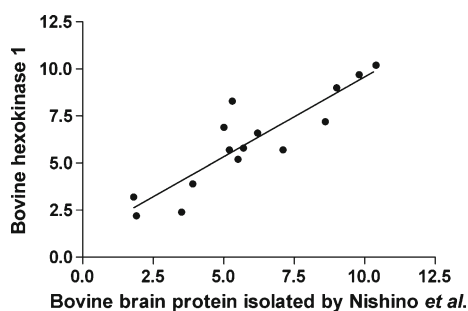


Fig. 2 Correlation between the amino acid composition of bovine hexokinase 1 and the enzyme purified by Nishino et al. (1983). The relative abundance of each amino acid of bovine hexokinase 1 is plotted against the relative amino acid abundance of the bovine brain protein isolated by Nishino et al., taking into account that the values for Asp and Glu represent the sum of respectively Asp + Asn and Glu + Gln. Cys, Trp and Pro were not determined by Nishino et al. [$F(1,13)=53.06$, $P<0.0001$, $R^2=0.8032$]

ThTP synthesis by adenylate kinases

Although ThTP generally accounts for less than 1 % of total thiamine, in a few tissues such as pig skeletal muscle (Egi et al. 1986), *E. electricus* electric organ (Bettendorff et al. 1987) and chicken white muscle (Miyoshi et al. 1990), ThTP is the major thiamine compound, accounting for >70 % of total thiamine (Table 2). Kawasaki and coworkers have suggested that this high ThTP content was correlated with the high amount of adenylate kinase 1 (AK1, myokinase, EC 2.7.4.3) found in skeletal muscle and electric organ. They indeed showed that, in vitro, the adenylate kinase isoform 1 (AK1) may synthesize ThTP according to the reaction: $\text{ThDP} + \text{ADP} \rightleftharpoons \text{ThTP} + \text{AMP}$ (Shikata et al. 1989b).

The same authors suggested that this enzyme was also responsible for ThTP synthesis in chicken white muscle in vivo (Miyoshi et al. 1990; Shioda et al. 1991). However, the significance of this reaction in vivo can be questioned as AK has a sharp pH profile with an optimum at 10 with ThTP as substrate (Shikata et al. 1989). Moreover, physiological concentrations of free ThDP in the cytosol are at best 10 μM (Bettendorff et al. 1994b), much lower than the K_m for ThDP reported for AK1 (830 μM). Thus, the rate of ThTP synthesis by AK1 is about 4 orders of magnitude lower than ATP synthesis under physiological conditions.

In rat skeletal muscle (quadriceps), ThTP content varied as a function of age: ThTP content increased until the age of 6–12 months and then decreased (Fig. 3a). This is in agreement with results from Matsuda et al. who showed an increase in rat skeletal muscle ThTP content between birth and 3 months, but they did not test older mice (Matsuda et al. 1989a). We observed a similar relationship between AK activity and age in rat skeletal muscle and a significant correlation between ThTP content and AK activity was observed ($R^2=0.68$; $p=0.0009$, Fig. 3b). No significant correlation was observed for the other thiamine derivatives (not shown). We observed a significant relationship between AK activity and lactate dehydrogenase ($R^2=0.38$, $p=0.032$). These results suggest that anaerobic metabolism increases until about the age of 12 months and then decreases. These results strongly suggest that, in rat skeletal muscle, ThTP is mainly synthesized by AK1 as was previously suggested by Kawasaki (1992a).

The accumulation of large amounts of cytosolic ThTP may be interpreted as follows: the equilibrium of the reaction $\text{ADP} + \text{ThDP} \rightleftharpoons \text{AMP} + \text{ThTP}$ will be shifted to the right because AMP reacts with ATP (which is in excess) to form 2 ADP. Both reactions are catalyzed by AK and the global reaction will be $\text{ThDP} + \text{ATP} \rightleftharpoons \text{ThTP} + \text{ADP}$. This equilibrium will also be shifted to the right because the muscle contains high amounts of phosphocreatine and creatine-kinase: $\text{ADP} + \text{phosphocreatine} \rightleftharpoons \text{ATP} + \text{creatine}$. The global process can thus be described by the reaction $\text{ThDP} + \text{phosphocreatine} \rightleftharpoons \text{ThTP} + \text{creatine}$.

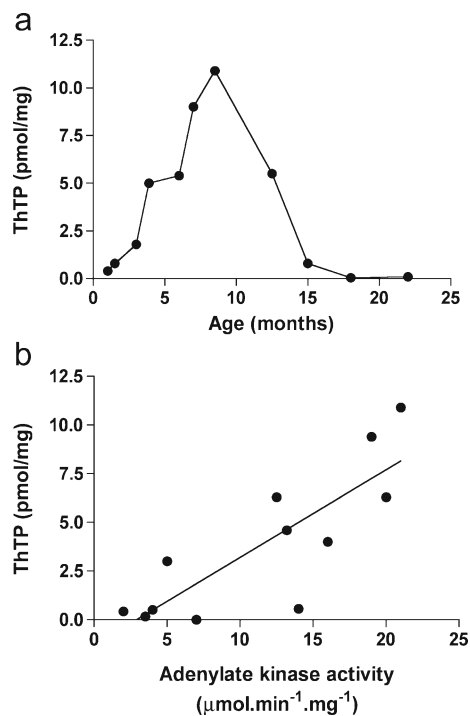


Fig. 3 ThTP content in rat skeletal muscle (quadriceps) as a function of age (a) and AK1 activity (b). ThTP and AK1 activity were determined in muscle cytosolic fractions as described (Makarchikov et al. 2002). [F(1,10)=21.39, $P=0.0009$, $R^2=0.6814$]

Therefore, it is likely that in skeletal muscle (and most probably electric organs) the main reaction responsible for ThTP synthesis is the one catalyzed by AK1. The role of AK1, which is a cytosolic enzyme, is in agreement with the observation that ThTP is essentially found in the cytosol of skeletal muscle (Egi et al. 1986; Matsuda et al. 1989c) and electric organs (Bettendorff et al. 1987; Eder and Dunant 1980).

However, it may not be the only ThTP synthesizing reaction. Indeed, in a previous study we showed that ThTP levels in adenylate kinase knock-out mice are very low, but the same as in wild-type animals (Makarchikov et al. 2002). Other isoforms of mammalian AK may also be responsible for ThTP synthesis. Hence, bacterial AKs are also able to synthesize ThTP at a low rate (Gigliobianco et al. 2008), but most probably another enzyme is involved.

ThTP synthesis by a chemiosmotic mechanism

In the 1990s, we reported a net synthesis of ThTP in a particulate fraction (synaptoneurosomes) isolated from rat brain (Bettendorff et al. 1993a, c, 1994a) with either thiamine or ThDP as substrate. ThTP was formed inside closed compartments that we thought to be synaptosomes. Recently, we reinvestigated this issue and found that ThTP synthesis occurred in mitochondria from ThDP and inorganic phosphate in the presence of substrates of the respiratory chain (Gangolf

et al. 2010b). Addition of external phosphate and ThDP to isolated rat brain mitochondria lead to an increase in ThTP synthesis. Indeed, ThDP can enter mitochondria via a specific transporter located in the internal membrane of the organelle (Marobbio et al. 2002; Lindhurst et al. 2006). Moreover, ThTP synthesis requires intact mitochondria and a functional respiratory chain. It is inhibited by uncouplers and by inhibitors of F_0F_1 -ATP synthase, suggesting that it might be synthesized by a chemiosmotic mechanism similar to ATP synthesis by oxidative phosphorylation: $\text{ThDP} + \text{P}_i \rightleftharpoons \text{ThTP}$. In order to test whether such a mechanism may be of physiological importance, we incubated brain slices with the uncoupler CCCP: ThTP levels decreased, suggesting that such a chemiosmotic mechanism is indeed operative in vivo.

As ThTP has been found in most types of organisms, it was of interest to investigate whether it could be produced through a similar mechanism in tissues other than the mammalian brain, and also in organisms that are phylogenetically distant from mammals, e.g. bacteria. Indeed, *E. coli* cells having a catalytically inactive ATP synthase or lacking the enzyme are unable to synthesize ThTP. In the latter case, ThTP synthesis can be restored by transformation of the bacteria with a plasmid containing the whole operon for coding for *E. coli* F_0F_1 -ATPase subunits (Gigliobianco et al. 2013).

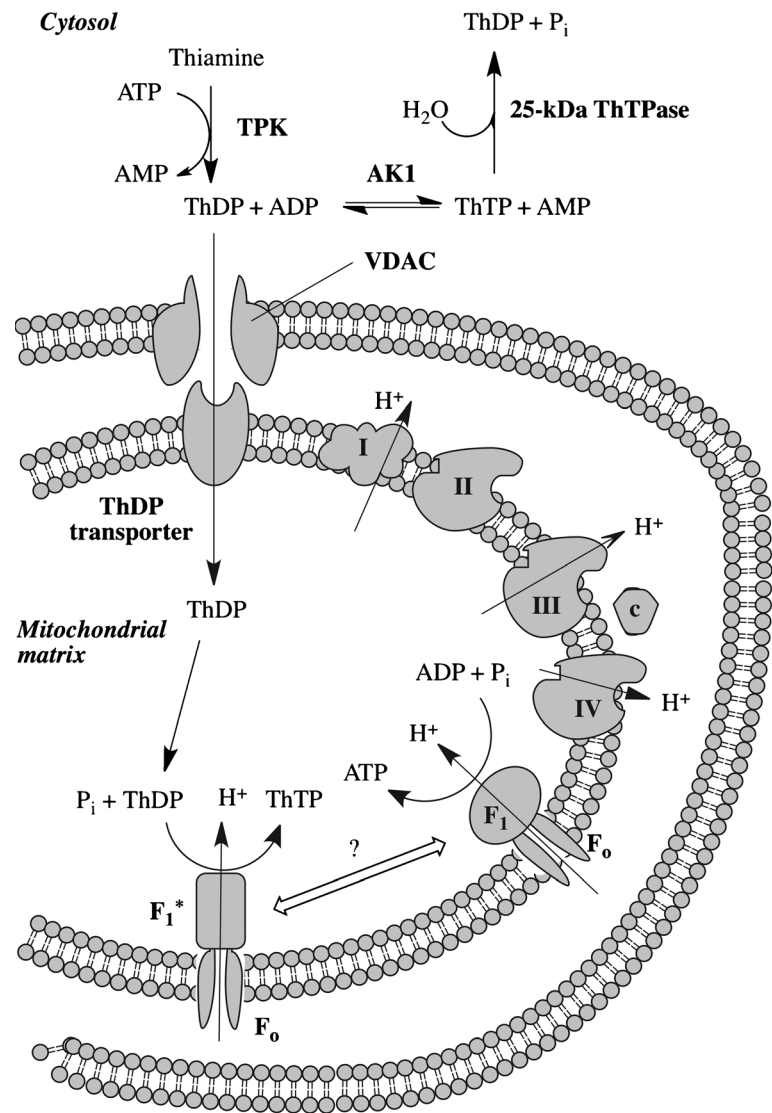
The occurrence of this chemiosmotic mechanism would account for the fact that in the mammalian brain, in contrast to skeletal muscle (see above), most ThTP is localized inside mitochondria. External phosphate increased the release of ThTP from the mitochondria (Gangolf et al. 2010b). It is not known whether this release is of physiological importance, but it might suggest that ThTP produced inside mitochondria could have a role either in the intermembrane space or in the cytosol (Fig. 4).

It could be argued that ThTP is merely a byproduct of F_0F_1 -ATPase without physiological significance. In this case, we would expect that ThTP would be synthesized in all mitochondrial preparations, but no such synthesis was observed in rat liver mitochondria for instance. These results suggest a tight, organ-specific, regulation of mitochondrial ThTP synthesis, possibly depending on metabolic differences between cells. This is in agreement with results obtained in *E. coli*, where ThTP is synthesized only in the absence of amino acids in the incubation medium, provided that a suitable carbon source is present (Lakaye et al. 2004c); in the absence of a carbon source, they synthesize AThTP (Bettendorff et al. 2007; Gigliobianco et al. 2010).

Conclusion

The aim of the present review was to carefully examine existing data on the mechanism of ThTP synthesis, its hydrolysis and its role. The data reviewed here summarize over

Fig. 4 Synthesis and hydrolysis of ThTP in a mammalian cell. ThTP may be synthesized in the cytosol by AK1. This reaction is only significant in tissues with high AK1 activity such as skeletal muscle and possibly erythrocytes. ThTP accumulates in the cytosol only when 25-kDa activity is low. In brain cells, ThTP may be synthesized in the mitochondrial matrix by a chemiosmotic mechanism and it may be exchanged with cytosolic inorganic phosphate (Gangolf et al. 2010b). ThDP may enter mitochondria by a specific transporter, probably by exchange against nucleotides (Lindhurst et al. 2006). I to IV, respiratory complexes; F_1^* : hypothetical modified conformation of F_1 that would bind ThDP rather than ADP



60 years of research on ThTP and especially the mechanism of its synthesis. It now appears that, because of the low concentration of this compound in most tissues, real progress was made only after the development of reliable and sensitive HPLC methods.

The situation was even more frustratingly complicated as four different mechanisms for the synthesis of ThTP had been proposed: ThDP:ATP phosphotransferase, a ThDP:ATP phosphotransferase using bound ThDP as substrate, AK1 and F_0F_1 -ATP synthase.

It is our opinion that there is no compelling evidence for a mechanism involving a ThDP:ATP phosphotransferase as proposed by several authors with various variations using either free or bound ThDP as substrate. Indeed, some of these studies are flawed by chromatographic artifacts and reliable determination of the small amounts of ThTP present in biological samples became only possible with the advent of

sensitive HPLC methods, beginning of the 1980s. In other studies, the compound detected was probably not ThTP, but the recently discovered AThTP. On the other hand, it is most probable that the only cytosolic and soluble ThDP-binding protein is transketolase, not involved in ThTP synthesis.

It has been convincingly demonstrated that AK1 may constitutively synthesize ThTP at a very slow rate. This reaction is probably relevant only in tissues with a high AK1 content such as skeletal muscle and electric organs. In these tissues, which have a low 25-kDa ThTPase activity, ThTP can accumulate to high levels and even become the major thiamine compound. This is the case in pig and chicken skeletal muscle and *E. electricus* electric organ. In view of the observation that ThTP is by far the major thiamine compound in electric organs of *E. electricus*, we, probably erroneously, postulated that ThTP might be involved in bioelectrogenesis (Bettendorff et al. 1987; Bettendorff 1994b), a hypothesis that

would have been in accord with previous studies suggesting a role of ThTP in membrane excitability (Cooper and Pincus 1979). However, the fact that ThTP accumulation in these tissues is the result of two unrelated factors, which was not known at that time, is not in favor of a physiological role in these tissues.

Recently we demonstrated a third mechanism for ThTP synthesis (Gangolf et al. 2010b; Gigliobianco et al. 2013). According to these data, ThTP is synthesized inside mitochondria following the reaction $\text{ThDP} + \text{P}_i \rightleftharpoons \text{ThTP}$ by a chemiosmotic mechanism similar to oxidative phosphorylation (Fig. 3). ThTP can be released from mitochondria in the presence of external P_i . Therefore, cytosolic ThTP may have two different origins, either by exit from mitochondria or synthesis by cytosolic AK. In most mammalian tissues, with the exception of those mentioned above, 25-kDa ThTPase rapidly hydrolyzes cytosolic ThTP. This enzyme, especially in rodents, has a very high catalytic efficiency ($k_{\text{cat}}/K_m = 10^6 - 10^7 \text{ s}^{-1} \text{ M}^{-1}$). Therefore, ThTP is efficiently hydrolyzed, even when its cytoplasmic concentrations are very low, i. e. in the submicromolar range, which is generally the case. It has been proposed that ThTP results from metabolite (ThDP) damage and that 25-kDa ThTPase would be a kind of repair enzyme, converting ThTP to ThDP (Linster et al. 2013). Though this hypothesis cannot be excluded, there are two arguments against it: (1) as stated above, in skeletal muscle and electric organs ThTP accumulates in the absence of any apparent damage; (2) synthesis of ThTP by the chemiosmotic mechanism is tissue-specific.

Moreover, ThTP synthesis by F_0F_1 -ATP synthase in bacteria is highly dependent on metabolic conditions and occurs only transiently at the onset of amino acid starvation (Lakaye et al. 2004c). In this organism, no specific ThTPase is present and the control of ThTP concentration occurs at the level of synthesis involving F_0F_1 -ATP synthase.

As mitochondria have probably evolved from endosymbiotic bacteria, this raises the interesting hypothesis that in animal cells the role of ThTP may be mitochondrial rather than cytoplasmic. Hence, a cytoplasmic accumulation of ThTP as a result of high AK1 activity, as observed in some skeletal muscles and electric organs, would therefore not be physiologically relevant.

The data reviewed here also emphasize the uniqueness of thiamine, which, to our knowledge, is the only molecule existing in its mono-, di-, and triphosphate forms that is not a nucleotide. Therefore, the metabolism of thiamine is more reminiscent of a nucleotide such as adenosine, than that of other vitamins. The parallelism between ThTP and ATP is further strengthened by the observation that they are synthesized by the same enzymes: adenylate kinase and F_0F_1 -ATP synthase. Moreover, like ATP, ThTP may phosphorylate rapsyn as well as several other brain proteins, though this is probably by autophosphorylation (Nghiem et al. 2000).

Finally, the discovery of AThTP, another thiamine triphosphorylated derivative is not meant to simplify the picture.

Now that the mechanisms of ThTP synthesis have been elucidated and that a specific ThTP-hydrolyzing enzyme has been identified, future work should focus on its targets. In this respect, the study of protein phosphorylation by ThTP should be helpful. Organisms such as *E. coli* and higher plants, in which ThTP appears under very specific stress situations should give interesting insights into the physiological role of this compound. Finally, in mammalian cells, strategies aiming at silencing ThTPase expression (knockout mice, siRNA) should represent a promising approaches.

Acknowledgments This work was funded by the “Fonds de la Recherche Scientifique Collective” (grant 2.4558.04). L. Bettendorff is Research Director and B. Lakaye Reserch Associate at the Funds for Scientific Research (F.R.S.-FNRS, Belgium). The data from Fig. 2 were obtained with the technical assistance of Olivier Hennen.

Conflict of interest The authors declare that they have no competing interests.

References

- Barchi RL, Braun PE (1972) A membrane-associated thiamine triphosphatase from rat brain. Properties of the enzyme. *J Biol Chem* 247:7668–7673
- Berman K, Fishman RA (1975) Thiamine phosphate metabolism and possible coenzyme-independent functions of thiamine in brain. *J Neurochem* 24:457–465
- Bettendorff L (1994a) The compartmentation of phosphorylated thiamine derivatives in cultured neuroblastoma cells. *Biochim Biophys Acta* 1222:7–14
- Bettendorff L (1994b) Thiamine in excitable tissues: reflections on a non-cofactor role. *Metab Brain Dis* 9:183–209
- Bettendorff L, Wins P (2013) Thiamine triphosphatase and the CYTH family of proteins. *FEBS J* 280:6443–6455
- Bettendorff L, Grandfils C, De Rycker C, Schoffeniels E (1986) Determination of thiamine and its phosphate esters in human blood serum at femtomole levels. *J Chromatogr* 382:297–302
- Bettendorff L, Michel-Cahay C, Grandfils C, De Rycker C, Schoffeniels E (1987) Thiamine triphosphate and membrane-associated thiamine phosphatases in the electric organ of *Electrophorus electricus*. *J Neurochem* 49:495–502
- Bettendorff L, Wins P, Schoffeniels E (1988) Thiamine triphosphatase from *Electrophorus electricus* is anion-dependent and irreversibly inhibited by 4,4'-diisothiocyanostilbene-2,2'-disulfonic acid. *Biochem Biophys Res Commun* 154:942–947
- Bettendorff L, Grandfils C, Wins P, Schoffeniels E (1989a) Thiamine triphosphatase in the membranes of the main electric organ of *Electrophorus electricus*: substrate-enzyme interactions. *J Neurochem* 53:738–746
- Bettendorff L, Schoffeniels E, Naquet R, Silva-Barrat C, Riche D, Menini C (1989b) Phosphorylated thiamine derivatives and cortical activity in the baboon *Papio papio*: effect of intermittent light stimulation. *J Neurochem* 53:80–87

- Bettendorff L, Weekers L, Wins P, Schoffeniels E (1990a) Injection of sulbutiamine induces an increase in thiamine triphosphate in rat tissues. *Biochem Pharmacol* 40:2557–2560
- Bettendorff L, Wins P, Schoffeniels E (1990b) Regulation of ion uptake in membrane vesicles from rat brain by thiamine compounds. *Biochem Biophys Res Commun* 171:1137–1144
- Bettendorff L, Peeters M, Jouan C, Wins P, Schoffeniels E (1991) Determination of thiamin and its phosphate esters in cultured neurons and astrocytes using an ion-pair reversed-phase high-performance liquid chromatographic method. *Anal Biochem* 198:52–59
- Bettendorff L, Hennuy B, Wins P, Schoffeniels E (1993a) Thiamin and derivatives as modulators of rat brain chloride channels. *Neuroscience* 52:1009–1017
- Bettendorff L, Kolb HA, Schoffeniels E (1993b) Thiamine triphosphate activates an anion channel of large unit conductance in neuroblastoma cells. *J Membr Biol* 136:281–288
- Bettendorff L, Peeters M, Wins P, Schoffeniels E (1993c) Metabolism of thiamine triphosphate in rat brain: correlation with chloride permeability. *J Neurochem* 60:423–434
- Bettendorff L, Hennuy B, De Clerck A, Wins P (1994a) Chloride permeability of rat brain membrane vesicles correlates with thiamine triphosphate content. *Brain Res* 652:157–160
- Bettendorff L, Wins P, Lesourd M (1994b) Subcellular localization and compartmentation of thiamine derivatives in rat brain. *Biochim Biophys Acta* 1222:1–6
- Bettendorff L, Mastrogiacomio F, Kish SJ, Grisar T (1996) Thiamine, thiamine phosphates, and their metabolizing enzymes in human brain. *J Neurochem* 66:250–258
- Bettendorff L, Wirtzfeld B, Makarchikov AF, Mazzucchelli G, Frédéric M, Gigliobianco T, Gangolf M, De Pauw E, Angenot L, Wins P (2007) Discovery of a natural thiamine adenine nucleotide. *Nat Chem Biol* 3:211–212
- Bontemps J, Philippe P, Bettendorff L, Lombet J, Dandriofosse G, Schoffeniels E, Crommen J (1984) Determination of thiamine and thiamine phosphates in excitable tissues as thiochrome derivatives by reversed-phase high-performance liquid chromatography on octadecyl silica. *J Chromatogr* 307:283–294
- Calingasan NY, Sheu KF, Baker H, Jung EH, Paoletti F, Gibson GE (1995) Heterogeneous expression of transketolase in rat brain. *J Neurochem* 64:1034–1044
- Chernikevich IP, Luchko V, Voskoboev AI, Ostrovsky YM (1984) Purification and properties of ATP:thiamine diphosphate phosphotransferase from brewer's yeast. *Biokhimiya* 49:899–907
- Cooper JR, Pincus JH (1979) The role of thiamine in nervous tissue. *Neurochem Res* 4:223–239
- Cooper JR, Roth RH, Kini MM (1963) Biochemical and physiological function of thiamine in nervous tissue. *Nature* 199:609–610
- Cooper JR, Itokawa Y, Pincus JH (1969) Thiamine triphosphate deficiency in subacute necrotizing encephalomyelopathy. *Science* 164:74–75
- Cooper JR, Pincus JH, Itokawa Y, Piro K (1970) Experience with phosphoryl transferase inhibition in subacute necrotizing encephalomyelopathy. *N Engl J Med* 283:793–795
- Cooper JR, Nishino K, Nishino N, Piro K (1982) The enzymatic synthesis of thiamin triphosphate. *Ann N Y Acad Sci* 378:177–187
- Czemiecki J, Chanas G, Verlaet M, Bettendorff L, Makarchikov AF, Leprince P, Wins P, Grisar T, Lakaye B (2004) Neuronal localization of the 25-kDa specific thiamine triphosphatase in rodent brain. *Neuroscience* 125:833–840
- De La Fuente G, Diaz-Cadavieci R (1954) Cocarboxylase activity of thiamine triphosphoric esters. *Nature* 174:1014
- Delvaux D, Kerff F, Murty MR, Lakaye B, Czemiecki J, Kohn G, Wins P, Herman R, Gabelica V, Heuze F, Tordo X, Maree R, Matagne A, Charlier P, De Pauw E, Bettendorff L (2013) Structural determinants of specificity and catalytic mechanism in mammalian 25-kDa thiamine triphosphatase. *Biochim Biophys Acta* 1830:4513–4523
- Di Rocco M, Lamba LD, Minniti G, Caruso U, Naito E (2000) Outcome of thiamine treatment in a child with Leigh disease due to thiamine-responsive pyruvate dehydrogenase deficiency. *Eur J Paediatr Neurol* 4:115–117
- Dubyak GR (2012) Function without form: an ongoing search for maxi-anion channel proteins. Focus on “Maxi-anion channel and pannexin 1 hemichannel constitute separate pathways for swelling-induced ATP release in murine L929 fibrosarcoma cells”. *Am J Physiol Cell Physiol* 303:C913–C915
- Eckert T, Möbus W (1964) Über eine ATP:thiaminediphosphat-phosphotransferase—Aktivität im Nervengewebe. *H-S Z Physiol Chem* 338:286–288
- Eder L, Dunant Y (1980) Thiamine and cholinergic transmission in the electric organ of Torpedo. I. Cellular localization and functional changes of thiamine and thiamine phosphate esters. *J Neurochem* 35:1278–1286
- Egi Y, Koyama S, Shikata H, Yamada K, Kawasaki T (1986) Content of thiamin phosphate esters in mammalian tissues—an extremely high concentration of thiamin triphosphate in pig skeletal muscle. *Biochem Int* 12:385–390
- Finsterer J (2008) Leigh and Leigh-like syndrome in children and adults. *Pediatr Neurol* 39:223–235
- Frédéric M, Delvaux D, Gigliobianco T, Gangolf M, Dive G, Mazzucchelli G, Elias B, De Pauw E, Angenot L, Wins P, Bettendorff L (2009) Thiaminylated adenine nucleotides. Chemical synthesis, structural characterization and natural occurrence. *FEBS J* 276:3256–3268
- Gaitonde MK, Evans GM (1983) Metabolism of thiamin in rat brain. *Biochem Soc Trans* 11:695–696
- Gangolf M, Czemiecki J, Rademacker M, Detry O, Nisolle M, Jouan C, Martin D, Chantraine F, Lakaye B, Wins P, Grisar T, Bettendorff L (2010a) Thiamine status in humans and content of phosphorylated thiamine derivatives in biopsies and cultured cells. *PLoS One* 5:e13616
- Gangolf M, Wins P, Thiry M, El Moulaj B, Bettendorff L (2010b) Thiamine triphosphate synthesis in rat brain occurs in mitochondria and is coupled to the respiratory chain. *J Biol Chem* 285:583–594
- Gautam M, Noakes PG, Mudd J, Nichol M, Chu GC, Sanes JR, Merlie JP (1995) Failure of postsynaptic specialization to develop at neuromuscular junctions of rapsyn-deficient mice. *Nature* 377:232–236
- Gigliobianco T, Lakaye B, Makarchikov AF, Wins P, Bettendorff L (2008) Adenylate kinase-independent thiamine triphosphate accumulation under severe energy stress in *Escherichia coli*. *BMC Microbiol* 8:16
- Gigliobianco T, Lakaye B, Wins P, El Moulaj B, Zorzi W, Bettendorff L (2010) Adenosine thiamine triphosphate accumulates in *Escherichia coli* cells in response to specific conditions of metabolic stress. *BMC Microbiol* 10:148
- Gigliobianco T, Gangolf M, Lakaye B, Piron B, von Ballmoos C, Wins P, Bettendorff L (2013) An alternative role of FoF1-ATP synthase in *Escherichia coli*: synthesis of thiamine triphosphate. *Sci Rep* 3:1071
- Greiling H, Kiesow L (1956) Die enzymatische Phosphorylierung von Glucose mit Thiamintriphosphorsäureester. *Z Naturforsch* 11b:491
- Greiling H, Kiesow L (1958) Zur Biochemie des Thiamintriphosphorsäure IV. Mitt.: Das Vorkommen von thiamintriphosphate im tierischen Organismus. *Z Naturforsch* 13b:251–252
- Gurtner HP (1961) Aneurin und Nervenerregung. Versuche mit 35S markiertem Aneurin und Aneurinantimetaboliten. *Helv Physiol Acta Suppl.* XI:1–47
- Hashitani Y, Cooper JR (1972) The partial purification of thiamine triphosphatase from rat brain. *J Biol Chem* 247:2117–2119
- Hazell AS, Butterworth RF (2009) Update of cell damage mechanisms in thiamine deficiency: focus on oxidative stress, excitotoxicity and inflammation. *Alcohol Alcohol* 44:141–147
- Ishii K, Sarai K, Sanemori H, Kawasaki T (1979a) Analysis of thiamine and its phosphate esters by high-performance liquid chromatography. *Anal Biochem* 97:191–195

- Ishii K, Sarai K, Sanemori H, Kawasaki T (1979b) Concentrations of thiamine and its phosphate esters in rat tissues determined by high-performance liquid chromatography. *J Nutr Sci Vitaminol (Tokyo)* 25:517–523
- Itokawa Y, Cooper JR (1968) The enzymatic synthesis of triphosphothiamin. *Biochim Biophys Acta* 158:180–182
- Itokawa Y, Cooper JR (1970) Electrophoretic separation and fluorometric determination of thiamine and its phosphate esters. *Methods Enzymol* 18A:91–92
- Iwata H, Yabushita Y, Doi T, Matsuda T (1985) Synthesis of thiamine triphosphate in rat brain in vivo. *Neurochem Res* 10:779–787
- Iyer LM, Aravind L (2002) The catalytic domains of thiamine triphosphatase and CyaB-like adenylyl cyclase define a novel superfamily of domains that bind organic phosphates. *BMC Genomics* 3:33
- Kawasaki T (1992a) Thiamin triphosphate synthesis in animals. *J Nutr Sci Vitaminol (Tokyo) Spec No* :383–386
- Kawasaki T (1992b) Vitamin B1: thiamine. In: De Leenheer AP, Lambert WE, Nelis HJ (eds) *Modern chromatographic analysis of vitamins*, vol 60. *Chromatographic science series*, 2nd edn. Marcel Dekker, Inc, New York, pp 319–354
- Kiessling K-H (1953) Thiamine triphosphate in bakers' yeast. *Nature* 172:1187–1188
- Kunz HA (1956) Über die Wirkung von Antimetaboliten de Aneurins auf die einzelne markhaltige Nervenfaser. *Helv Physiol Acta* 14:411–423
- Laforenza U, Patrini C, Mazzarello P, Poloni M, Rindi G (1990) Thiamine, thiamine phosphates and thiamine metabolizing enzymes in synaptosomes of rat brain. *Basic Appl Histochem* 34:249–257
- Lakaye B, Makarchikov AF, Antunes AF, Zorzi W, Coumans B, De Pauw E, Wins P, Grisar T, Bettendorff L (2002) Molecular characterization of a specific thiamine triphosphatase widely expressed in mammalian tissues. *J Biol Chem* 277:13771–13777
- Lakaye B, Makarchikov AF, Wins P, Margineanu I, Roland S, Lins L, Aichour R, Lebeau L, El Moualij B, Zorzi W, Coumans B, Grisar T, Bettendorff L (2004a) Human recombinant thiamine triphosphatase: purification, secondary structure and catalytic properties. *Int J Biochem Cell Biol* 36:1348–1364
- Lakaye B, Verlaet M, Dubail J, Czerniecki J, Bontems S, Makarchikov AF, Wins P, Piette J, Grisar T, Bettendorff L (2004b) Expression of 25 kDa thiamine triphosphatase in rodent tissues using quantitative PCR and characterization of its mRNA. *Int J Biochem Cell Biol* 36:2032–2041
- Lakaye B, Wirtzfeld B, Wins P, Grisar T, Bettendorff L (2004c) Thiamine triphosphate, a new signal required for optimal growth of *Escherichia coli* during amino acid starvation. *J Biol Chem* 279:17142–17147
- Leigh D (1951) Subacute necrotizing encephalomyelopathy in an infant. *J Neurol Neurosurg Psychiatry* 14:216–221
- Lindhurst MJ, Fiermonte G, Song S, Struys E, De Leonardi F, Schwartzberg PL, Chen A, Castegna A, Verhoeven N, Mathews CK, Palmieri F, Biesecker LG (2006) Knockout of Slc25a19 causes mitochondrial thiamine pyrophosphate depletion, embryonic lethality, CNS malformations, and anemia. *Proc Natl Acad Sci U S A* 103:15927–15932
- Linster CL, Van Schaftingen E, Hanson AD (2013) Metabolite damage and its repair or pre-emption. *Nat Chem Biol* 9:72–80
- Lohmann K, Schuster P (1937) Untersuchungen über die Cocarboxylase. *Biochem Z* 294:188
- Lynch PL, Young IS (2000) Determination of thiamine by high-performance liquid chromatography [in process citation]. *J Chromatogr A* 881:267–284
- Makarchikov AF, Chemikevich IP (1992) Purification and characterization of thiamine triphosphatase from bovine brain. *Biochim Biophys Acta* 1117:326–332
- Makarchikov AF, Wins P, Janssen E, Wieringa B, Grisar T, Bettendorff L (2002) Adenylyl kinase 1 knockout mice have normal thiamine triphosphate levels. *Biochim Biophys Acta* 1592:117–121
- Makarchikov AF, Lakaye B, Gulyai IE, Czerniecki J, Coumans B, Wins P, Grisar T, Bettendorff L (2003) Thiamine triphosphate and thiamine triphosphatase activities: from bacteria to mammals. *Cell Mol Life Sci* 60:1477–1488
- Makarchikov AF, Brans A, Bettendorff L (2007) Thiamine diphosphate adenylyl transferase from *E. coli*: functional characterization of the enzyme synthesizing adenosine thiamine triphosphate. *BMC Biochem* 8:17
- Marobbio CM, Voza A, Harding M, Bisaccia F, Palmieri F, Walker JE (2002) Identification and reconstitution of the yeast mitochondrial transporter for thiamine pyrophosphate. *EMBO J* 21:5653–5661
- Matsuda T, Cooper JR (1981a) The separation and determination of thiamine and its phosphate esters in brain. *Anal Biochem* 117:203–207
- Matsuda T, Cooper JR (1981b) Thiamine as an integral component of brain synaptosomal membranes. *Proc Natl Acad Sci U S A* 78:5886–5889
- Matsuda T, Doi T, Tonomura H, Baba A, Iwata H (1989a) Postnatal development of thiamine metabolism in rat brain. *J Neurochem* 52:842–846
- Matsuda T, Tonomura H, Baba A, Iwata H (1989b) Difference in thiamine metabolism between extensor digitorum longus and soleus muscles. *Comp Biochem Physiol B* 94:399–403
- Matsuda T, Tonomura H, Baba A, Iwata H (1989c) Tissue difference in cellular localization of thiamine phosphate esters. *Comp Biochem Physiol B* 94:405–409
- Matsuda T, Tonomura H, Baba A, Iwata H (1991) Membrane-associated thiamine triphosphatase in rat skeletal muscle. *Int J Biochem* 23:1111–1114
- Minz B (1938) Sur la libération de la vitamine B1 par le tronc isolé du nerf pneumogastrique soumis à l'excitation électrique. *C R Soc Biol (Paris)* 127:1251–1253
- Miyoshi K, Egi Y, Shioda T, Kawasaki T (1990) Evidence for in vivo synthesis of thiamin triphosphate by cytosolic adenylate kinase in chicken skeletal muscle. *J Biochem (Tokyo)* 108:267–270
- Murphy JV (1976) Neurochemical changes in Leigh's disease. *J Nutr Sci Vitaminol (Tokyo)* 22 SUPPL:69–73
- Naito E, Ito M, Yokota I, Saijo T, Matsuda J, Osaka H, Kimura S, Kuroda Y (1997) Biochemical and molecular analysis of an X-linked case of Leigh syndrome associated with thiamin-responsive pyruvate dehydrogenase deficiency. *J Inher Metab Dis* 20:539–548
- Nghiêm HO, Bettendorff L, Changeux JP (2000) Specific phosphorylation of *Torpedo* 43K rapsyn by endogenous kinase(s) with thiamine triphosphate as the phosphate donor. *FASEB J* 14:543–554
- Nishino K, Itokawa Y, Nishino N, Piros K, Cooper JR (1983) Enzyme system involved in the synthesis of thiamin triphosphate. I. Purification and characterization of protein-bound thiamin diphosphate: ATP phosphoryltransferase. *J Biol Chem* 258:11871–11878
- Pincus JH, Solitare GB, Cooper JR (1976) Thiamine triphosphate levels and histopathology. Correlation in Leigh disease. *Arch Neurol* 33:759–763
- Postoenko VA, Parkhomenko YM, Vovk AI, Khalmuradov AG, Donchenko GV (1988) Isolation and certain properties of the thiamine-binding protein of rat brain synaptosomes. *Biokhimiya* 52:1792–1797
- Redkar VD, Kenkare UW (1972) Bovine brain mitochondrial hexokinase. Solubilization, purification, and role of sulfhydryl residues. *J Biol Chem* 247:7576–7584
- Rossi-Fanelli A, Siliprandi N, Fasella P (1952) On the presence of the triphosphothiamine (TPT) in the liver. *Science* 116:711–713
- Rossi-Fanelli A, Siliprandi N, Siliprandi P, Ciccarone P (1955) Triphosphothiamine. I. Preparation and crystallization of the pure compound, some chemical and enzymatic properties. *Arch Biochem Biophys* 58:237–243
- Ruenwongsa P, Cooper JR (1977) The role of bound thiamine pyrophosphate in the synthesis of thiamine triphosphate in rat liver. *Biochim Biophys Acta* 482:64–70

- Sanemori H, Kawasaki T (1982) Thiamine triphosphate metabolism and its turnover in the rat liver. *Experientia* 38:1044–1045
- Sanemori H, Ueki H, Kawasaki T (1980) Reversed-phase high-performance liquid chromatographic analysis of thiamine phosphate esters at subpicomole levels. *Anal Biochem* 107:451–455
- Schrijver J, Dias T, Hommes FA (1978) Studies on ATP: thiamine diphosphate phosphotransferase activity in rat brain. *Neurochem Res* 3:699–709
- Shikata H, Egi Y, Koyama S, Yamada K, Kawasaki T (1989) Properties of the thiamin triphosphate-synthesizing activity catalyzed by adenylate kinase (isoenzyme 1). *Biochem Int* 18:943–949
- Shioda T, Egi Y, Yamada K, Kawasaki T (1991) Properties of thiamin triphosphate-synthesizing activity of chicken cytosolic adenylate kinase and the effect of adenine nucleotides. *Biochim Biophys Acta* 1115:30–35
- Sidorova AA, Stepanenko SP, Parkhomenko Iu M (2009) Characteristics of thiamine triphosphatase from neural cells plasma membranes. *Ukr Biokhim Zh* 81:57–65
- Sismeiro O, Trotot P, Biville F, Vivares C, Danchin A (1998) *Aeromonas hydrophila* adenylate cyclase 2: a new class of adenylate cyclases with thermophilic properties and sequence similarities to proteins from hyperthermophilic archaeobacteria. *J Bacteriol* 180:3339–3344
- Song J, Bettendorff L, Tonelli M, Markley JL (2008) Structural basis for the catalytic mechanism of mammalian 25-kDa thiamine triphosphatase. *J Biol Chem* 283:10939–10948
- Srinivas S, Watanabe T, Lin CS, William CM, Tanabe Y, Jessell TM, Costantini F (2001) Cre reporter strains produced by targeted insertion of EYFP and ECFP into the ROSA26 locus. *BMC Dev Biol* 1:4
- Sui D, Wilson JE (2002) Purification of the Type II and Type III isozymes of rat hexokinase, expressed in yeast. *Protein Expr Purif* 24:83–89
- Szyniarowski P, Lakaye B, Czerniecki J, Makarchikov AF, Wins P, Margineanu I, Coumans B, Grisar T, Bettendorff L (2005) Pig tissues express a catalytically inefficient 25-kDa thiamine triphosphatase: insight in the catalytic mechanisms of this enzyme. *Biochim Biophys Acta* 1725:93–102
- Velluz L, Amiard G, Bartos J (1948) Acide thiamine-triphosphorique. *C R Acad Sci (Paris)* 226:735–736
- Velluz L, Amiard G, Bartos J (1949) Thiamine triphosphoric acid, its relation to the thiamine pyrophosphate (cocarboxylase) of Lohmann and Schuster. *J Biol Chem* 180:1137–1145
- Von Mural A (1942) Über den Nachweis von Aktionssubstanzen des Nervenregung. *Pflugers Arch* 245:604–632
- Von Mural A (1947) Thiamine and peripheral neurophysiology. In: Harris RS, Thimann KV (eds) *Vitamins and hormones*, vol 5. Academic, New York, pp 93–118
- Von Mural A, Zemp J (1943) Über die Freisetzung von Aneurin bei der Nervenregung. *Pflugers Arch* 246:746–748
- Voskoboev AI, Chernikevich IP (1985) Biosynthesis of thiamine triphosphate and identification of thiamine diphosphate-binding protein of rat liver hyaloplasm. *Biokhimiya* 50:1421–1427
- Voskoboev AI, Luchko VS (1980) Isolation and radiometric determination of rat liver ATP: thiamine diphosphate phosphotransferase activity. *Vopr Med Khim* 26:564–568
- Voskoboyev AI, Chernikevich IP, Luchko VS (1987) Studies on thiamine diphosphate kinase (EC 2.7.4.15) from brewer's yeast: purification and some properties. *Biomed Biochim Acta* 46:3–13
- Wilson JE (2003) Isozymes of mammalian hexokinase: structure, subcellular localization and metabolic function. *J Exp Biol* 206:2049–2057
- Yoshioka H, Nishino K, Miyake T, Ohshio G, Kimura T, Hamashima Y (1987) Immunohistochemical localization of a new thiamine diphosphate-binding protein in the rat nervous system. *Neurosci Lett* 77:10–14
- Yusa T (1961) Thiamine triphosphate in yeasts and some plant materials. *Plant Cell Physiol* 2:471–474
- Yusa T (1962) Studies on thiamine triphosphate II. Thiamine triphosphate as phosphate donor. *Plant Cell Physiol* 3:95–103

